University of Denver
Digital Commons @ DU

Electronic Theses and Dissertations | Graduate Studies

1-1-2009

Analysis and Treatment of Emerging Polar Contaminants

Daniel E. Connors
University of Denver

Follow this and additional works at: https://digitalcommons.du.edu/etd

 Part of the Environmental Chemistry Commons

Recommended Citation

Connors, Daniel E., "Analysis and Treatment of Emerging Polar Contaminants" (2009). *Electronic Theses and Dissertations*. 788.
https://digitalcommons.du.edu/etd/788

This Dissertation is brought to you for free and open access by the Graduate Studies at Digital Commons @ DU. It has been accepted for inclusion in Electronic Theses and Dissertations by an authorized administrator of Digital Commons @ DU. For more information, please contact jennifer.cox@du.edu,dig-commons@du.edu.

ANALYSIS AND TREATMENT OF EMERGING POLAR CONTAMINANTS

_____

A Dissertation

Presented to

The Faculty of Natural Sciences and Mathematics

University of Denver

_____

In Partial Fulfillment

of the Requirements for the Degree

Doctor of Philosophy

_____

by

Daniel E. Connors

June 2009

Advisor: Keith E. Miller

Author: Daniel E. Connors
Title: Analysis and Treatment of Emerging Contaminants
Advisor: Keith E. Miller
Degree Date: June 2009

Abstract

Two major classes of polar compounds have recently become a major focus as sources of contamination of water systems. Pharmaceuticals and personal care products (PPCPs) enter water through wastewater streams, and many of these compounds survive current wastewater treatment processes. High production volume chemicals (HPVCs), defined as chemicals produced in excess of one million pounds per year have numerous entries into surface and drinking waters due to their ubiquity. The commonality between many of these compounds is their polarity, which makes them water-soluble.

While both PPCPs and HPVCs have been entering into the environment for decades, advances in analyte detection have increased the ability of scientists to identify these compounds in surface, waste and drinking waters. Methods for polar compound suites have been developed using a number of technologies, however these processes are often time consuming and require specialized instrumentation.

In this study, a fast, robust method for the detection and treatment of emerging polar contaminants was developed with accompanying instrumentation. A liquid chromatography system, hyphenated to a universal gas phase detector,

flame ionization detector (FID), was designed. By using pure subcritical water as a mobile phase, temperature was used to control chromatographic retention. This instrument may be used for rapid screening of environmental samples with minimal preparation. Using subcritical water chromatography allowed for testing of mass transfer between subcritical water and organic phases, which provides data on the transport of polar contaminants between solvent phases.

A second component of the work in this dissertation was to test a treatment protocol for waste streams, which demonstrated the reduction of selected analytes within the PPCP and HPVC classes. Subcritical water wet oxidation allowed for the breakdown of all polar organic molecules dissolved in a water sample. As a thermochemical process, the oxidation reaction further reduced select compounds that remain after current biological waste removal processes, and provided a value-added process to current wastewater treatment, in which a needed process, disinfection, can be coupled to additional contaminant removal.

Acknowledgements

I wish to thank Keith Miller for his support through my tenure at the University of Denver. Keith made a challenge in my early graduate career into an opportunity for learning, and I am richer for the experience. I specifically want to thank Keith for giving me the guidance I needed when I needed it, and the freedom to explore and build my own research directions.

I appreciate the support of Don Stedman and Todd Wells. Having Don available always meant there was a way to solve a research problem by building the solution. Todd provided invaluable suggestions throughout my graduate tenure, especially when tricky ideas about negative refractive indices needed to be turned into a prop oral.

I appreciate the support of Randy Shearer for his donations of instrumentation and expertise, and Stephen Ellis and Blair Corning for their support during my internship at South Adams Water and Sanitation District. I also appreciate the support and interest of Dr. Jay McGrew with his work on the VTR system.

I also need to thank the constant support of my family and friends, especially Dr. Susan Connors for her help in the preparation of this dissertation. Special thanks goes to Arsalan Rivsi, Jessi Snyder, Joe Zemetra, Behrang Mahjoub, Mike Swanson, Jeff Caulfield, Tiffany Gustafson, Allison Peddle and Brooke Woolman, as well as past and current members of the analytical section.

TABLE OF CONTENTS

LIST OF FIGURES

LIST OF TABLES

Chapter 1: Introduction

> Seldom if ever does Nature operate in closed and separate compartments, and she has not done so in distributing the earth's water supply.
>
> -Rachel Carson, *Silent Spring* (1962)

When *Silent Spring* was published, the idea that human-made chemicals could negatively impact the environment was a radical concept. Rachel Carson was referring to the environmental effects of dichlorodiphenyltricholoroethane (DDT) in this quotation, but the lessons of this compound's environmental effect still resonate. Despite criticism of the eventual ban on DDT in recent years, *Silent Spring* demonstrated how human activity can directly impact environmental quality and how unintended consequences of seemingly benign compounds can cause changes in the ecosystem. This dissertation research was designed to contribute to the understanding of the presence of new environmental contaminants, as well as to improve the methods necessary to remove compounds that could cause environmental damage.

While many of the compounds of concern in the 1960s have been removed from common usage, new classes of chemicals presumed to be safe have been found to affect ecosystems. Low concentrations of these chemicals can affect wildlife, and detection of these chemicals has largely been limited to modern analytical chemistry methods. Great advances in mass spectrometry and separation techniques have allowed for a more thorough understanding of the environmental impact of anthropogenic (coming from a human source) chemicals. A major study by the United States Geological Survey (USGS) demonstrated the ubiquity of biologically active polar organic contaminants in U.S. waterways originating from human pharmaceutical and personal care product usage (Kolpin et al., 2002). Further studies have demonstrated the appearance of flame-retardants in the Arctic (Brown and Wania, 2008) and the common antibacterial compound triclocarban in surface waters (Halden and Paull, 2004). The anthropogenic marker caffeine has been demonstrated to be remarkably common in surface water, indicating the transport of trace contaminants of human origin into the environment (Buerge et al., 2003). Concentrations of these types of compounds are found frequently in the part per million to part per trillion range, depending on the chemical usage rate and sampling location.

Once in the environment, the effects of anthropogenic contaminants are unpredictable. Some products are transformed through biological or physical

processes, resulting in the creation of unique new compounds, such as the discovery of Q1, a contaminant with the formula $C_9H_3Cl_7N_2$, that appears to be anthropogenic in origin but does not match any published reference to known chemicals (Vetter et al., 1999). Later research demonstrated Q1 to be 2,3,3', 4,4',5,5'-heptachloro-1'-methyl-1,2'-bipyrrole, which has no obvious source, but is found widely in the Atlantic Ocean in the Southern hemisphere (Vetter and Jun, 2002). Other compounds that were thought to be environmentally benign, like alkylphenolic surfactants, have been proven to strongly mimic estrogens in vertebrates, causing dramatic changes in the endocrinology of reporter species in surface waters (Jobling et al., 1996). Complex transfer processes in the environment for polar contaminants makes the eventual environmental fate extremely difficult to predict based solely on contaminant structure.

Three important problems exist for the understanding and prevention of environmental damage due to polar contaminants:

1. Determining the presence of anthropogenic polar contaminants in surface, waste and drinking waters;
2. Understanding the physical processes that make some chemicals environmentally benign and others dangerous; and
3. Finding where contamination events occur, likely in wastewater treatment plants, and changing how treatment is performed to prevent contamination.

1.1 Research Objectives

The goals of this study were to develop new analytical methods for the detection of emerging polar contaminants in the environment, to correlate physical structures of polar contaminants to their retention behaviors, and to develop new methods of remediating these contaminants before they enter the environment.

New and innovative approaches to the detection of polar compounds are required to increase understanding of the problem of polar contaminants in the environment. Since aqueous systems were the major focus of this research, reversed-phase liquid chromatographic (RPLC) techniques were a natural first step in the development of analytical techniques. Because many contaminants of interest are polar and have weak chromophores, RPLC hyphenated to mass spectrometry (MS) has been a major method of environmental analysis in the literature (Richardson, 2006, 2008). However, due to the expense and length of time required for MS analysis, other low cost and efficient methods for the detection of organic molecules are required as initial screening methods for improved environmental monitoring. Thus, the instrument design of a liquid chromatographic (LC) system with universal organic detection was undertaken as a new method of initial screening for environmental contamination. While the instrumentation designed in this work is not able to match the sensitivity or structural identification capabilities of MS techniques, little sample preparation is

required, and multiple target organic compounds in an aqueous sample can be quantified. Using chemical reference standards, a quick screening instrument allows for the rapid identification of samples containing compounds of concern and excludes clean samples; thus, fewer samples would require additional analysis with more sensitive techniques like MS for structural analysis.

The physical structure aids in the prediction of compounds with likely environmental toxicity. However, the mechanisms of environmental transport are often based upon bulk approximations of interactions with polar and non-polar phases (e.g., bulk partitioning measurements such as octanol-water partition coefficients). In order to better understand the processes in which polar analytes partition between polar and non-polar phases, chromatographic processes are often used as model systems. Using a pure-water system and a chromatographic column as analogs for non-polar environments, as well as computational modeling of the interaction of molecules in these phases, new insights into the retention of analytes can be correlated to environmental accessibility, which will help to predict when and if a chemical is an environmental risk (Szabo et al., 1990; Pussemier et al., 1990; Guo et al., 2002). An Organization for Economic Cooperation and Development method, OECD 106, has been specifically developed for the prediction of soil partitioning of environmental contaminants using high performance liquid chromatography (HPLC) retention factors, with a particular focus on the partitioning between water and organic carbon (Kördel et

al., 1995). Although only about 1% by mass of soil is organic carbon, Kördel et al. estimated that about 70% of mass transfer of contaminants was controlled by this portion of soils.

Treatment processes for polar contaminants are required in order to prevent entry into surface waters. As many of the contaminants of interest originate from pharmaceuticals, personal care products, and high production volume chemicals, wastewater treatment facilities are a likely place where treatment can occur. Municipal wastewater treatment facilities are designed for the removal of bulk organic wastes and biological oxygen demand. Current research on modifying treatment methods seeks to target micro-contaminants for removal, which may in the long term be the best solution for the prevention of new environmental contaminants from ever reaching surface waters.

1.2 Universal Detection of Polar Organic Molecules

While LC- MS and LC with ultraviolet-visible (UV-Vis) absorbance detection have been the primary methods of analyzing polar organics in aqueous systems, neither system can universally detect organic molecules. MS detection of small molecules is poor, which could miss many high production volume chemicals in environmental samples. Absorbance methods require analytes have inherently strong chromophores or an extraction and derivatization process to

allow for gas phase detection (modifying analyte volatility) or UV detection (addition of a chromophore).

A different approach for the detection of organic compounds is to directly hyphenate the separation system to a universal organic detector, the flame ionization detector (FID). Following the work of Miller and Hawthorne (1997), a subcritical water chromatography system with flame ionization detection (SWC-FID) was designed, using subcritical water as a mobile phase. Subcritical water is water that has been heated above 100ºC at pressures above 1 atmosphere, but below the critical point of 474ºC and 218 atm. Subcritical water was demonstrated to have the same ability to elute organics from a stationary phase as an aqueous phase modified with an organic solvent like methanol or acetonitrile. Detection limits were found in this system to be less than 1ng injected for many compounds, and the FID linearity is comparable to the linearity observed for gas chromatography-FID systems. Separations of small polar organics (e.g., alcohols, ketones and carboxylic acids, substituted phenols and benzenes) were demonstrated in this dissertation study, all of which have relevance to the analysis of high production volume polar chemicals.

While universal carbon detection is useful for the analysis of complex aqueous samples, additional sample specificity is useful. Chemiluminescence detectors for nitrogen and sulfur are available that can interface directly to FIDs and can provide an additional selective data channel of separation. The use of a

chemiluminescent detector for sulfur was demonstrated with the SWC-FID system with the potential for applications to environmental analysis and food quality.

1.3 Describing the Behavior of Polar Organics in Complex Systems

In the context of predicting mass transport, the chromatographic behavior of a compound in a separation can be correlated to the more complex environmental system where molecules can reside in aqueous phases, organic phases, or adsorb onto mineral surfaces (Pan et al*.,* 2008). The behavior of a molecule in this complex system can provide insight as to whether it will be bioavailable, or if it will sorb to a surface or phase that will enhance biodegradation or physical degradation. A recent review of pharmaceutical and personal care products' environmental fate demonstrated the complexity of polar compound transport in natural waters, with possible interactions occurring for solutes between organic, aqueous, and mineral phases in water and sediments (Pan et al*.,* 2009). In order to model this complex process, the analysis of polar analytes in a chromatographic separation can provide detailed correlations between molecular structure and partitioning characteristics. While this process is not new in the field of liquid chromatography, recent insights into the molecular behavior of polar analytes in hydroorganic (aqueous solutions with organic modifiers) mobile phases and non-polar stationary phases have indicated the

mechanisms of retention in chromatography strongly mirror the mechanisms of mass transfer in the environment (Zhang et al., 2005; Zhang et al., 2006, Rafferty et al., 2008).

Experimental procedures were undertaken in this study to describe the mass transfer of polar organics from a pure water phase into a non-polar one. Using a pure water mobile phase allowed for accurate representations of transport between aqueous phases and organic phases, without other dissolved aqueous phase organics. Using the SWC-FID system outlined in section 1.2, pure water could be used instead of an organically modified aqueous mobile phase. This system is more reflective of mass transfers between aqueous phases and non-polar ones, as no organic solvent interface is found in a pure water system. Monitoring the retention of polar analyte classes as a function of temperature allowed for the prediction of mechanisms of transfer in terms of the attributes of chemical structure and also allowed for a description of organic molecules interacting directly with a subcritical aqueous phase. Due to the simplicity of the mobile phase, correlations of phase modification to mass transport were produced, without the complication of a hydroorganic phase.

1.4 Removal of Micro-Contaminants with Subcritical Water Wet Oxidation

Wastewater treatment plants are a logical setting for improved treatment of polar contaminants. However, as is described by Teske et al., (2008),

wastewater plants were designed for the removal of bulk products with oxygen demand, not the breakdown of trace analytes. Value-added treatment processes that compliment current technologies would be desirable, as trace organics could be removed, and other necessary processes in wastewater treatment, like disinfection, could be performed simultaneously. Using a wet oxidation process for chemical treatment of trace analytes can be a significantly different reaction process from current wastewater removal, which is biologically treated.

In wastewater treatment plants, the addition of a subcritical water oxidation reactor can assist in the removal of micro-contaminants that survive typical biological wastewater treatment. In addition, subcritical water oxidation can sterilize wastewater without any chemical additions, providing an efficient decontamination and tertiary treatment.

Subcritical water is a benign reaction medium for organic reactions. In addition to the natural acceleration provided by a strong polar solvent at elevated temperatures, subcritical water acts as a strong acid-base catalyst, which dramatically increases the efficiency of breakdown of organic molecules. When molecular oxygen is added to subcritical water, free radical oxidation of organics is observed, further enhancing organic breakdown (Li et al., 1991). In this work, a lab-scale reactor was tested for effects on residual solids, organic content, and the removal of specific micro-contaminants. Oxidation was favored over hydrothermolysis (the breakdown of organic molecules in high temperature

water) when molecular oxygen is more efficiently transported into the liquid phase (Li et al., 1999). A Taylor bubble (Nigmatulin, 2001), which is a specific bubble shape in narrow tubes, was used to create a large liquid-vapor interface, improving oxygen transport. In associated studies of the efficiency of a lab-scale subcritical water oxidation reactor, solids were efficiently removed from both model solutions and actual waste matrices, with removal percentages up to 99% for model systems and 90% in solutions derived from actual waste products. Total organic content, measured as chemical oxygen demand, was reduced by up to 80% in model solutions and 75% in actual samples. Antibiotics were removed efficiently, demonstrating reductions approaching 100%, limited by the detection method of analysis.

1.5 Study Design and Dissertation Format

In this work, three studies were performed. The first study measured the efficacy of a SWC-FID system in terms of detection limits, linear range, and separation efficiency, and explored how a SWC-FID system could be extended for environmental analytical monitoring. The second study explored the mechanisms of transport for polar analytes in subcritical water; with the goal in future work to extrapolate data collected in the subcritical phase to partitioning effects of polar analytes in natural waters. Finally, the third study sought to use a

lab-scale wet air oxidation reactor for the removal of emerging contaminants from wastewater streams, as a method of preventing environmental damage.

A critical literature review of the detection methods and removal processes of polar contaminants is provided in Chapter 2. Chapter 3 provides a literature review of the theory and mechanisms of the systems used in this study, while Chapter 4 provides details on the materials, methods, and specific instrumentation used or designed in this work. Results for the three studies listed are collected in Chapters 5-7, and conclusions are provided in Chapter 8. Two appendices are also provided; Appendix A lists computational input files, while Appendix B briefly outlines chloride stress corrosion, which was discovered in the wet air oxidation reactor.

Chapter 2: Critical Review of Emerging Polar Contaminant Research

The study of anthropogenic polar contaminants has become a major research area in the fields of water quality and environmental analytical chemistry. These chemicals have been demonstrated to be common in wastewaters, as well as surface and drinking waters, indicating a current lack of effective wastewater treatment (Conn et al., 2006; Teske and Arnold, 2008). Many of these chemicals, which are derived from industrial, medical, and personal care product sources, have been found to have endocrine disrupting effects even at extremely low concentrations. A significant amount of research into the processes of prevention, transport and identification of polar contaminants has been conducted in the hopes of limiting environmental damage as well as unforeseen effects on the human population. In this section, the historical discovery of polar contaminants in the environment is discussed as well as the differing philosophies on how environmental monitoring should be performed. Next, common analytical methods are discussed for the detection of

polar contaminants. Finally in this chapter, work is reviewed on the removal of environmental contaminants in wastewater treatment.

2.1 The Discovery of Emerging Polar Contaminants in the Environment

Historically, much of environmental analytical chemistry has focused on persistent organic compounds such as polychlorinated products, pesticides, dioxins and polyaromatic hydrocarbons (PAHs) (Croley et al., 2000; Szabo et al., 1990; Richardson, 2000). A dramatic change in focus occurred when the endocrine disrupting characteristics of a number of anthropogenic chemicals that enter surface water through wastewater treatment plants were discovered. Endocrine disruption is the change in hormonal activity of vertebrates due to exposure to natural or artificial compounds. A groundbreaking study performed by the USGS on a network of 139 streams in 30 states found organic polar contaminants correlated to wastewater sources in 80% of the studied streams (Kolpin et al., 2002). The contaminants found in this reconnaissance fit into several broad categories:

1. Pharmaceuticals, especially over the counter drugs and antibiotics
2. Wastewater chemicals, frequently treatment additives
3. Industrial and agricultural compounds such as insecticides, plastic production chemicals and surfactants
4. Steroids and hormones

This study led to a great number of publications on the identification and detection of polar and highly soluble compounds that could pass through wastewater treatment or be deposited in surface water through other transport mechanisms. A review of groundwater used for drinking water in the U.S. found volatile organic compounds (VOCs), as well as pesticides and anthropogenic nitrate (an indication of mixing with treated wastewater), most frequently in the ng to low μg L^{-1} concentration range (Squillace et al., 2002). A current biennial review performed by Susan D. Richardson and colleagues through the National Exposure Research Laboratory at the Environmental Protection Agency has greatly expanded the list of analytes to include chemical warfare agents, personal care products such as UV filters in sunscreen, organometallic compounds, combustion engine additives like methyl *tert*-butyl ether and the degradation products of all of these compounds (Richardson and Ternes, 2005; Richardson, 2006, 2008). An extensive review of the known pharmaceuticals in surface waters indicates there are hundreds of potential contaminants in common usage, along with accompanying degradation products. The ecotoxicity of these compounds is at best poorly understood (Khetan and Collins, 2007).

While most of these compounds were found to be in low part per billion (ppb) concentrations, a great number of these chemicals have demonstrable endocrine disrupting activity to vertebrates in this concentration range (Jobling et al., 1996; Routledge et al., 1998). Alkylphenols and related structures have been

linked in particular with disruption of sexual development in fish (Tyler and Jobling, 2008). The large number of chemicals present in water has also been implicated in stress-response changes in human embryonic cells; morphological changes are noted at ng L^{-1} (part per trillion) concentrations of a mixture of compounds (Pomati et al*.,* 2006).

With the discovery of this contaminant class, treatment and prevention becomes fundamentally important. The easiest prevention is to stop using non-biodegradable products with endocrine activity and replace high production volume chemicals with more environmentally benign methods (Boethling et al., 2007). Otherwise, removal must take place in wastewater treatment plants (WWTPs), so that anthropogenic contaminants never reach surface waters. Ultimately, anthropogenic contaminants must be prevented from entering drinking water from surface waters, requiring a full understanding of the breakdown processes involved with polar organics (Stackelberg et al., 2004).

2.2 Methodological Philosophies of Environmental Monitoring

Several philosophies exist for the prioritization the analysis of polar analytes in the environment. Analysis can focus on identifying all compounds in a sample or quantifying a few compounds of major importance. Water samples can be selected for screening because of a history of contamination or because an anthropogenic marker is found at a high concentration. Because surveys may

begin in wastewater plants and continue into streams, aquifers or drinking water treatment plants, detection methods must handle many different concentrations and sample matrices. Three different philosophies are outlined sections 2.2.1 through 2.2.3. The first method described in section 2.2.1 uses predictive statistical models to attempt to describe the contaminants of interest and how these contaminants interact with the environment once released into surface waters. The next approach, in section 2.2.2, suggests the monitoring of high concentration anthropogenic markers as a method for determining contamination. Finally, in 2.2.3, *de novo* analysis seeks to identify as many compounds as possible in an environmental sample and then determine environmental effects.

2.2.1 Environmental Contamination Predictions with Theoretical Modeling

One philosophy of monitoring seeks to determine contaminants based upon predictions of environmental fate from chemical models. Both the European Union (E.U.) and U.S. have lists of predicted major contaminants, and researchers have used these lists as starting points for estimations of environmental toxicology (Cunningham and Rosenkranz, 2001). Free energy relationships have been used to predict structural characteristics that would cause a compound to stay in solution versus partitioning into soils or sediments in surface waters, indicating the potential for environmental interactions (Nguyen et al., 2005). Risk assessment protocols can also be used to estimate the

likelihood of contamination of a watershed. Sanderson et al. (2006) used a weight of evidence risk assessment protocol to suggest that alkyl sulfates and other charged surfactants pose a low risk to biota via predicted and measured compound concentration and correlation to measured macro-invertebrate life.

Lucas and Jauzein (2008) used principal component analysis to predict the size, shape and relative risk of plumes of chlorinated solvents in groundwater through a variability index methods. This approach allowed for the design of an appropriate testing region for the spread of the plume. A toxic pressure calculation has also been used to describe the effects of high production volume chemicals in the environment in the North Sea by the estimation of a given chemical's "toxic stress" potential and then correlation with expected concentrations (Harbers et al*.,* 2006). Klopman and Chakravarti (2003) used a structural training algorithm to predict chemical structures with likely endocrine disrupting capacities; unfortunately, the most likely structure is that of phenols, indicating a large number of chemicals as potential endocrine disruptors.

Brown and Wania (2008) demonstrated how prioritization of potential contaminants could assist in the design of an analytical approach. They used two parallel screening methods to select for analytes, based upon properties that would 1.) favor long-term survival in aqueous solution (partition coefficients) and 2.) match the structural similarity of other known contaminants. Of the 82,000 chemicals they screened, 4,291 were identified as likely to become Arctic

contaminants, of which 120 were found to be high production volume chemicals (> 1 million pounds produced by EPA standards, EPA-HQ-OPPT-2005-0033; 2006). Perfluorinated alkyl-compounds were determined to be a likely target for further study in Arctic watersheds. These compounds were determined to be found in high concentrations, have partitioning coefficients that favored aqueous transport, and are similar to known compounds with known environmental toxicity.

Using a logical framework to identify new analytes is often difficult. Milman (2005) points out that often the analytes targeted for analysis have a direct correlation to the number of times they are cited in the media and in literature, and the screening of generalized compounds is difficult, even with advanced detection methods such as tandem mass spectroscopy. Often, some combination of likelihood ranking along with basic species identification (e.g., phenols, antibiotics) followed by more intensive analysis with multiple detection regimes is required, as is seen in Kolpin et al. (2002) and Gibson et al. (2005).

2.2.2 Anthropogenic Markers

When choosing a sample for analysis, a high concentration marker can be used as indication of anthropogenic contamination. Buerge et al. (2003) suggested caffeine, which is largely anthropogenic in origin, might be a reasonable marker. It has been found to be ubiquitous downstream of urban

centers in surface waters in concentrations from 6-250 ng L^{-1} in the study cited. In addition, time resolution of the study showed spikes in caffeine concentrations in rivers and ponds after heavy rains when wastewater treatment facilities were overwhelmed. Caffeine readily partitions to clay minerals (Caulfield, 2008), creating a concentration sink. Aqueous caffeine concentration can therefore provide a relatively instantaneous picture of the total contamination from designated wastewater sources but not measure all upstream contamination occurrences.

Sirivedhin and Gray (2005) suggested the best anthropogenic marker system was a measure of the overall content of organic carbon in a given water sample. This study determined that organic material from treated wastewater was identifiable, via factor analysis, by a higher concentration of halogens and nitrogen than organic material from non-anthropogenic sources, allowing for the determination of anthropogenic contamination, without the requirement of one specific marker. With the great variability seen in environmental contamination, using a factor analysis of organic components would likely identify anthropogenic sources more accurately than tracing a single analyte.

Certain rare markers can be used for specific analytes, such as boron (identified via inductively coupled plasma mass spectrometry, ICP-MS), which correlates well with nitrosamine contaminants (Schreiber and Mitch, 2006). Anthropogenic nitrate concentrations have also been tracked via isotopic ratios of

oxygen and nitrogen to trace contamination from farming runoff in Guiyang, China (Liu et al., 2006).

Tracing emerging contaminants from wastewater treatment through large watershed is extremely difficult, and several methods have been suggested for different compound classes. A study by Heberer (2002) of pharmaceuticals in an industrialized German city followed the concentrations of a series of pharmaceutical compounds through a WWTP and downstream into drinking water sources. While some compounds (clofibric acid, diclfenac) diminished with distance from the WWTP, others (carbamazepine, salicylic acid) were found to have relatively constant concentrations or even increased. By using a comparison of rapidly degrading product concentrations against compounds with constant concentrations, the input point can be confirmed. In this case the WWTP was demonstrated to be the pharmaceutical source. Benfenati et al. (2003) tracked industrial contaminants downstream from industrial dump sources to determine the size of environmental effects. In more complex watersheds with multiple wastewater inflow points, the process of contaminant sourcing is increasingly difficult, which ultimately requires the usage of special tracers for source confirmation.

2.2.3 *De Novo* Analysis of Environmental Samples

Contrasting with the usage of anthropogenic markers, a different strategy of measuring contaminants in the environment is to use minimal selectivity, which instead attempts to describe all compounds present in a given sample. This approach has been described alternatively as non-targeted screening, holistic analysis or *de novo* analysis. This method allows for the description of all compounds with a significant concentration present in the sample and has clear advantages for the identification of new compounds of interest, with the understanding that no approach can be truly universal, nor can detection limits be expected to be comparable to selective analysis. *De novo* analysis has only become possible with the "omics" approach to extremely high peak capacity chromatographic separations, especially when coupled with highly specific tandem mass spectroscopy for compound identification (Bajad and Shulaev, 2007). Like the biological measurement of metabolites or genetic products with metabolomics and genomics, respectively, the "omics" approach to identification is to use chromatographic techniques with such high resolution as to be able to identify all compounds in a sample separately, which is attractive for complex environmental samples.

Several methods have been described for non-target or holistic screening of organic contaminants in water using solid phase extraction coupled to LC-MS or GC-MS (SPE-LC-ESI-MS) (Loos et al., 2003), SPE-GC-TOF (Hernández et al.,

2007) and SPE-μLC-QTOF (Ibáñez et al., 2005). This approach has proved fruitful in the detection of new analytes that may be a product of bioconversion or other natural process, as in the case of the compound Q1, a heptachlorinated bipyrrole, (Vetter et al. 1999) or in the identification of chlorinated pesticide degradation products on food (García-Reyes et al. 2005). A related technique using a secondary separation mechanism in Q-TOF analysis, high field asymmetric waveform ion mobility spectroscopy (FAIMS) allows for the creation of massive libraries of compounds with unique mass/charge ratios and specific ion mobilities. FAIMS has been able to provide structural identification of numerous compounds in a sample without previous analyte selection, which proves to be useful in extending MS identification into smaller molecules such as haloacetic acids (Gabryelski et al., 2003; Sultan and Gabryelski, 2006).

2.3 Detection Methods for Environmental Polar Contaminants

The main difficulty in the study of emerging polar contaminants is detection. Compounds of interest are often found in the low μg L^{-1} to ng L^{-1} concentration range, requiring very sensitive detection methods and frequently pre-analysis concentration methods. Detection in wastewater requires selective concentration of target analytes in a very complex sample matrix with many competing compounds. In addition, many compounds of interest are small, have low inherent volatilities, and may not have intrinsic chromophores. Typically, this

combination of analyte attributes would favor LC methods with mass spectrometric detection (e.g., Halden and Paull, 2004). However, many other approaches have been suggested, as reviewed by Koester and Moulik (2005), including gas chromatography, LC with mass spectrometry and other detection regimes, and immunoassays.

2.3.1 Sample Pre-Concentration Methods

For relatively simple matrices such as surface and drinking water, all organic compounds present may be relevant to polar contaminant analysis. A simple pre-concentration step may be all that is required to bring samples into a detectable concentration range. Castillo et al. (1999) used non-polar and mixed mode anion exchange solid phase extraction (SPE) cartridges to extract linear alkyl benzene sulfonates and other organics present in contaminated groundwater near tanneries and textile plants. The extracts were then analyzed using LC-MS with electrospray or atmospheric pressure ionization, with selective ions monitored for maximum sensitivity. Method detection limits of ~3ng L^{-1} (decyl benzene sulfonate) to ~1µg L^{-1} (2,4-dinitrophenol) were determined, with actual concentrations in contaminated groundwater from 1-2400µg L^{-1}.

Reddersen and Heberer (2003) used a non-polar SPE method combined with sample derivatization for GC-MS separation and detection. This study looked for pharmaceuticals in groundwater, and the combined SPE-GC-MS

method reported many compounds with method detection limits less than 1ng L^{-1}. A complimentary study performed solid-phase microextraction (SPME), followed by derivatization on the SPME cartridge on a series of endocrine disrupting alkylphenols reported method detection limits of 1-3ng L^{-1} in several sample matrices (Pan and Tsai, 2008). A third study used a liquid-liquid extraction method with ionic liquids for the non-aqueous phase (McFarlane et al., 2005). This study demonstrated that non-polar analytes readily partitioned into the ionic liquid (which is favorable due to pi-stacking on the anionic component), and this method was suggested as a pre-concentration step for the monitoring of development waters downstream of oil and gas development.

2.3.2 Analysis of Derivatized or Semi-Volatile Compounds with GC and GC-MS

Many compounds of concern have functional groups that can be easily targeted for derivatization, and some analytes have enough vapor pressure for separation via gas chromatography. This is especially true for substituted phenols and other aromatic compounds or for high production volume chemicals used as organic solvents. Isaacson et al. (2006) used SPE extraction of groundwater samples along with GC with tandem mass spectrometry for the quantification of 1,4-dioxane, 1,1,1-trichloroethane (TCA) and tetrahydrofuran in a contaminated aquifer. In addition to being able to track the movement of these

three HPVCs in the aquifer, the concentrations of each compound relative to the distance from the contamination source gives a measure of biodegradation. TCA was found to biodegrade much more rapidly than 1,4-dioxane, but the dioxane degraded more rapidly when THF was available as a co-contaminant.

For the comprehensive analysis of many compounds in a complex system, two-dimensional GC (GC×GC) with FID detection can dramatically increase the peak capacity of a given separation. Beens et al. (2001) used a GC×GC method for the separation of an artificial mixture of 80 organic micro-contaminants found in surface waters, demonstrating full resolution of all compounds in one 50-minute separation. This method has a significant advantage over single separation methods in that the 2D chromatogram has greater peak capacity and can resolve more compounds. A prediction of the analyte characteristics of unknowns can also be created by correlation to nearby known reference compounds. However, the separation with flame ionization detection cannot formally identify a compound to the sample level of specificity that a mass spectrum could.

GC-MS methods have more limited resolution when monitoring the total ion chromatogram as opposed to selected ions, and in complex systems, the number of total ions may be very large, requiring multiple ionizations and large fragmentation libraries for identification. However, the high-resolution capability of many mass spectrometers can be a huge benefit in the tracing of isotopic

concentrations, which can assist in the determination of the source of a given contaminant. Grange and Sovocool (2007) demonstrated a high resolution MS technique to predict the sourcing of a number of organic contaminants and to demonstrate that due to unusual isotopic abundance, compounds must have come from anthropogenic sources instead presence in the background matrix. This is similar to the study by Sirivedhin and Gray (2005) who used factor analysis of organic compound composition to determine anthropogenic sourcing.

2.3.3 Polar Contaminant Analysis with LC and LC-MS Methods

The most logical method for the analysis of polar compounds in aqueous media is reversed phase liquid chromatography (RPLC), with UV-Visible detection or mass spectrometry for compound identification. RPLC methods have the advantage of working well with more polar analytes, and samples do not have to be volatile for detection. Given the size of many compounds of interest, electrospray ionization (ESI)-quadrupole and ESI-tandem mass spectrometry have been very common detection methods for polar analytes after LC separation; these methods also have the advantage of identifying possible breakdown products from bio- or photodegradation. Tandem mass spectrometry has the advantage of adding a second collision cell for more accurate ion

fragmentation libraries, while single quad methods are less expensive and time consuming.

A LC-ESI-MS method with a single quadrupole detector used by Halden and Paull (2004) successfully followed triclocarban through urban waterways in Baltimore, MD. Triclocarban is a common antimicrobial agent and pesticide found in personal care products, and as such is anthropogenic in origin; any detected triclocarban in surface waters indicates a lack of removal during wastewater treatment. The detection method used a neutral/lipophilic SPE extraction followed by elution into methanol/acetonitrile/acetic acid. No compound derivatization is required for this method, although the acetic acid-triclocarban adduct was observed in the mass spectra as a confirmatory ion. An isocratic method of LC separation allowed for detection of triclocarban in river and drinking waters with detection limits of less than 1ng. A gradient LC method was also usable in this method for river and wastewater samples, with reported limits of detection around 2ng. With this method, triclocarban was found in waste, river, and groundwater samples, as well as in wells used for drinking water. Evidence of triclocarban in ground and well water demonstrates poor removal in WWTPs. In addition, though not likely within the limit of quantification (LOQ) of the method, triclocarban was found in finished drinking water, indicating that neither waste water nor drinking water treatment methods were completely successful in the removal of this contaminant.

Nonylphenol and its ethoxylates and derivatives were analyzed by ESI-quadrupole from river sources, drinking waters, and fish tissues using several different clean up methods. This method was sensitive enough to follow the time dependent changes in concentrations in river and drinking water in Chongqing, China, and also detect nonylphenol in the muscle, gill and liver tissues of fish at concentrations relevant to cause endocrine disruption. Several other methods also used either ESI-quadrupole or atmospheric pressure ionization followed by quadrupole detection (Petrovic and Barceló, 2000; Croley et al*.,* 2000; Benijts et al., 2002).

Many tandem mass spectrometric detection methods for emerging contaminants have been reported. Vanderford et al. (2003) reported detection limits of endocrine disrupting compounds of 1pg injected, corresponding to matrix concentrations of ~1ng L^{-1}. Loos et al. (2007) also used a tandem mass spectrometry detection method for the detection of polar contaminants (e.g., herbicides, pharmaceuticals, alkylphenols and derivatives, and fluorinated surfactants) in the drinking and surface waters near Lake Maggiore in Northern Italy, downstream of the major city of Piemonte. This study successfully identified a number of common compounds, including endocrine disruptors, drug residues and the anthropogenic marker caffeine in both lake and treated drinking water in the ng L^{-1} range. Thirty-three compounds of significant concern to water quality were quantified via a LC-MS/MS method after SPE (Baugros et al*.,* 2008).

Two other important mass spectral techniques that have been used for environmental monitoring are accelerated-time-of-flight MS and the high-field asymmetric waveform ion mobility spectrometry (FAIMS). Accelerated TOF methods often use hybrid quadupoles (Q-TOF) either as the only detector or in combination with a secondary ionization and detector arrangement, and can assist in the structural identification of unusual compounds in complex matrices by giving extremely accurate compound masses from the TOF detector (Petrovic and Barceló, 2006). This technique was used to identify an unknown contaminant species in surface water by an exact mass from the TOF combined with structural data from different collision energies from a Q-TOF-MS-MS method (Bobeldijk et al., 2001). This type of detection has also been used for the screening of chemicals for potential pharmacological or toxicological effect (Polettini et al., 2008).

FAIMS is effectively a separation method after a sample has been ionized via ESI, which could be incorporated after a standard chromatographic separation (Sultan and Gabryelski, 2006). Ions enter an electrode field with cycles of high and low dc voltage; ions are then sorted according to their relative mobility in these two field strengths. Once separated, ions are swept into a TOF or Q-TOF system via a compensation voltage ramp, which balances the separation electric field and causes ions to transport into the detector. This particular system has the advantage of providing a completely orthogonal

separation mechanism to typical chromatographic separations, providing a method for two-dimensional analysis. In addition, all of the typical advances made with MS detection (mass identification, compound fragmentation) can be combined with a specific separation regime for high resolution of the specific ions created via the ionization method.

While a large portion of the literature has focused on mass spectrometry detection for LC separations due to the structural identification of compounds, other detection regimes are also frequently used. The most frequently used LC detection method is standard UV-Visible absorbance, and this method is reasonable for compounds with strong chromophores. Estrogens and nonylphenol ethoxylates were extracted from a wastewater pilot plant effluent using SPE, and then cleaned and transferred into methanol or dichloromethane and detected using UV absorbance (Esperanza et al*.,* 2004). Nonylphenol ethoxylates were detected at around 250-500ng L^{-1} using a standard diode array detector at 300nm (Lee et al*.,* 1997). This detection limit is significantly higher than for mass spectrometry but is still reasonable for the matrix, which had concentrations of these surfactants in the 10-1000µg L^{-1} range.

When the compound of interest is known, another powerful method of detection is via combination with chemiluminescence. Serrano and Silva (2006) used a known chemiluminescent reaction -- luminol and peroxide in the presence of copper (II). Aminoglycosides inhibit the reaction by complexing strongly with

copper, thus causing detection in a continuous flow chemiluminescence reactor. Limits of Detection (LOD) for this method were reported in the μg L^{-1} range and it requires very little sample preparation. High detector selectivity was due to the interaction strength between the metal and the analyte.

2.3.4 Immunoassays and Yeast Estrogen Receptor Transcription Screens

A final method for the screening of analytes with biological activity is through selective colorimetric immunoassays. Immunoassays have significant advantages in the testing of biologically active compounds such as very high specificity for a given analyte and the ability to isolate low concentrations of analyte in messy sample matrices, as the selection for target analytes is via immunological interactions with antibodies or antigens. Enzyme-linked immunosorbent assays (ELISA) use antibodies structured for selectivity to a given hapten and then stacked antibodies to produce a detection response, frequently the activity of a peroxidase with a reporter compound. ELISAs for nonylphenol and nonylphenol ethoxylates have been produced with low cross reactivity and high specificity in complex matrices (Mart'ianov et al., 2005). Farré et al. (2006) used an ELISA designed for linear alkyl benzenesulfonates and were able to extract several variants of the compound class from wastewater influent using a simple dilution step instead of sample extraction and concentration. Castillo et al. (2000) compared an ELISA method to a SPE-LC-MS

and LC-fluorescence method for the identification of surfactants in wastewaters, with reproducible results for both methods.

Gibson et al. (2005) used fish bile from fish exposed to wastewater effluent as a screening sample for estrogens, and one method used was the yeast estrogen receptor transcription bioassay (YES). In this assay, a human estrogen receptor gene is inserted onto a plasmid containing a estrogen-reporter element linked to a *Lac*-Z operon, and the plasmid is then transformed into yeast. If an estrogen analog is present, the plasmid activates and produces β-galactosidase, which can convert a reporter compound, chlorophenol red-β-galactopyranoside, into chlorophenol red, which can be measured by absorbance to predict estrogenic concentration. This study was able to then validate the results of the YES assay by GC-MS analysis, confirming the presence of nonylphenolic contaminants in fish bile.

2.4 Measuring Wastewater Removal of Polar Contaminants

If the main transport mechanism of polar contaminants into surface waters is through wastewater treatment plants, then monitoring of the breakdown of polar contaminants in water through typical treatment processes is the best way to reduce environmental risk. In addition, it is important to ensure the removal of contaminants in raw water occurs during the treatment of drinking water to prevent risk to human populations. Several common polar contaminants (e.g.,

benzotriazole, nonylphenol and derivatives) can survive conventional wastewater treatment at biologically relevant concentrations, showing how important new removal strategies are for preventing further contamination (Voutsa et al., 2006).

Conn et al. (2006) surveyed the efficacy of treatment of organic contaminants at thirty decentralized onsite wastewater treatment plants in Jefferson and Summit County, CO for the post treatment detection of a series of surfactants and PPCPs. Decentralized wastewater treatment is often less thorough than centralized municipal treatment. Of the treatment methods surveyed, none successfully removed all compounds, and in many cases the effluent resulted in concentrations of biological relevance; nonylphenol was found at median concentrations of 19μg L^{-1} in 34 samples of nonresidential septic tank effluents. This type of decentralized treatment is uncommon in highly centralized urban areas but used widely enough to be of significant concern as a source of organic wastewater contaminants.

Teske and Arnold (2008) examined the removal of endocrine disruptors in wastewater plants that used a much more typical treatment mechanism for centralized WWTPs -- activated sludge. Activated sludge treatment, which uses a biological floc of microorganisms in oxygenated wastewater to consume and degrade biologically relevant compounds, is typical of municipal scale WWTPs. However, as the authors point out, activated sludge methods were designed for clarification and removal of biological nutrients observed through reductions in

suspended solids and biological oxygen demand, not the removal of trace organics. The authors found estrogenic compounds were removed at rates as low as 0% to as high as 100%, with the median being close to 60%. Methods with separate nitrification/denitrification steps were found to be more effective at removal than traditional one step activated sludge treatment. While many compounds present in the influent of the plant were identified, in some studies cited in Teske et al., the overall effluent estrogenic activity was actually higher than the influent, indicating that the treatment process may in fact concentrate some analytes or create degradation products with stronger endocrine disrupting effects than the starting material through biological transformation.

Due to the high likelihood of alkylphenols and their ethoxylates to partition to sludge or suspended solids, these contaminants are of particular concern to survive wastewater treatment. Loyo-Rosales et al. (2007) traced the concentrations of 5 common alkylphenol ethoxylates through three different activated sludge WWTPs before and after treatment and found that all compounds had reduction on the order of 95%; however, carboxylates of alkylphenols were formed in the wastewater plants. A more careful examination of the mass balance of total alkylphenols indicate 20-40% of the compound was released in effluent untreated or as a degradation product; 19-64% of the compounds were found to actually partition to the sludge and suspended solids, and the remainder degraded beyond detectability. This study indicated that a

non-trivial portion of alkylphenols survived activated sludge treatment. As a result, alkylphenols maintain relevant concentrations in effluent, and can provide a risk if sludge is allowed to contact surface water or soils. Andreu et al. (2007) were able to quantify alkylphenols from 0.02 to 5mg Kg^{-1} in soils exposed to post reactor sludge, indicating that sludge partitioning is not truly removal.

A newer WWTP treatment method called the membrane bioreactor (MBR) uses microorganisms embedded on a support matrix or in a flow through membrane instead of an activated sludge floc and has been suggested to be more efficient in the breakdown of organic contaminants. A parallel pilot-scale MBR running alongside of an activated sludge treatment plant was used by González et al. (2007) to test the efficacy of both methods in alkylphenol removal. The large contact surface between the membrane bound bacteria and the wastewater explain the higher removal efficiency (94% removal of all compounds, versus 54% for the activated sludge), as well having greater consistency in the removal of organics regardless of structure. MBR treatment has the promise of removing many more contaminants of interest during normal biological treatment; however, tertiary treatments may further reduce specific contaminants below biologically relevant concentrations.

The most common tertiary treatment after biological wastewater treatment is with chlorine either as a gas, liquid or in the form of sodium hypochlorite. Chlorine treatment is largely used to sterilize biological effluent, as well as to

remove minor residual contaminants; however, other tertiary treatments may be able to further reduce organic trace contaminants not removed during the biological treatment stage. Both ozonation and UV exposure have been used as sterilization methods for wastewater effluents, and many compounds may be photodegradable or oxidized into a more benign form with ozone. Sulfamethoxazole has been observed to rapidly breakdown in the presence of ozone, UV exposure at 254nm and a titania catalyst (Béltran et al., 2008; Dantas et al., 2008). This antibiotic may not fully break down in biological treatment, thus ozonation adds a tertiary treatment process, while at the same time disinfecting effluent without the use of chlorine.

2.5 Summary

A class of polar organic contaminants has been discovered in waste, surface, and drinking waters. These contaminants enter surface waters largely through treated wastewater effluents and are composed of pharmaceuticals, personal care products, detergents, industrial surfactants, and high production volume organic solvents. Due to their potential toxicity and endocrine disruption at extremely low concentrations, as well as their ubiquity in world water systems, the removal of polar organics has become a focus of environmental protection policy and research. Both gas and liquid chromatographic methods have been developed for analysis of this class of structures, frequently with mass

spectrometry as a detection method for identification of compounds and their degradation products. Immunoassays have also been utilized in the identification of relevant compounds, to predict the endocrine disrupting function of putative contaminants and degradants. Many studies have been performed on the actual treatment of organic contaminants in wastewater treatment plants, which indicate both the current limitations of typical treatment regimes and the potential for more efficient and environmentally friendly removal of polar contaminants. Of particular promise to the removal of microcontaminants in wastewater are biological treatment processes that favor breakdown of polar organics (membrane bioreactors), as well as the addition of tertiary treatment processes like ozonation and UV treatment.

Chapter 3: Review of Methods Literature and Theory

The work in this dissertation seeks to build upon current techniques for detection and prevention of emerging polar contaminants and provide a simple and efficient method for analysis without advanced analytical techniques such as separation techniques hyphenated to tandem mass spectrometry. The first major analytical process employed to characterize complex environmental samples is chromatographic separations of analytes. Therefore, basic chromatography theory is described in this chapter, along with the analytical measurements of chromatography.

Next, the theories of chromatographic separation mechanisms are examined in detail, including the classical sorption mechanism and modern molecular modeling descriptions. Several techniques are used for the prediction of retention in chromatography: linear solvation energy relationships (LSERs), van't Hoff relationships of enthalpies of transfer between phases, and configurational-bias Monte Carlo (CBMC) simulations of phase interactions.

The physical attributes of subcritical water are uniquely suited as a chromatographic mobile phase, especially for the separation of polar compounds in aqueous media. High temperature water chromatography instrumentation differs from traditional LC, but has added benefits in terms of speed and solvent usage.

Finally, in this chapter, the use of subcritical water as a beneficially reactive medium for oxidation is explored. Subcritical water's increased dissociation and increased solvation strength make for an advantageous and green reaction solvent for environmental treatment.

3.1 Basic Liquid Chromatography Theory

Chromatography is the separation of a mixture of compounds due to differences in residence times between some stationary phase and a mobile phase (Skoog et al., 1998; Skoog et al., 2004 and Harris, 2007). The more favorable a compound is to reside in the mobile phase, the faster it elutes, and, given a sufficiently large difference in elution time, compounds can be resolved from each other (Skoog et al., 1998). Liquid chromatography works by sorting compounds by their partitioning coefficient *K* from a stationary phase to a liquid mobile phase. This partitioning behavior is controlled by a difference in the polarity of the phases. In normal phase chromatography, analytes transfer between a non-polar mobile phase and polar stationary phase, so the least polar

analytes elute first, and the most polar analytes elute last. Current technology now favors reversed-phase liquid chromatography (RPLC), with a polar mobile phase and non-polar stationary phase, due to a significantly greater flexibility with the stationary phase and mobile phase makeup.

Chromatographic separations are controlled by differences in partition coefficients between analytes. Partition coefficients are defined by the following equation, where c_S is the molar concentration of an analyte on the stationary phase, and c_M is the molar concentration of the analyte in the mobile phase.

$$K = c_S / c_M \qquad [3.1]$$

The greater the difference in partition coefficients, the greater the resolution in a chromatographic separation. The selectivity of a chromatographic separation for one compound *A* over a different compound *B* is given by equation 3.2.

$$\alpha = K_B / K_A \qquad [3.2]$$

The time a compound takes to elute from a given column is called the retention time, t_R, and is defined by equation 3.3, where *L* is the column length and *v* is the linear rate of migration.

$$t_R = L/v \quad [3.3]$$

Most compounds will have some retention on the stationary phase, so the retention time of a compound should be larger than the dead time t_M, which is the time for the mobile phase to move through the column. This value is normally the column length divided by mobile phase flow rate under the assumption that the mobile phase has no net adherence to the stationary phase. As column dead times are specific to a given set of parameters and a specific column, retention factors are values that are comparable between systems.

$$k'_A = (t_R - t_M) / t_M \quad [3.4]$$

Finally, in order to measure how well a given separation resolved two analytes, the definition of compound resolution is given in equation 3.5, where W is the width of two respective chromatographic peaks *A* and *B*.

$$R_S = 2[(t_R)_B - (t_R)_A]/(W_A + W_B) \quad [3.5]$$

The resolution of two peaks is considered to be complete if $R_S = 1.5$ or greater. The reason for broader peaks is covered in the discussion of chromatographic efficiency.

3.1.1 Plate Theory and Chromatographic Efficiency

The classical description of how efficient a chromatographic separation occurs is based upon the theoretical plate height *H*. A theoretical plate is equivalent to a cross section of column with a finite likelihood of causing partitioning to the stationary phase. The number of theoretical plates (*N*) in a column is given by equation 3.6 where *H* is the plate height and *L* is the column length.

$$N = L/H \qquad [3.6]$$

The greater the number of theoretical plates per given column length, the lower the peak height, and the more efficient the column.

Given a number of theoretical plates, a collection of analyte molecules moving through a column will have a statistical likelihood of transferring to each plate, giving a chromatographic peak a Gaussian shape, with the most likely transfer rate found at the center of the peak, and the peak width relative to the standard deviation of this transfer. Partitioning is therefore based off of a normal distribution of events, creating a Gaussian (normal) curve. This is demonstrated in Figure 3.1, which shows the resolution of two peaks at low and high plate heights.

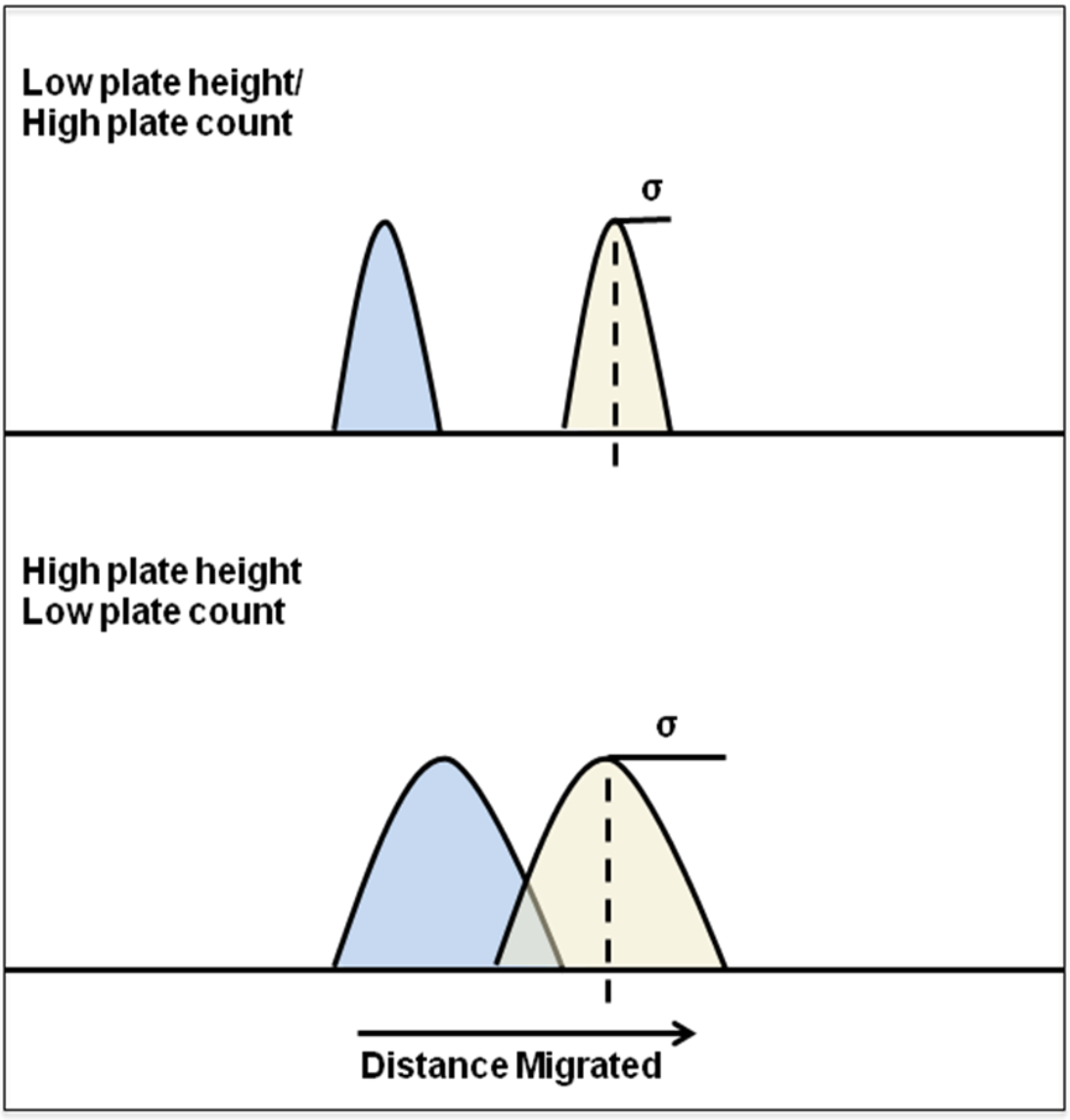

Figure 3.1 Resolution of two analytes in an efficient and inefficient column. The greater the number of plates, the narrower the analyte peaks, and the greater the resolution.

If the theoretical plate height is low (i.e., the number of opportunities for mass to transfer between phases is high) the standard deviation of transfer occurrences is small, and as such, the peak is narrower. Likewise, if the plate height is high or plate count is low, then the standard deviation of the collection of molecules will be larger, as a greater variance is possible in the number of mass transfer interactions, and as such, the peak will be wider. Plate counts can most easily be calculated from the retention times and peak widths of a given chromatographic peak:

$$N = 16\ (t_R / W)^2 \qquad [3.7]$$

$$H = LW^2 / 16t_R^2 \qquad [3.8]$$

If the variance of a peak (the square of the standard deviation of the Gaussian peak) is known, another convenient description of column height is given by:

$$H = \sigma^2 / L \qquad [3.9]$$

3.1.2 Kinetic Rate Theory of Chromatographic Efficiency

While the theoretical plate methods is useful in the description of idealized separations, the actual mechanism of separation is far more complex, and has

contributions from mass transfer, diffusion, and the fact that many paths exist for a mobile phase to flow through a column. The simplistic theoretical plate description cannot account for all of these factors, and as such tends to ignore significant effects on column efficiency from mobile phase makeup, flow rates and temperature. The kinetic rate theory of chromatographic separation, on the other hand, seeks to describe separation efficiency in terms of physical constants, resulting in the van Deemter equation of plate height, given in equation 3.10, where h is the reduced plate height (cm or mm), A is the expression for multiple path lengths in a given column, B is the longitudinal diffusion, C_S and C_M the mass transfer coefficients for the stationary and mobile phase, respectively, and u the linear flow rate of the mobile phase.

$$h = A + B / u + (C_S + C_M)\, u \qquad [3.10]$$

This equation is important because all of the terms can be derived from physical constants of the column or of the separation parameters, and as such, can predict the efficiency of a column at any given flow rate. This equation is more fully described in this form given in equation 3.11, where λ and γ depend on the column packing, D_S and D_M are the diffusion coefficients for the stationary and mobile phases, d_F is the thickness of the liquid surface on the stationary phase and d_P is the stationary phase particle diameter.

$$h = 2\lambda d_P + 2\gamma D_M / u + [\, f_S(k')\, d_F^2\, D_S^{-1} + f_M(k')\, d_P^2\, D_M^{-1}] \, u \qquad [3.11]$$

While many of these constants are specific to a given column design, several components have specific meaning in terms of the makeup and flow rates of the mobile phase. Yang (2006) extended this expression to explicitly include factors such as solvent viscosity and temperature, both of which affect the diffusion coefficients.

$$h = A + 2\gamma k_B T / 3\pi\eta d u + [C_S + C_M]\, u / T \qquad [3.12]$$

Solvent viscosity (η) is also inversely proportional to temperature, and water's viscosity can be approximated in the subcritical range by equation 3.13, where the dynamic viscosity η is given in Pa*s:

$$\eta = 27.45 / (T - 273) \qquad [3.13]$$

As such, the effective van Deemter equation with regards to temperature is:

$$H = A + b(T^2 - 273T) / u + c \times u / T \qquad [3.14]$$

Column behavior and efficiency are therefore fundamentally correlated to temperature and flow effects of the mobile phase, and as such, the mechanism of transfer can be controlled by temperature as well as by solvent makeup. An example of column efficiency effects as a function of temperature is presented in Figure 3.2. At low linear flow rates, the longitudinal diffusion coefficient dominates, and a greater temperature causes an increase in plate height. However, at optimal flow rates where mass transfer dominates, the plate height is inversely proportional to temperature, and the greater the temperature, the better the column efficiency.

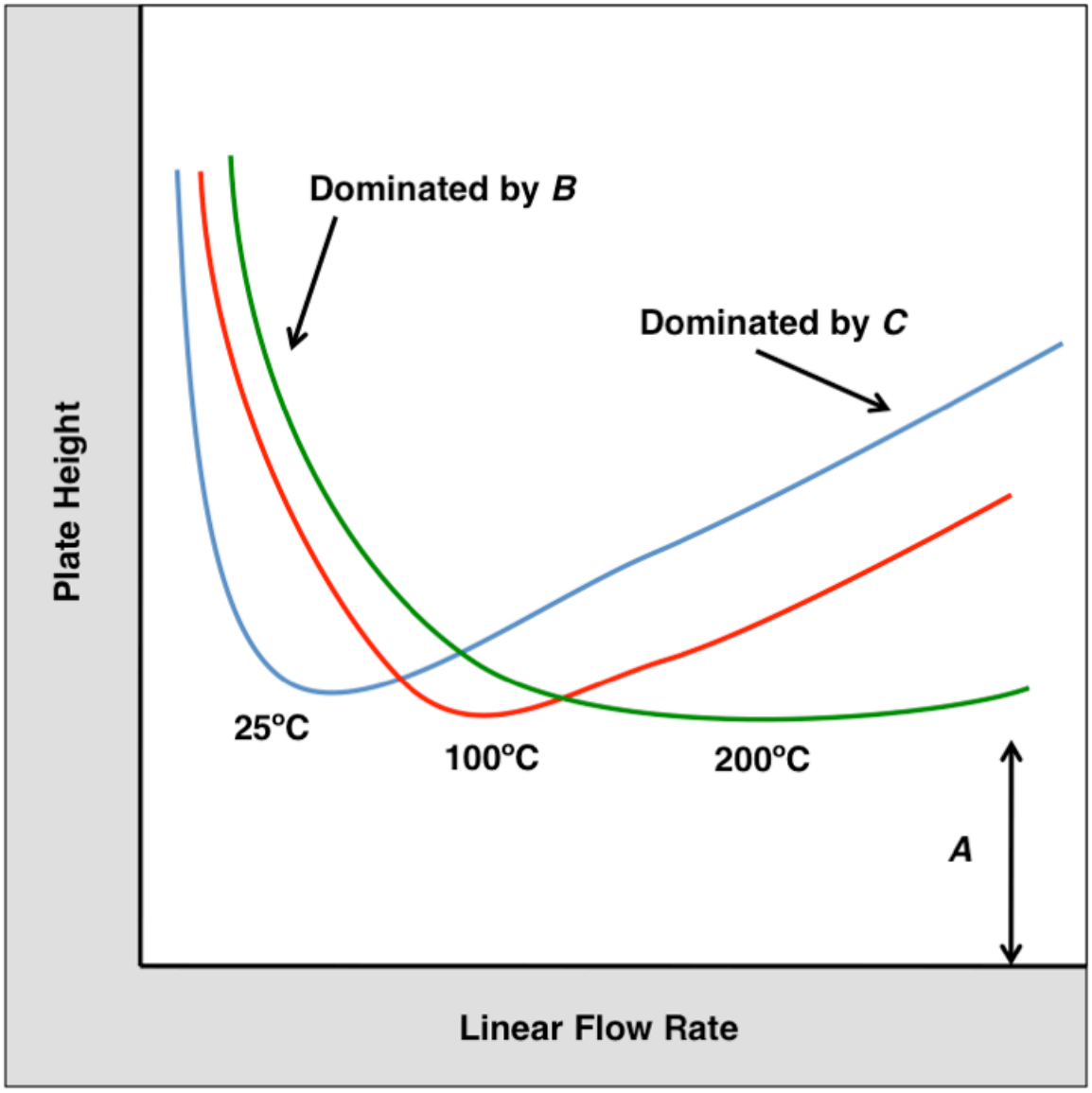

Figure 3.2 van Deemter plots as a function of temperature for a liquid chromatographic system. In low flow rates, the longitudinal diffusion component dominates plate height, whereas mass transfer rates dominate at higher flow rates. *A* is independent of flow rate, and thus does not change with temperature, mobile phase flow or mobile phase makeup. Adapted from Yang, 2006.

3.2 Advanced Theories of Solute Retention in Liquid Chromatography

While the chromatographic efficiency of a separation is well described by the kinetic rate theory, this theory does not explain why a given analyte might have a greater retention than any other. Facile descriptions of the partitioning mechanism exist for all chromatographic methods. Gas chromatographic separations have differences due to analyte volatility and liquid chromatography separations occur due to differences in partitioning between a polar and non-polar phase. In supercritical fluid chromatography, both of these factors occur to some extent. Mechanistically, the actual processes involved with liquid chromatography are considerably more complex than those seen in gas chromatography, making the prediction of analyte retention much more difficult. Gas chromatographic mobile phases behave like non-interacting ideal gases, and, therefore, all selectivity in a GC separation is due to analyte interactions with the stationary phase. In LC, solubility and solvation energetics can cause partitioning mechanisms driven by exclusion from the mobile phase or attraction to the mobile phase, stationary phase, or even the residual support structures (the silica of the stationary phase particles) beneath the stationary phase modifiers (Carr et al*.,* 1993)

In gas chromatography, the retention of an analyte can be predicted in a GC method by correlation to Kováts retention indices of *n*-alkanes, and the behavior of a given stationary phase can be described by the retention of

standard set of probe molecules (Poole, 2003; and Barry, 2004). No true correlation to the Kováts retention indices of analytes or MacReynolds constants for descriptions of stationary phases exist for liquid chromatography due to the more complex partitioning mechanism. As such, several competing methods have been described as possible methods for the prediction of analyte behavior in a generalized manner for liquid chromatography, including the description of the enthalpy of transfer between phases, the prediction of phase interactions through training algorithms, and the computational prediction of phase behavior at the molecular level.

3.2.1 The Solvophobic Theory of Reversed-Phase Retention

The solvophobic (sometimes described also as lipophilic) mechanism for reversed-phase retention assumes that analytes are retained in RPLC largely through partitioning between the organic stationary phase and the hydroorganic mobile phase. A partitioning mechanism implies an analyte forces the formation of a solvent cavity in the new phase, a transfer event occurs moving the analyte to the new phase, and then the solvent cavity closes in the old phase (Vailaya and Horváth, 1998). In contrast, in an adsorption process an analyte interacts with a “solid” phase, displacing solvent coverage of the stationary phase, which is favorable due to hydrophobic exclusion. If the net free energy of this transfer is negative, then the transfer is favored to occur, the free energy is equivalent to the

sum of all interactions that occur in this transition where ΔG_{cavity} is the difference in free energy due to the formation of a new cavity and collapse of an old cavity in the previous phase, and are calculated from interactions of hydrogen bonding and Van der Waals forces in each phase.

$$\Delta G_{Transfer} = \Delta G_{cavity} + \Delta G_{intermolecular} + \Delta G_{solvent} - RT \ln (RT/V_s) \qquad [3.15]$$

$\Delta G_{intermolecular}$ includes all of the changes in interactions between an analyte and the surrounding phase, including Van der Waals, dispersion effects, and coulombic forces. Solvent free energy components ($\Delta G_{solvent}$) include effects of solvent mediation on coulombic interactions (especially relevant to exposed silanols in reversed phase stationary phases) and interactions and repulsions between phases. In reality the polar and non-polar phases are not mutually exclusive, and are saturated with solvent, making pure transitions between phases difficult to describe. The final term in this expression is the change in free volume as a function of transition, with V_s the molar volume of the solvent at 0.1MPa. Cavity formation terms are likely to dominate this expression.

If an analyte is reasonably non-polar, a solvophobic mechanism can describe reversed-phase retention (Vailaya and Horváth, 1997). In this arrangement, non-polar analytes are preferentially excluded from the mobile phase and partitioned into the stationary phase. Selectivity comes from the

relative free energy of transfer for analytes, with less polar analytes forced out of the mobile phase with more energetic favorability than more polar analytes. Implicit in this description is the fact that little interaction is occurring between analytes and stationary phase modifiers. Thus, the driving force behind retention is the aqueous phase makeup, not the modification of the stationary phase surface. This framework becomes suspect if the analyte is polar; a polar functional group should at least partially reduce the energetic favorability of exclusion, as hydrogen bonds between analyte and mobile phase should allow for solubility and prevent favorable mass transfer. In addition, polar compounds should be energetically excluded from interaction with a non-polar phase, as partitioning into a non-polar phase would remove hydrogen bonding from the analyte, without compensating by creating a new hydrogen bonding network.

In a slightly different description of the solvophobic mechanism, Carr et al. (1993) describe the energetics of transfer between a mobile phase and stationary non-polar phase with an ideal gas phase intermediate. The free energy of transfer of an analyte between a polar liquid phase and an ideal gas phase, and also between a stationary phase and gas phase, completes a thermodynamic cycle to model the free energy of mobile to stationary phase transfer.

$$\Delta G_{transfer} = \Delta G_{mobile/gas} - \Delta G_{gas/stationary} \quad [3.16]$$

By measuring the individual free energies in this arrangement, it was determined that methylene solvation in organic solvents from a gas phase is favorable, but methylene solvation is always unfavorable into water. In organic solvents, methylene solvation has favorable dispersion interactions with the solvent (induced dipole-dipole) that are greater than the unfavorable solute cavity formation. In water the dispersion forces are less than the energy of cavity formation and as such are unfavorable. In mixed mobile phases, mobile phase modifiers cause a solvophilic interaction between analyte and mobile phase, balancing methylene exclusion.

When the other half of equation 3.16 is examined, it becomes clear that stationary phase interactions must at least be on the same scale as those in the mobile phase. In fact, Carr et al. (1993) suggest methylene selectivity is largely a function of stationary phase makeup, with a relatively small endergonic term of the bulk organic phase creating a cavity versus a large exergonic term for solute-solvent interactions. Because this model implies an attractive force between non-polar analytes and the non-polar phase, this is sometimes referred to the lipophilic mechanism instead of the solvophobic mechanism.

The authors admit this is hard to reconcile with polar compounds, which should have large endergonic terms for forcing a polar analyte into a non-polar phase and breaking a hydrogen bonding network. Strongly polar analytes should effectively behave in the exact opposite manner to the non-polar analytes

described, with solvophilic interactions with water, and solvophobic interactions with a stationary phase. Rafferty et al. (2007) offer one possible explanation for the retention of polar compounds in reversed phase mechanisms, suggesting that the problem with the solvophobicity model is the less rigorous modeling of the non-polar phase.

3.2.2 Reversed-Phase Retention with Realistic Stationary Phases

As is implicit in Figure 3.3, as well as in the previous section, most classical models of reversed-phase retention imply a uniform non-polar liquid as the stationary phase, similar to the non-polar phase observed in liquid-liquid partition chromatography. In actual reversed-phases, this is not realistic, as the non-polar phase is immobilized on a normal-phase support material at a given coverage concentration. Coverage levels of stationary phase modifiers are on the order of 3μmol m^{-2}, which leaves a significant amount of the polar support material exposed (Rafferty et al., 2008).

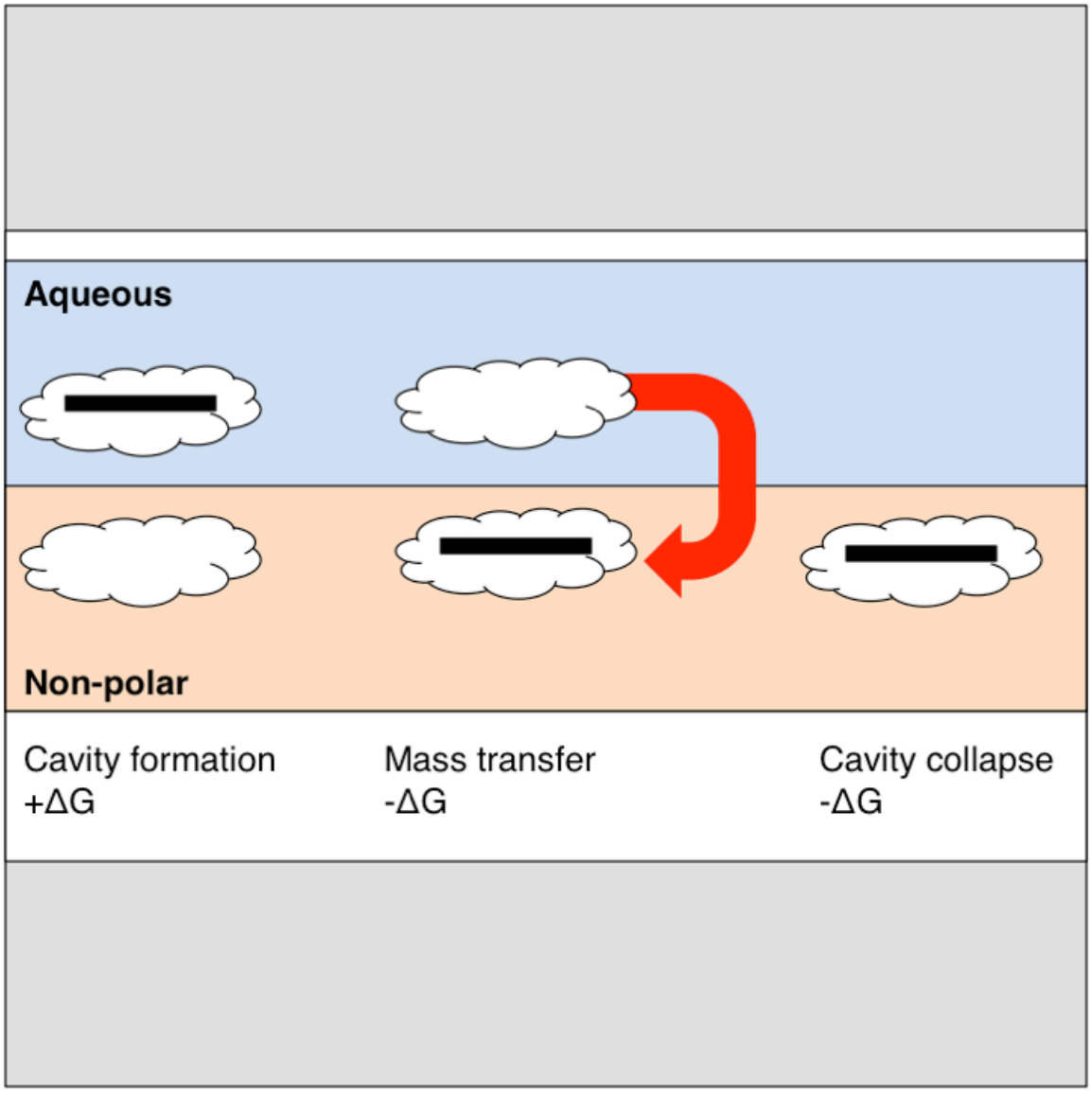

Figure 3.3 Thermodynamic cycle for mass transfer in the solvophobic mechanism. A non-polar analyte with an unfavorable hydrogen bonding arrangement in the aqueous phase is transferred completely to the non-polar phase in a net exergonic process.

Exposed surface silanols (as most common stationary phases use silica as a support material) have been demonstrated to have specific interactions with polar analyte probes, which is described as a silanophilic interaction (Berek and Tarbajovská, 2002). In addition, despite significant efforts at deactivating surface silanols such as trimethylsilanation, exposed silanols remain in most traditional stationary phases (Engelhardt et al., 1991). IR and NMR studies of passivated stationary phases suggest that even after phase modification and passivation, around 40% of the silanol groups are still exposed (Köhler et al., 1986). This should not be surprising, as the mineral surface of silica, even though relatively amorphous, is equivalent to a <111> face of β-cristobalite silica crystals (Zhuravlev et al., 2001). Even the maximal case of ~5μmol m^{-2}, demonstrated in Figure 3.4, demonstrates accessible silanols.

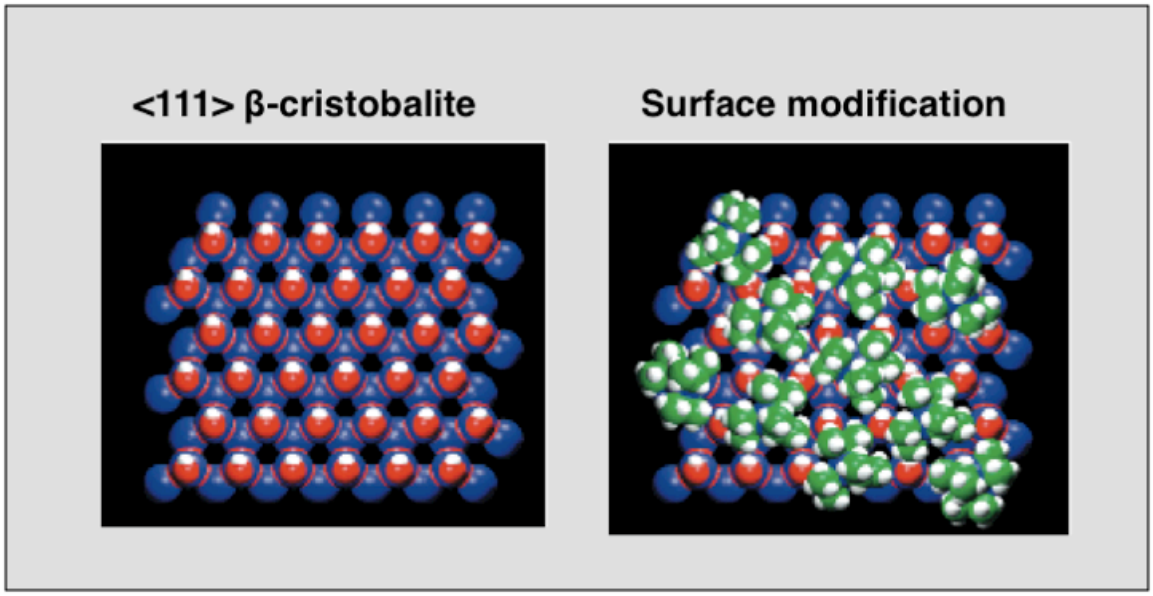

Figure 3.4 Surface silanols as modeled by the <111> surface of crystalline silica. Residual silanol oxygens are shown in red, with hydrogens in white. Surface modification with triisopropyl ligands are shown, with carbons in green. From Zhuravlev et al. (2001).

With the exposed silanols, hydration of the silica surface is energetically favorable, although bulky side groups may make this impossible. Cox (1993) suggests that even after heat treatment to reduce silanol concentrations, in liquid chromatography, at least a slow rehydration of residual silanols should be expected. Thus, the description of the stationary phase as uniform and purely non-polar is likely unrealistic. This has been demonstrated in Monte Carlo simulations by Rafferty et al. (2008), in which chains of hydrogen bonded solvent exist between the bulk phase and the residual silanols (Figure 3.5). In addition, while a nonpolar analyte is shown to behave according to the solvophobic partitioning model, a polar analyte (1-propanol) is shown to directly interact with the surface silanols and is not fully embedded in the non-polar phase. Thus, the actual mechanism of reversed-phase retention is much more complex with polar analytes than for non-polar compounds and should be expected to include both adsorption to the silanol surface and partitioning contributions, along with orientation biasing to prevent endergonic (energetically unfavorable) hydrogen bond disruption of polar functional groups.

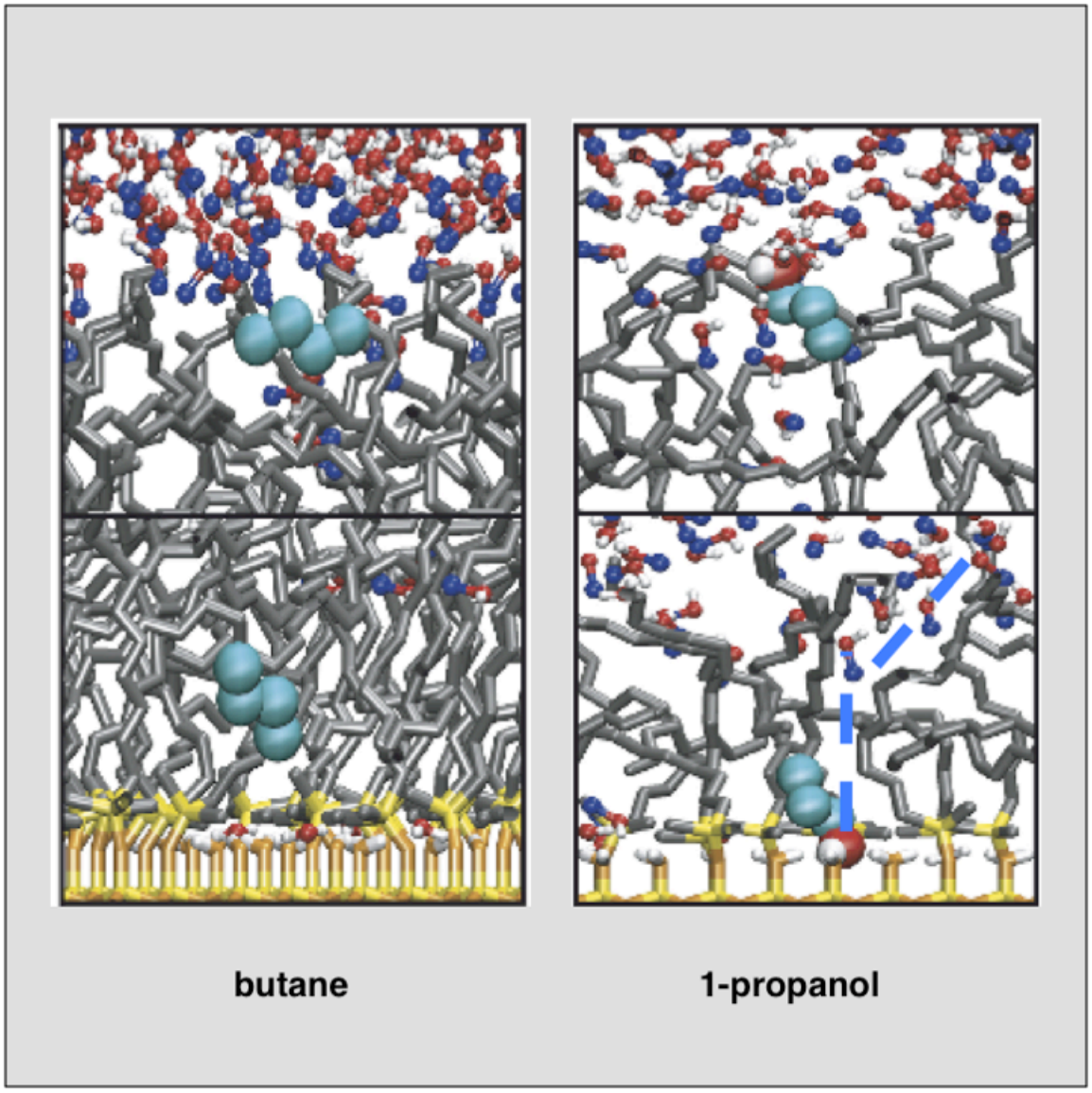

Figure 3.5 Simulations of the retention mechanisms of butane and 1-propanol. While the density of the stationary phase is higher, the butane is shown to embed deeply in the octadecanes. 1-propanol is shown in two configurations: with the hydroxyl group excluded from the octadecanes (upper pane), and adsorbed to the silanol (lower pane). Note the hydrogen bonding chain of water and methanol molecules linking the 1-propanol to the bulk mobile phase (highlighted with the blue dashed line) and the sorbed solvent molecules at the silica surface. From Rafferty et al. (2008, pp 20-27).

3.2.3 Mechanistic Views of Mobile Phase Modification

Typical reversed-phase retention assumes the modification of the mobile phase is uniform and occurs through the decrease in solvent polarity (usually measured via dielectric constants of the bulk material). This causes the solvophobic interaction between non-polar groups and water to decrease and results in a mass transfer back to the mobile phase. However, a uniform mobile phase is somewhat unrealistic, even with modifiers like acetonitrile and methanol that are fully miscible with water, as these modifiers are much more amenable to interactions with a fully, non-polar stationary phase than water (Wick et al., 2004). This is observed in simulations, in which the local concentration of modifier increased at the mobile phase/stationary phase interface (Zhang et al*.,* 2006). As this effect is present in all mixed mobile phases, pure mobile phases and temperature controlled elution effects would create different mobile phase environments, which would change mass transfer effects (Zhang et al*.,* 2005).

Temperature and mobile phase mixing mechanisms have both been used as dielectric constant modifiers; but using these two mechanisms may result in subtle changes in how mass transfer occurs. Most of the early literature on temperature modification of mobile phases sought to directly compare the two processes as equivalent, with Chen and Horváth (1997) developing the correlation that a temperature increase of 5ºC is equivalent to the increase in acetonitrile concentration of 1%. Houdiere et al. (1997) used temperature

gradients in combination with solvent mixing gradients for accelerated separations, which significantly changed the selectivity of late eluting analytes.

3.2.4 Predicting Reversed-Phase Selectivity and Retention

While mechanistically, analyte transfer is complex and involves both adsorption and partition effects in an orientationally specific manner to a given analyte, many simplified descriptions of the process have been used to estimate analyte retention based on macroscopic descriptors of analytes and chromatographic systems. The simplest predictive model of retention can correlate linear alkanes or linearly related homologues (i.e., alkylbenzenes), Where A is the absolute intercept of the homologue series, B is correlated to the free energy of transfer ($\Delta G_{CH2} = -2.3RTB$) and n_{CH2} is the number of methylenes beyond the first homologue (Tchapla et al., 1984):

$$log\ k' = A + Bn_{CH2} \qquad [3.17]$$

This process is similar to the comparison to Kováts retention indices used for the description of GC retention. Clearly, this is of limited transferability between analytes, and is not useful for polar compounds. In the thermodynamic cycle described by Carr et al. (1993) a direct measure of the free energy of transfer is derived from the retention factor and the volume ratio of the two phases:

$$\Delta G_{Transfer} = -RT \ln k' + RT \ln \Phi \quad [3.18]$$

This is often rearranged to the form below where the natural logarithm of retention factor *k'* is plotted against 1/*T* in Kelvin:

$$\ln k' = -\Delta H^{o}/RT + \Delta S^{o}/R + \ln \Phi \quad [3.19]$$

The slope of this line is the enthalpy of transfer ΔH^{o}, and the intercept is a combination of the entropy of transfer, ΔS^{o} and the natural logarithm of the phase volume ϕ. The rearranged van't Hoff relationship implies that phase ratio is constant and independent of column temperature and is easier to calculate experimentally than 3.18 (Cole and Dorsey, 1992). Constant mobile phase makeup can be correlated to the enthalpy of transfer by this relation, and the retention behavior of an analyte across stationary phases or of multiple analytes on the same stationary phase can be described in this manner (Cole et al., 1992). By subtracting the enthalpy value of one analyte from another, the result gives the energetic selectivity in a given chromatographic environment.

The phase ratio is likely to change as a function of temperature, as it is explicitly related to the density of both phases. Therefore, non-linear van't Hoff plots may be observed when retention factor is correlated to temperature

(Chester and Coym, 2003). The authors in this study demonstrated that differential van't Hoff plots between related analytes gave temperature independent enthalpies without a phase contribution. These authors extended the study of mobile phase modification by temperature from just solvent makeup to also include temperature, up to the subcritical range. Guillarme et al. (2004) note that curvilinear van't Hoff plots should be expected in the subcritical range, which correlates to changes in the heat capacity phases, giving the relationship:

$$\ln k' = b_0 + b_1 T^{-1} + b_2 T^{-2} + \ln \phi \qquad [3.20]$$

Given the selectivity, temperature effects on retention can be more formally correlated to the effect of mobile phase modifier, allowing for extrapolation to the temperature independent selectivity of a reversed-phase without any mobile phase modifier (Coym and Dorsey, 2004). Extrapolations to pure water mobile phases at room temperature from a series of temperature regressions of mixed mobile phases have not been demonstrated to effectively model analyte retention between pure water and a stationary phase; polar molecules are demonstrably less well predicted by this type of analysis. This may be due to the poor transferability between chemical species. While the free energy of transfer of an analyte is described, no mechanistic concerns are directly probed, and only the relative favorability can be examined.

A second approach to the description of retention of analytes from easily accessible chromatographic parameters uses linear solvation energy relationships (LSERs) of a training set of solute parameters to predict chromatographic solvent behaviors. The modern solvation parameter model is based upon the Hildebrand regular solution model (Hildebrand et al., 1962) and the solvent selectivity parameters of Snyder (1974), and uses a multiple linear regression process to describe chromatographic processes in terms of a series of parameters. The modern LSER correlation, provided in equation 3.21, uses solute parameters: E, the excess polarizability relative to a comparable *n*-alkane (excess molar refraction); S, the combined polarizability and dipolarity; A, the hydrogen bonding acidity or donation; B, the hydrogen bonding acceptance or basicity and V, the molecular volume (McGowan's characteristic volume/100) (Vitha and Carr, 2006):

$$log\ k' = c + eE + sS + aA + bB + vV \qquad [3.21]$$

All of these parameters are solute specific, and several libraries are available for a great number of relevant probe solutes for liquid, gas and supercritical fluid chromatographic systems (Abraham et al., 2004; Blackwell and Stringham, 1997; Torres-Lapasió et al., 2004; Quina et al., 2005). From multiple linear regression of solute parameters and retention factors, solute descriptors (lower case in

equation 3.21) can be calculated. The descriptor *e* measures the favorability of solvation, *s* measures solvent dipolarity and polarizability, *a* measures solvent hydrogen bond acceptance, *b* measures solvent hydrogen bond donation and *v* measures solvent hydrophobicity. It should be noted that the solvent descriptors are complimentary to the solute parameters, and, in a two-phase system, the sign of the solvent descriptors indicates which phase is affected. Since retention factor is the regressed function, positive descriptor signs indicate a favorable interaction with the stationary phase, and negative signs indicate favorable interactions with the mobile phase.

Using LSER regressions, the interactions of analytes can be described in greater detail than with previous theoretical models The five relatively orthogonal parameters in this model can describe a wider number of solute-solvent and solvent-solvent interactions, including polarizability and electron pair interactions not seen in any previous model, along with standard parameters like the favorability of cavity formation and solvent hydrogen bonding. The LSER system can accurately predict retention in traditional reversed-phase chromatography with solvent programming (Poole et al., 2006); elevated temperature programming with polymer type stationary phases (Pawlowski and Poole, 1999); and a combination of both techniques (Bolliet and Poole, 1998). These studies all indicate that mobile phase polarity and hydrogen bonding are balanced by

stationary phase hydrophobicity and solvation, with selectivity of a given analyte predicted by a composite effect of all five parameters.

3.3 Subcritical Water

Subcritical water is simply water at temperatures above the standard 0.1MPa boiling point, but at pressures high enough to maintain a liquid phase. This range runs from 100-374ºC and from pressures from atmospheric to ~100MPa. In this temperature and pressure range, a number of interesting changes occur in the behavior and solvation characteristics of water. It begins to behave more like a non-polar organic solvent with weaker hydrogen bonding. The higher the temperature, the less it behaves like room temperature water. At room temperature and atmospheric pressure, the dielectric constant (more properly the relative static permittivity), ε_r, is 78.46, indicating a very high degree of polarity, as compared to n-hexane, which has a value of 1.89 at the same temperature and pressure (Lide, 2004). However, as temperature and pressure increase and water becomes a subcritical fluid, the dielectric constant rapidly decreases; at 100ºC and 0.5MPa, ε_r is 55.43; at 350ºC and 100MPa, ε_r is only 20.29, which is comparable to pure acetonitrile or methanol (Umematsu and Franck, 1980). An approximate prediction of ε_r is provided by equation 3.22 where T_0 is 298.15K, T is the actual temperature in Kelvin, ρ is the actual liquid density in Kg m^{-3} and ρ_0 is 1000 Kg m^{-3}:

$$\varepsilon_r = 1 + (7.62571 * T_0 / T) * \rho/\rho_0 \quad [3.22]$$

In subcritical water, the dissociation constant, K_W , increases as temperature increases. This is due to greater variance in localized charges and hydrogen bonding that is observed at higher temperatures, which accelerates the autoionization mechanism (Geissler et al., 2001). The effect on ion concentration is seen in Figure 3.6, which demonstrates pK_W of pure water from 0-300ºC. At elevated temperatures, water is effectively acidic, which will be discussed later in the usage of subcritical water as a reaction medium. Tabulated effects on subcritical water dielectric constant, density and pK_W are provided in Table 3.1, calculated by Wagner and Pruss (2002).

Table 3.1 Temperature effects on subcritical water.

Temperature, K	**Density g cm^{-3} at 5MPa**	**log K_W at 0.1MPa**	**Dielectric Constant, ε at 5MPa**
273	1.0023	14.946	88.05
298	0.9987	13.995	78.65
373	0.9593	12.252	55.59
423	0.9225	11.641	44.12
473	0.8709	11.310	34.90
523	0.8049	11.205	27.15

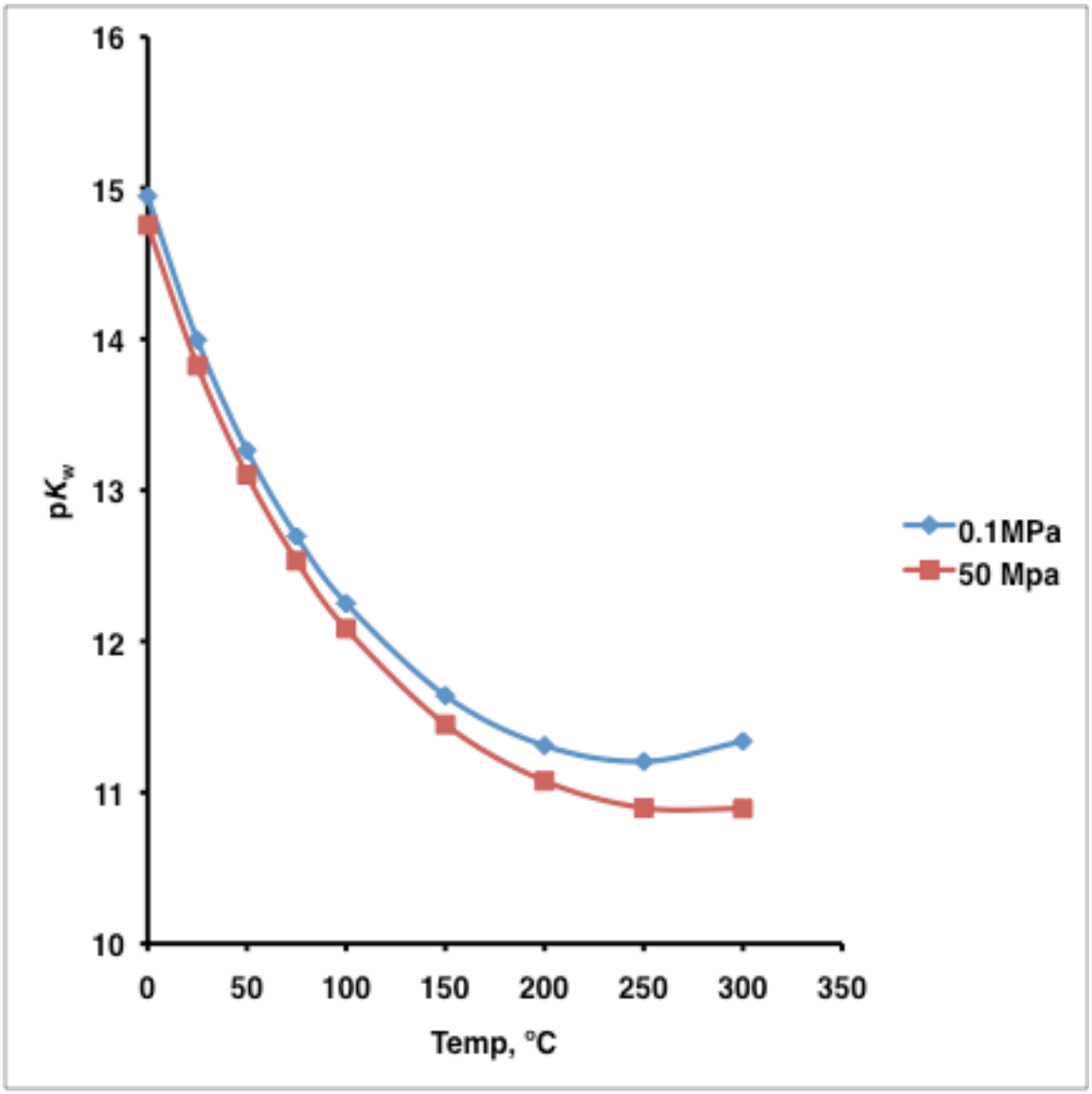

Figure 3.6 pK_W of pure water as a function of temperature, at 0.1MPa (ambient) and 50 MPa, typical of experiments involving subcritical water. With the pK_W values listed, the pH of water is approximately 5 in subcritical water. From Bandura and Lvov (2006).

3.3.1 Solvatochromic Effects and Brownian Motion in Subcritical Water

While the dielectric constant is a valuable measure of solvent strength and polarity for chromatographic purposes, the value has limited predictive capabilities in terms of describing polarizability or hydrogen bonding characteristics, both of which are relevant to the solvation of compounds in subcritical water. Instead, many researchers have sought to describe the changes in water in terms of Kamlet-Taft parameters of a solute's polarizability (π^*), hydrogen bond donation or acidity (α) and hydrogen bond acceptor or basicity (β). These values can be derived experimentally through solvatochromic measurements at relevant temperatures and pressures, in which reporter molecules in solution undergo spectral shifts relative to the behavioral changes in the solvent. The spectral shift can be deconvoluted depending on the specific probe to give the equation 3.23, where A is absorbance where no solvent-solute interaction occurs, S is the spectral shift due to dipolarity or polarizability, D is the shift due to solvent hydrogen bond acceptance, and E is the shift due to solvent hydrogen bond donation:

$$\nu_{MAX} = A + S\pi^* + D\alpha + E\beta \qquad [3.23]$$

Osada et al. (2003) used quinoline in water as a reporter for the estimation of hydrogen bonding changes in subcritical water, with the result indicating a

dramatic shift in hydrogen bonding ordering. This was observed because quinoline readily hydrogen bonds through the substituted nitrogen on the napthyl ring, causing an inductive effect on the rest of the aromatic structure and a corresponding shift in the UV- absorbance of the π-π* transition. The perturbation at elevated temperature indicates a specific reduction in the hydrogen bond donation to quinoline (resulting in net electronic withdrawal at the nitrogen, and a corresponding blue shift in v_{MAX}), which correlates to a decrease in overall hydrogen bonding in the solvent.

Lu et al. (2001) described the Kamlet-Taft parameters for subcritical water from room temperature to 275ºC using the solvatochromic shifts in several reporter molecules. The probe 4-nitroanisole was used for the π* measurement of polarizability of the solvent, with cyclohexane (π*=0) and dimethyl sulfoxide (π*=1) used for references, and the spectral shift observed as a function of the polarizability of water affecting the reporter. In a similar manner, dichloro-betaine [2,6-dichloro-4-(2,4,6-triphenyl-1-pyridinio)phenolate] was used as a deprotonated standard for a probe of water hydrogen bond donation (α), and *N,N*-dimethyl-4-nitroaniline used for hydrogen bond acceptor (β) measurements. The result of this series of measurements indicates water becomes less polarizable at higher temperatures and the hydrogen bond acidity decreases by a similar margin. Hydrogen bonding basicity is slightly increased (from a β value of

0.15 to around 0.2) at elevated temperatures, demonstrating an increased favorability in accepting hydrogen bonds.

Using a similar approach to Osada et al., Minami et al. (2006) used pyridazine as a reporter molecule to measure the changes in local density and hydrogen bonding in sub- and supercritical water. Pyridazine has spectral shifts due both to changes in polarizability and hydrogen bonding, and cannot be used to isolate specific effects in the Kamlet-Taft equation. However, the authors used a 4^{th} order polynomial fit of the spectral shift to predict solvent density, and then the difference in measured density against predicted density indicated that, in subcritical water, the local solvent density is actually higher near the probe molecule than in bulk solution. Solvent density enrichment decreases as the solvent temperature increases, which the authors attribute to a breakdown in the hydrogen bonding between the probe and the solvent, which correlates well with previous work.

A related technique for measuring the solvent effects of subcritical water was described by Mukai et al. (2006) using video microscopy to observe the motion of 2μm diameter polystyrene beads. Unlike chemical probes used in the solvatochromic studies, this study used a physical marker to observe the changes in diffusion as water temperature increases. As expected, the measured diffusion coefficient increased with temperature according to the Stokes-Einstein relationship, given in equation 3.24, where the diffusion coefficient D is calculated

from k_b, the Boltzmann constant, the temperature T in Kelvin, the solvent viscosity η and the particle radius R:

$$D = k_b\, T/(6\pi\eta R) \qquad [3.24]$$

Differences between measured and theoretical diffusion coefficients were attributed to the large particle size in this study; however, this study demonstrates the effect of temperature on particle mobility in subcritical water.

3.3.2 Computational Simulations of Subcritical Water

To compliment the experimental studies of subcritical water hydrogen bonding, several research groups have attempted to describe hydrogen bonding through molecular dynamics and Monte Carlo simulations. Both of these techniques depend on forcefield definitions of atoms in a given thermodynamic situation, solved for Newtonian equations of motion (Frenkel and Smit, 1996). Monte Carlo processes predict the most likely next move for a given molecule by measuring the change in energy caused by the movement against the likelihood in a Boltzmann distribution at a given temperature and pressure. Molecular dynamics calculations predict the likelihood of a given set of movements in a complex system in a given time step (frequently on the scale of picoseconds). Both approaches allow enough trial steps (where all molecules in a system move

1 step, according to determined statistical likelihoods) until a theoretical equilibrium state is reached. Monte Carlo and molecular dynamics programs have been used extensively for the prediction of fluid behavior, surface effects (Zangwill, 1988; Pesek and Leigh, 1994), and processes involved with chromatography (Wick et al., 2004).

Touba and Mansoori (1998) predicted density and radial distribution functions for water from ambient to subcritical temperature ranges using a series of computational techniques to explain hydrogen bonding in terms of equations of state. The primary finding in this study is that by including the prediction of chains of hydrogen bonds in cubic state equations, the model can accurately predict fluid densities and bond likelihoods in high temperature water.

A molecular simulation study by Liew et al. (1998) was able to describe actual hydrogen bonding orientations and favorabilities in ambient and supercritical water. The interesting aspect of this study is that a second type of hydrogen bonding is observed in supercritical water, demonstrated in Figure 3.7. While traditional linear hydrogen bonding is observed both in ambient and supercritical water, so-called bifurcated hydrogen bonding, in which dipoles of two water molecules are aligned and two bond interactions occur between the two molecules, also exists in supercritical water at significant concentrations.

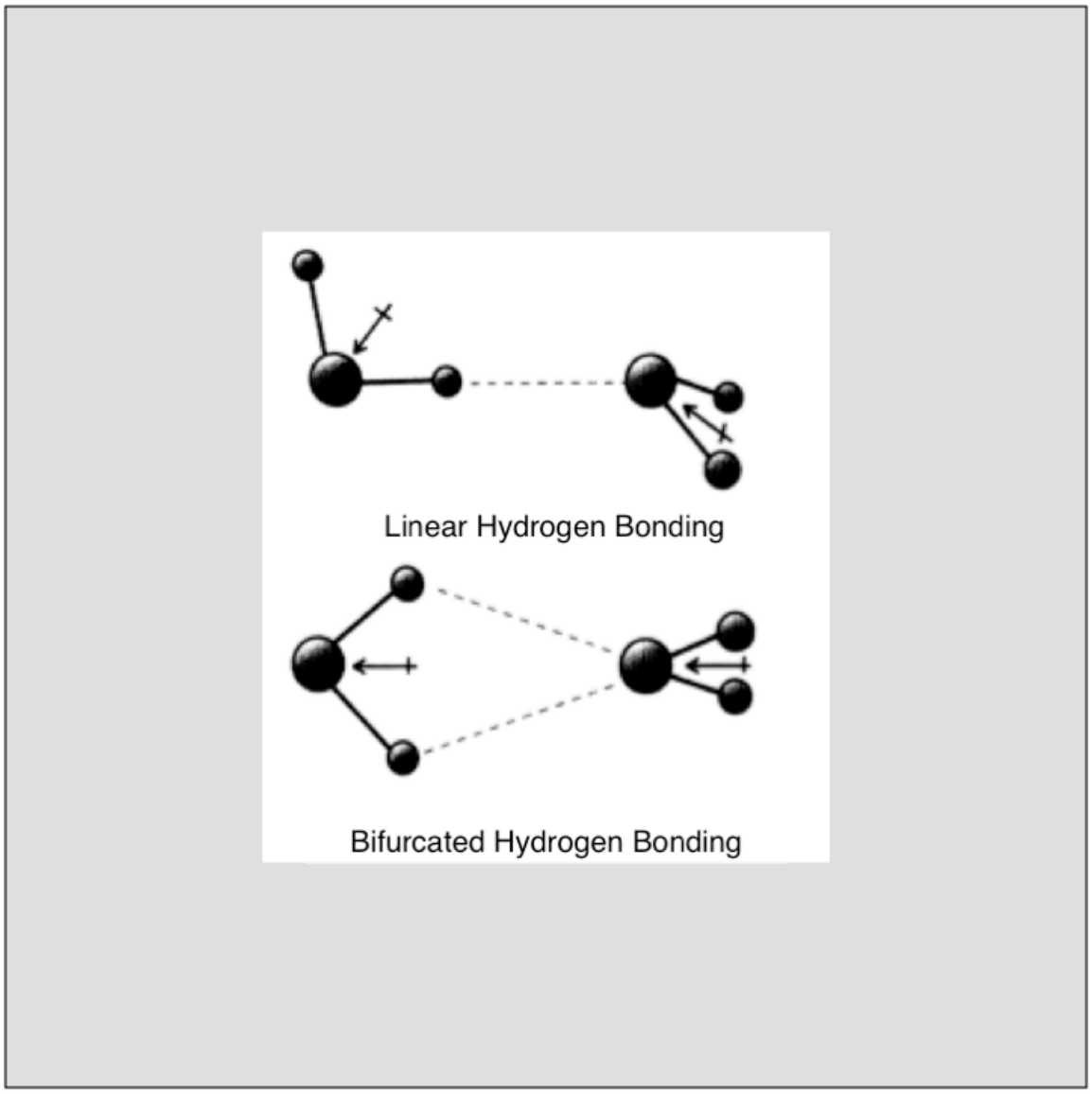

Figure 3.7 Hydrogen bonding orientations for water in sub and supercritical water. The bifurcated arrangement is found only in supercritical water. From Liew et al. (1998)

To compare the difference between forcefields, two studies were performed to determine which system best models water in the actual environment. The first methods used the TIP4P model of water, which creates a localized negative charge outside of the oxygen atom to simulate the electron density in unhybridized p orbitals (Jorgensen et al., 1983). Mountain (1989) specifically used the TIP4P model in high temperature water to both validate the model's predictions of the phase diagram, and also calculate the predicted hydrogen bond distribution for this hard-sphere model. Pairing distances (g_{OO} g_{OH} and g_{HH}) were found to shift slightly for subcritical water, and the TIP4P model also predicted local structures that were not actually observed in supercritical water. Yoshii et al. (1998) used a polarizable potential model of water, which allows for local interactions that polarize the point charges residing on the oxygen and hydrogens, which better reflects actual water effects. This study observed temperatures and pressures from ambient to supercritical conditions and found correlations between shifts in the radial distribution functions and hydrogen bond predictions seen in experimental data. Diffusion coefficients were also calculated and observed to increase in a manner consistent with experiment up to the critical point.

One final study of the hydrogen bonding of water in ambient and supercritical situations used molecular dynamics, which uses finite time steps, to

predict the mean lifetime of hydrogen bonds (Martí, 2000). This study concluded that using a molecular dynamics simulation will accurately predict a given water-water hydrogen bond will exist for about 1ps in ambient water. In supercritical water this timeframe is significantly reduced, although the total number of hydrogen bonds is still significant and hydrogen bonding networks do not disappear in supercritical water.

3.3.3 Solubility and Elution from Stationary Phases with Subcritical Water

At a molecular level, subcritical water behaves more like a polar organic solvent then ambient water, with a corresponding reorganization of hydrogen bonding and decreased polarity. This would suggest that, as a solvent, subcritical water would behave significantly differently than ambient water and likely more similar to methanol or acetonitrile.

Miller and Hawthorne (1998) used a modified GC oven with a pair of LC pumps, the first pump moved water through a saturation vial saturated with naphthalene or benzo[*a*]pyrene in sand. The GC oven was used to bring the sample to subcritical temperatures and pressures; water was pumped through the cell to produce a saturated sample. As soon as water was collected, the second LC pump inserted chloroform into the effluent to prevent sample deposition in the line, and the amount of the analyte was then quantified with GC-FID or GC-MS. The experiment gave solubility values for naphthalene at 36 ± 1

μg g^{-1} at 25ºC and 0.1MPa, up to 216 ± 1 μg g^{-1} at 65ºC and 3MPa. Benzo[*a*]pyrene was found to have a solubility in water at 0.04 ± 0.1 μg g^{-1} or less at 100ºC, but 1100 ± 50 μg g^{-1} at 250ºC and ~6MPa. In addition, although this temperature is above the ambient pressure melting point of benzo[*a*]pyrene, the authors suggest that at the elevated and temperature, the increased solubility is not due to sample melting.

Miller et al. (1998) continued the work on the measured solubility of polycyclic aromatic hydrocarbons in subcritical water, and Mathis et al. (2004) extended solubility measurements for alkylbenzenes. A summary of these solubility results is found in Table 3.2.

Table 3.2 Relative solubilities of hydrophobic compounds in subcritical water. Adapted from Miller et al. (1998) and Mathis et al. (2004).

Temperature, K	**Relative Solubility (based upon mole fraction solubility at 298K)**		
	Anthracene	**Ethylbenzene**	**1,2-dichlorobenzene**
373	40	3.3	3.2
423	1100	8.6	11
473	26000	29	34

As non-polar and weakly polar compounds are much more soluble in subcritical water as compared to ambient, the effective solvent strength of water increases dramatically as temperature increases. Yang et al. (1998) used a similar series of phenols, polycyclic aromatic hydrocarbons, and aliphatic hydrocarbons saturated on LC stationary phases, and then used elution volumes

of water at higher temperatures and pressures from 50-250ºC to test the temperature of water required for elution and the recovery percentage. Samples were first tested on typical normal phase packings (e.g., glass, alumina, fluorosil). Typical recoveries were from 80-110% from these materials, and the elution temperature depended on the point at which the sample became favorably soluble; phenols and amines would elute at ~50ºC whereas PAHs and linear alkanes would not elute from the normal phase packing until the temperature reached 250ºC. C18 and polymer modified packings used as reversed phase stationary phases were also tested for elution efficiency. Compounds required significantly higher temperatures (well above 100ºC) to successfully elute compounds from C18 column packing. A less polar polymer packing material shifted the elution temperature about 50ºC higher than the C18 indicating that subcritical water has insufficient solvent strength for most reversed-phase elutions until the temperature is significantly above 100ºC.

3.4 Subcritical Water Chromatography

Using subcritical water as a chromatographic mobile phase requires a different description of the retention mechanism, as well as adaptations of instrumentation to tolerate high temperatures and pressures. From theory, it is known that temperature modification of a mobile phase is not exactly equivalent to the addition of an organic modifier. In addition, high temperatures are required

for pure water chromatography due to the relatively weak solvent strength of water even at temperatures up to 250°C. At these temperatures, many typical stationary phase modifications are hydrolyzed, which would be unacceptable for actual operation. Advantages of using subcritical water as an eluent, such as relevant separation processes for highly polar analytes and aqueous samples, along with the possibility of general organic detection regimes, have driven research in SWC despite these challenges.

3.4.1 Thermally Stable Stationary Phases

The first concern of using subcritical water with chromatography is its corrosivity towards standard stationary phases. Most silica-based stationary phases have a single siloxane bond between the modifier and the silica surface, and at elevated temperatures and pressures these bonds are known to hydrolyze, ruining the chromatographic column. Research into thermally stable stationary phases has suggested several reasonable alternatives to traditional silica-base columns. Young et al. (1998) synthesized branched and linear silica based stationary phases, which had multiple silanation sites, resulting in high carbon loads and steric hindrance to prevent hydrolysis in the context of subcritical water extraction.

Instead of using silica as a stationary phase support, Li et al. (1997) suggested using modified zirconia as an alternative stationary phase, as carbon-

zirconium bonds are believed to be less likely to hydrolyze in subcritical conditions. Using a hydrophobic selectivity model, Zhao and Carr (2000) determined that the selectivity of polybutadiene and polystyrene modified zirconia was similar to a moderately polar phenyl-siloxane stationary phase in 50:50 water acetonitrile mobile phase. With LSER descriptions a PBD-ZrO_2 stationary phase was amenable to temperature and methanol mobile phase modification; however, the selectivity was unique from similar carbon load silica stationary phases (Li and Carr, 1996). This type of column has been very successful in high temperature chromatographic separation. Fields et al. (2001) demonstrated the stability of polymer-zirconia columns up to 200ºC for the separation of steroidal hormones. Selectivity on the polybutadiene stationary phase system differed significantly from a standard C18-silica column at identical temperatures and mobile phase makeup. Interestingly, unlike predicted column efficiency models including temperature, the Van Deemter curve reported in this study did not show any significant shift from ambient to 165ºC. Instead of a polymer modification, Dugo et al. (2007) used octadecyl-coated zirconia for a separation of parabens in subcritical water (modified with up to 40% acetonitrile) and thermal stability was observed to at least 200ºC.

While zirconia is an interesting support material for subcritical water chromatographic columns, it does have some significant differences from silica based columns. Specifically, unlike silica, which has exposed silanol groups,

zirconia has exposed zirconium atoms, which can act like lewis acids and interact with a mobile phase as an ion or ligand exchange site (Dugo et al., 2007). Thus, several other high temperature columns have also been designed, using polymer backing, in the case of the Hamilton PRP-1 column, or multiply bridged stationary phase modifiers, as is seen in the Waters XBridge® column. An evaluation of the multiply bridged column demonstrated selectivity much more like traditional silica-C18 columns; however, this column was not generally evaluated without organic mobile phase modification (Liu et al. 2005)

A cross comparison of commercially available high temperature columns evaluated the efficiency and pH tolerance, and then correlated retention behavior for columns in different mobile phase modifications (Marin et al., 2004). Peak capacity was increased for some columns using a temperature program as opposed to a solvent program, while it was comparable for others. Acidic and basic conditions had no effect on stationary phase behavior; however the authors did note that zirconia columns are likely unacceptable for thermal programming applications with UV-Visible detection, as the columns caused an unacceptable baseline absorbance at high temperatures. A second study by He and Yang (2003) of the long-term thermal stability of the same class of columns indicated reproducibility is not a significant problem for most high temperature columns. Stable columns like the PRP-1 showed retention stability for at least 9000 column volumes at elevated temperature. HTLC separations were also compared to

similar normal and reversed-phase columns at ambient and high temperatures in water: acetonitrile mobile phases; in some cases full reversal of elution order was observed for a series of octylphenol ethoxylates (Vanhoenacker and Sandra, 2005).

3.4.2 High-Temperature Liquid Chromatography Instrumentation

In addition to requirements of a stationary phase that can tolerate high temperatures, instrumentation for subcritical water or high temperature liquid chromatography must provide a mechanism for injection, temperature controls that can cause thermal gradients through a separation, back pressure to maintain the liquid mobile phase at subcritical temperatures, and a detection regime that can tolerate high temperatures. The simplest designs for HTLC systems used liquid chromatography pumps and injectors attached to columns inside of GC ovens, which have the requisite thermal controls (Smith, 2006). As most HTLC systems use standard LC UV-Visible detection, after separation a cooling chamber is used, and the cooled eluent enters the detection cell; a backpressure regulator is placed after the detection cell to maintain the liquid phase (Yang, 2007). As long as UV-Visible detection is used, mobile phases can be modified by both temperature and organic modifiers.

An example of this type of HTLC system is provided in Figure 3.8, which illustrates a typical instrument using a GC oven, LC pump and UV detector, from Smith (2008).

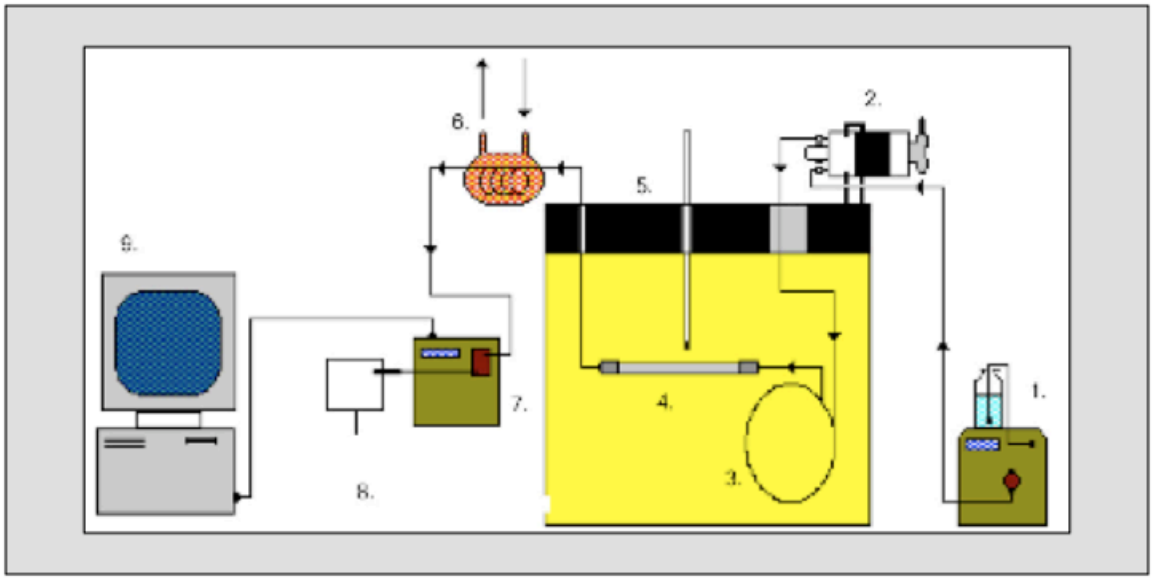

Figure 3.8 Schematic for a typical lab-built HTLC system with UV detection. 1. HPLC pump. 2. Injection system. 3. Preheating coil. 4. HTLC stationary phase column. 5. GC oven. 6. Cooling loop. 7. UV detector. 8. Back pressure regulator. 9. Signal integration. From Smith (2008).

While few commercial instruments have been designed for HTLC, research groups have developed simple modifications of commercially available equipment for this type of chromatographic system (Cabooter et al., 2007).

With HTLC, much of the focus has been on the use of a thermal mechanism as an accelerated separation for a second dimension in two-dimensional liquid chromatography (2DLC) (Stoll et al., 2006). When thermal gradients are combined with solvent gradients in small columns, very rapid (< 10s) separations are possible, and this is required for the second separation dimension in 2DLC. A review of the use of HTLC systems in 2DLC is provided by McNeff et al. (2007) and this study highlights how using two separation mechanisms (solvent and temperature gradients) can fine tune separation parameters for high peak capacities and orthogonality from the first separation dimension.

3.4.3 Gas-Phase Detection with Subcritical Water Chromatography

Zhang et al. (2008) highlight a common complaint about traditional liquid chromatography -- there is no easily applied general detector equivalent to the general organic detection possible with GC with flame ionization detection (FID). While UV detection can allow for the detection of many molecules with chromophores, and short wavelength refractive index (RI) or evaporative light scattering detectors (ELSD) are often cited as universal LC detectors, both have

disadvantages. RI detectors only work for polarizable compounds, and ELSDs are expensive and have limited dynamic ranges. Thus, the combination of a pure water mobile phase has been suggested as a possible method for the use of gas phase FID systems, as the FID is insensitive to steam. Flame ionization detectors work by ionizing all compounds in an effluent stream in a hydrogen and oxygen flame, then measuring the current at the burner tip, which has a voltage potential applied to it (Skoog et al., 1998). Oxidized compounds like CO_2 and H_2O produce no ions at the temperatures of the flame and, therefore, have no impact on the detector. As reduced carbons provide the major component of any organic analyte, the FID response is effectively a carbon counter, with mass sensitive detection limits in the range of 0.1pg s^{-1}. As FIDs had already been heavily used with GC and supercritical fluid chromatography and many of the components for HTLC are adapted from GC equipment, the FID appeared to be a natural fit with high temperature liquid chromatography. Two significant problems exist with this adaptation however. The mobile phase must have minimal organic modifier to prevent swamping out analyte signal, and the mobile phase must efficiently be converted to steam before the flame in a way that prevents analyte from depositing on the transfer line or extinguishing the flame.

The first citation of a subcritical water chromatography system with flame ionization detection (SWC-FID) was by Miller and Hawthorne in 1997. A supercritical fluid restrictor was used to maintain a liquid mobile phase in the

column while allowing the effluent to flash into steam before the FID. Alcohol concentrations in beverages were determined with this method, taking advantage of the large linear range of the FID. In addition, phenols and amino acids were also detected. This study used an instrument fairly similar to the HTLC-UV instrument described earlier; however, other methods have also been examined. Bruckner et al. (1997) performed a pure water chromatographic separation at room temperature, followed by UV absorbance detection and drop headspace extraction of volatiles into a FID. Wu et al. (2001) performed a high temperature aqueous separation in a wide bore packed capillary column in a similar manner to SWC, but this study did not force the mobile phase to remain a liquid, and a liquid to steam gradient was seen in the column. This method was useful for volatile polar compounds that were difficult to separate in conventional GC.

Several studies were undertaken to optimize SWC-FID interfaces in different approaches. Ingelse et al. (1998) designed a similar system to Miller and Hawthorne but used a 1mm internal diameter LC column for separations, as the optimal column flow rate could be reduced to 50µL min^{-1} or less so as to prevent flame extinguishing. Feng et al. (2001) used this approach with capillary and packed GC columns for narrower internal diameter columns. Using a micro-LC setup, Hooijschuur et al. (2000) took ambient LC effluent and superheated it after the separation with an inductive RF heater, which then fed into an inverted FID for detection. This system is more similar to a thermospray ionization source

seen in mass spectrometry than the other described systems. Yang et al. (2002) used more standard SWC separation methods but split the effluent after separation to feed into the FID; this method sacrificed sensitivity for improved separation efficiency at higher flow rates.

Several studies applied SWC-FID techniques to separations that are difficult with LC or GC. Neff et al. (2001) tagged positional isomers of triacylglycerides (TAGs) with bromine to make the analytes more water soluble, and then used SWC-FID for separation and detection. Several pairs of positional TAG isomers were fully resolved and quantified, which was not possible using a comparable LC-MS technique. Yarita et al. (2002) quantified mass percentages of alcohol in alcoholic beverages as a quality control screen. The SWC-FID method was found to correlate determined masses well with a GC method and with labeled values. The potential for QC control with the SWC-FID system has advantages in rapid screens of other polar compounds in alcoholic beverages that may have low volatility, which would not be accessible to a GC method. Guillarme et al. (2005) also suggested the use of SWC-FID for the separation of alcohols. This study also carefully determined the likely parameters that SWC-FID systems could tolerate in terms of column temperature, FID gas flow rates and mobile phase flow rates. The parameter space is large, suggesting the SWC-FID system is relatively flexible and could be optimized to specific separation needs.

Briefly, another gas phase detector can also potentially be adaptated to subcritical water chromatography. The sulfur chemiluminescence detector (SCD) is a selective detector that uses ozone to oxidize sulfur monoxide (produced in FIDs) into SO_2 in a luminescent reaction:

$$SO_{(g)} + O_{3(g)} \rightarrow SO_2^* + O_2 \qquad [3.25]$$

$$SO_2^* \rightarrow SO_2 + h\nu \qquad [3.26]$$

As this reaction produces light through chemical excitation instead of fluorescent excitation, all light produced is due to chemiluminescent emission, which occurs between 300-400nm. Since no light excitation is used, careful measurement of all light production is possible, giving an equimolar detector response to sulfur present (Benner and Stedman, 1989). Emerging environmental contaminants often contain sulfur and are not highly volatile, suggesting a SWC-FID-SCD arrangement may be able to specifically analyze emerging contaminants in aqueous media. While SCDs have been used for a long time with supercritical fluid chromatography with CO_2 mobile phases (Shearer and Skelton, 1994), little research has occurred on the hyphenation of SCD to LC systems. However Ryerson et al. (1994) suggested the design of LC-SCD using a subcritical water breakdown system to convert sulfur compounds to SO, which was then extracted

from the liquid phase via a drying apparatus. This apparatus is somewhat complex and does not provide a carbon specific analysis channel; in addition, the sensitivity was low for sulfur containing analytes. A micro-LC-SCD system is described by Howard et al. (1994) but used methanol-programmed separations at ambient temperatures to volatilize compounds in a FID before entry into the SCD. With this arrangement, high concentrations of methanol were required, and no clear trend emerged in the detector response to chromatographic conditions, with actual detection limits in the ppm range.

3.5 Subcritical Water as an Oxidation Medium for Benign Organic Treatment

While much of the earlier investigation of subcritical water focused on organic solubility and the potential of subcritical water as a chromatographic mobile phase, this ignores another possibility of subcritical water as a reaction medium. Due to the increased acidity of subcritical water, along with the greatly increased ability to solvate organic molecules, subcritical water behaves more like an acidic organic solvent such as acetic acid than ambient water, which has a dramatic change on organic reactions in the solvent. Hydrolysis and dehydration reactions are observed to occur at much faster rates in subcritical water due to a combination of these factors. This section focuses on the usage of

subcritical water as a solvent for rapid hydrothermolysis and oxidation of organic molecules, with applications to the breakdown of wastewater organics.

3.5.1 Hydrothermal Breakdown of Organic Contaminants

Jin et al. (2004) tested the breakdown of cellulose in subcritical water, and found that both acid-catalyzed and base-catalyzed reactions occurred in subcritical water, even when another strong acid or strong base was added to the solution. Thus, subcritical water by itself acts as a strong acid-base catalyst. Erythromycin, a common antibiotic, has been shown to breakdown in subcritical water as a function of time, with acid-catalyzed breakdown products observed (Butler and Weber, 2005). Hydrothermal breakdown processes have also been used to successfully remove bisphenol E, an endocrine disruptor (Savage et al., 2006). Again, breakdown product analysis suggests that the reaction proceeds through an acid-catalyzed mechanism, which is enhanced in subcritical water. This study further suggests carbocations are stabilized in subcritical water, allowing for different breakdown processes than are seen in ambient water. Hydrothermal breakdown processes have been widely adapted, and the breakdown of chlorinated compounds (Kubátova et al., 2002), biomass (Jin et al., 2008), and carbohydrates (Asghari and Yoshida, 2007) have been demonstrated.

3.5.2 Oxidation of Organic Compounds in Subcritical Water

Due to the high solubility of organic compounds and molecular oxygen in subcritical water, oxidation reactions can be combined with acid-catalyzed hydrolysis for more complete breakdown of contaminants in solution. Wet oxidation in subcritical water has been attempted in a number of different ways, using a combination of catalysts, oxidants and target materials. One early study of the oxidation of alkyl aromatics with molecular oxygen in subcritical water allowed for a relatively efficient conversion of the alkyl aromatic compound to the acid form with ~60% efficiency; additional compounds were formed through partial oxidation or through decarboxylation (Holliday et al., 1998). Ozen and Kus (2006) demonstrated that molecular oxygen readily oxidized alcohols to aldehydes or ketones and arenes to quinones with a straightforward oxidation mechanism; in this study, no additional catalysts were required. The difficulty in analyzing subcritical water oxidation and breakdown is in the complexity of the mechanism. Due to acid and base catalyzed hydrolysis, dehydration reactions, and oxidation, a wide variety of possible products can be observed in the breakdown of organic compounds. Figure 3.9 demonstrates the possible breakdown products of lactic acid, which is used as a simplified analyte to model carbohydrate breakdown (Li et al., 1999). This study also highlights how oxygen additions affect product ratios; the major product in an oxidizing reaction is acetic

acid, whereas acetaldehyde is the major product in a strictly hydrothermal reaction.

Dadkhah et al. (2006) extracted polycyclic aromatic hydrocarbons (PAHs) using subcritical water from contaminated soil samples. Once extracted, the PAHs were rapidly oxidized by the addition of hydrogen peroxide; after 2-6 hours of treatment, most high concentration PAHs were reduced to below the detection limit of the GC method used for quantification. PAH oxidation is rate controlled by the residence time in solution, so greater temperatures enhanced oxidation rates. This study also observed that a vast amount of the oxidation process occurred in the first 30-60 minutes of treatment.

Wet oxidation can be decoupled from hydrothermal degradation into a two-step process. Jin et al. (2006) used a previously described hydrothermal degradation of cellulose into 5-hydroxymethyl-2-furaldehyde, 2-furaldehyde, and lactic acid. Next, these reaction products were reacted with hydrogen peroxide at stoichiometric quantities, producing a high yield of acetic acid, which is a likely oxidation endpoint for the breakdown of carbohydrates. The two-step reaction the authors used in this study produced a greater yield of acetic acid than a one-step wet oxidation and degradation and also yielded a higher purity of end products, indicating less partial reactions of degradation products.

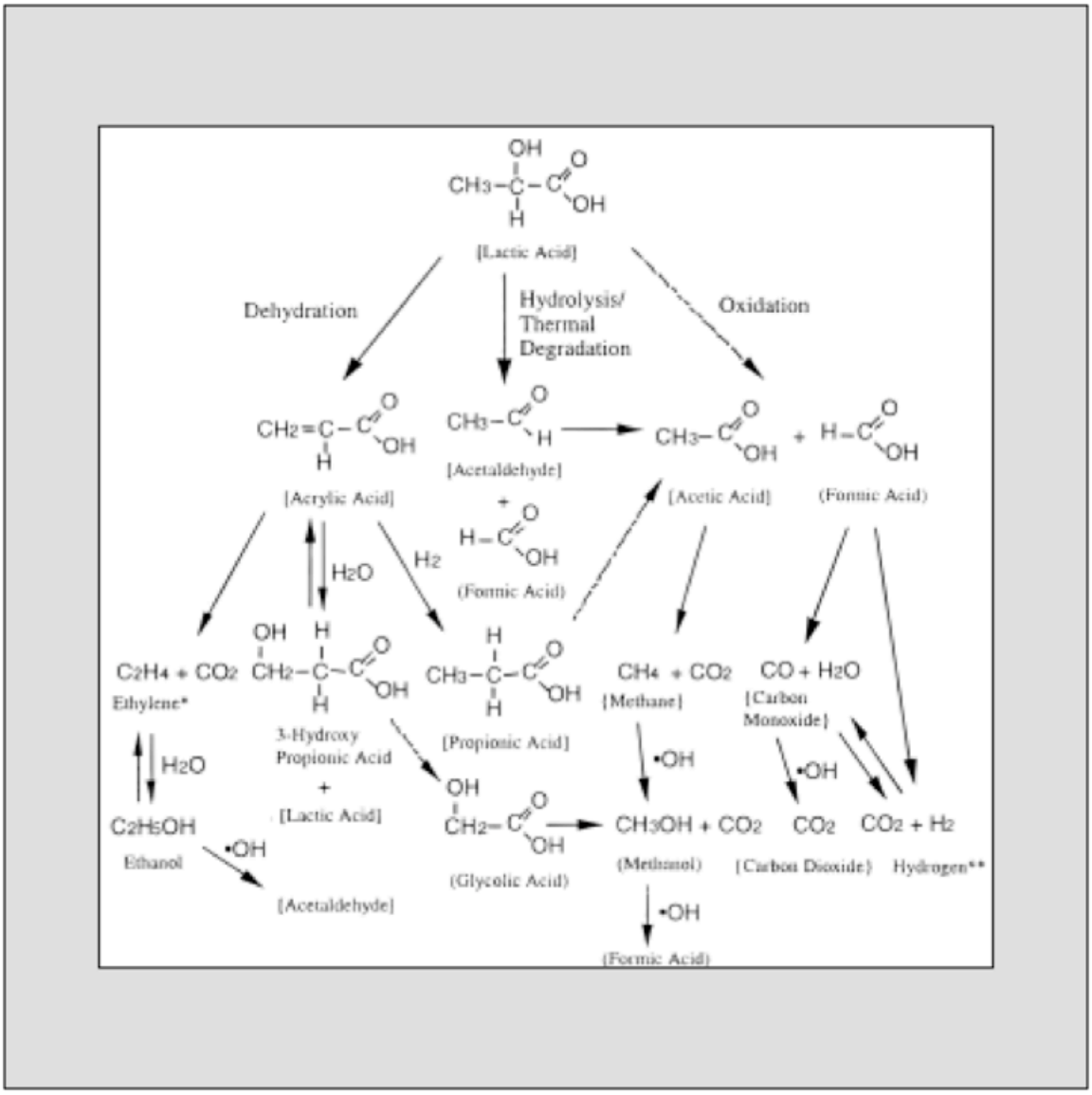

Figure 3.9 Breakdown mechanisms for lactic acid in subcritical water oxidation. System parameters determine specific production favorabilities, with acetic acid being the most likely product if oxygen is present, and acetaldehyde if oxygen is absent. From Li *et al*. (1999).

3.5.3 Wet Oxidation in Subcritical Water for Wastewater Treatment

In addition to the treatment of model organic contaminants, wet oxidation processes in subcritical water have been used for the direct treatment of sewage sludge for treatment. A commercial scale supercritical water treatment facility was first described in 2002, which used a cyclic processing method to bring wastewater sludge up to supercritical temperatures and pressures. The feedstocks for this plant were domestic and industrial waste, and the supercritical treatment was used to reduce chemical oxygen demand (COD) and total solids concentrations (Griffith and Raymond, 2002). COD measures the residual dissolved organic concentration, while solids measurements reflect insoluble organics. This was an extremely endothermic reaction; a great deal of energy was required to bring the sludge up to treatment temperatures. The process was then upscaled from a pilot plant (0.4 gallons per minute effluent) to a commercial scale treatment system (12.5 gpm).

Shanableh (2005) describes the kinetics of decomposition of organics during hydrothermal oxidation treatment. The change in COD is effectively controlled by system temperature by the Arrhenius relationship where the reaction rate constant is related to the pre-exponential value k^0_{COD}, the activation energy required for breakdown, and the temperature T:

$$k_{COD} = k^0_{COD} \exp(-E_A/RT) \qquad [3.27]$$

The change in COD can then be correlated to the concentration of reactants and oxygen by equation 3.28, where [COD] is the concentration of organic molecules, [O] is the oxidizer concentration, and m and n are reaction orders:

$$dCOD/dt = -k_{COD}[COD]^{M}[O]^{N} \quad [3.28]$$

For the study listed, the reaction is first order with respect to COD. An important note in this study is that often the oxidizer concentration is rate limiting and first order but steady states are used as approximations due to the large excess of oxidizer used in most hydrothermal reactions. This is somewhat inaccurate, as the rate limitations are due to the slow mass transfer of oxygen in subcritical water. Shanableh and Imteaz (2008) later expanded this work to determine the activation energy required for COD reduction, with the intent of determining if pre-digestion of sludge (typical in most wastewater treatment plants) was required for effective removal with supercritical water treatment. This study suggested that the typical k_{COD} was on the scale of 60000 and the activation energy was on the scale of 10KJ mol^{-1} whether or not the sludge was pretreated.

Due to the ease of application, compressed air has been considered an oxidant of interest for wet oxidation instead of pure oxygen, as it is considerably cheaper and safer for large-scale usage. Chung et al. (2009) released a study of the wet air oxidation of sludge using a lab scale stirred tube reactor to measure

the reduction of COD and solids during a subcritical water wet oxidation process. Subcritical water has been suggested to have practical benefits over supercritical water in this regard, as supercritical water is caustic enough to cause significant damage to reactors and using supercritical water results in higher maintenance cost for large-scale processes. Using the wet air oxidation process, solid and total COD were reduced in sludge up to 80%. A frequently seen effect of the oxidation is the rapid decrease in COD from solid sources, with a corresponding increase in soluble COD, which eventually decreases, causing a total COD reduction. Solid organics are rapidly dissolved in the subcritical solvent before actual degradation begins.

3.6 Summary

In this chapter, the basic theory of chromatographic separations was reviewed. Because of advances in molecular simulations of the liquid chromatographic process, it is clear that the retention mechanism of liquid chromatography is complex, and complexity is increased when the mobile phase is changed from a purely aqueous system to a hydroorganic one. In order to better understand the mechanistic contributions to retention, several techniques and theoretical models have been employed to attempt to predict the retention of analytes in a liquid chromatographic system, with varying degrees of generality.

Subcritical water was examined as an alternative mobile phase in liquid chromatography. Due to its specific differences in dielectric values, and its different hydrogen bond ordering, subcritical water behaves more like a hydroorganic mobile phase, with a corresponding increase in solvent strength relative to ambient water. However, subcritical water is a homogenous fluid, unlike the real concentration variances present in hydroorganic mobile phases, which may subtly change the interactions between phase interfaces in chromatographic systems.

Using subcritical water as a chromatographic medium has significant advantages beyond mechanistic concerns. Water is inexpensive, environmentally benign, and the subcritical mobile phase is compatible with gas phase detectors, allowing for universal organic molecule detection. This is a significant benefit for environmental analysis, as many analytes of interest are too small or polar for gas chromatography or mass spectral detection. The development of high temperature and subcritical water chromatographic systems has allowed for the testing of thermal effects on retention, as well as thermally controlled liquid chromatography.

The use of subcritical water as a reaction medium was also explored in terms of the breakdown of organic molecules. Due to the greater dissociation of water at elevated temperatures, subcritical water can act both as a strong acid and strong base catalyst. As many molecules that are insoluble in ambient water

are much more soluble in subcritical water, the efficiency of organic reactions is greatly increased. When an oxidizer is added to subcritical water, oxidation reactions can occur that would not be favorable at ambient temperatures. Due to its greater solubility in subcritical water, molecular oxygen can be efficiently used as an oxidizer in hydrothermal oxidations. This technique has been used both for creating green organic chemical processes and for the removal of organic wastes from wastewater. The hydrothermal oxidation approach is chemical, unlike the typically biological processes used in primary treatment of wastewater and, as such, is more likely to remove compounds that biological treatment cannot.

Chapter 4: Materials, Methods and Instrumentation

In this chapter, the materials and methods for all experiments are described. In addition, the design schematics for the two experimental instruments are provided. Specific experimental parameters and included in later chapters with the individual experiments. Theoretical discussions related to these methods and instruments were reviewed in Chapter 3.

4.1 Design of a SWC-FID Instrument

This study includes the experimental design and optimization of a subcritical water chromatography system with flame ionization detection (SWC-FID). This system is built from commercially available components, so as to maximize compatibility of widely available technologies of both liquid chromatography and gas phase detection. This flexibility is intended to allow for easy adaptation of new column and detector technologies into the SWC-FID system without additional interface or injection modifications.

4.1.1 SWC-FID System Overview

The basic SWC-FID system requires a temperature-controlled chamber for the liquid chromatography column, an injection system, a conventional isocratic LC pump, a LC column that can tolerate elevated temperatures up to 200ºC, and an interface to a FID. Since gas chromatography ovens are easily temperature controlled and can be built with integrated FID controls, a GC system is the ideal starting point. The base system used in this study is a modified Agilent 6890 GC system with an integrated FID (Agilent, Santa Clara, CA). The mobile phase was delivered with an ESA 582 isocratic LC pump (ESA, Chelmsford, MA). A basic SWC-FID schematic is provided in Figure 4.1. Initial system designs in this study are similar to the original SWC-FID design provided by Miller and Hawthorne (1997), but were later modified for internal sample heating and injection.

4.1.2. Mobile Phase Preheating and Sample Injection

GC injection ports are incompatible with samples that are to be kept in the liquid phase; therefore adapted LC injection ports are the logical starting instrumentation for an injection system. In addition, the mobile phase must be brought to the subcritical temperature range before sample injection, so as to minimize band broadening due to thermal mismatch. Temperatures relevant to

subcritical water chromatography are damaging to many common LC connectors and ports, so care must be taken to prevent contact with the subcritical water.

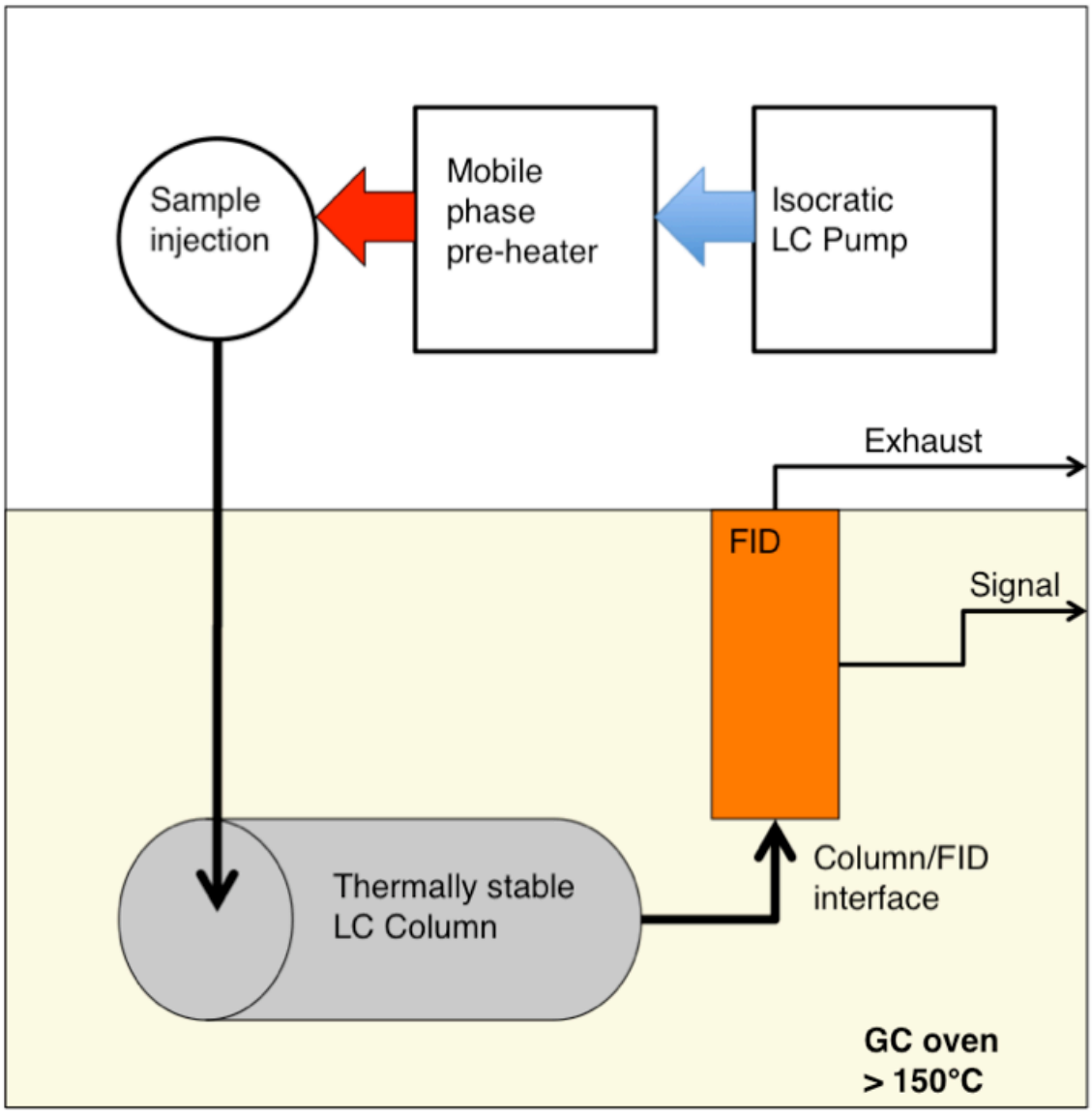

Figure 4.1 Box diagram of the SWC-FID system.

In early designs for this instrumentation, a Brinkmann CH-500 column heater (Brinkmann, Westbury, NY) was used to pre-heat the mobile phase to near boiling, but within the thermal tolerances of a Rheodyne® 7725i manual LC injector port (Agilent, Santa Clara, CA). As this methods only brings the mobile phase and sample to near boiling, polyetheretherketone (PEEK) tubing and connectors standard to LC can be used for connection to the pump (1/16" o.d. by 0.010" PEEK tubing; VICI, Houston, TX, USA) and for the sample injection loop (5µL, Grace, Deerfield Il, USA). The sample injector is outside of the column oven, and a 50cm stainless steel tubing with Valco type fittings is used to connect the injector to the column inside the oven (1/16" o.d. 0.005" i.d.,VICI, Houston, TX, USA). A detailed schematic of this injector arrangement is provided in Figure 4.2.

While this injection system provided a reasonable method for incorporating the sample and mobile phase into the column, it suffers from a significant drawback. While the mobile phase is warm, it is not subcritical, and as such weakly soluble compounds may not be readily carried into the column. In addition, the difference between temperatures of the injected sample, mobile phase and column is great (in some cases as much as 100^{o}C), which is certain to cause thermal mismatch broadening in the chromatography (Yang et al., 2002).

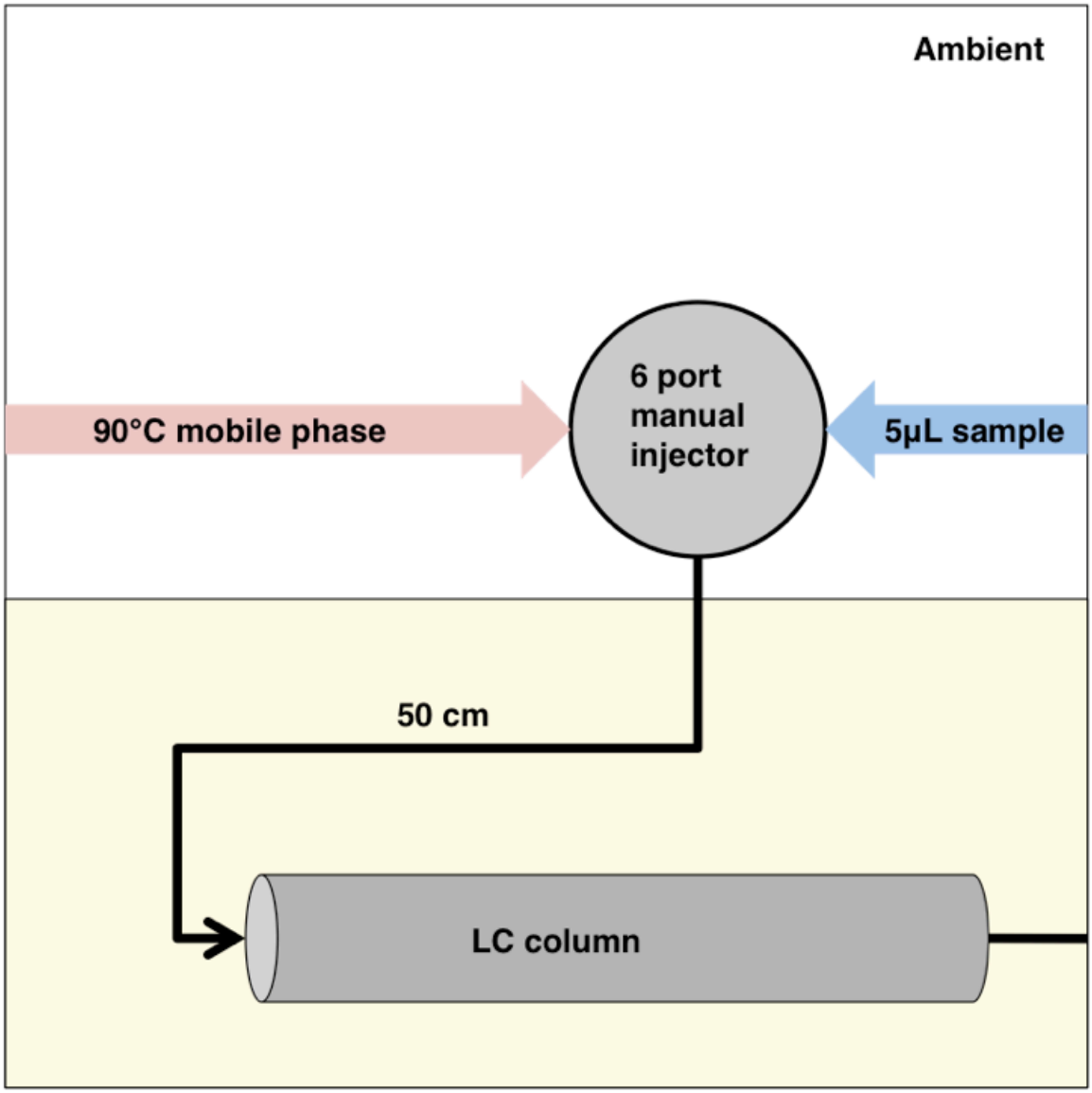

Figure 4.2 Schematic of external injection loop with sub-boiling mobile phase preheating

A second injector and mobile phase pre-heater is described in Figure 4.3. In this configuration, a model 6C4UWT high temperature, manual 6 port switching valve with a 6” standoff was placed inside the GC oven (VICI, Houston, TX). The mobile phase was delivered from the isocratic pump to the switching valve via a 100cm stainless steel tube (1/16” o.d., 0.005” i.d.), in which the excess 90 cm are looped within the oven in order to preheat the mobile phase before sample addition. A 10µL stainless steel sample loop was connected to the valve, and two 25 cm stainless steel tubes (1/16” o.d.,0.005” i.d.) were used to connect the external sample injection port and exhaust port to the valve. Due to the heating of the sample and mobile phase, ball valves were placed on the sample injection port and the exhaust port, so that sample can be kept in the injection loop until ready for injection (Swagelock, Solon, OH). A modified 1/16” swage fitting was placed on top of the injection valve that held down a 4mm SGE medium temperature septum (04018490, SGE, Austin, TX), allowing for liquid injection into the preheated system.

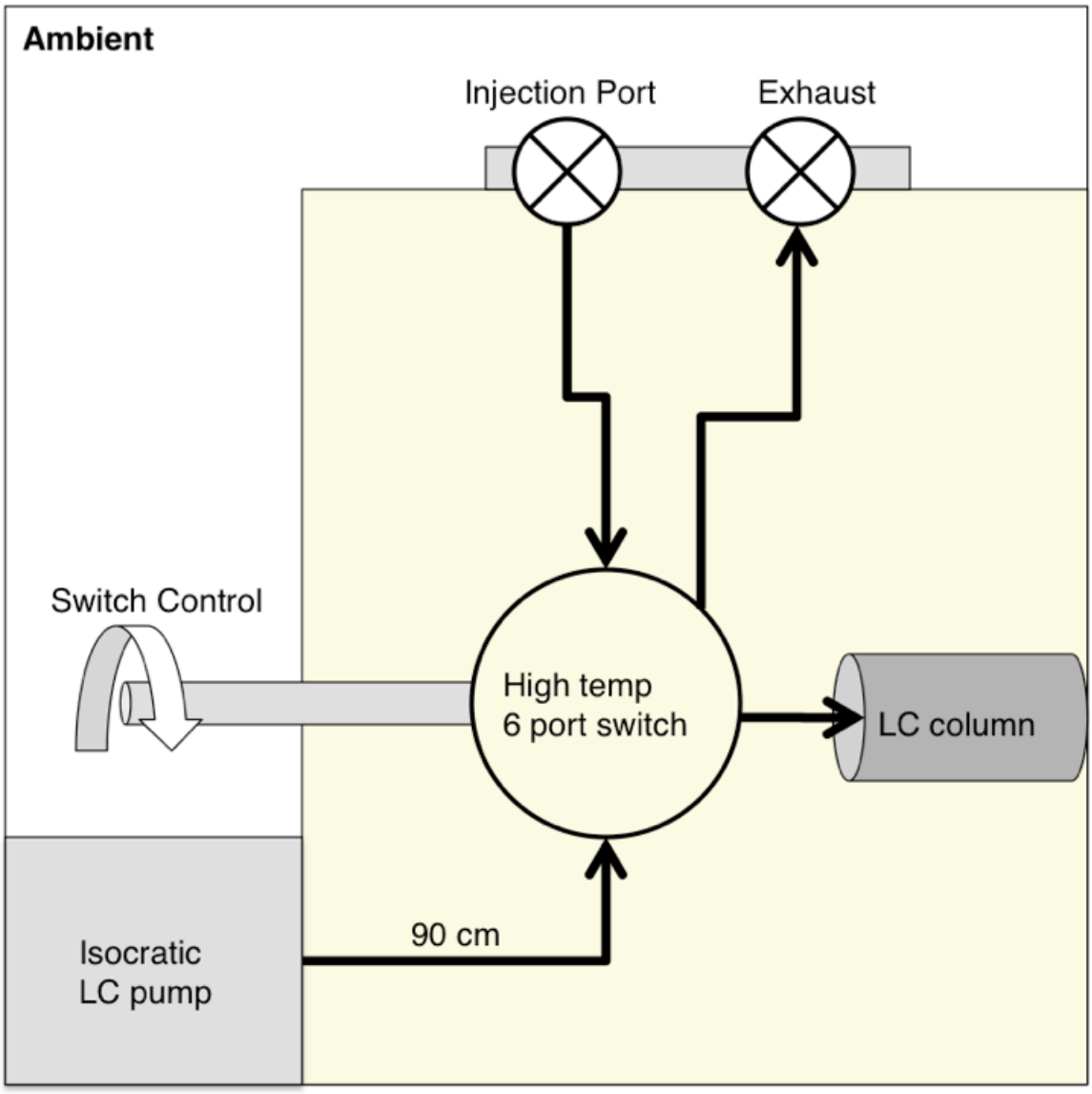

Figure 4.3 Internal injection and mobile phase pre-heating arrangement**.**

4.1.3 LC Column Selection

In the past, the main constraint for SWC-FID was the lack of acceptable stationary phases for use with subcritical water. Most conventional LC columns have an upper temperature limit of around 60ºC. Above this temperature the silanol bonds to the stationary phase can hydrolyze and rapidly degrade the column. However, several columns have been created which can be used for high temperature separations. In all optimization and application studies cited in chapter 5, a Zirchrom® Diamondbond-C18® zirconia column (5μm, 100mm X 2.1mm i.d., Zirchrom, Anoka, MN) was used. This column uses carbon-clad zirconia instead of silica for the stationary phase particle. Carbon-zirconia bonds have been shown to be less susceptible to hydrolysis at high temperatures, thus allowing for the greater temperature tolerance for surface modifications, and the carbon cladding reduces stationary phase interactions with the mobile phase (Zhao and Carr, 2000). Stationary phases that have been successfully used with the SWC-FID system are described in Table 4.1.

Table 4.1 High temperature tolerant LC columns

Column (Maker)	Particle composition	Surface Modification	Temperature Limit
Diamondbond® C-18 (Zirchrom)	Zirconia coated with carbon	Uncapped C-18	200ºC
PRP-1 (Hamilton)	Poly(styrene-divinylbenzene)	none	150ºC
X-bridge C-18 (Waters)	Silica	C-18 with three bonds to silanol surface	80ºC (200ºC was used without degradation)
Discovery Zr-PBD (Sigma-Aldrich)	Zirconia	Polybutadiene	150ºC
Discovery Zr-CarbonC18 (Sigma-Aldrich)	Zirconia coated with carbon	Uncapped C-18	200ºC

4.1.4 LC Column to FID Interface

A component that causes difficulties for SWC-FID systems is the interface between the column effluent and the FID intake. If the pressure from the column is released too quickly, the mobile phase will flash into steam before carrying low volatility analytes into the detector. However, if the mobile phase remains a liquid inside the FID, the flame will be destabilized and detector sensitivity will be lost. This system used a narrow capillary as a back pressure restrictor to prevent early mobile phase nebulization but allows for gradual reduction in pressure as the

mobile phase moves through the capillary, so that most of the mobile phase is converted to steam near the inlet of the FID.

A 10cm section of 127μm i.d. stainless steel tubing connects the column to a Valco 0.25mm i.d. internal/external union (VICI Houston, TX), which then connects to a 30cm section of 21μm i.d. Silcosteel® (Restek Bellefonte, PA). Based upon monitored back pressure via the LC pump, the restrictor created about 3.5-4 MPa of back pressure on the system, which is sufficient to maintain a liquid mobile phase up to about 250ºC. The ideal arrangement would be to use silcosteel for the entire interface, as some systematic broadening will occur due to the change from the stainless to silcosteel internal diameters, but this connection was not possible due to the narrow o.d. of the silcosteel, which is incompatible with typical LC column fittings.

The opposite end of the Silcosteel® tubing is inserted 2.5cm into the FID jet. To accommodate the relatively wide bore of the Silcosteel® line, a model G1531-80620 wide bore FID jet was used (Agilent, Santa Clara, CA). The FID temperature was found to be optimal at 400ºC, facilitating the rapid conversion of mobile phase to dry steam. The LC-FID interface is depicted in Figure 4.4.

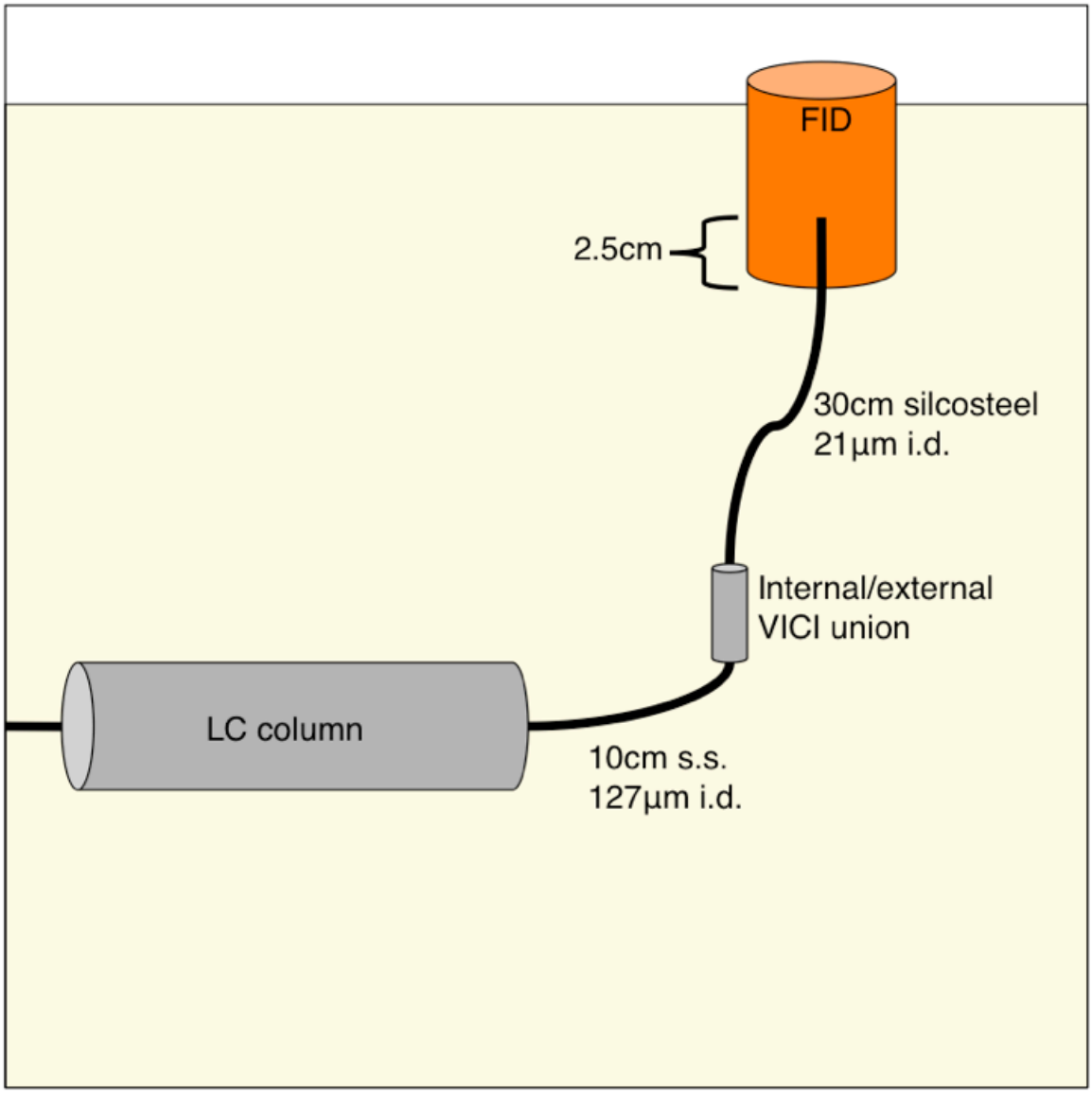

Figure 4.4 Schematic diagram of LC column-FID interface.

4.1.5. Detector Description and Hyphenation

The detector used for all of the experiments in Chapters 5 and 6 is the flame ionization detector installed in the Agilent 6890 GC. Other than the wide-bore jet, which is used to accommodate the silcosteel® interface, the FID was used as is. Zero air was used as the oxidant for the system. Generally the system used a high flow of oxidant (>250 standard cubic centimeters per minute (sccm), corresponding to a regulator pressure of 150PSI). Hydrogen was used from a regulator at ~25-50sccm and nitrogen was used as a makeup gas. All experiments used a FID temperature of at least 300ºC; most experiments were run at a temperature of 400ºC.

Data integration for the FID was performed via the signal integration channel provided, which allowed for the use of Agilent Chemstation® as a data logger for system control. Typical data sampling rates were at 0.5hz. All sample integrations were performed using the automatic peak picking methods included with the software to minimize sampler bias. Chromatogram data collection was initiated through an autostart signal from the injector as to minimize retention time drift from a manual triggering system.

For gas phase detection extension experiments, a Sievers model 255 nitrogen chemiluminescence detector (NCD) with dual plasma controller and burner was modified for use as a sulfur chemiluminescence detector (SCD) (Agilent, Santa Clara, CA). NCD and SCD systems are identical except for the

chemiluminescence wavelength monitored. Thus, the 800nm red cutoff filter used for the NCD system was replaced with a 300-400nm UV band pass filter from Sievers. Oxygen, zero air, and hydrogen were regulated and connected to the SCD without further purification. An oil-sealed vacuum pump was used to maintain a constant pressure of 5 torr in the mixing chamber to increase the rate of interaction between the ozone and effluent from the plasma burner. The dual plasma control was directly connected to collect FID exhaust, collecting between 10-20% of the exhaust for analysis. The ozone regulator was used with 5sccm of air per instrument instructions with the FID adapter (Sievers Model 355 SCD Manual). The plasma temperature was kept at 800ºC for all experiments. As ozone is damaging to the vacuum pump, a chemical trap containing Hopcalite® from Sievers was used to neutralize any residual ozone in the post-detection exhaust. Hopcalite® is a 3:1 combination of manganese and copper oxide, which acts as a catalyst to convert ozone and CO to O_2 and CO_2 respectively.

Signal integration was performed via the voltage out connections on the SCD, with Vernier LoggerPro® software used for data collection. A Vernier LabPro data logger was used to collect the signal for computer analysis. The LoggerPro® software was also used for data integration. As there was no software control of the SCD, all chromatograms were manually triggered and manually integrated. A diagram of the SCD is provided in Figure 4.5.

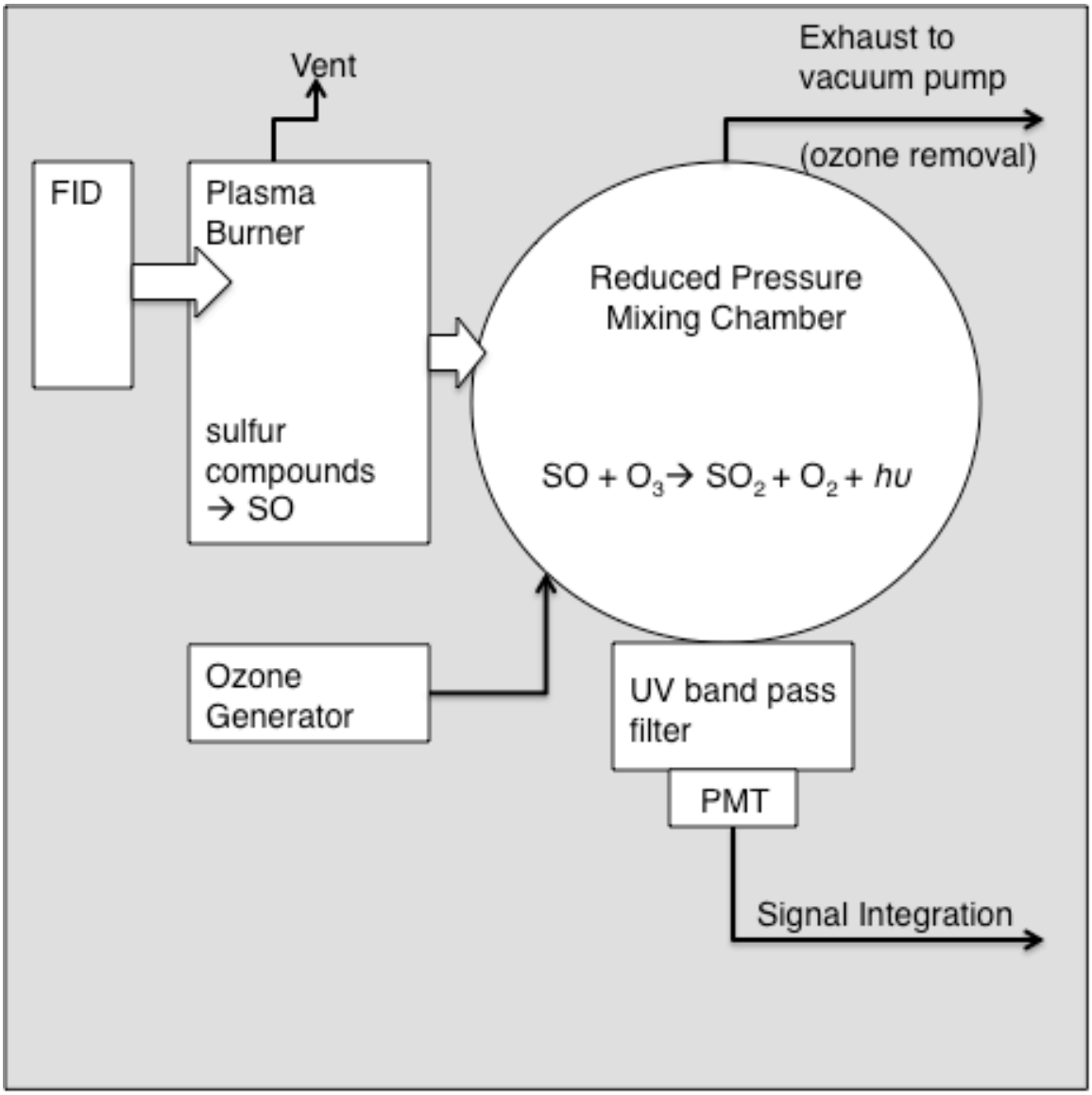

Figure 4.5 SCD schematic description

4.1.6 Chemicals

For the studies described in Chapters 5 and 6, the SWC-FID system was used. Analyte solutions were made for these studies in 18MΩ resistivity deionized water from a Millipore Milli-Q purification system (Billerica, MA). Typical solutions were made in the 100-1000ppm concentration range, depending on the study goal; additional concentrations were made by serial dilution. Table 4.2 summarizes of the sources of all chemicals and reagent grades used in the studies in Chapters 5 and 6. Compound sources are listed in the table note.

Table 4.2 Summary of chemicals used in experiments with SWC-FID

Compound	Stated % Purity
Alcohols, diols and mercaptans	
methanol[1]	99.99
ethanol[1]	99.5
1-propanol[2]	99
2-propanol[2]	99
1-butanol[2]	99.5
1-pentanol[3]	99
1-hexanol[2]	97
1-heptanol[2]	97
1-octanol[3]	99
1-nonanol[4]	97
2-methyl-2-propanol[3]	99.5
1,2-propanediol[4]	97
benzyl alcohol[3]	99
β-mercaptoethanol[3]	--
Aldehydes, ketones and ethers	
propionaldehyde[3]	99.9
benzaldehyde[3]	99
2-butanone[3]	99
4-heptanone[3]	98
acetone[1]	99
cyclohexanone[2]	97

Table 4.2 Chemicals used with SWC-FID, Continued

acetophenone[1]	97
tetrahydrofuran[5]	99.93
tetrahydrothiophene[4]	97
Benzene and derivatives	
benzene[1]	99.9
toluene[3]	99.95
ethylbenzene[6]	99.8
m-xylene[3]	99
n-butylbenzene[3]	99
aniline[6]	97
nitrobenzene[2]	99.9
methoxybenzene[7]	97
pyridine[2]	97
1,2-dichlorobenzene[3]	99.9
4-chlorotoluene[3]	98
Phenol and derivatives	
phenol[2]	99
1,4-dihydroxybenzene[7]	97
2-methylphenol[3]	99
4-chlorophenol[3]	99
4-methoxyphenol[3]	99
4-nitrophenol[3]	97
4-iodophenol[3]	99
2-naphthol[3]	97
Other chemicals	
1,1,2-trichloroethane[3]	98
acetonitrile[5]	99.9
acetic acid[1]	99
d-fructose[3]	99
d-glucose[1]	99
sucrose[3]	99.9
n-hexylamine[3]	99

[1] Fisher Scientific (Pittsburgh, PA)
[2] Mallinckrodt (Hazlewood, MO)
[3] Sigma-Aldrich (St. Louis, MO)
[4] Eastman-Kodak (Rochester, NY)
[5] Pharmco (Shelbyville, KY)
[6] Acros Organics (Geel, BE)
[7] MCB (Whitehouse Station, NJ)

4.2 Design of a Subcritical Water Wet Oxidation Reactor with a Taylor Bubble Mixing Mechanism

This study entailed the analysis of a lab scale wet oxidation reactor that uses Taylor bubble mixing to enhance oxidation. This reactor uses a longitudinally rotated tube to mix pressurized air with a liquid of interest, using the surface tension of the liquid as a mechanism for increasing the size of the air/liquid interface. At subcritical temperatures and pressures, oxidation is accelerated due to the greater solvation of organic compounds, the increased solubility of oxidants, and the medium's inherent strong acid and strong base catalytic behavior. Rapid breakdown of complex organic molecules into smaller and less environmentally hazardous products results from the efficient oxidation process.

4.2.1 System Overview

The basic schematic of a wet oxidation reactor is provided in Figure 4.6. The basic components of the reactor are minimal -- an apparatus for the addition of liquid sample, an air pressurization system and a rotating tube that is insulated and heated with conductive heating tape. The reactor tube must be narrow in diameter relative to the length of the tube so that a bolus of vapor can move through the liquid as the tube is inverted.

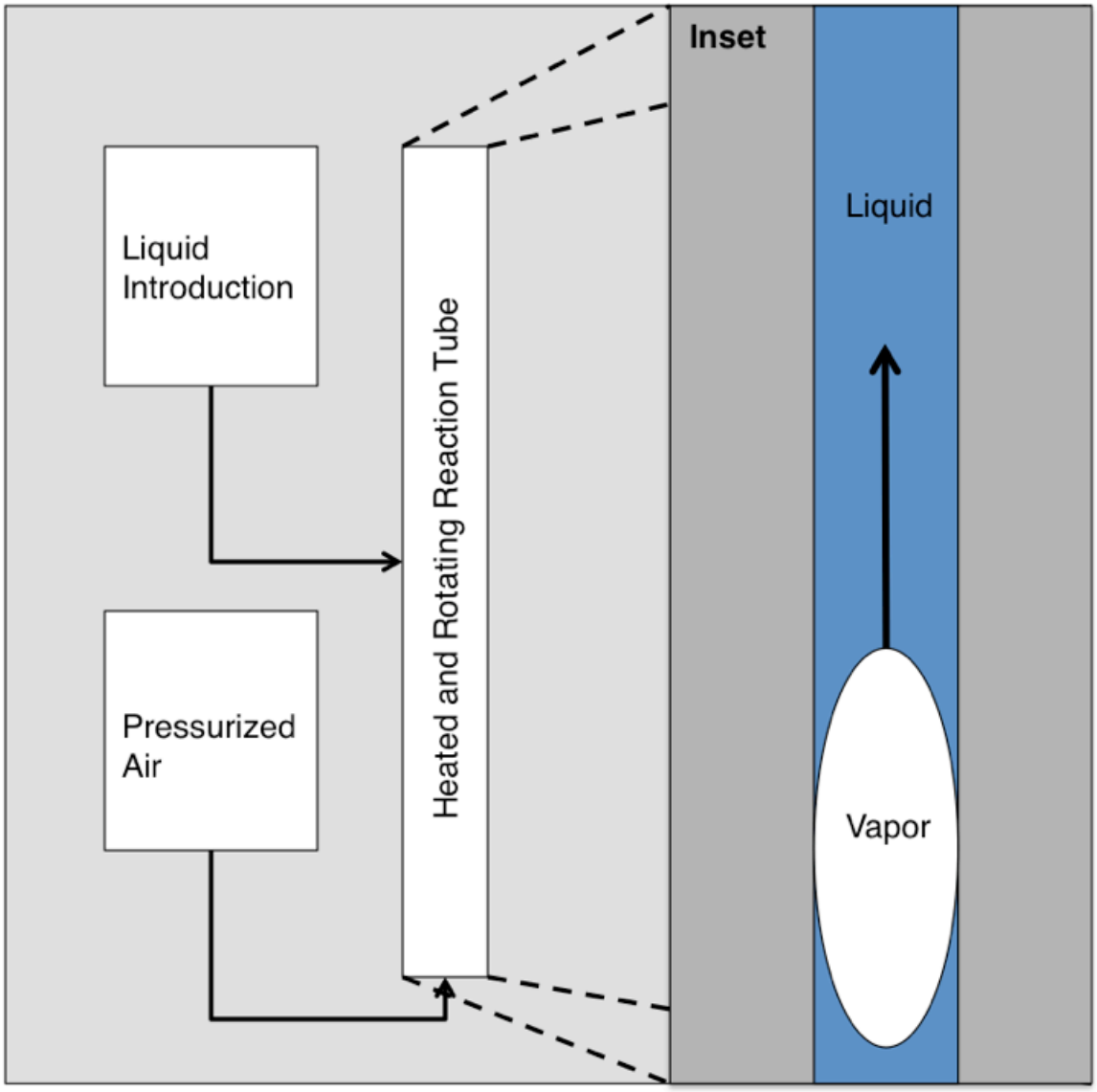

Figure 4.6 Schematic of a wet oxidation reactor. Inset: Model Taylor bubble, with a large, moving liquid/vapor interface

The shape of the vapor bolus is approximately bullet shaped, and as a result, the surface interface between vapor and liquid is very large relative to tube diameter (Nigmatulin, 2001). The surface area of the air-water interface is about 160 times that of the static surface area in the tube, allowing for efficient mass transfer rate between the oxidant (air) and the subcritical reaction medium, and the interface becomes larger as temperature increases and kinematic viscosity decreases, resulting in extremely efficient mixing.

A detailed schematic diagram of this experimental reactor is provided in Figure 4.7. A liquid sample charge vessel, shown in the Figure 4.7 inset, was built out of stainless steel, which was connected to a low-pressure (house) air source**.** After sample addition, the house air is turned on to move the sample into the reaction chamber, which is 2m by 2.1cm diameter. The volume of the reaction chamber is approximately 1L. Typical liquid sample volumes were 500mL in order to provide adequate mixing space with the vapor phase. To maximize surface area, the bubble length must be at least 5 times the diameter, which corresponds to the reactor geometry.

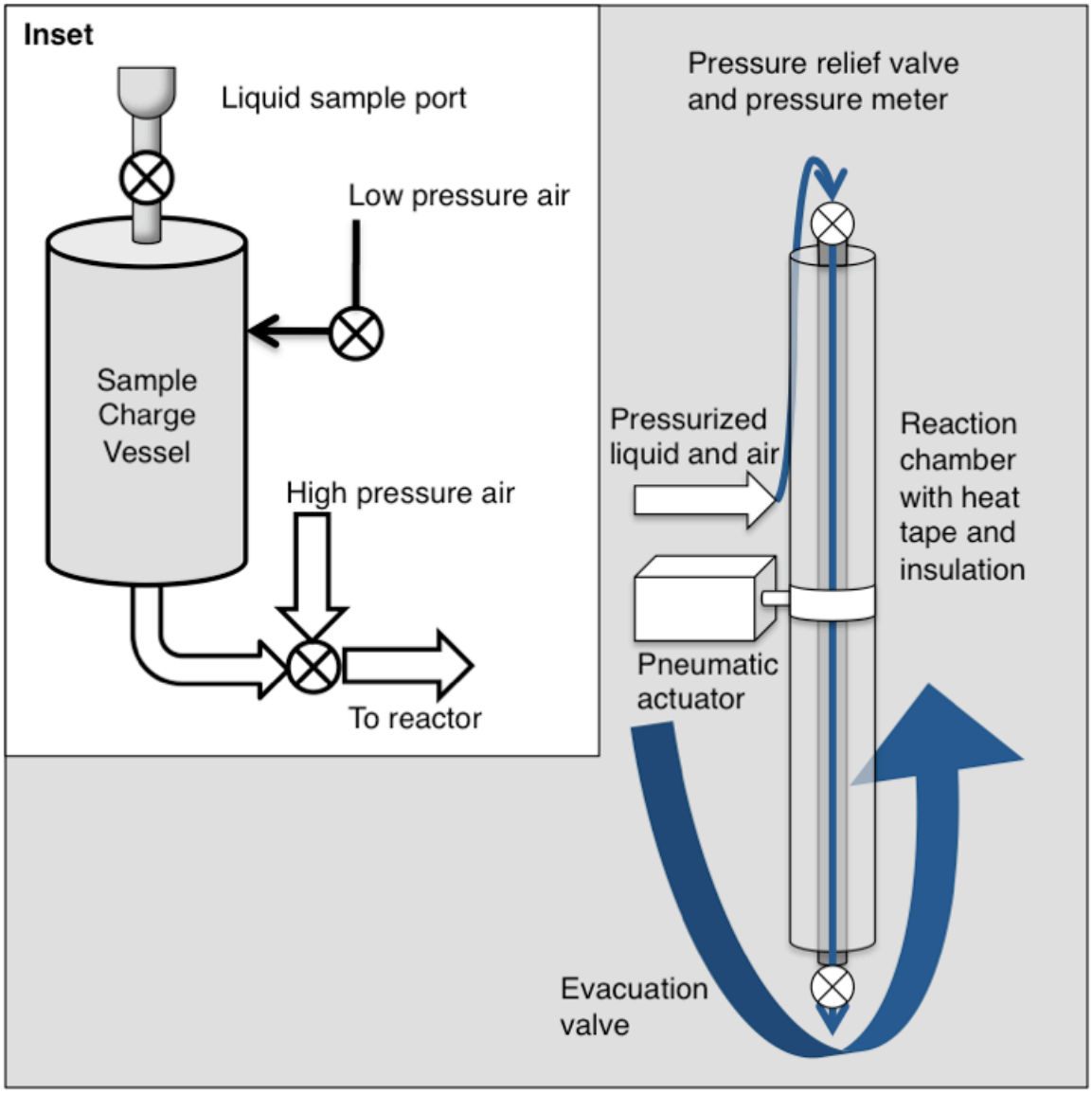

Figure 4.7 Detailed schematic of rotating vertical tube reactor. Inset: Liquid sample introduction apparatus

Once the liquid sample is added to the reaction chamber, the charge vessel can be isolated, and high-pressure air can be added to charge the reaction chamber to the desired pressure. For all studies, high-pressure air was provided by a cylinder of breathing air without additional purification. The reactor vessel was wrapped with heat tape and conductive heating wire, which was temperature controlled via a rheostat. Three K-type thermocouples are used to monitor the reaction temperature at each end and the middle of the tube.

The pressure is monitored via a pressure sensor during both the initial charging of the system and during operation. A pressure relief valve is placed after the pressure sensor to prevent pressures above 15.2MPa (2000PSI). The reactor tube was rotated via a Pneuturn® air actuator, which was charged with a regulated nitrogen cylinder (Bimba, Monee, Il). In order to facilitate rapid cooling of the reaction chamber after operation, house air was connected to a cooling tube running alongside the reaction tube, causing rapid heat transfer out of the chamber. An evacuation valve is placed at the end of the reactor tube for the release of treated sample.

4.2.2 Chemicals and Materials

Deionized and high purity water for all solutions and mobile phases was prepared using a Milli-Q water purification system (Millipore, Billerica, MA). All chemical standards were reagent grade purity or higher and used without further

purification. Acetonitrile was obtained from Pharmco (Shelbyville, KY). Glacial acetic acid and glucose were obtained from Fisher Scientific (Pittsburgh, PA). Formic acid was obtained from EMD (Gibbstown, NJ). Glycolic acid was obtained from VWR International (West Chester, PA). Sodium carbonate and sodium bicarbonate were purchased from Baker (Lopatcong, NJ).

High purity cellulose was produced through homogenization of #40 Whatman filter paper in water. Samples of bovine and hog manure were provided from farms local to the Denver metropolitan area and prepared with approximate concentrations of 10g L^{-1} after homogenization in water. The FDA Denver District Laboratory provided the sulfonamides sulfadiazine and sulfadimethoxine, and solutions were made either in pure water or 75:25 water: acetonitrile for sulfadimethoxine. Glucose was added if necessary to bring the treatment mixture to an appropriate initial chemical oxygen demand, to better model actual waste streams with polar contaminants.

4.3 Analytical Methods

For studies using the SWC-FID system, the instrument was used to derive chromatographic values such as retention factor and peak area. To analyze the effluent of the wet oxidation reactor, several techniques were used and depended on the analyte in question. All wet oxidation reactor effluent was tested for pH, conductivity, total solids, and chemical oxygen demand. In addition, some effluent was analyzed for anion content, especially for organic acid and nitrate concentrations as a measure of nitrification and organic molecule conversion in the reaction process. To quantify the removal of sulfonamide antibiotics, a HPLC method with UV detection was used.

4.3.1 Determination of Limits of Detection for SWC-FID System

A simplistic determination of limits of detection is performed by calculating the relative standard deviation of a series of low concentration analytes, determining the signal to noise ratio (s/n), and calculating the equivalent concentration with a s/n=3. This is generally an unacceptable method, as the relative standard deviation is likely to be variable with the concentration of the analyte injected, and, as such, the predicted limit of detection is arbitrary (Long and Winefordner, 1983). A more accurate method of modeling the standard deviation of system noise is by using the standard deviation of a regression value, $s_{Y/X}$ as the noise deviation, and then determining a limit of detection from

the equivalent injection of a mass with signal $=3s_{Y/X}$ (Vial and Jardy, 1999). Typical regressions of concentration versus signal are linear; however it is likely that the variance at different concentrations is not equivalent. While the relative standard deviation of a signal is likely to be smaller at higher concentrations, the raw error is also larger, so normal least squares regressions will attempt to minimize this error. A more appropriate regression value for heteroscedastic data is the weighted least squares analysis. Weights are calculated by the inverse of the individual variance of each measurement, which is normalized to the population size *n* and then multiplied by the measurement, thus equally weighting error contributions from lower concentration samples with higher ones. For this study, normal least squares analysis was calculated in Microsoft Excel, and weighted least squares analysis was calculated via the java-based Linear Least Squares Calculator (Bertrand, 2000). For all LOD measurements, the standard value of 3σ is used as a coverage factor.

4.3.2 Retention of Analytes in Subcritical Water Chromatography

Data used in Chapters 5 and 6 were generated on the custom SWC-FID system described in section 4.1.5, using a Zirchrom® Diamondbond-C18® zirconia column. For all data reported, retention of analytes was determined via a peak area measure of the FID chromatogram, and retention factors were determined against the minimally retained analyte methanol. All reported

retention factors are recorded as an average of at least 3 replicates. Sample solution injections of 10µL were used in all cases except where specifically noted. The SWC-FID system has an operational temperature range from about 125ºC to 200ºC with a mobile phase flow rate from 40-100µL min^{-1}. For all mechanistic studies in Chapter 6, the mobile phase flow rate was 100µL min^{-1} to maximize column efficiency.

In the mechanistic studies of retention, two theoretical models were used. The first method used the linear solvation energy relationships of analyte retention. A custom library of compound solute characteristics was derived from two published sources (Torres-Lapasió et al., 2004; Quina et al., 2005). Regressions of analyte characteristics and retention factors of 34 analytes was performed using Microsoft Excel and are listed in Chapter 6. This number of analytes is sufficient to accurately fit all 5 of the analyte solute descriptors, and analytes were selected for a wide coverage of analyte descriptor values and to break covariance trends (Vitha and Carr, 2006).

For the relationships of enthalpy of transfer, the van't Hoff equation was used to relate retention factors as a function of temperature, with methods derived from Coym and Dorsey (2004) and Cole et al. (1992); a linear regression of the natural logarithm of the retention factor was plotted against 1/T in K, using linear and polynomial fits built into Microsoft Excel.

4.3.3 HPLC with UV Detection

For the analysis of breakdown products of the wet oxidation reactor, reversed-phase LC (RPLC) with UV detection was used to measure the concentration of analytes with readily available chromophores. This was used to specifically quantify the breakdown of sulfonamide antibiotics during reactor treatment. An Agilent 1100 Series binary HPLC system with a multiple wavelength detector and autosampler was used for all separations (Agilent, Santa Clara, CA). Samples were injected without further treatment. Five (5) µL sample volumes were separated isocratically with 80:20 water: acetonitrile on an Xterra RP_8 column (3.5µm, 4.6 × 50 mm; Waters Corporation, Milford, MA, USA). Detection was performed at 270nm, and quantification was based upon peak areas integrated with the Agilent ChemStation® software. A limit of detection of 0.06ng μL^{-1} was determined for sulfadiazine, and 0.02ng μL^{-1} for sulfadimethoxine using the WLS method previously described in section 4.3.1.

4.3.4 Ion Chromatography

Organic acids and other inorganic anions were quantified using a Dionex DX-120 ion chromatography (IC) system in anion mode (Dionex, Sunnyvale, CA). The IC was equipped with a 10µL sample injection loop and an Alltech Element A-1 anion column (7µm, 4.6 × 50 mm; Grace, Deerfield, IL, USA) was used for separations, using suppressed conductivity detection. An eluent composed of

1.4mM sodium bicarbonate, 1.1mM sodium carbonate, and 1% acetonitrile was used for all IC separations. Samples were prepared for IC by dilution of the sample 1:10 or 1:100 in the anion eluent and then filtered with a 13mm syringe filter (0.45µm PTFE membrane, VWR; West Chester, PA).

4.3.5 Descriptive Analysis of Wet Oxidation Reactor Products

Chemical oxygen demand (COD) was tested via the ASTM-508 method with dichromate oxidation. Briefly, all organic molecules are converted to CO_2 (NO_3^- for nitrogen) in this reaction by potassium dichromate in strong acid, causing a color change as the dichromate is consumed and $Cr^{3+}_{(aq)}$ is produced. A standardized reactor digestion tube method was purchased to perform this quantification (part # 21259-15; Hach, Loveland, CO), which was validated against a solution of 100ppm glucose. The linear range of this method is from 0-1500 mg L^{-1}; thus all test solutions were diluted 1:5 in water before analysis.

Total solids were measured via the ASTM-208A method for quantification of total residue at 103-105ºC. Briefly, a sample of 20-50mL of sample was dried in a tared crucible for 4-24 hours at 103ºC, and the residue was measured after cooling in a dessicator. After additional dessicator time, the measurement was repeated, as needed if the sample appeared to still have moisture.

Conductivity and pH measurements of reactor breakdown products were performed with a Hanna 98129 combo pH and conductivity meter (Hanna, Woonsocket, RI).

4.4 Configurational-Bias Monte Carlo Simulations

For studies of subcritical water behavior, a simulation methods was developed for the description of hydrogen bonding ordering, density, and volume phase ratio as compared to a model stationary phase using a configurational-bias Monte Carlo (CBMC) simulation. For the simulator, Towhee, a freely available Unix application was installed on a local server (Siepmann and Martin, 1999). Towhee has an advantage over other common molecular dynamics simulators, as it is specifically written for CBMC as opposed to other conventional molecular dynamics (MD) or Monte Carlo (MC) simulation types and has been used extensively to model systems with vapor-liquid equilibria or with multiple phases in thermodynamic contact. Configurational-bias MC was chosen to favor interactions that would be enhanced by positions which are favored by hydrogen bonding, as opposed to sampling all space, which can result in chemically improbable conformations for the long molecules seen in the model stationary phase. This program has also proven useful for high pressure and temperature calculations (Rai et al., 2007).

For modeling of water, the TIP4P forcefield was used (Jorgensen et al., 1983). TIP4P is a hard sphere model of a water molecule, with a strongly localized negative charge outside of the oxygen atom to simulate electron density in the extended p orbitals. Typical experiments used 1000 water molecules. Octadecane was used as a model stationary phase, and was modeled using the TraPPE-UA forcefield (Martin and Siepmann, 1999). This united-atom forcefield was selected due to its ability to selectively arrange long chain molecules in specific torsions for initial configurations, thus removing system bias in the initial arrangement of molecules. Typical experiments used 5 octadecane molecules, which approximate the surface concentration of octadecane in a typical C18 phase, ~2.5µmol m^{-2}.

The isobaric-isothermal (constant moles, pressure and temperature, referred to as NPT) ensemble was used for all simulations. This is the correct ensemble for usage as no change in the moles of analytes is expected, and, in real world experiments, an isobaric bath is provided by system backpressure. For both water only and multi-phase experiments, the volume of the experimental box was allowed to change significantly (an isotropic volume move of 5Å allowed at every cycle) so as to allow the system equilibrate at the given temperature. A pressure of 1500kPa was used for all experiments; this pressure is sufficient to maintain a liquid phase to approximately 275ºC. Initial box dimensions were set to 40Å in all directions, and two boxes were used for volume interactions in the

phase ratio experiment. Input files for simulation experiments are provided in Appendix A.

In order to interpret hydrogen bond densities, the radial distribution function was derived using the program's internal "movie" descriptor function. Radial distribution functions were derived from pairing distance frequencies of atoms. For all simulations, the radial density values of atoms were calculated to a resolution of 0.08Å.

Atomic distribution functions were used for the calculation of spatial distributions of molecules. Atomic distributions were normalized by the program function to 1 along each box axis, and twenty points were used for distribution steps, allowing for comparison of simulation boxes with different final sizes. All distributions were calculated by determining the product of distributions in the x and y direction; this is equivalent to observing the atomic distribution compressed to a two dimensional map along the z-axis.

For water, a normalizing function was used to correlate pairing densities of individual atoms to the overall radial density; this function is derived from neutron scattering values, as cited by Chen and Teixeira (1986) and by Martí (2000), and is provided in equation 4.2, where $g_{OO}(r)$ is the pairing density between one oxygen atom and another; $g_{OH}(r)$ is the pairing density between one oxygen atom and one hydrogen atom, and $g_{HH}(r)$ is the pairing density between two hydrogen atoms

$$g(r) = 0.092g_{OO}(r) + 0.422g_{OH}(r) + 0.486g_{HH}(r) \quad [4.2]$$

Chapter 5: Applications of Subcritical Water Chromatography with Flame Ionization Detection (SWC-FID)

The next three chapters in this dissertation summarize results of the three studies discussed in Chapters 3 and 4. Chapter 5 describes the optimization and utilization of SWC-FID as a screening tool for organic contaminants. Chapter 6 outlines the mechanistic studies of solute retention in subcritical water, and Chapter 7 gives the results of the subcritical water wet oxidation reactor.

Using a fast screening instrument as a first identification of contamination greatly reduces analysis time, as uncontaminated samples do not require the workup and analysis associated with very specific and sensitive methods. SWC-FID is an example of a fast screen; while FID detection does not provide sample structural identification, the detector is universal for organic molecules. Using carefully selected standards, individual analytes and classes of contaminants can be identified in samples; these samples can then in turn undergo more comprehensive analysis with techniques such as LC-MS. In order to be an acceptable fast screen, the instrument must have detection limits in the range of

expected analyte concentrations, which in this case would likely be in the ppb range. The techniques must also tolerate high concentrations, requiring a large dynamic range. Extensions of this basic SWC-FID instrument are discussed for more selective detection, but the main advantage of using FID detection is its universality. By coupling a liquid chromatography technique to a FID, universal organic detection is extended to the study of polar environmental contaminants.

5.1 Optimization of SWC-FID Detection

In order to maximize detector sensitivity, a series of experiments were performed to probe the variable parameter space of the SWC-FID. Of these variables, the detector fuel ratio, temperature, and makeup gas flow rates were determined to be the primary targets for system optimization because they would likely be constant for all separation methods. Initial system parameters were modeled after the parameters measured by Guillarme et al. (2004) and Ingelse et al. (1998). The mobile phase flow rate, injection volumes, and stationary phase temperatures were not considered in the optimization experiments since they were allowed to vary to suit the specific requirements of a given separation method. For each optimization parameter range, the peak area of a 4μg methanol injection was measured at a constant mobile phase flow rate (75μL min^{-1}) and column temperature (150ºC). The initial parameters for the SWC-FID system are listed in Table 5.1. The signal to noise ratio (s/n) and the peak areas

were determined in each trial for system evaluation through a minimum of 3 replicate injections. After each parameter was probed, the value with the maximum s/n was used as a constant for the next parameter.

Table 5.1 SWC-FID optimization parameters

Parameter	Initial value	Working Parameter
FID temperature	400°C	400°C
FID hydrogen flow rate	50 sccm	55 sccm
FID air flow rate	250 sccm	375 sccm
FID makeup gas flow rate	0 sccm	0-25 sccm
Mobile phase flow rate	75μL min^{-1}	50-100μL min^{-1}
GC oven temperature	150°C	125°C-200°C

5.1.1 Hydrogen and Air Gas Flow Rates in the FID

The hydrogen and air flow rates were tested to determine the optimal flow rates at each. The hydrogen flow rate into the FID was tested from 40 to 100 sccm at a constant airflow rate of 250sccm. Previous studies have suggested that hydrogen flow rates have the most dramatic impact on the detector response, (Guillarme et al., 2004; Hooijschuur et al., 2000) which is confirmed by these data. In Figure 5.1, the s/n is graphed in terms of the H_2:O_2 fuel ratio. A brief note: all s/n ratios in this section are displayed in red, whereas direct peak area values are presented in blue. All hydrogen flow rates are beneath the equimolar fuel ratio, making the flame oxygen rich. From this plot, an equivalent flow rate of 55sccm hydrogen was found to be optimal. Air flow rates from 250 to 500 sccm were then tested at the optimized hydrogen flow rate. Changing the

airflow rate had a less dramatic effect on s/n, suggesting a wider parameter range is possible for airflow, so long as the approximate fuel ratio is maintained. An airflow rate of 375 sccm was used for most experiments. A typical setup for the same detector in capillary GC would be 30sccm hydrogen, 400sccm air and 25sccm makeup gas, indicating that optimized operation for the SWC-FID required slightly richer fuel ratios than detector setups for traditional GC (from HP 6890 Service Manual).

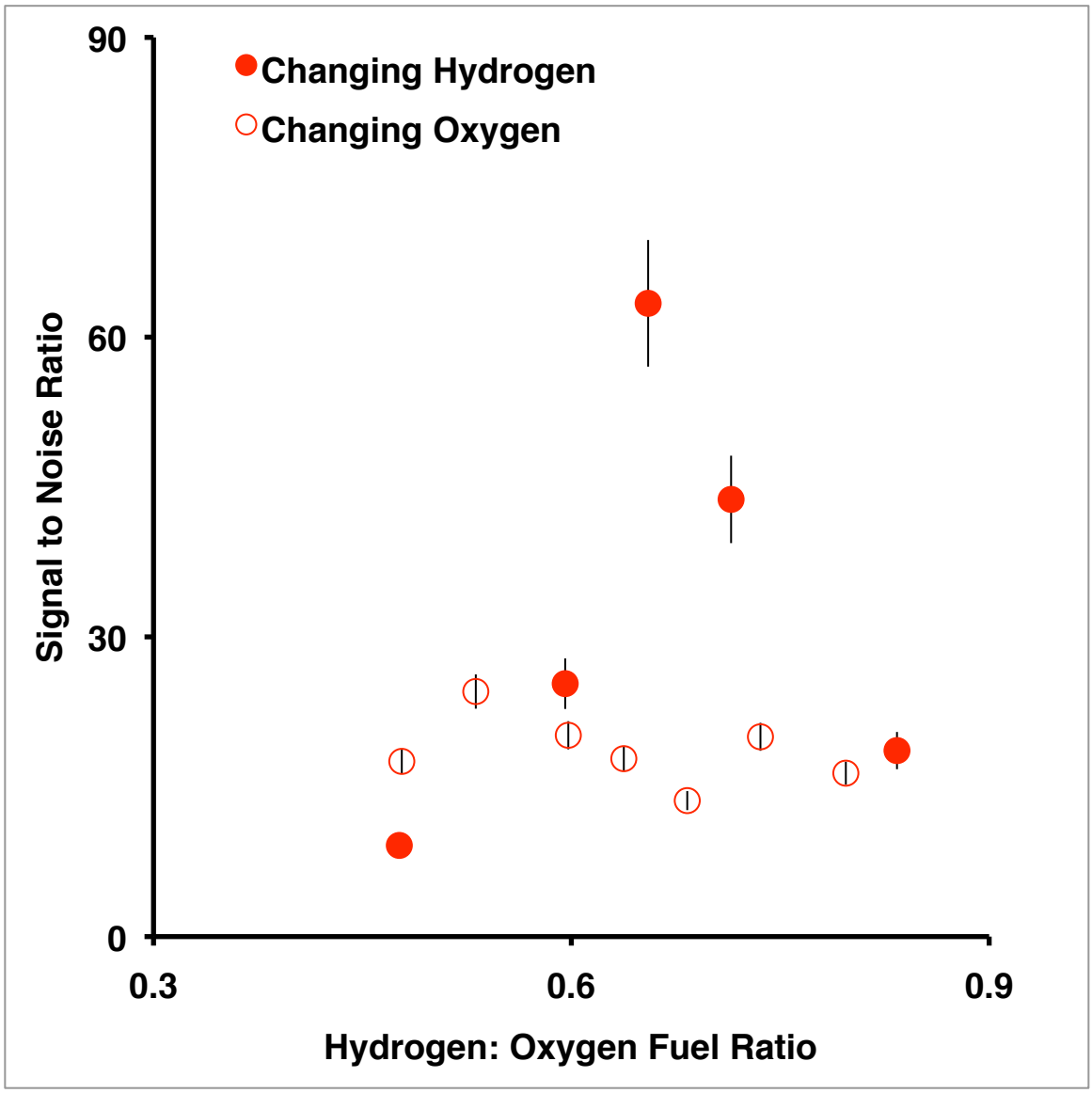

Figure 5.1 FID fuel ratio optimization. Hydrogen flow rate changes have a more dramatic impact than air flow rate changes, and the maximum s/n for each parameter is used as a system constant in successive experiments. Error bar values reflect the percent error value as compared to signal size.

5.1.2 FID Temperature and Makeup Gas Optimization

Higher than typical FID temperatures result in better analyte response in SWC-FID systems, as a high temperature is required to flash the subcritical water into steam efficiently. The temperature of the detector was tested from 300 to 400°C. As shown in Figure 5.2, the s/n was plotted as a function of detector temperature. Improved sensitivity is seen at higher temperatures, as graphed in Figure 5.3. Despite the highest s/n being found at 300ºC, the relative homoscedasticity of the variance in peak areas suggested that the temperature with the greatest mean peak area was actually optimal. Typical operation for a GC-FID is at 300ºC, indicating another difference between FID operation for SWC-FID.

Nitrogen was used as a makeup gas in order to potentially enhance nebulization of the mobile phase stream without changing the FID fuel ratio. Nitrogen was tested as an additive up to 40sccm at the optimized fuel ratio and FID temperature. A s/n improvement is seen at nitrogen flow rates from 20-25 sccm, depicted in Figure 5.4. However, as seen in Figure 5.5, the addition of makeup gas had a weakly negative effect on peak area detection, and therefore, makeup gas usage was omitted from further studies.

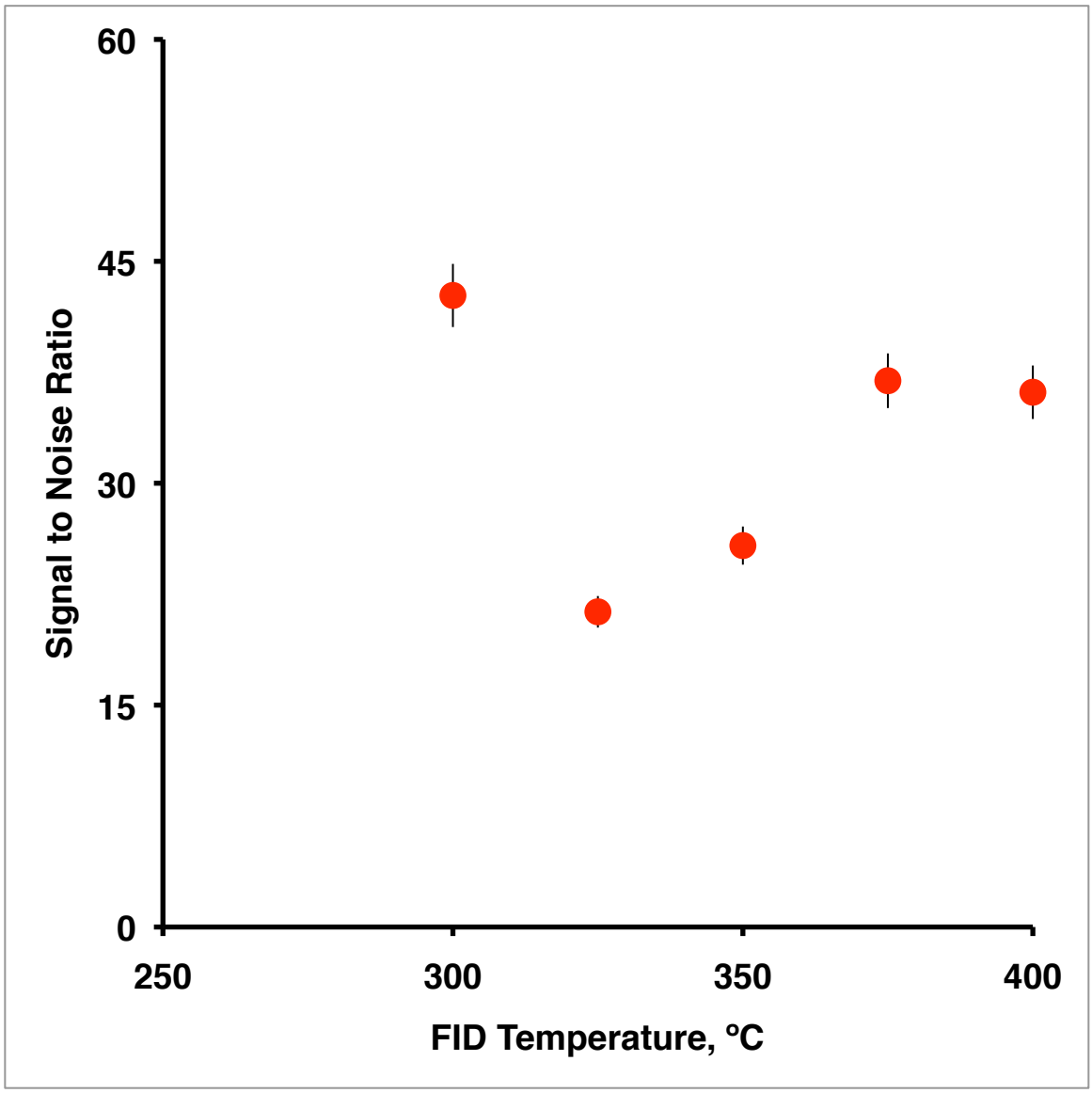

Figure 5.2 s/n of detector response due to FID temperature. The s/n was highest at the lowest temperature, 300°C. Note the relative variance in s/n, as compared to Figure 5.1, in which a more dramatic effect is observed. Error bar values reflect the percent error value as compared to signal size.

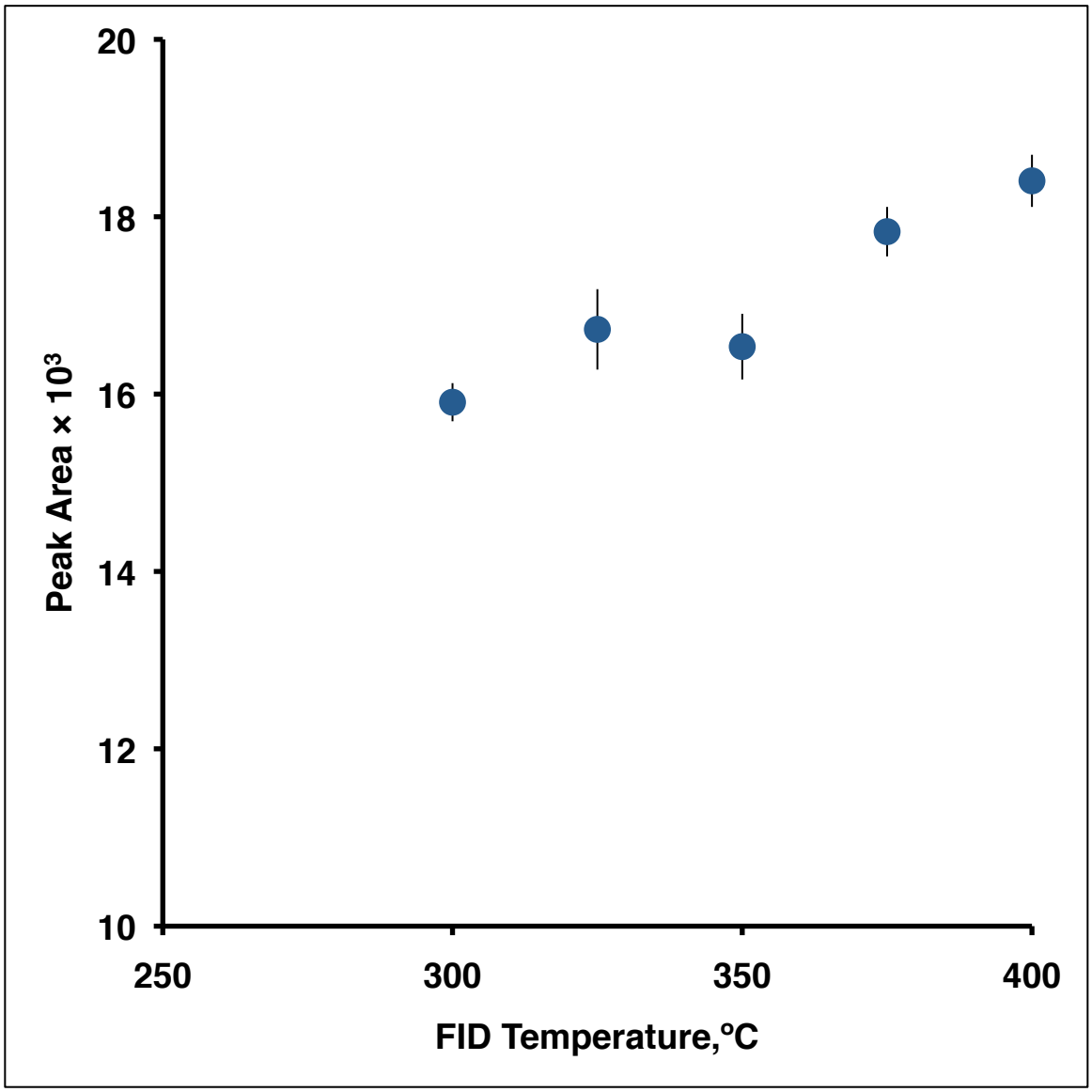

Figure 5.3 Peak area as a function of FID temperature. Although the peak area variance is smallest at the lowest temperature, the peak area of higher temperatures is greater, and the variance is relatively homoscedastic. Error bars are the standard error of the average peak area.

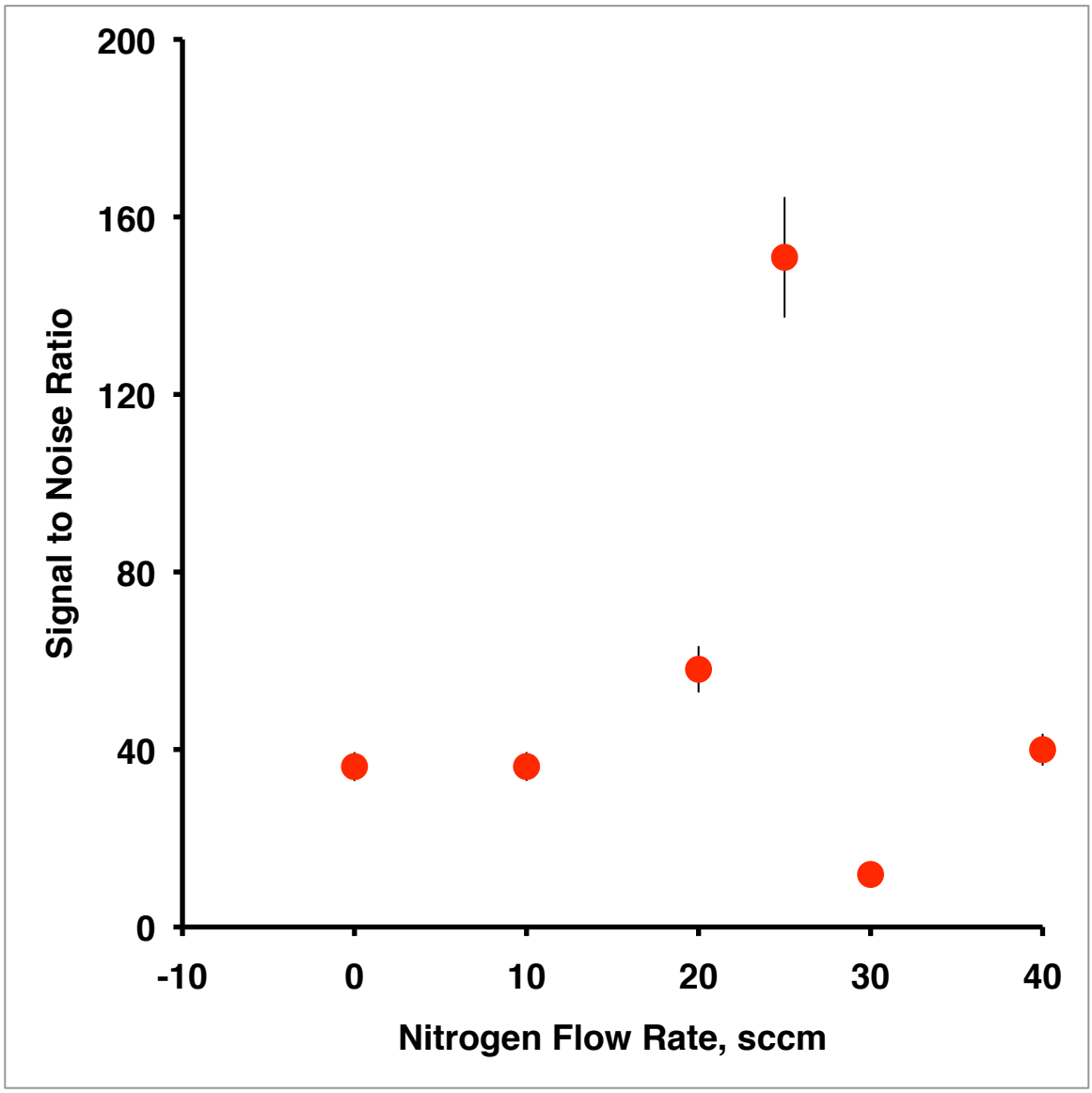

Figure 5.4 s/n of detector response to the addition of nitrogen as makeup gas. The maximum s/n is found at 25sccm. Error bar values reflect the percent error value as compared to signal size.

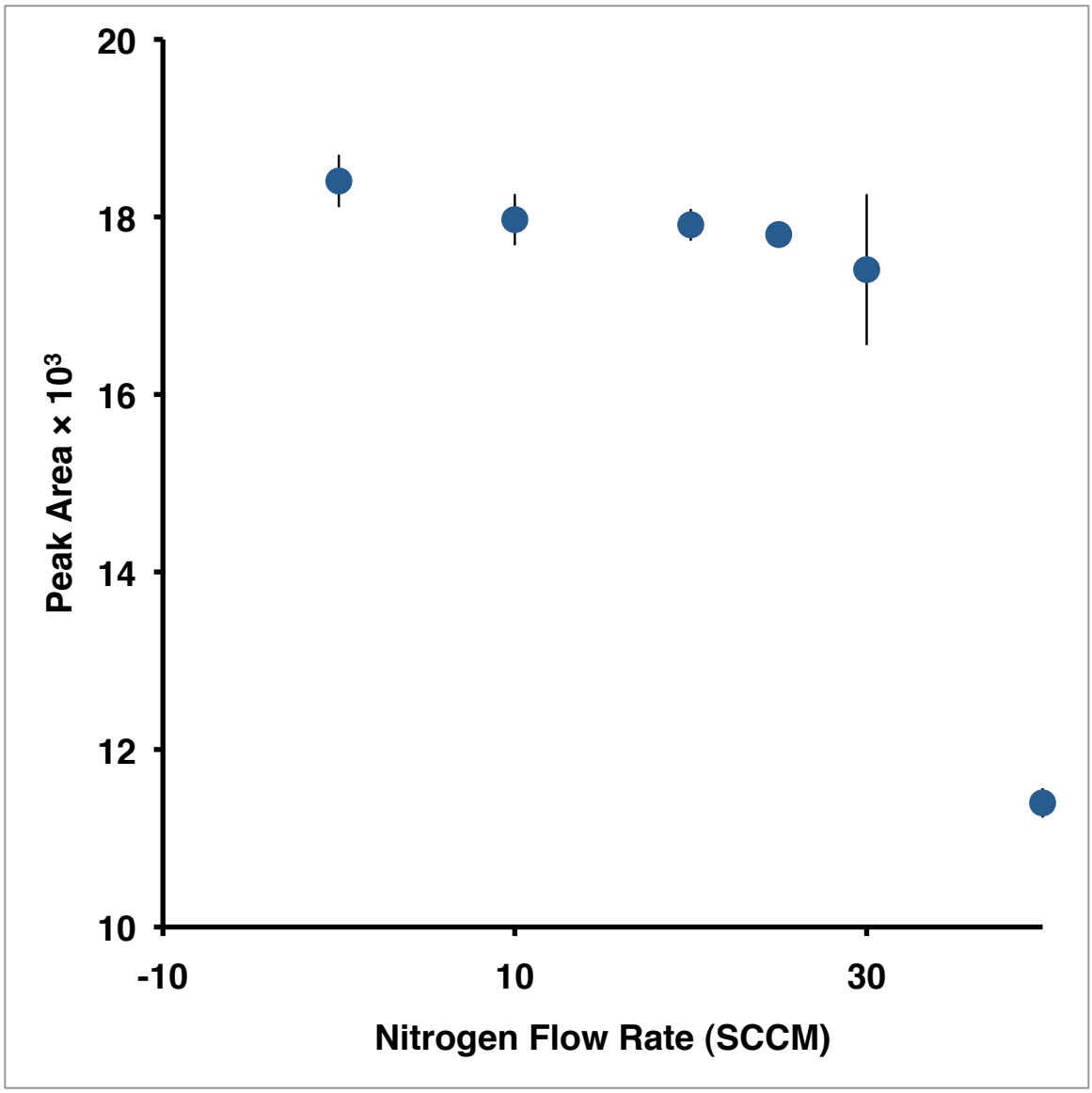

Figure 5.5 Peak area as a function of nitrogen makeup gas addition. While s/n is smallest at 25 sccm (error bars smaller than marker), the effect on peak area is slightly negative. Error bars are the standard error of the average peak area.

5.2 Improved detector sensitivity with SWC-FID

Previous work in SWC has often focused on detection of analytes that make up 0.1-10% of the overall solution. Using the optimized SWC-FID configuration with direct injection, the limit of detection was determined for a series of compounds previously reported in other SWC systems. The linear range of the FID was also used to extend the operational flexibility of the instrument.

5.2.1 Limits of detection using the optimized SWC-FID

Traditional LC methods for determining the LOD for a given analyte generally use a flow injection methods without a stationary phase in place, so as to provide a pure measurement of the detector response to the injection of analyte without any concentration or broadening from the separation mechanism. However, for this system, the traditional method is not possible, as detector stability depends on the back pressure provided by the back pressure capillary and the column; thus all LODs were determined with the column in place.

A common method to estimate a limit of detection is to use a dilute concentration of sample and determine the s/n of replicates at that dilution; then the mass injected is scaled to have a s/n=3. This method is performed because it is difficult, and somewhat arbitrary, to estimate background noise from a chromatogram baseline peak to peak noise. Also, as the dilution of the sample is assumed to be sufficiently close to infinite dilution that the standard deviation of

the noise measured is equivalent to the noise, σ_B, of the system background. This method ignores the high likelihood of error due to the relative scale of the sample concentration; for lower test concentrations, the relative standard deviation is greater, causing an over prediction of σ_B, with the opposite being true at higher concentrations. This effect is demonstrated in Figure 5.6, which plots the RSD of several test analytes in the SWC-FID system as a function of the logarithm of the mass injected. The analyte mass injected has an impact on predicted LODs when system noise is directly correlated to baseline (blank) noise.

A regression method uses multiple concentrations and determines the $\sigma_{Y/X}$, the variance of the regression, which can then be extrapolated to infinite dilution for a measurement of background noise (Vial and Jardy, 1999). The value of $\sigma_{Y/X}$ can be derived from an ordinary least squares (OLS) regression, but this is only valid if the variances measured are homoscedastic. As the concentration series was determined to have heteroscedastic variance, a weighted least squares (WLS) regression is a more accurate way to determine the regression variance, in order to prevent large mass addition values from dominating the regression statistics. Heteroscedasticity in sample concentration variance should not be surprising. If the tested concentration range is large, the raw values of the largest mass injection variances are substantially larger than low mass variances, despite the RSD being lower at high concentrations.

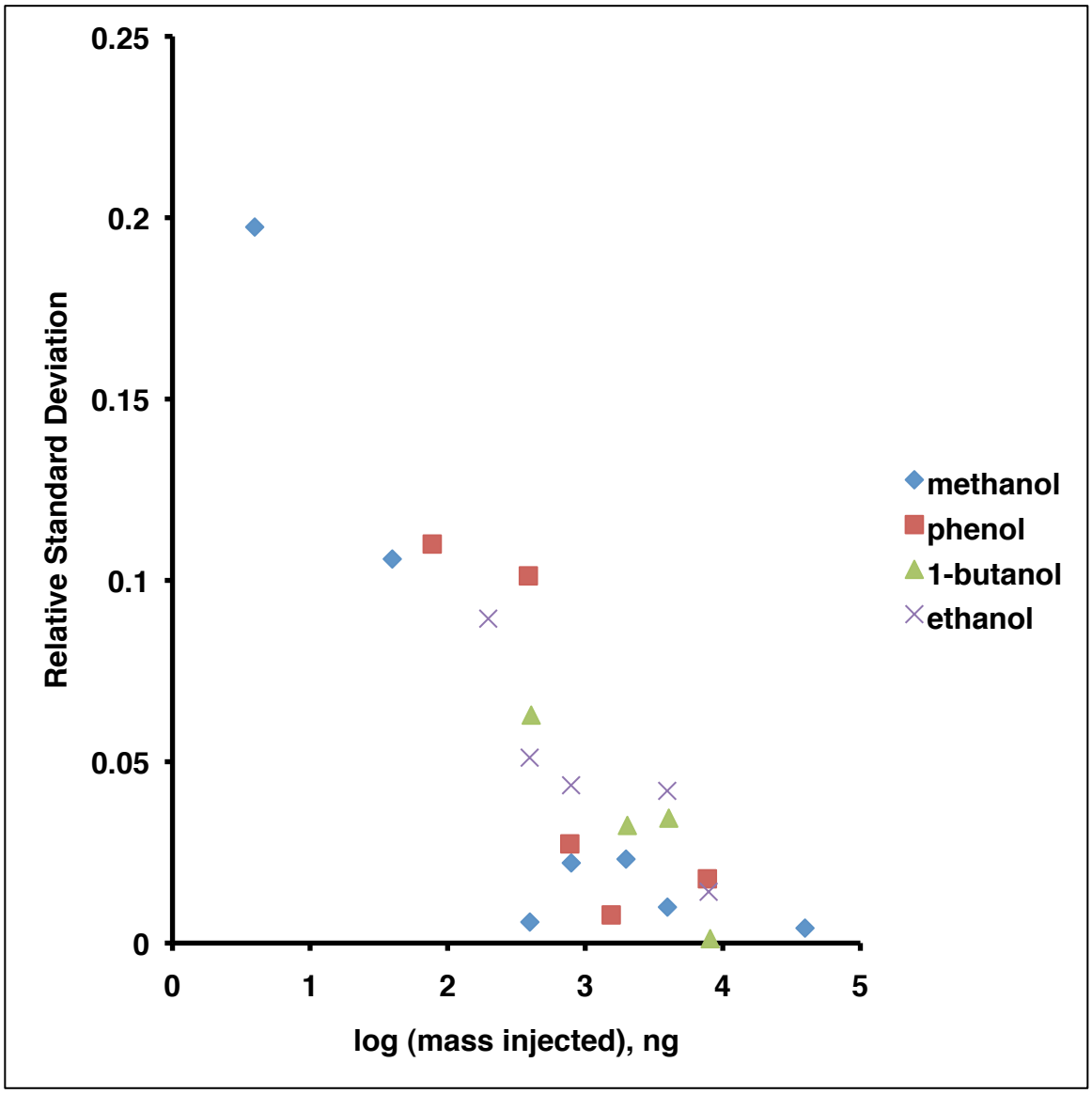

Figure 5.6 RSD of a series of analyte peak areas as a function of the mass injected.

In Table 5.2, the LODs of several compounds are reported from literature values. Many of these values were reported as s/n=3 calculations; analytes with LODs determined by a regression are noted with an asterisk. For each sample with a single point calculation, the s/n=3 LOD is reported, along with the mass injected from literature and used in this study. This is done to compare approximately equal RSD values as from the literature values cited in the table; however, significant variance between literature and this study are observed, resulting in poor correlation.

Table 5.2 Literature and experimental LODs with SWC-FID methods.

Compound	**Literature LOD, ng (mass injected)**	**s/n =3, ng (mass injected)**	**OLS area=3$\sigma_{y/x}$**	**WLS area=3$\sigma_{y/x}$**
methanol[1]	0.84 (140)	3.8 (40)	0.04	0.050
propion-aldehyde[1]	5 (500)	9.5 (2000)	0.42	0.32
tert-butanol[2]	1*	-	0.23	0.16
fructose[3]	63 (612)	180 (5000)	0.45	0.64
ethanol[4]	3 (200)	1.6 (200)	0.09	0.20
phenol[4]	0.2 (160)	0.74 (80)	0.080	0.074
1-butanol[5]	0.18*	-	0.32	0.0067
1,1,2-trichloroethane	0.06*	-	0.19	0.096
benzene❖	-	82 (440)	0.26	0.63
tetrahydro-thiophene❖	-	89 (250)	0.098	0.084

[1]Ingelse et al. (1998)
[2]Miller and Hawthorne (1997)
[3]Yang et al. (2002)
[4]Hooijschuur et al. (2000)
[5]Bruckner et al.. (1997)
*Literature LODs were determined using a regression instead of the s/n method.
❖No Literature LOD reported

Also provided in Table 5.2 are the LOD determined from an ordinary and weighted least squares analysis. These values are comparable to the detection limits reported for 1-butanol and 1,1,2-trichloroethane, which were measured using an analogous drop headspace analysis method, with LODs determined by regression analysis. One sample in literature (Miller and Hawthorne, 1997) used a regression style measurement of LOD with a directly comparable SWC-FID instrument, *tert*-butanol. A factor of 5 sensitivity improvement was seen in this sample, indicating the optimization of the FID interface was successful. Applying the regression analysis to other compounds suggests a factor of 5 or greater improvement in detection from reported values.

5.2.2. Detector Linearity

FIDs have extremely large ranges of equimolar response to carbon in the flame, and this system was found to be able to respond linearly to concentrations of analyte from the nanogram to mass % range or of at least 6 orders of magnitude. Response linearity was determined via replicate injections of methanol from 4ng to 400µg, which is summarized in Table 5.3. A correlation coefficient of 0.9922 was found for this regression.

Table 5.3 Methanol linearity data

Methanol Linearity Data	Value
Slope (Standard Deviation)	4.24 (0.073)
Intercept (Standard Deviation)	233 (48)
Observations	28
Range	4ng -400µg
Correlation Coefficient^2 (R^2)	0.9922

In Figure 5.7, the peak shape of example chromatograms of methanol concentrations are shown to align with similar peak shapes. Due to low separation efficiency and the isocratic and isothermal separation parameters for this study, tailing was expected for each of the peaks and does not indicate sample overloading.

Extrapolating from the peak to peak noise observed in the lowest (4ng) peak, an approximate LOD of 1ng would be predicted, demonstrating that 4ng is within the LOQ of this method. However, by performing the regression analysis, average values for system noise were reported, and actual LODs are predicted to be lower than in specific examples in this figure, in which higher system noise is observed. The main problem with interpreting noise directly from this chromatogram was how to non-arbitrarily assign a window of signal that would be equivalent across chromatograms, and then to correlate that value to the blank variance; even if the window was assumed to be the size of a peak width (or half height peak width), system noise assignments would be relatively arbitrary, and would lend themselves to underprediction of actual system noise.

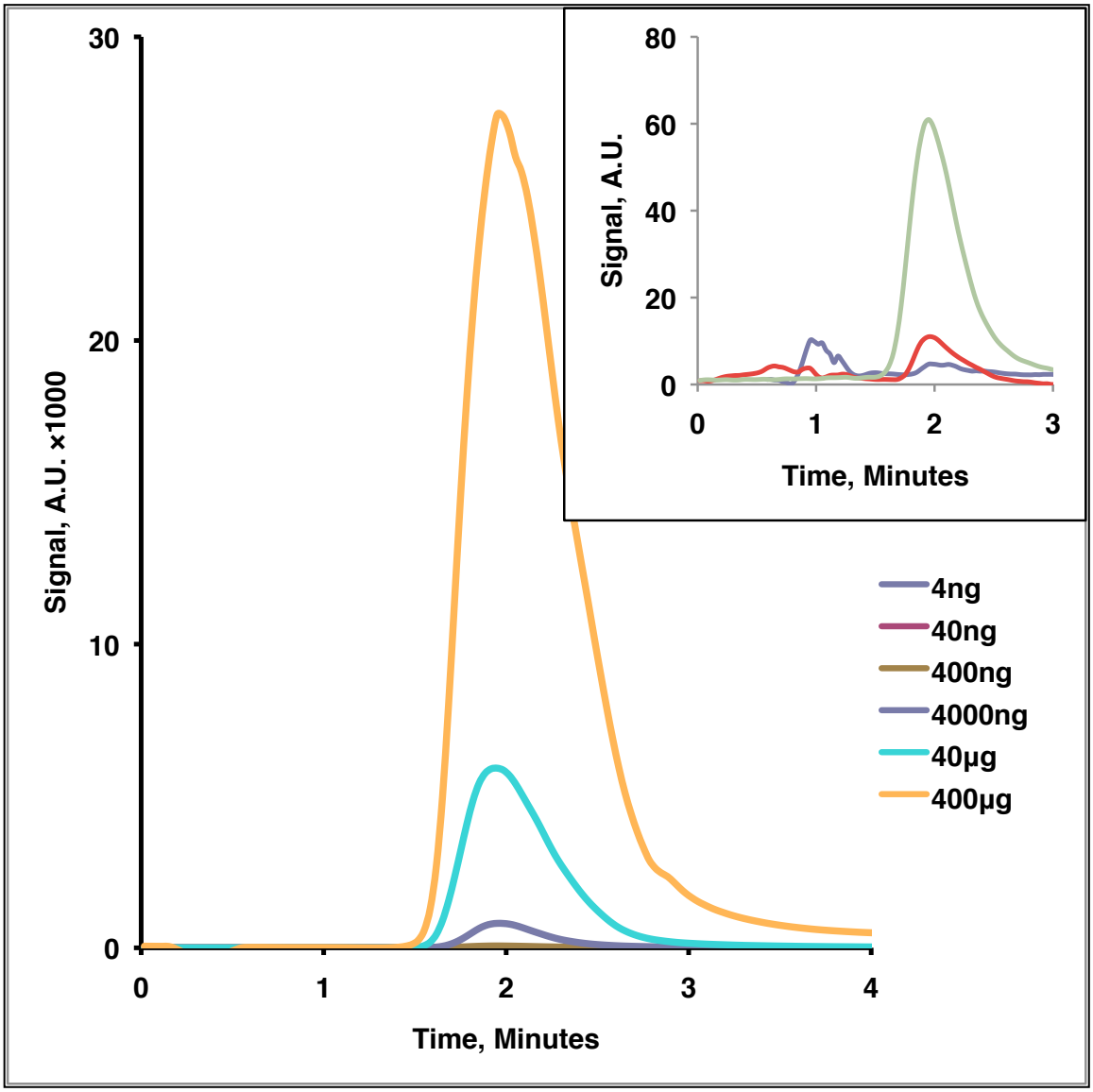

Figure 5.7 Peak shape of methanol injections at concentrations from 4ng to 400µg.

5.3 Separations with SWC-FID

Although this system was optimized for detection, several separations were performed to demonstrate the universality of the FID detector in conjunction with aqueous analytes. For all of these separations, the previously described Zirchrom® column was used with a pure water mobile phase. FID parameters were the parameters described in section 5.1, and the variable parameters are described for each separation.

5.3.1 Separation Efficiency

Typical flow rates for a column with a 2.1mm diameter should be greater than the 100µL min^{-1} flow rate used, but this was not possible with a direct hyphenation to a FID. Thus, with flow rates beneath optimal, the system efficiency is best at the maximum tolerated flow rate, approximately 100µL min^{-1}. System efficiency is also affected by column temperature, as the factors that control plate height predictions (viscosity, diffusion) are temperature dependent. This is observed in Figure 5.8, which is the experimentally determined van Deemter plot of methanol at 175 and 200ºC at various linear flow rates. The downward trend at both temperatures suggests that the dominant contribution to plate height is due to the longitudinal diffusion coefficient.

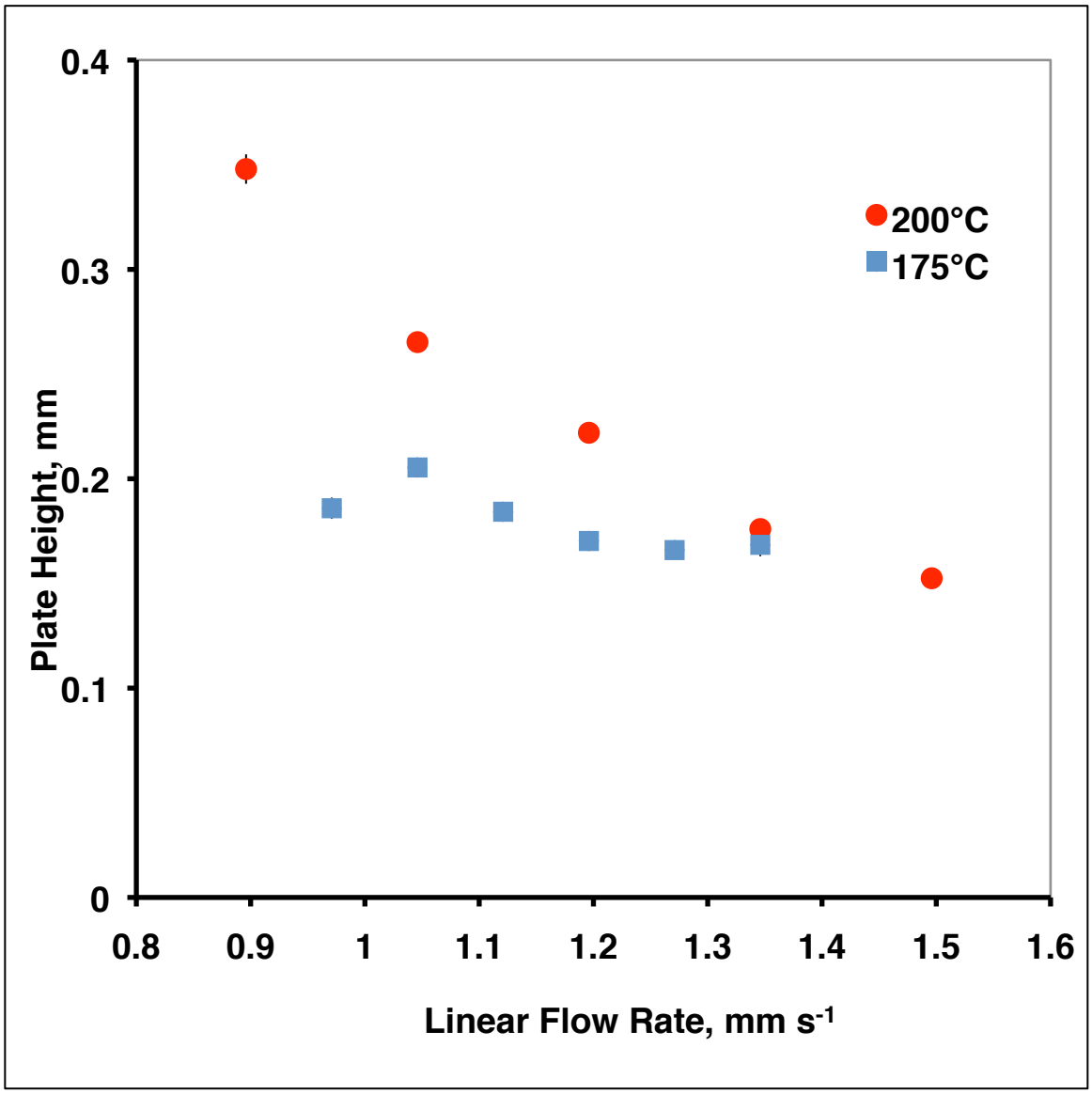

Figure 5.8 van Deemter plot of methanol retention at 175 and 200ºC. Because the B term of the van Deemter equation is directly related to temperature, the plate height is greater at 200ºC than at 175ºC for comparable flow rates, however this would be reversed at optimal flow rates, where the C term dominates, as C is inversely proportional to temperature. Error bars reflect the standard deviation of calculated plate height in mm, and are smaller than the markers used.

5.3.2 Separation of Linear Alcohols

In Figure 5.9, the separation of 6 linear alcohols is depicted. The separation was performed with a 10µL injection of a mixture of 100mg/L of methanol, *n*-pentanol, *n*-hexanol, *n*-heptanol, *n*-octanol and *n*-nonanol. The separation was performed with a mobile phase flow rate of 100µL min^{-1} at an isothermal column temperature of 200ºC. Full resolution of each of the analytes was seen and while the order of elution reflects the sample volatility, at the pressure of operation (4MPa above ambient), it is likely the analytes are still liquids until they entered the FID interface. Most of the analytes should remain in a liquid phase during the separation until elution to the FID where they are combusted. Thus, the separation mechanism must reflect the relative polarity and size of the analytes, which would provide this elution order; less polar and larger analytes can transition from the dense aqueous phase to the less dense and less polar stationary phase with greater favorability.

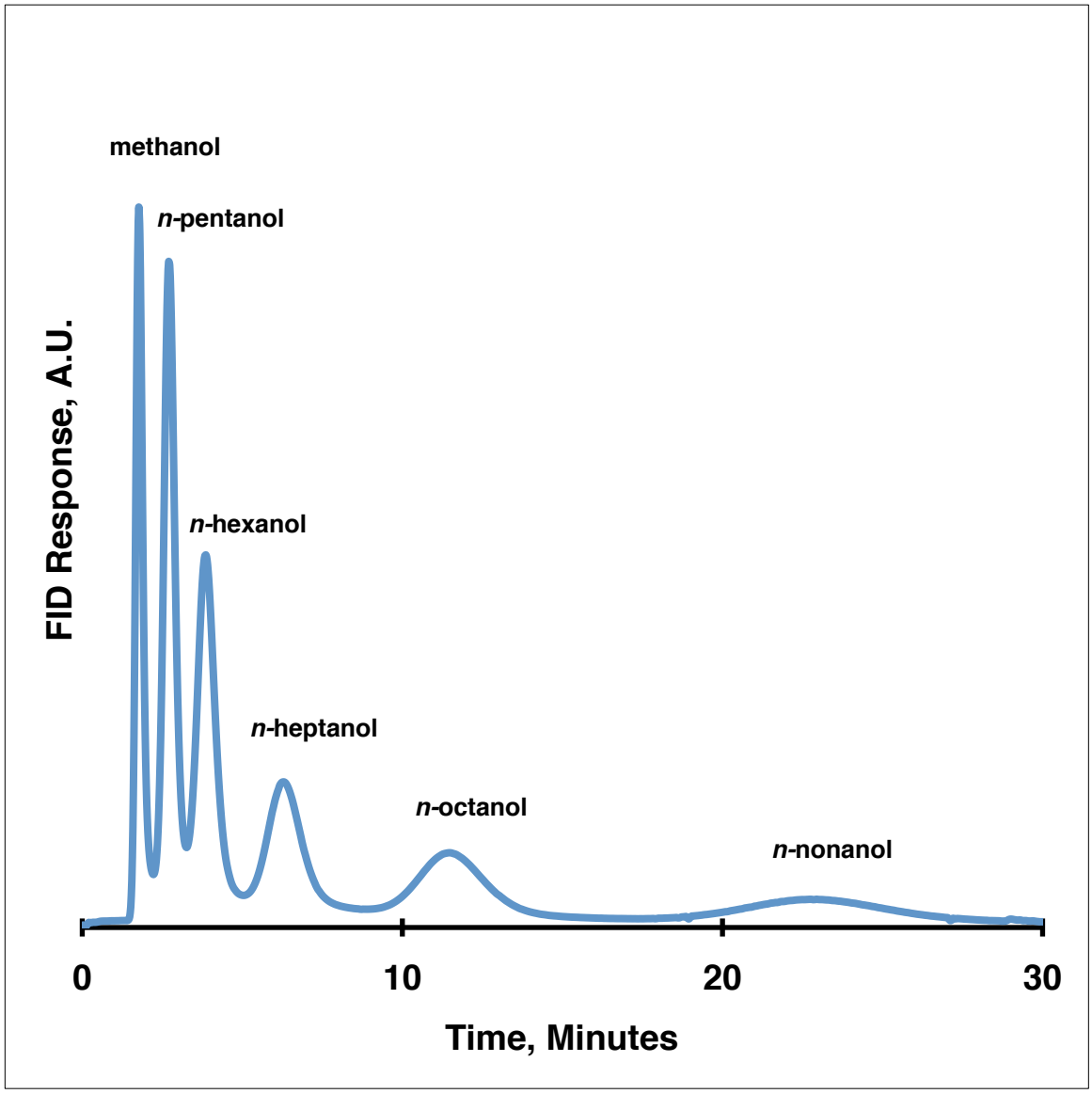

Figure 5.9 Isothermal separation of linear alcohols

5.3.3 Separation of Benzene Derivatives

Figure 5.10 shows a separation of a mixture of 500mg L^{-1} each of benzene, toluene, ethylbenzene and *m*-xylene, with methanol used as a minimally retained analyte. This separation was performed using a column temperature ramp, beginning at 175ºC and ramping to 200ºC at 1.25ºC min^{-1}. The mobile phase flow rate was 75µL min^{-1}. The dominant separation mechanism was related to analyte size. While separation efficiency was low, peak shape is improved by the thermal ramp, which acts analogously to a solvent mixing ramp in traditional reversed phase chromatography. This was demonstrated in comparison to the isothermal separation in Figure 5.9, where peak width increases dramatically for late eluting analytes. In this separation, peak width was relatively narrow for late eluting samples, allowing for greater peak capacity and separation efficiency, as is seen in solvent ramps with conventional LC.

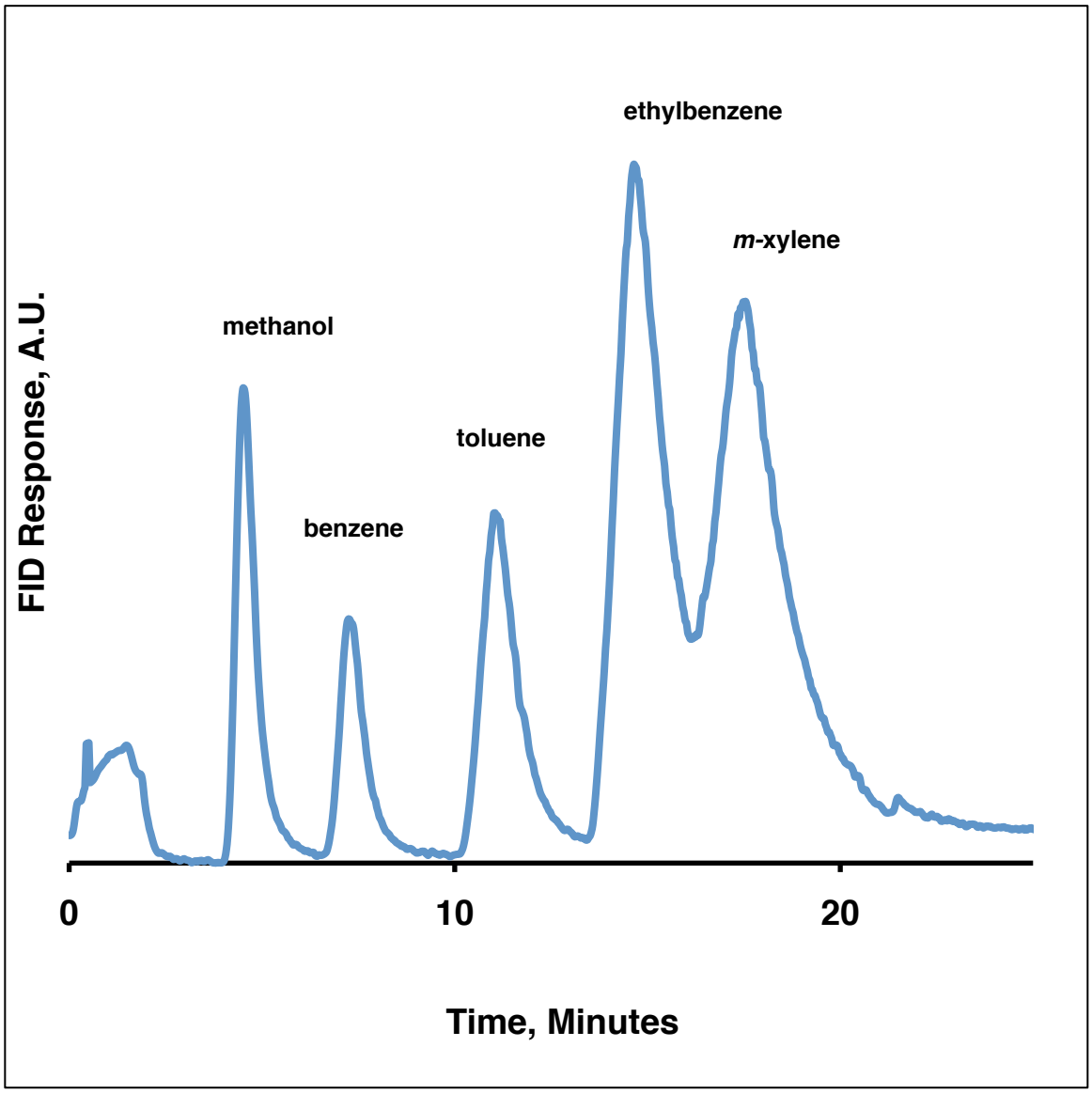

Figure 5.10 Separation of benzene derivatives

5.3.4 Separation of Substituted Phenols

In this separation, the effects of temperature on separation rate were examined, along with predictions of elution order by analyte polarity. Mixtures of 500 mg L^{-1} 1,4-dihydroxybenzene, phenol, 2-methylphenol and 4-chlorophenol were separated at 3 temperatures, 160ºC, 180ºC and 200ºC isothermally, as demonstrated in Figure 5.11. All mobile phase flow rates were 70µL min^{-1}. In Figure 5.12, the same analytes are separated using a temperature ramp, starting at 160ºC and holding for 5 minutes, followed by a 5ºC min^{-1} ramp to 200ºC. Separation efficiency was improved with the addition of a temperature ramp, and calculated efficiency values were calculated for 5 separation methods in Table 5.4. Peak capacity (the number of fully resolved peaks in a given separation) calculations for isothermal separations were performed via the method described by Stoll et al. (2008), while gradient peak capacities were calculated by the method given by Neue (2005). Theoretical plates were determined via equation 3.7.

Table 5.4 Phenol separation efficiency values

Separation Temperature Parameter	Peak Capacity	Number of Theoretical Plates
160ºC Isothermal	6.34	964
180ºC Isothermal	3.05	245
200ºC Isothermal	3.40	325
3ºC min^{-1} Temperature Gradient	11.8	872
5ºC min^{-1} Temperature Gradient	12.3	1370

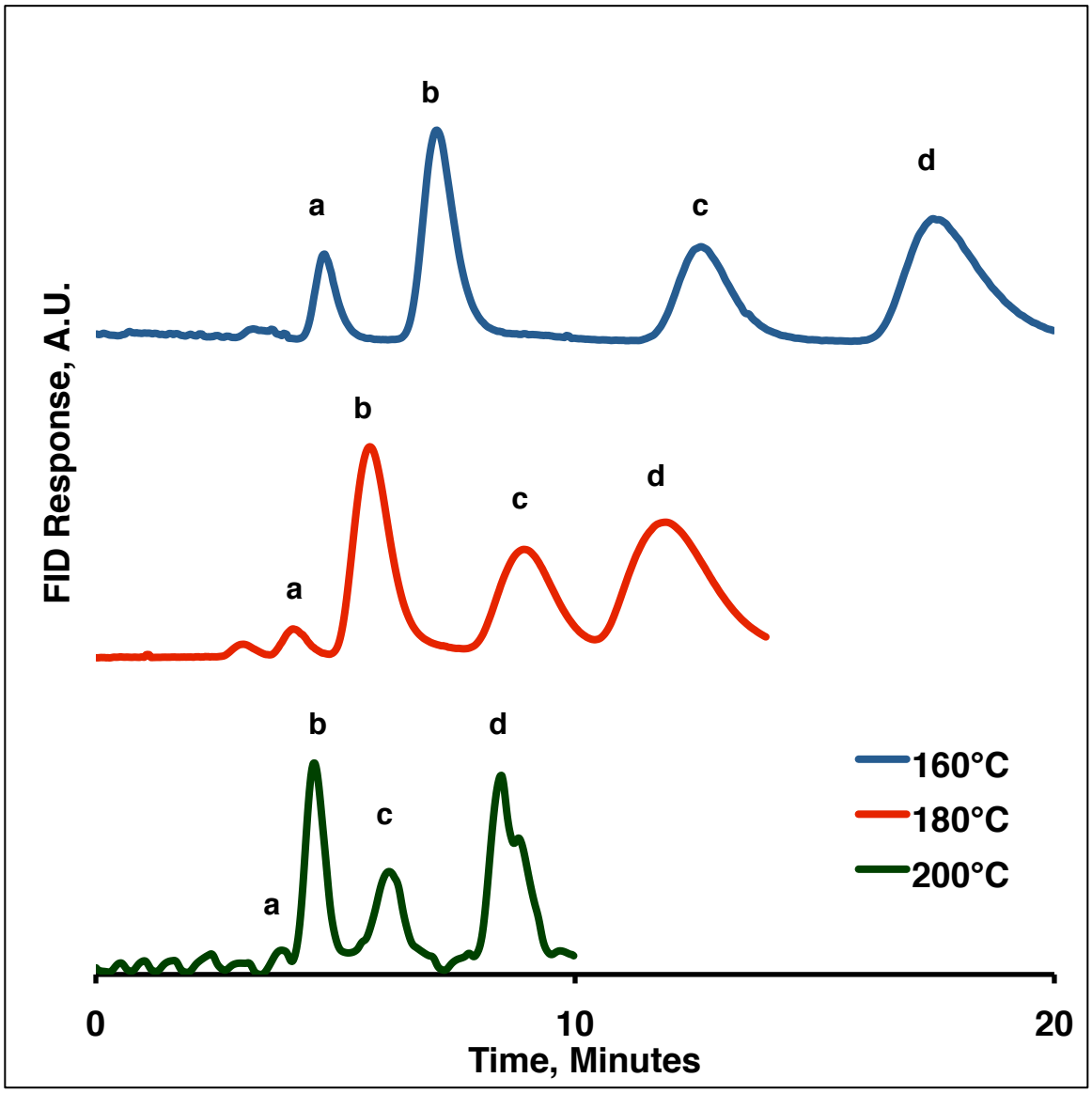

Figure 5.11 Isothermal separations of substituted phenols. (a) 1,4-dihydroxybenzene, (b) phenol, (c) 2-methylphenol, (d) 4-chlorophenol.

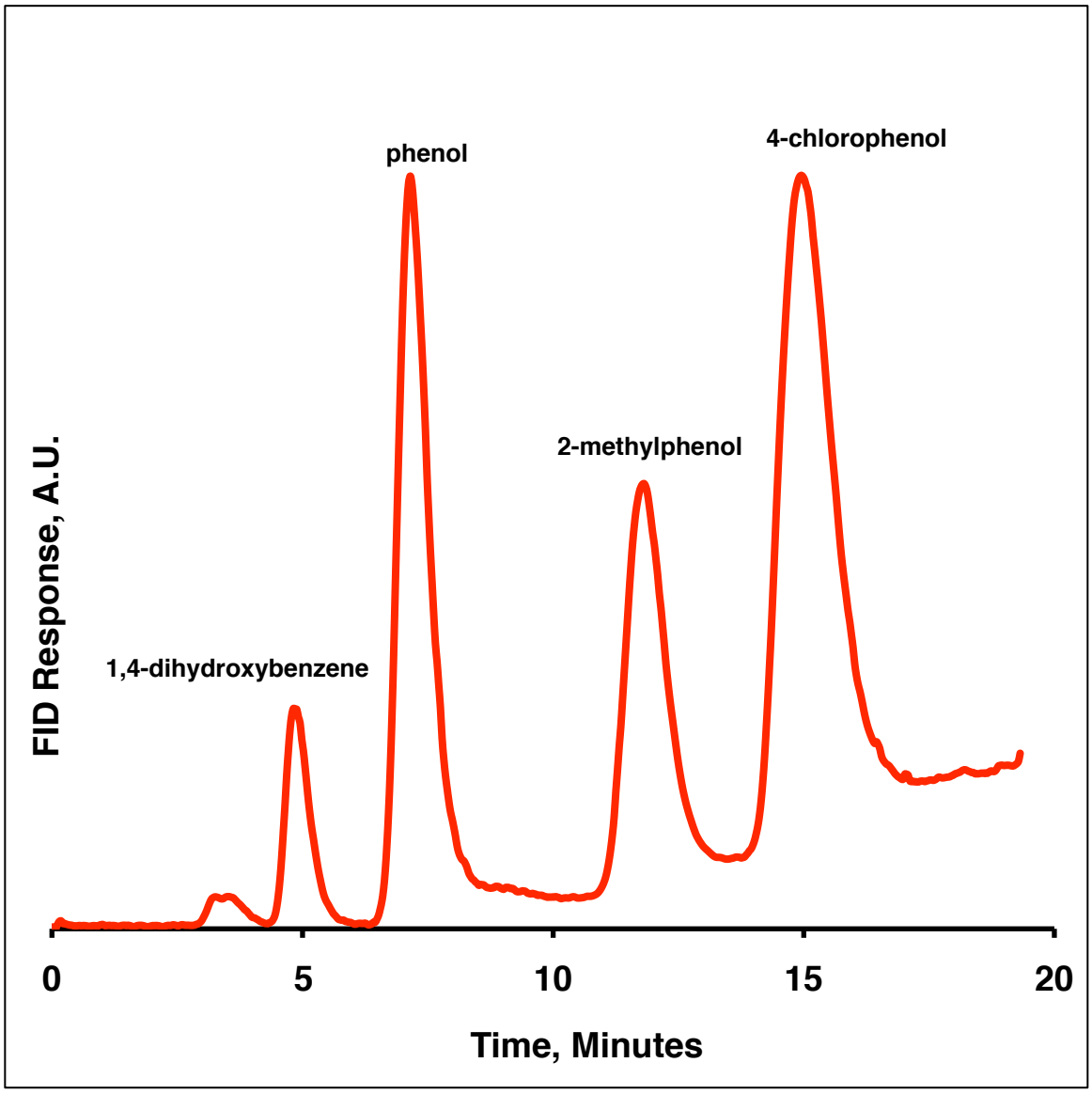

Figure 5.12 Thermal program separation of substituted phenols

In this separation series, the elution order was predicted by the analyte polarity. As analyte size is relatively similar, the polarity was the most significant difference between analytes. The mechanism of separation must be due to the favorability of mass transfer of analyte between the stationary and mobile phase.

Analyte retention was diminished as the temperature of the column was increased, indicating a decrease in the relative polarity of the mobile phase, but the order of analytes did not change, indicating that mass transfer rates were being changed by the thermal gradient instead of any modification in the retention mechanism.

5.4 Thermal effects on analyte retention

The temperature of the column and mobile phase has a measureable impact on the retention of analytes, as mass transfer is temperature dependent. However, at pressures and temperatures above 100ºC for water, the mobile phase polarity and hydrogen bonding characteristics are also modified as a function of temperature, with the dielectric constant of water dropping, and hydrogen bonding becoming less ordered. This is equivalent to mixing solvents in traditional LC, and has a similar result on analyte retention. In Figure 5.13, the retention factors of 10µL injections of 1000mg L^{-1} benzene and acetonitrile are depicted as a function of system temperature; methanol was used as a minimally retained analyte for retention factor calculations.

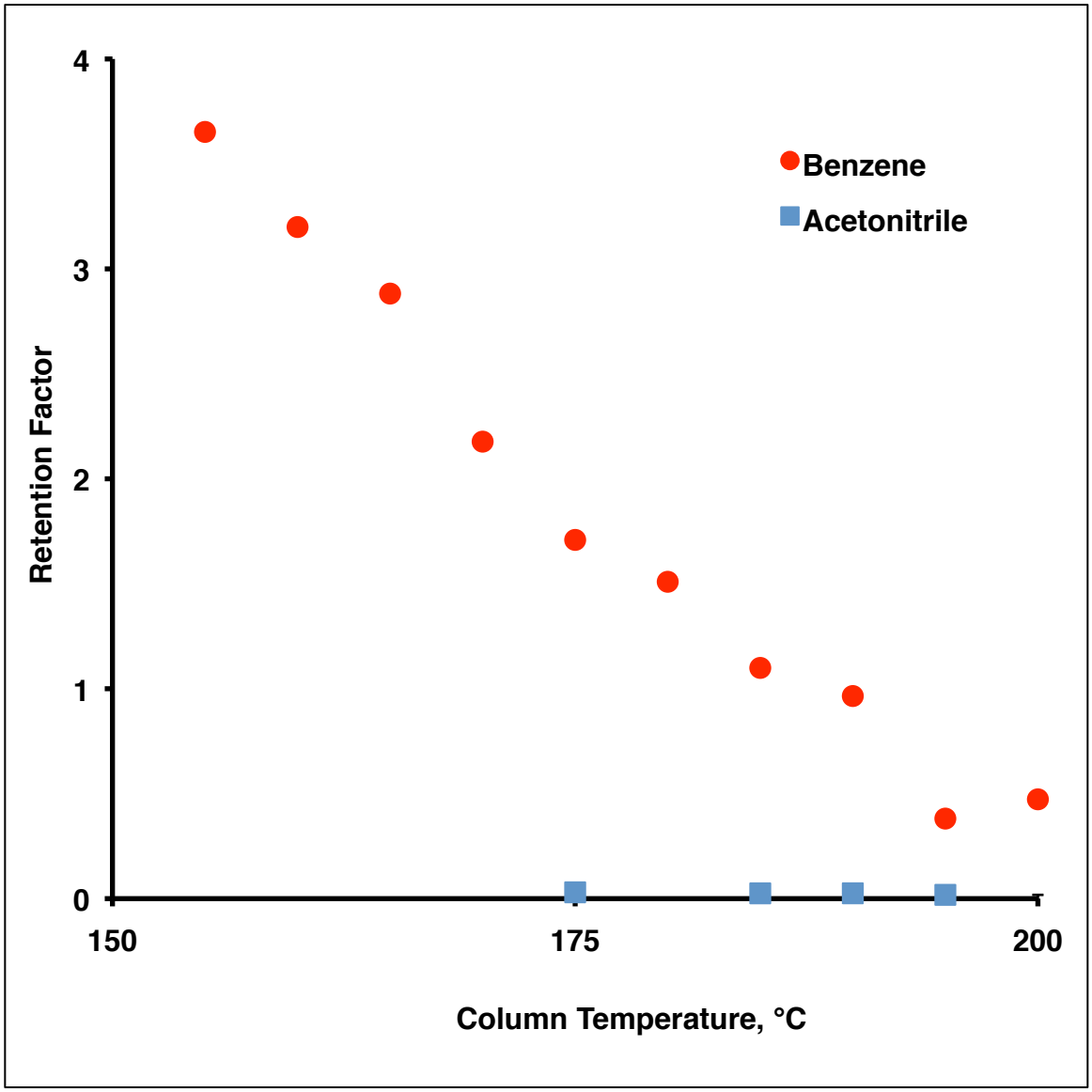

Figure 5.13 Temperature dependent retention factors of acetonitrile and benzene, with methanol used as a minimally retained analyte. Error bars, which reflect the standard deviation of the retention factor are smaller than the markers used.

While the minimally retained acetonitrile was relatively unaffected by the temperature change, benzene showed a factor of 4 reduction in retention factor from 150ºC to 200ºC. One possible explanation for this effect is a shift in column efficiency due to the temperature dependence of mass transfer coefficients. However, benzene and acetonitrile would be affected by the change in mass transfer coefficients relatively equally, and no real change in retention factor would be expected. However, the solubility of the two analytes changes at different points in the temperature range. While acetonitrile is readily solvated at all temperatures, benzene is very weakly soluble in room temperature water. At higher temperatures, the negative energetic favorability of solvating benzene is diminished, as the hydrogen bonding donor network is less organized and the overall solvent polarity is diminished, so benzene transfers to the mobile phase much more favorably.

5.5 Hyphenation of SWC-FID with Sulfur Chemiluminescence Detection

One of the significant advantages of gas phase detection with an FID is hyphenation with a number of available specific detectors, most notably the chemiluminescent detectors developed for sulfur and nitrogen specificity (Benner and Stedman, 1989; Hao et al., 1994). The sulfur chemiluminescent detector was of particular interest for initial adaptation, with the intent of detecting sulfur-containing antibiotics; however, current stationary phase technology did not allow

for the direct testing of this compound class. The commercially available SCD has the advantage of connection directly to the exhaust of a FID but only about 10% of the exhaust is sampled, leading to a ten-fold reduction in the amount of analyte flux as compared to the FID. Since the mechanism of the detector is insensitive to steam, adaptation to a SWC system was possible.

5.5.1 SCD Detector Sensitivity

Initial system parameters for the SCD were based on the suggested values for the SCD (Sievers 355 SCD operation manual), and are summarized in Table 5.5. This type of SCD allows for a connection of a plasma chamber after the FID exhaust and was used to convert any unburned compounds into elemental gas components. First, tetrahydrothiophene was used as a test analyte, as its high volatility allowed for easy conversion to gas for detection.

Table 5.5 SCD working parameters.

Detector Parameter	System Operation Value
Plasma temperature	800ºC
Secondary heater temperature	200ºC
Hydrogen flow rate (sccm)	40
Air flow rate (sccm)	65
Oxygen flow rate (sccm)	8

Note: for initial experiments, a zero air source was used as oxidizer. For later experiments, pure oxygen was used.

To test the sensitivity of analytes relative to the optimized FID, tetrahydrothiophene LODs were determined for both the SCD and FID, which are summarized in Table 5.6.

Table 5.6 LOD of tetrahydrothiophene via the FID and SCD detectors. All values reported in ng.

Detector Type	OLS area=$3\sigma_{y/x}$	WLS area=$3\sigma_{y/x}$
FID	0.098	0.084
FID per carbon	0.025	0.021
SCD	0.23	0.15

5.5.2 SCD detector selectivity

The advantage of the SCD is its selectivity for sulfur containing species. If the system were optimized for separation efficiency, an overlay of the SCD signal with the FID signal would show which analytes had responses to both detectors, providing an additional selective data channel. To prove the selectivity of the SCD, a simple mixture of benzene and tetrahydrothiophene was separated and the aligned FID and SCD chromatograms were plotted together in Figure 5.14. From this chromatogram, the relative selectivity of the SCD response between sulfur and carbon was at least a factor of 26. In typical operation, the detector response is reported to be 2×10^7 times greater for each gram sulfur per gram carbon in optimized separations (Sievers 355 SCD operation manual).

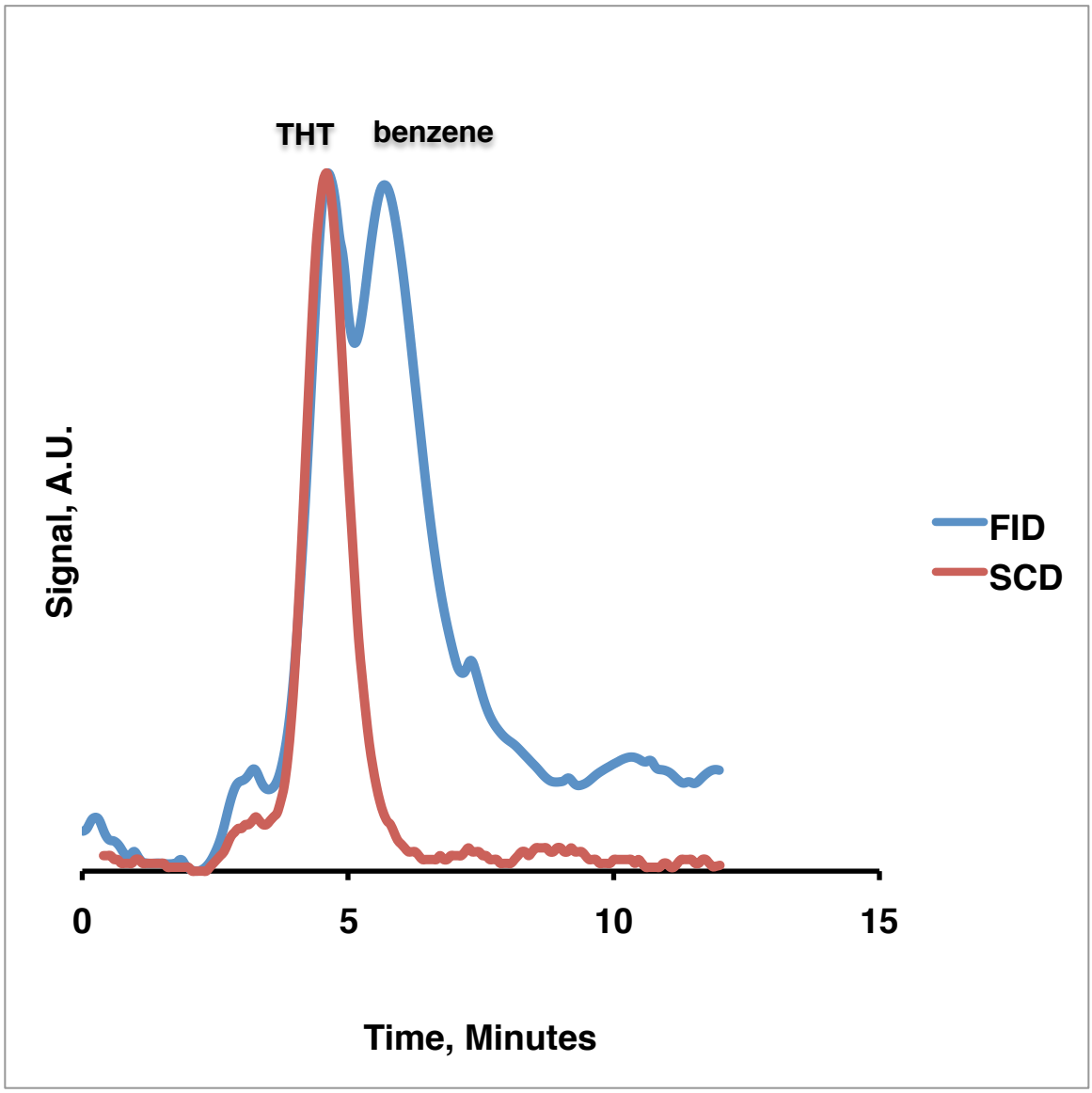

Figure 5.14 Non-optimized separation of tetrahydrothiophene (THT) and benzene. This demonstrates that adding the sulfur selective data channel increases the effective peak capacity, as the THT peak can be fully resolved on the SCD channel.

While the actual separation efficiency and peak capacity are unaffected by the second detector, the selectivity of the SCD could identify additional peaks overlaid in the FID chromatogram, thus effectively increasing the amount of peaks that can be resolved in a separation. This separation has a resolution value of 0.37 using the FID channel only but using the SCD channel to determine approximate peak widths, an effective resolution of 0.91 was observed.

In Figure 5.15, a separation of ethanol and β-mercaptoethanol is depicted. This was performed in a matrix of 1:10 domestic beer diluted with deionized water, with a 100ppm spike of β-mercaptoethanol. The mercaptan was used as an analog of the mercaptans observed in beer products that result in the "skunking" of beer. Typical mercaptans have a sensory threshold in the ppb range, so it is important for samples containing mercaptans that detection of these compounds is not overwhelmed by the high concentration of ethanol. In this chromatogram, the relatively large spike of β-ME was clearly visible in both the FID and SCD peaks; however despite the mass percentage concentration of ethanol in the sample, the SCD displayed no correlated peak to the ethanol, and in fact detected a secondary sulfur-containing peak that was overlaid in the FID signal. This secondary peak was a contaminant in the β-ME, likely the sulfhydral dimer, and does represent any contribution from the matrix, as demonstrated in Figure 5.16, the FID and SCD peaks of the beer sample without the β-ME spike.

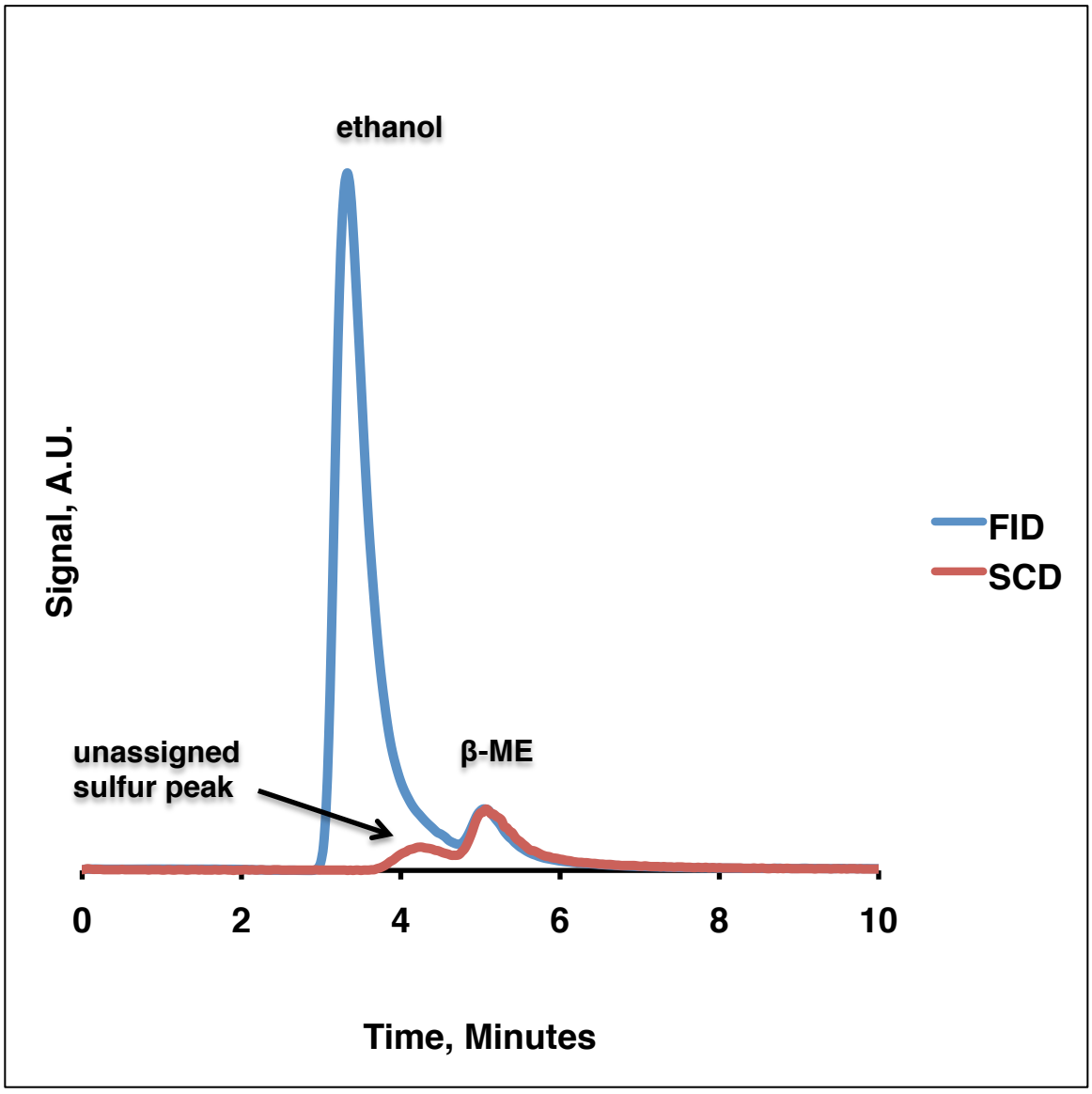

Figure 5.15 Chromatogram of 1:10 domestic beer spiked with β-mercaptoethanol (β-ME). Approximate ethanol concentration was 0.4%, or 16µg injected; β-ME was 100ppm or 555ng injected.

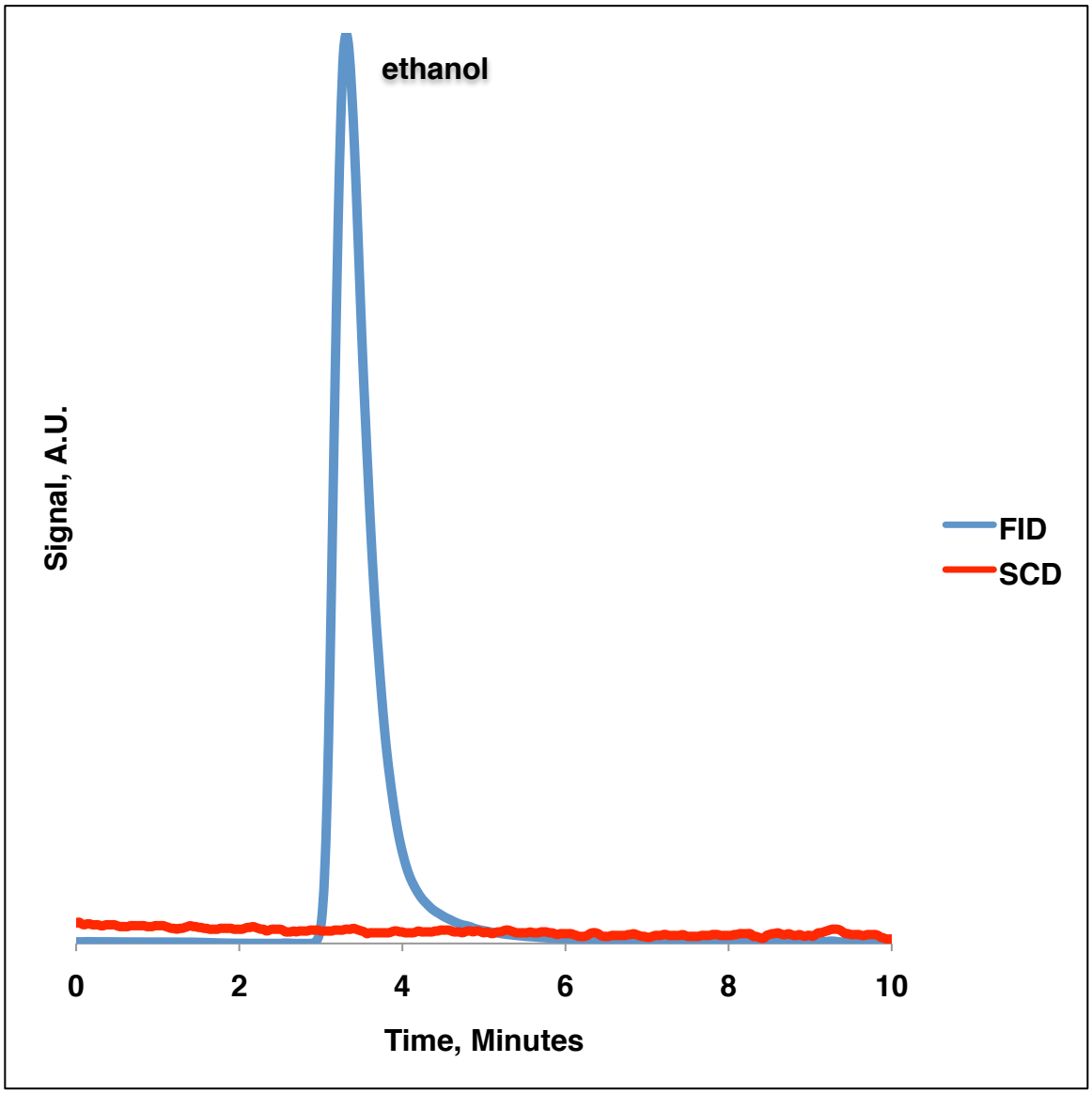

Figure 5.16 Ethanol from beer, without the addition of β-ME .

5.6 Summary

A subcritical water chromatography system with flame ionization detection was designed to improve upon reported detection limits of trace analytes, especially for small polar compounds difficult to detect using other LC methods. This system was found to have LODs in the range of 0.04 to 0.7ng for several tested analytes, with a range of linear detector response from the low ng to hundreds of μg injected, corresponding to a dynamic range of at least 6 orders of magnitude.

Several separations were performed with this system to demonstrate the likely mechanism of separation was based upon the mass transfer of analytes between the stationary and mobile phase due to solute parameters such as analyte size and polarity. The temperature dependence of retention was demonstrated using a comparison of retention factors between a strongly and weakly retained analyte, where strongly retained analytes respond much more dramatically to increased temperatures due both to changes in mass transfer and the mobile phase polarity. The temperature programming methods was also demonstrated as analogous to a solvent programming method in conventional LC.

The FID detector was hyphenated with a SCD for the addition of sulfur selective detection. This hyphenation allowed for the effective enhancement of peak capacity, even when the relative separation efficiency is low. An application

to the detection of mercaptans in food products was demonstrated. The data provided demonstrated SWC-FID systems are likely underutilized in the study of polar analytes, and due to the flexibility of the detection method, this system offers potential for the study of small polar compounds in aqueous systems.

Chapter 6: Mechanistic Studies of Retention in Subcritical Water

In a subcritical water chromatographic separation, mass transfer is controlled by changing the polarity and hydrogen-bonding characteristics of water through changes in temperature, as was demonstrated in Chapter 5. This results in a different interface between the polar and non-polar phases than seen in hydroorganic mobile phases, which have an organic-rich mobile phase layer contacting the non-polar phase. Thus, mass transfer is predominantly related to the changes in the polarity and hydrogen bonding of the water. Because chromatographic parameters (specifically solute retentions) can be correlated to descriptions of the mass transfer of analytes, energetic descriptions (free energy values) of transfer of polar organics can be extrapolated to complex interfaces between organic and aqueous phases (Pan et al., 2009). Efforts toward describing organic partitioning processes in pure water and extrapolation from conventional RPLC may cause subtle discrepancies between observed processes because organic solvent driven partitioning may have a different driving force than is observed in temperature driven partitioning. Thermodynamic

processes, phase parameters and micro-scale simulations were used in this study to elucidate the processes that drive partitioning between pure water and organic layers.

6.1 Thermodynamic Mass Transfer Processes

Established processes for the descriptions of partition chromatography use the van't Hoff equation to correlate retention factors to the free energy of mass transfer. Large free energy terms suggest strong energetic favorability for probe solutes to reside in the non-polar phase. This is described by equation 6.1, where K is the partition coefficient, k' is the retention factor and ϕ is the phase volume ratio:

$$\Delta G^{o} = -RT \ln K = -RT (\ln k' - \ln \phi) \qquad [6.1]$$

Using the Gibbs' equation, this can be rearranged to the van't Hoff formulation, where the enthalpy of mass transfer is correlated to the slope of the regression of $\ln k'$ against $1/T$:

$$\ln k' = -\Delta H^{o}/RT + \Delta S^{o}/R + \ln \phi \qquad [6.2]$$

If the enthalpy of transfer, entropy of transfer and phase ratio are all temperature independent, then the van't Hoff equation will be linear. However, phase ratio is likely to have some temperature dependence, especially in the subcritical temperature range because water density is expected to dramatically change at temperatures above the normal boiling point. In addition, if the mobile phase is sufficiently polar, the brush phase is likely to collapse due to hydrophobic exclusion, so a phase transition could be observed in high-temperature pure water phases. Relevant water physical parameters are provided in Table 6.1, as calculated by Wagner and Pruss (2002).

Table 6.1 Literature physical property values for subcritical water.

Temperature, K	**Density g cm^{-3} at 5MPa**	**log K_W at 0.1MPa**	**Dielectric Constant, ε at 5MPa**
273	1.0023	14.946	88.05
298	0.9987	13.995	78.65
373	0.9593	12.252	55.59
423	0.9225	11.641	44.12
473	0.8709	11.310	34.90
523	0.8049	11.205	27.15

Chester and Coym (2003) extended the van't Hoff formula to correlate the energetic favorability of transfer to the selectivity factor α, which is phase ratio independent. As a result, a linear selectivity plot is expected, so any non-linearity in selectivity is correlated to changes in transfer enthalpy as a function of temperature. The selectivity equation is as follows:

$$ln\ \alpha = ln\ k'_2 - ln\ k'_1 = (-\Delta H^o_2 + \Delta H^o_1)/RT + (\Delta S^o_2 - \Delta S^o_1)/R \quad . \qquad [6.3]$$

6.1.1 van't Hoff Regressions of Probe Analytes

Six probe solutes were used to correlate retention factor to temperature, in the subcritical temperature range from 155ºC to 200ºC. Each injection was 5µL of an approximately 1000ng μL^{-1} stock solution of each analyte. From previous work described in Chapter 5, additional band broadening due to sample overloading was not observed at this concentration, so this was acceptable for the determination of retention factor. All retention factors were determined by the standard formulation in equation 6.4 with methanol retention time used as a minimally retained analyte (T_M) for the determination of the retention of the mobile phase and the analyte retention time T_A:

$$k' = (T_A - T_M)/\ T_M \qquad [6.4]$$

For some very low retention analytes, independent injections of methanol were performed in the same day as injection of the probe to determine retention factor. All retention factors were measured in triplicate.

Probe selection was based upon the assumptions of the van't Hoff analysis approach, in which the driving force of retention is through the free

energy change of moving a non-polar analyte from a polar phase into a non-polar one. As such, explicitly non-polar analytes were used for probes. Benzene was expected to entirely partition into the non-polar phase according to the solvophobic theory of retention. Adding methylene or ethylene groups was expected to increase the magnitude of the free energy change, so toluene and ethylbenzene were also tested. 4-chlorotoluene was predicted to change the free energy by polarizing the aromatic ring, resulting in a diminished free energy magnitude relative to ethylbenzene, which has a similar molecular size and corresponding energetic favorability for the formation of solvent cavities.

To explicitly test the effect of a polarizable, but non-polar analyte without aromaticity,4-heptanone was used. This compound has the same number of carbons as toluene, but any polarization of the compound was expected only affect the carbonyl, leaving the remainder of the compound effectively non-polar. Finally, pyridine, which was expected to favor polar solvation, was used as a comparison to the non-polar analytes. Solvent acid donation is enhanced in subcritical water, so the basic pyridine should demonstrate a greatly reduced energetic favorability relative to the corresponding benzene. The measured retention factors of all compounds are summarized in Table 6.2, and retention factors of all analytes are presented as a function of temperature in Figure 6.1.

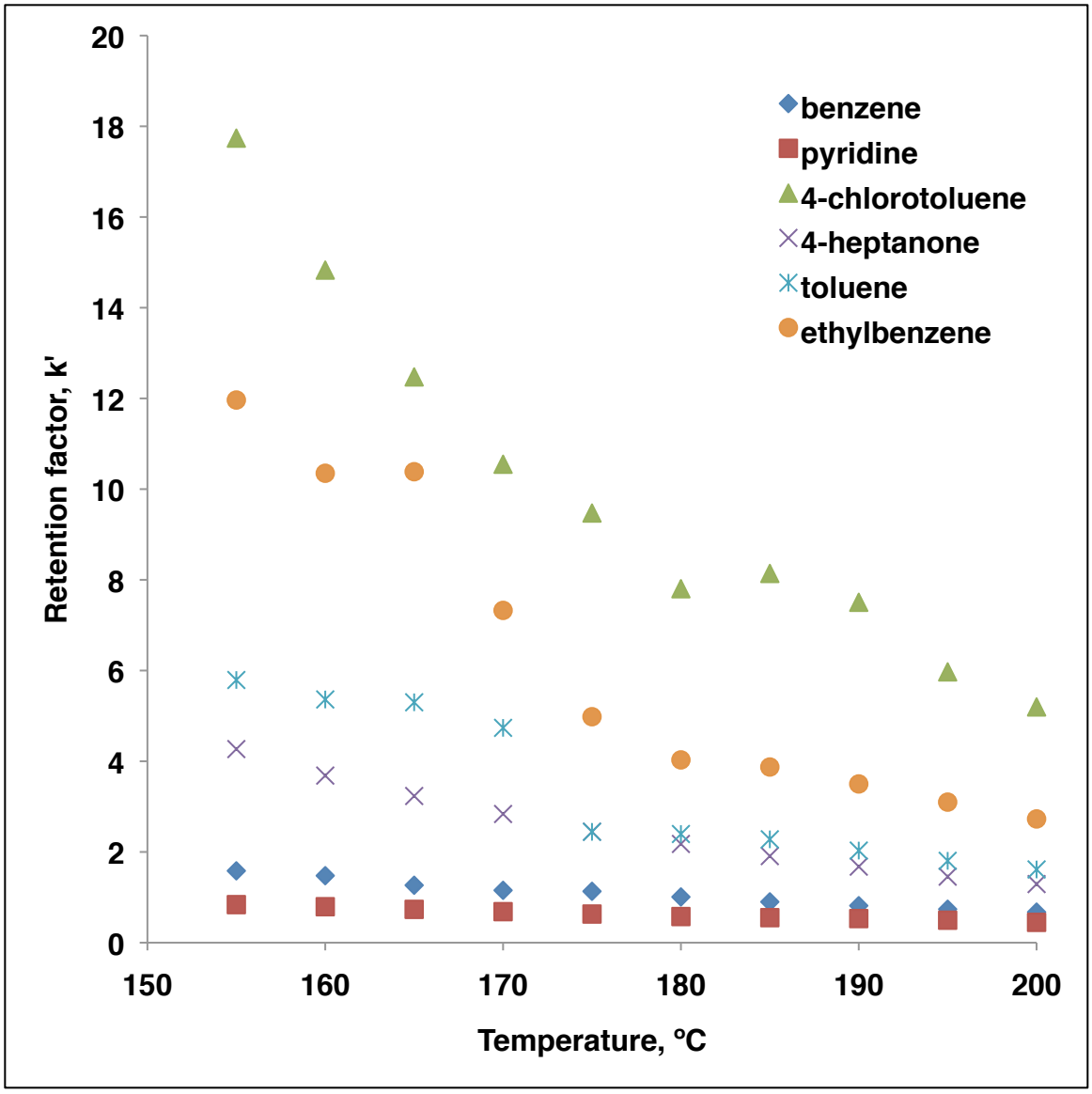

Figure 6.1 Retention factors of analytes as a function of temperature. Error bars are smaller than markers

Table 6.2 Retention factors of probe analytes from 155ºC to 200ºC.

Temperature, °C	Retention Factor (k')					
	benzene	pyridine	4-chlorotoluene	4-heptanone	toluene	ethylbenzene
155	1.58 (0.02)	0.84 (0.005)	17.7 (0.18)	4.27 (0.04)	5.79 (0.06)	12.0 (0.12)
160	1.48 (0.01)	0.79 (0.005)	14.8 (0.15)	3.68 (0.04)	5.36 (0.05)	10.4 (0.10)
165	1.27 (0.01)	0.73 (0.004)	12.5 (0.13)	3.23 (0.03)	5.30 (0.05)	10.4 (0.10)
170	1.15 (0.01)	0.68 (0.004)	10.6 (0.11)	2.84 (0.03)	4.74 (0.05)	7.33 (0.07)
175	1.13 (0.01)	0.63 (0.004)	9.47 (0.10)	2.45 (0.02)	2.44 (0.02)	4.98 (0.05)
180	1.01 (0.01)	0.58 (0.003)	7.80 (0.08)	2.18 (0.02)	2.40 (0.02)	4.03 (0.04)
185	0.90 (0.009)	0.55 (0.003)	8.14 (0.08)	1.91 (0.02)	2.28 (0.02)	3.87 (0.04)
190	0.82 (0.008)	0.53 (0.003)	7.50 (0.08)	1.68 (0.02)	2.03 (0.02)	3.50 (0.04)
195	0.74 (0.007)	0.50 (0.003)	5.97 (0.06)	1.46 (0.02)	1.80 (0.02)	3.10 (0.03)
200	0.67 (0.007)	0.45 (0.003)	5.20 (0.05)	1.29 (0.01)	1.61 (0.02)	2.73 (0.03)

Note: standard deviations reported in parentheses.

Measured shifts in the retention factor were observed for all compounds through this temperature range, with highly retained analytes like ethylbenzene and 4-chlorotoluene demonstrating the most dramatic changes. Using the van't Hoff relationship, the enthalpy of transfer and residual values, which include the entropic and phase volume ratio were determined and summarized in Table 6.3.

Reported correlation coefficients (R^2), standard errors of regression, and F statistics are provided in this table as well (All F statistics provided indicated significant correlation to the regression).

Table 6.3 van't Hoff energetic values of probe solutes

Compound	ΔH°, kJ mol^{-1}	ΔS°/*R* + ln ϕ	R^2	SE	F
benzene	-32.5 (0.80)	-8.63 (0.21)	0.983	0.03	1646
pyridine	-23.4 (0.47)	-6.77 (0.12)	0.989	0.02	2510
4-chlorotoluene	-51.9 (1.24)	-11.5 (0.33)	0.995	0.03	1757
4-heptanone	-44.6 (0.35)	-11.1 (0.09)	0.999	0.01	16343
toluene	-50.5 (2.68)	-12.5 (0.71)	0.959	0.09	356
ethylbenzene	-56.5 (4.21)	-13.5 (1.12)	0.918	0.15	180

Note: SE in parentheses

Initial analysis of probe van't Hoff regressions indicated predicted enthalpies correlated with expected relative values from the solvophobic description. Polarizability or acidity/basicity reduced the transfer enthalpy (i.e., pyridine relative to benzene, 4-chlorotoluene relative to ethylbenzene, 4-heptanone relative to toluene or 4-chlorotoluene), and adding methyl or ethyl groups to a probe increased the magnitude transfer favorability, measured as an increase in the magnitude of the enthalpy. However, raw retention factors did not correlate to enthalpic values in all cases, such as 4-chlorotoluene, which is retained longer than ethylbenzene at all temperatures. The relative scale of the intercept term is 1000× smaller than the enthalpic (slope) term. However, the intercept term ($\Delta S^o/R + ln\ \phi$) appears to correlate more strongly to the

comparison of relative retentions, with lower magnitude intercept terms indicating lower overall retention at all temperatures. From observation, small changes in intercept correlated to very large changes in retention factor.

6.1.2 Linearity of van't Hoff Regressions

If the phase ratio, entropy and enthalpy of transfer of an analyte are temperature independent, then the van't Hoff relationship is predicted to be linear, and the slope is the enthalpic term (Chester and Coym, 2003). This was seen in this study for the plot of 4-heptanone, depicted in Figure 6.2, which has a correlation coefficient of R^2 =0.9995. Mechanistically, this indicated that the free energy of transfer of this analyte is behaving according to a solvophobic mechanism, with the driving force of transfer relative to the difference in polarity between phases.

Because 4-heptanone did not demonstrate any enthalpic or entropic dependence on temperature, this would indicated that any phase ratio changes have no impact on its retention, or that the change in phase ratio is compensated energetically in other processes. Other analytes examined did demonstrate some temperature dependence on retention, which resulted in non-linear van't Hoff plots. This was most evident in the plots of benzene derivatives, presented in Figure 6.3, in which a significant non-linearity was observed for ethylbenzene and toluene.

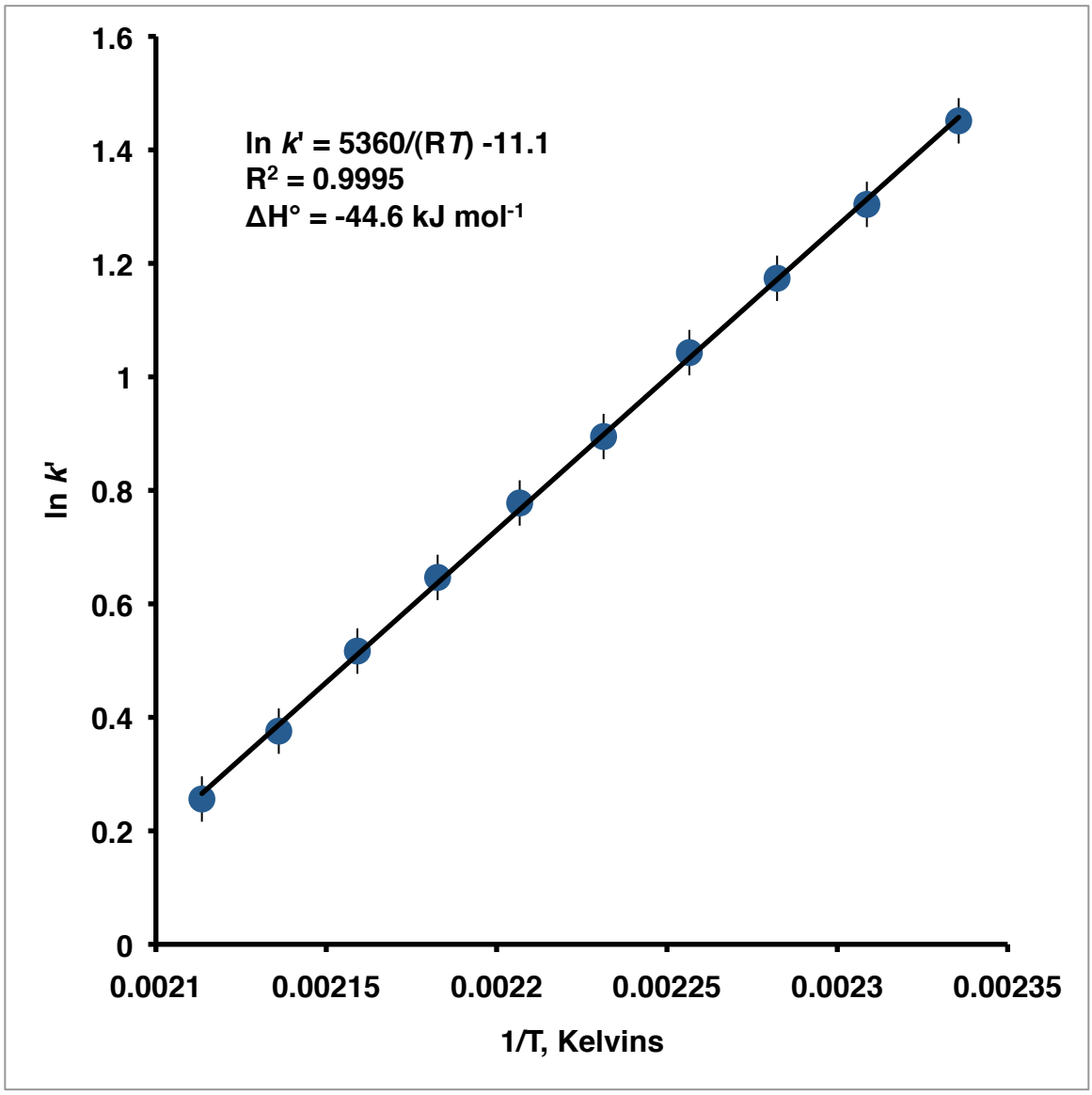

Figure 6.2 van't Hoff plot of 4-heptanone. A linear van't Hoff plot indicates that the enthalpy, entropy and phase ratio terms are not temperature dependent. Error bars reflect the standard deviation of the retention factor.

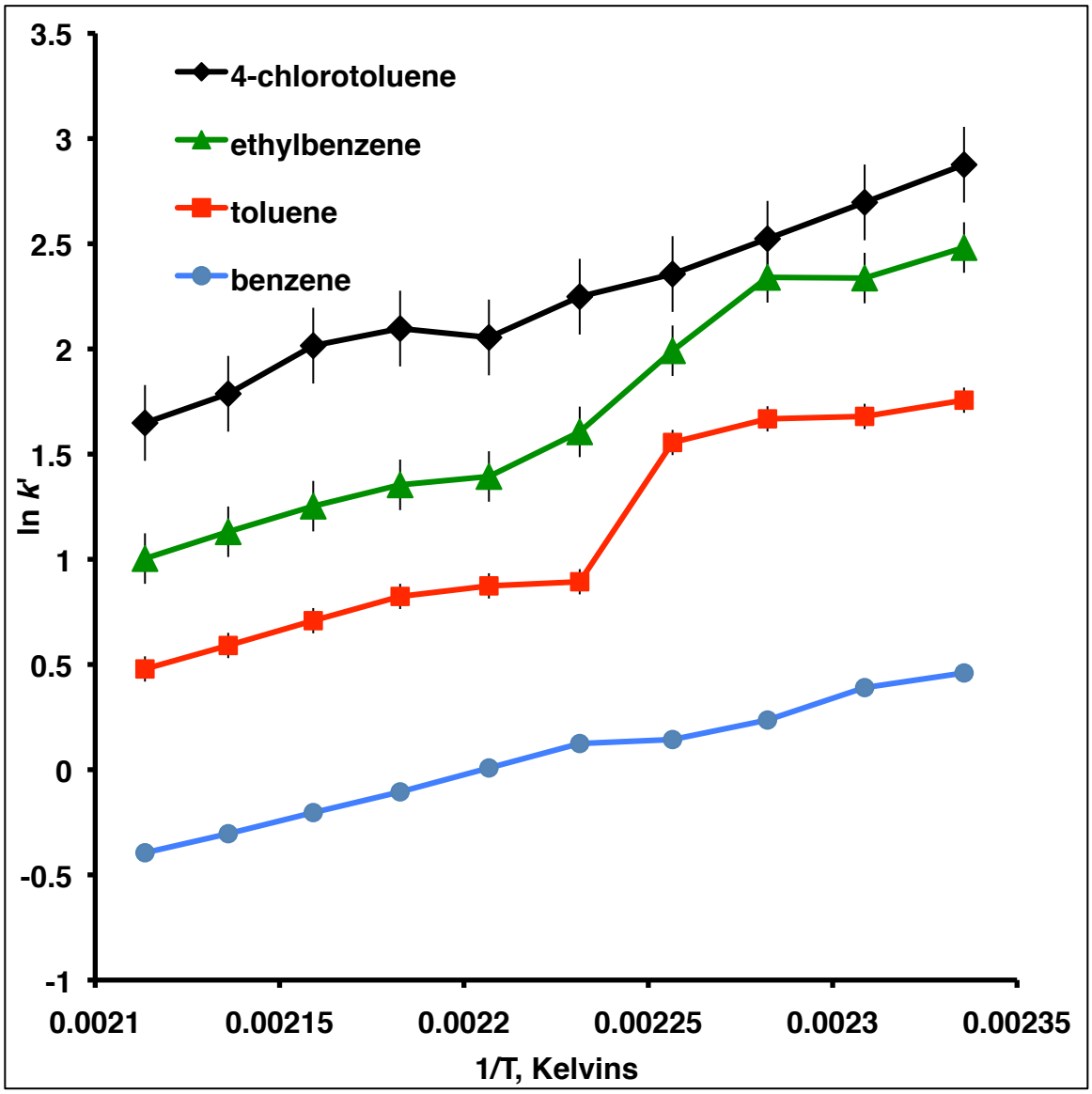

Figure 6.3 van't Hoff plots of benzene and substituted benzene derivatives. The addition of a methyl or ethyl group significantly changes the retention plot, which may partially be balanced by the addition of a polarizing chlorine group in 4-chlorotoluene. Errors reflect the standard deviation of the retention factor; toluene and benzene errors are smaller than the marker used.

6.1.3 Solute Selectivity

If only the phase ratio is changing, and enthalpic or entropic values are in fact temperature independent, then a plot of ln α versus 1/T would be expected result in a linear selectivity plot. Theoretically, contributions due to phase ratio should be cancelled out by the selectivity plot, so two comparisons were performed. Benzene was used as a reference analyte, providing the selectivity of a methylene or ethylene addition or pyridine substitution to substituted compounds. Secondly, as linear alkanes are not available for retention testing in LC, the 4-heptanone was used as an alkane analog to provide the selectivity value of a compound to a similarly sized linear molecule. Because 4-heptanone has solvation parameters similar to *n*-heptane, this comparison is analogous to a correlation to the retention factors of linear alkanes in gas chromatography.

Calculated selectivity values are provided in Table 6.4, with benzene and 4-heptanone used as reference solutes. A depiction of how the selectivity values relate to the individual solutes, in this case benzene and pyridine, is provided in Figure 6.3.

It is clear from the correlation coefficients in Table 6.4, and in the plots in Figure 6.4, that for most analytes selectivity plots show poor linearity. The most linear selectivity plots were between 4-heptanone and benzene, and between 4-heptanone and pyridine. At first glance, no correlations can be derived from these trends, other than the fact the selectivity of many analytes was temperature

dependent, contrary to the analyte pairs observed at lower temperatures by Chester and Coym (2004). In addition, Coym and Dorsey (2004) observed linear van't Hoff regressions of similar analytes in subcritical water from 125º-175ºC; however, a polybutadiene stationary phase was used instead of the carbon-clad zirconia-C18 in this work. The lower temperature range used by Coym and Dorsey may have caused their results to be linear.

Table 6.4 Selectivity regressions with benzene and 4-heptanone references

Selectivity versus benzene	**ΔHº, kJ mol^{-1}**	**ΔSº/*R***	**R^2**	**SE**	**F**
toluene	-21.6 (6.62)	-4.70 (1.77)	0.57	0.15	10.6
ethylbenzene	-28.1 (5.52)	-5.87 (1.48)	0.76	0.15	26
4-chlorotoluene	-11.0 (2.77)	-0.73 (0.74)	0.66	0.07	15
pyridine	8.79 (1.35)	1.83 (0.36)	0.84	0.03	43
Selectivity versus 4-heptanone	**ΔHº, kJ mol^{-1}**	**ΔSº/R**	**R^2**	**SE**	**F**
benzene	12.7 (1.08)	2.60 (0.29)	0.95	0.03	139
toluene	-8.86 (5.68)	-2.11 (1.51)	0.23	0.15	2.4
ethylbenzene	-15.4 (4.73)	-3.27 (1.26)	0.57	0.13	10.6
4-chlorotoluene	1.79 (2.50)	1.86 (0.67)	0.06	0.06	0.51
pyridine	21.5 (0.76)	4.42 (0.20)	0.99	0.02	805

Polybutadiene stationary phases are likely more resistant to solvent-driven stationary phase collapse than octadecane based stationary phases, and this may reflect the non-linearity observed in this work's selectivity data. The selectivity calculation removes contributions from phase ratio because:

$$\alpha = \frac{[K_A V_{A,S} / V_{A,M}]}{[K_A V_{B,S} / V_{B,M}]} \quad [6.5]$$

However, this assumes that the volume of the phases is equivalent for analytes. This is reasonable for most analytes in most chromatographic systems but if the mechanism of retention is significantly different for the two analytes, retention volumes may differ considerably.

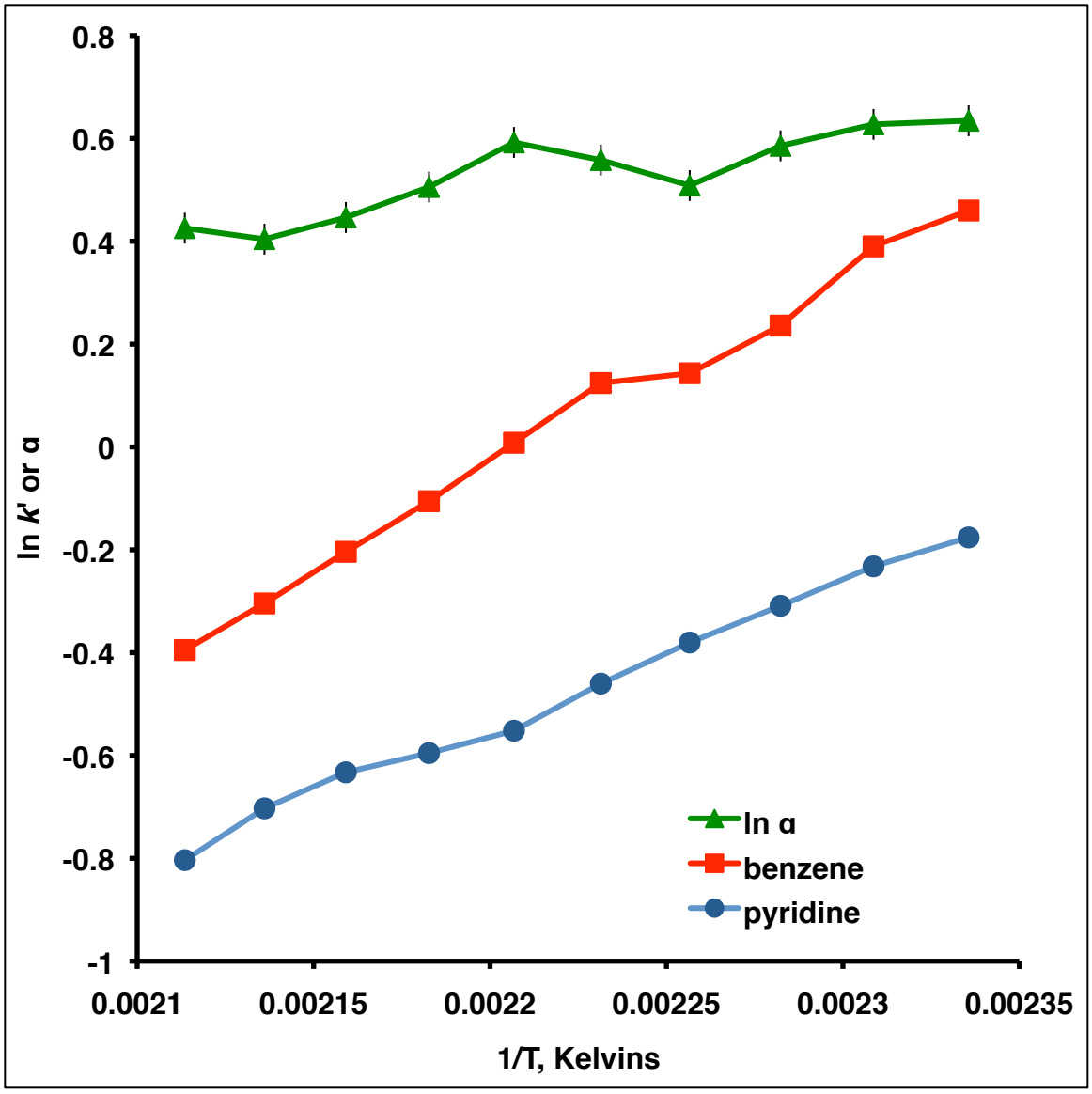

Figure 6.4 Demonstration of the van't Hoff relationship of benzene, pyridine, and the selectivity between analytes. In this case the selectivity regression value is greater than either analyte, indicating the energetic favorability of benzene mass transfer over pyridine at all temperatures probed. Error bars reflect the standard deviation of the retention factor for benzene and pyridine, and the standard error of the selectivity between the two compounds.

6.1.4 Temperature Dependent Stationary Phase Transitions

From solvophobic theory, it is known the driving force of molecular phase transfer is the favorable dispersion force in the non-polar phase balancing the unfavorable solvent cavity formation (Carr et al., 1993). The dispersion effect is seen most dramatically in methylene groups, which according to theory should be the most solvophobic. If the stationary phase is collapsed at some temperatures in the tested range, then the solvent cavity formation is much more energetically unfavorable due to steric hindrance of analyte partitioning. This effect would be most dramatically seen in analytes that could not align with collapsed octadecanes to partition (i.e., non-linear molecules) or analytes that would favor partitioning into deeper parts of the non-polar phase instead of those that could partially maintain contact with the polar phase (i.e., analytes without polarizable groups). Of these analytes, toluene and ethylbenzene are both non-linear and are less polarizable than benzene or pyridine; so partitioning for these analytes are expected to be most affected by a transition in the stationary phase.

Mobile phase polarity is temperature dependent and can be correlated to acetonitrile addition in traditional chromatography through the approximation that each 5ºC above boiling is equivalent to an increase of 1% acetonitrile in mobile phases (Bolliet and Poole, 1998). Traditional octadecane columns do not recommend mobile phases with less than 10-15% acetonitrile, which would correlate to a temperature of 150-175ºC with subcritical water mobile phases. In

Figure 6.4, the selectivities of pyridine, toluene, and ethylbenzene against benzene are plotted, with the critical temperature range highlighted in yellow. What is striking about this plot is how clearly selectivity variances occured in the range when a change in stationary phase solvation might happen, and the most dramatic shift was observed in the toluene selectivity. From solvophobic theory, the methylene addition should have the most dramatic effect on retention, as no steric shifts can resolve the cavity formation term. Once the stationary phase transition occurs, dispersion forces are suddenly much larger relative to the cavity formation, and a selectivity minimum is observed. The ethylene selectivity demonstrates a broader minimum, indicating that the lipophilic contribution to retention is smaller than is observed in toluene. Pyridine should not have to deeply partition into the stationary phase and thus is linear.

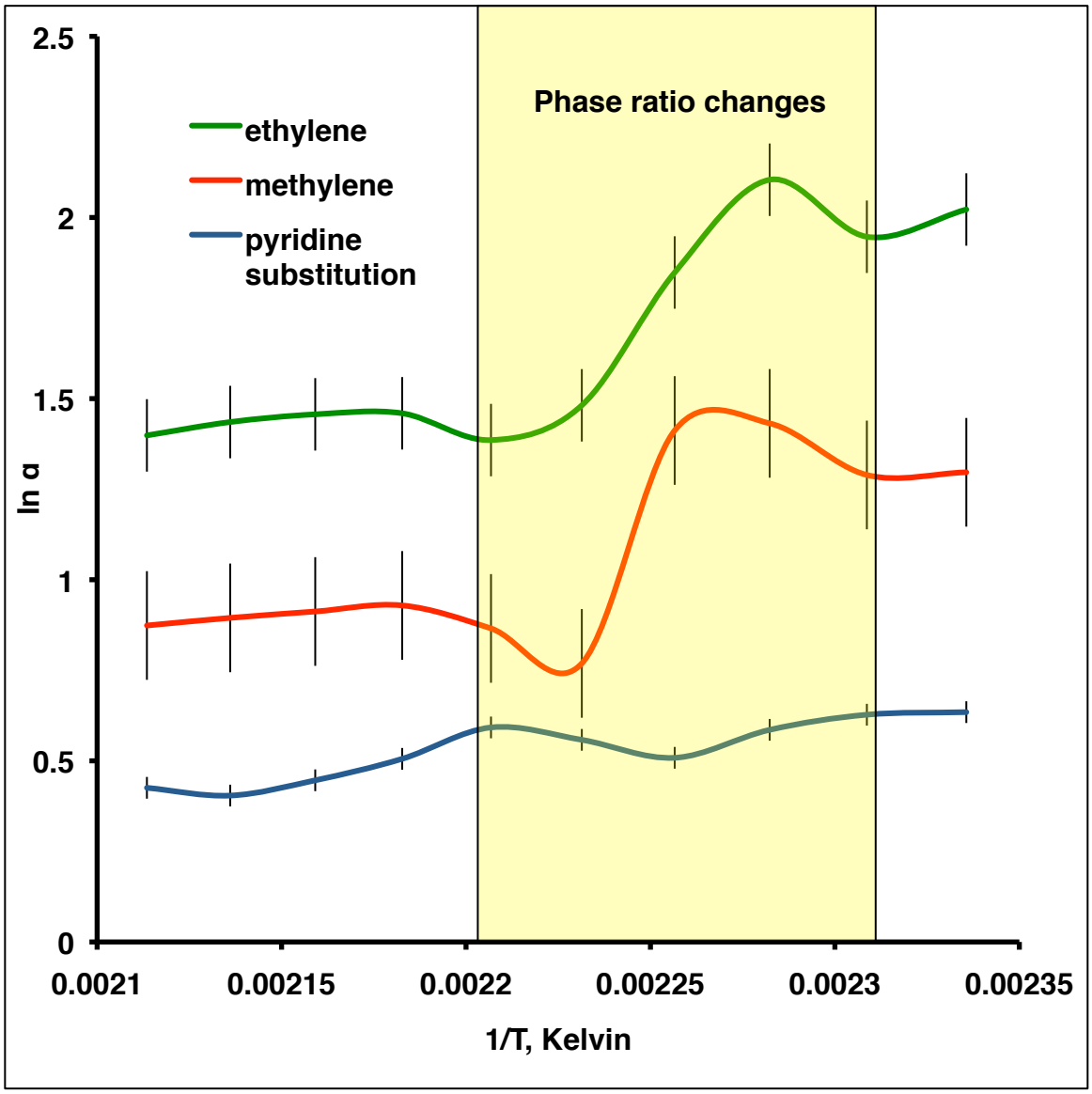

Figure 6.5 Selectivity regressions of analytes compared to benzene. The methylene selectivity demonstrates a significant dependence on temperature, which can be correlated to expected changes in the stationary phase; solvation of the stationary phase becomes favorable at approximately 175ºC, causing the octadecane phase to solvate and reorient. Error bars reflect the standard error of the selectivity values.

6.1.5 Retention Selectivity with a Linear Alkane Analog

Benzene was used as a reference analyte for the selectivity results in Figure 6.4; however, benzene could also be affected by the change in stationary phase orientation. As 4-heptanone demonstrated an extremely linear temperature response and would correlate as directly as is possible to a comparison to a linear alkane, selectivities were also tested against this analyte. Due to water exclusion, 4-heptanone could either partition to the surface of a non-polar phase, or deeply into a non-polar phase to bury the alkane groups, and thus would be expected partition independently of the orientation of the non-polar phase.

In Figure 6.6, the retention selectivities of all compounds against 4-heptanone are depicted. Pyridine and benzene have negative slopes in this plot, which indicated mass transfer relative to the reference analyte is more favorable at higher temperatures than at lower ones. From Table 6.4, the enthalpy of transfer for the pyridine: 4-heptanone selectivity is 21.5 kJ mol^{-1}, indicating enthalpic unfavorability for the transfer of pyridine as compared to 4-heptanone. In the comparison of 4-chlorotoluene and 4-heptanone there appears to be minimal temperature dependence on the selectivity between these analytes. As was also seen in the benzene selectivity plots in Figure 6.5, the selectivity values of ethylbenzene and toluene were non-linear in the range of proposed phase orientation transition.

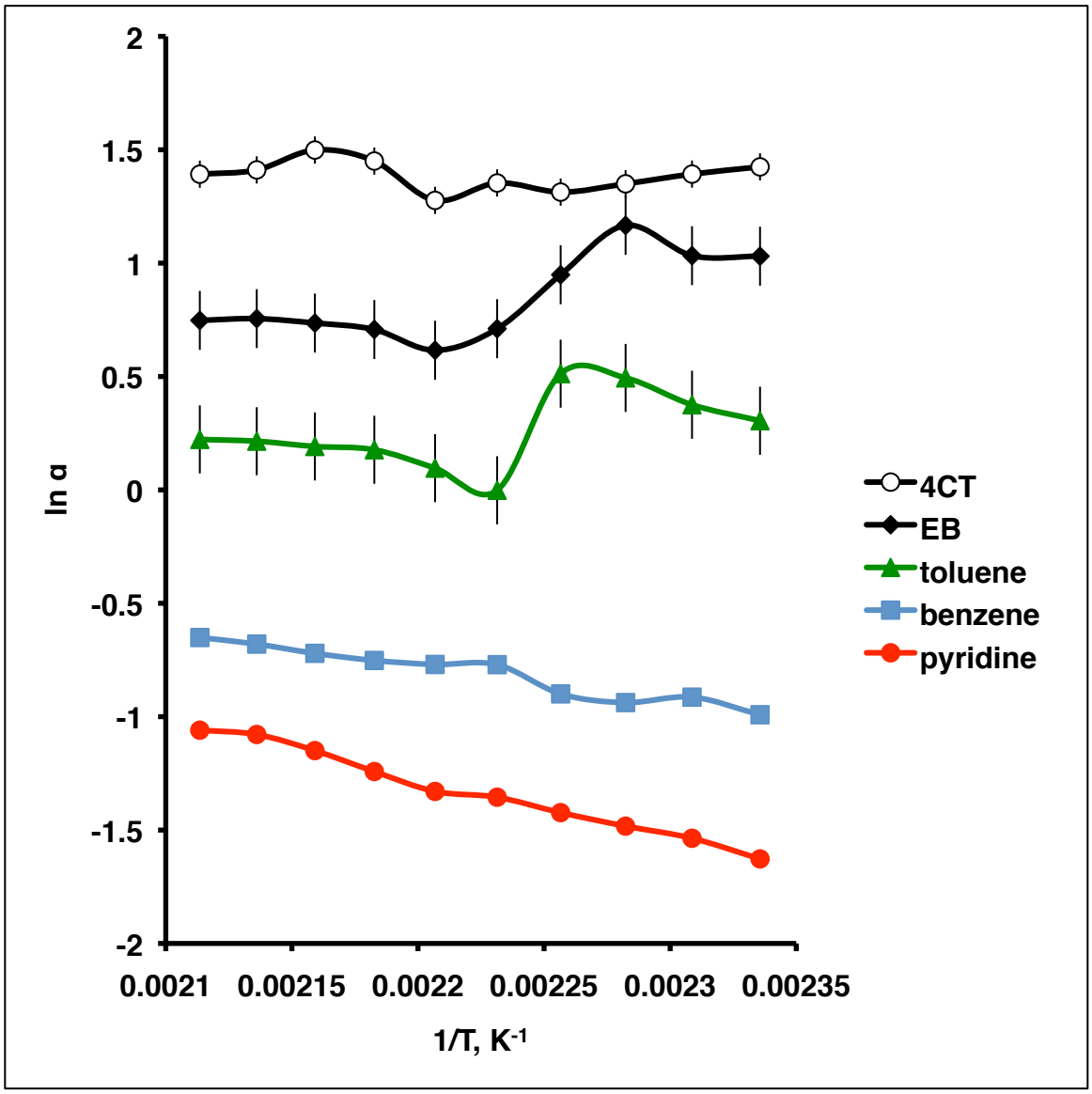

Figure 6.6 Selectivity as compared to 4-heptanone. Benzene and pyridine have negative slopes relative to 4-heptanone, indicating greater transfer favorability at high temperatures than at lower temperatures. Toluene and ethylbenzene demonstrate stationary phase transition effects, while the polarizable compounds demonstrate less phase dependence. Error bars reflect the standard error of the selectivity; values are smaller than marker for benzene and toluene.

6.2 Linear Solvation Energy Relationships of Solute Retention

While the van't Hoff analysis of probe analytes provides insight into the mechanisms of analyte retention in subcritical water, the transferability of the findings is limited. The driving force in the retention process is solvophobic exclusion, with polar analytes partitioning to the surface of the non-polar phase, and less polar analytes partitioning more deeply. However, this only provides a limited description of the processes involved with retention and does not provide much in the relative energetics of differing processes. For example, in the previous section, the relative partitioning effects of a methylene and ethylene addition to benzene demonstrated different results because of the combined favorable effects (Van der Waal's forces) and unfavorable forces (cavity formation). A more formal treatment of the energetic contributions to retention is to develop a set of solvent descriptors from a series of probe analytes. The process involved with this system is to choose a training series of probe analytes and correlate retention factors to the linear solvation energy relationships, with solvent descriptors in lower case and solute parameters in upper case developed by Abraham et al. (2004):

$$\log k' = c + eE + sS + aA + bB + vV \qquad [6.6]$$

The definition of each term is provided in Table 6.5. Solute parameters have been compiled for a wide variety of analytes, and correlation is performed via multiple linear regression.

Table 6.5 Linear Solvation Energy Relationship Definitions

Solute Parameters	Solvent Descriptors
E: Excess molar refraction	***e:*** Solvation favorability
S: Dipolarity/Polarizability	***s***: Dipolarity/Polarizability
A: Hydrogen bond donor (acidity)	***a***: Hydrogen bond acceptor (basicity)
B: Hydrogen bond acceptor (basicity)	***b***: Hydrogen bond donor (acidity)
V: McGowan volume/100	***v***: Hydrophobicity

Excess molar refraction is defined as the total polarizability of a molecule beyond that of an equivalent alkane. The McGowan Volume is the characteristic molecular volume of a molecule, divided by 100 (Abraham and McGowan, 1987). LSERs have the ability to quantify the structural contributions of analytes to the observed retention through description of the solvent. Thus, once a training set has produced a solvent description, any analyte's retention factor can be predicted by inputting the solvent parameters into the LSER equation.

6.2.1 LSER Study Design

For this study, multiple injections of a series of probes were performed to determine mean retention factors, with methanol as a reference analyte. A custom library of solute parameters was derived from two literature sources and designed for maximum coverage of parameter space. Analyte covariance is

always a concern for LSER parameter sets, as many contributions overlap, which may result in poor correlations to specific descriptors. This is a particular problem for the E and S parameters, both of which correlate to molecular polarizability. The analyte set used in this study sought to break covariance through the inclusion of analytes with dramatically different combinations of E and S parameters (e.g., 2-butanone, n-butylbenzene); however significant covariance is still observed in these two descriptors. The analyte parameter set is provided in Table 6.6.

In order to describe the events previously seen in the van't Hoff analysis study, three temperatures were chosen to determine probe retention factors. The lowest, 160ºC, was expected correlate to a partially collapsed stationary phase, and the highest, 200ºC, was expected to correlate to a fully solvated stationary phase, with the middle temperature, 180ºC near to the phase transition. A summary of measured retention factors is provided in Table 6.7. Covariance statistics of the solute set are provided in Table 6.8.

Table 6.6 Linear Solvation Energy Relationship solute parameters

Compound	E	S	A	B	V
1-butanol	0.224	0.42	0.37	0.48	0.731
1-pentanol	0.219	0.42	0.37	0.48	0.872
1-hexanol	0.21	0.42	0.37	0.48	1.013
1-heptanol	0.211	0.42	0.37	0.48	1.154
1-octanol	0.199	0.42	0.37	0.48	1.295
1-nonanol	0.193	0.42	0.37	0.48	1.435
2-methyl-2-propanol	0.18	0.31	0.31	0.6	0.731
benzyl alcohol	0.803	0.87	0.33	0.56	0.916
benzaldehyde	0.82	1	0	0.39	0.873
benzene	0.61	0.52	0	0.14	0.716
toluene	0.601	0.52	0	0.14	0.857
ethylbenzene	0.613	0.51	0	0.15	0.998
m-xylene	0.623	0.52	0	0.16	0.998
n-butylbenzene	0.6	0.51	0	0.15	1.28
aniline	0.955	0.96	0.26	0.41	0.816
nitrobenzene	0.871	1.11	0	0.28	0.891
methoxybenzene	0.708	0.75	0	0.29	0.916
pyridine	0.631	0.84	0	0.52	0.675
1,2-dichlorobenzene	0.872	0.78	0	0.04	0.961
4-chlorotoluene	0.705	0.67	0	0.07	0.98
phenol*	0.805	0.89	0.6	0.3	0.775
1,4-dihydroxybenzene*	1	1	1.16	0.6	0.834
2-methylphenol*	0.84	0.86	0.52	0.3	0.916
4-chlorophenol*	0.915	1.08	0.67	0.2	0.898
4-methoxyphenol*	0.9	1.17	0.57	0.48	0.975
4-nitrophenol*	1.07	1.72	0.82	0.26	0.949
4-iodophenol*	1.38	1.22	0.68	0.2	1.033
2-butanone	0.166	0.7	0	0.51	0.688
4-heptanone	0.113	0.66	0	0.51	1.111
cyclohexanone	0.403	0.86	0	0.56	0.861
acetophenone	0.818	1.01	0	0.48	1.014
tetrahydrofuran	0.289	0.52	0	0.48	0.622
1,1,2-trichloroethane	0.499	0.68	0.13	0.13	0.757
n-Hexylamine	0.197	0.35	0.16	0.61	1.054

Solute parameters were derived from Quina et al. (2005) except for *, which were derived from Torres-Lapasió et al. (2004).

Table 6.7 Temperature dependent retentions of probe solutes

Compound	log *k'* (SD)		
	160ºC	180ºC	200ºC
1-butanol	-0.37 (0.01)	-0.47 (0.01)	-0.63 (0.01)
1-pentanol	0.032 (0.01)	-0.113 (0.01)	-0.30 (0.03)
1-hexanol	0.44 (0.02)	0.26 (0.01)	0.048 (0.05)
1-heptanol	0.85 (0.01)	0.64 (0.02)	0.39 (0.09)
1-octanol	1.28 (0.01)	1.02 (0.02)	0.72 (0.21)
1-nonanol	1.51 (0.47)	1.17 (0.47)	1.06 (0.47)
2-methyl-2-propanol	-0.60 (0.01)	-0.63 (0.01)	-0.70 (0.01)
benzyl alcohol	0.065 (0.01)	-0.034 (0.02)	-0.136 (0.01)
benzaldehyde	0.48 (0.06)	0.15 (0.01)	0.041 (0.01)
benzene	0.38 (0.51)	0.14 (0.24)	0.045 (0.26)
toluene	0.83 (0.86)	0.59 (0.01)	0.47 (0.02)
ethylbenzene	1.16 (0.14)	0.72 (0.21)	0.71 (0.18)
m-xylene	1.24 (0.36)	0.85 (0.21)	0.66 (0.18)
n-butylbenzene	1.8 (0.14)	1.40 (0.21)	1.29 (0.18)
aniline	-0.04 (0.01)	-0.15 (0.01)	-0.24 (0.01)
nitrobenzene	0.61 (0.04)	0.30 (0.10)	0.23 (0.38)
methoxybenzene	0.66 (0.01)	0.44 (0.05)	0.25 (0.01)
1,2-dichlorobenzene	1.32 (0.12)	0.97 (0.56)	0.80 (0.01)
4-chlorotoluene	1.29 (0.36)	0.98 (0.36)	0.76 (0.36)
phenol	-0.059 (0.01)	-0.12 (0.04)	-0.23 (0.01)
1,4-dihydroxybenzene	-0.36 (0.02)	-0.50 (0.01)	-0.76 (0.01)
2-methylphenol	0.30 (0.01)	0.20 (0.03)	0.075 (0.01)
4-chlorophenol	0.47 (0.07)	0.36 (0.01)	0.22 (0.03)
4-methoxyphenol	0.27 (0.03)	-0.19 (0.01)	-0.26 (0.01)
4-nitrophenol	0.33 (0.28)	0.019 (0.13)	-0.12 (0.01)
4-iodophenol	0.90 (0.04)	0.62 (0.02)	0.59 (0.02)
2-butanone	-0.47 (0.01)	-0.73 (0.01)	-0.92 (0.1)
4-heptanone	0.79 (0.29)	0.34 (0.02)	0.27 (0.29)
cyclohexanone	-0.056 (0.01)	-0.19 (0.01)	-0.28 (0.06)
acetophenone	0.67 (0.01)	0.34 (0.03)	0.18 (0.01)
tetrahydrofuran	-0.51 (0.06)	-0.66 (0.01)	-0.90 (0.01)
1,1,2-trichloroethane	0.050 (0.01)	-0.095 (0.01)	-0.17 (0.01)
n-Hexylamine	0.56 (0.02)	0.35 (0.02)	0.11 (0.02)

Note: Standard Deviation of Retention factor in parentheses

Table 6.8 LSER covariance statistics

	E	S	A	B	V
E	1				
S	0.81	1			
A	0.35	0.41	1		
B	-0.45	-0.14	0.2	1	
V	-0.11	-0.15	0.07	-0.045	1

Several possible regressions were performed on this data set. The first regression included all 34 analytes. Vitha and Carr (2006) suggested the minimum number of analytes in a training set should be 4 times the number of regression parameters, so 20 analytes would be the minimal set required for a statistically relevant set. Generally, compounds with retention factors less than 1 (log k' less than 0) are suspect, so a regression of analytes with all analytes with retention factors greater than 1 at 160ºC was also performed. A subset of all aromatic compounds was also tested, as was a correlation of probe parameters to the literature octanol/water partition coefficient, $k_{OW,}$ which would demonstrate if a simpler analyte descriptor could sufficiently account for retention behavior. A summary of LSER regression descriptors is provided in Table 6.9.

Table 6.9 Summary of LSER Solvent Descriptors

Descriptor	**All solutes**			***k'* > 1 solutes**		
(SE)	**160**	**180**	**200**	**160**	**180**	**200**
c	-1.61	-1.45	-1.62	-1.27	-1.15	-1.39
	(0.14)	(0.14)	(0.12)	(0.16)	(0.18)	(0.11)
e	0.41	0.48	0.53	**0.21**	0.33	0.40
	(0.13)	(0.13)	(0.11)	**(0.13)**	(0.14)	(0.09)
s	-0.28	-0.46	-0.42	**-0.18**	-0.43	-0.38
	(0.11)	(0.12)	(0.10)	**(0.10)**	(0.11)	(0.07)
a	-0.52	-0.34	-0.41	-0.53	-0.23	-0.30
	(0.08)	(0.08)	(0.07)	(0.07)	(0.08)	(0.05)
b	-1.3	-1.16	-1.19	-1.48	-1.26	-1.30
	(0.15)	(0.15)	(0.13)	(0.15)	(0.17)	(0.11)
v	2.83	2.42	2.40	2.63	2.21	2.25
	(0.11)	(0.11)	(0.09)	(0.12)	0.14)	(0.09)
R	0.97	0.96	0.97	0.97	0.95	0.98
SE	0.11	0.11	0.10	0.07	0.085	0.05
F	212	160	213	135	84	215

Descriptor	**Aromatics Only**			**log k_{OW}**
(SE)	**160**	**180**	**200**	
c	-1.18	-0.94	-1.14	**-0.04**
	(0.22)	(0.21)	(0.18)	**(0.19)**
e	**0.21**	**0.31**	0.44	**0.21**
	(0.23)	**(0.22)**	(0.19)	**(0.17)**
s	**-0.18**	-0.34	-0.33	-0.77
	(0.14)	(0.14)	(0.12)	(0.16)
a	-0.49	-0.35	-0.43	**0.02**
	(0.10)	(0.09)	(0.08)	**(0.11)**
b	-1.49	-1.38	-1.38	-3.72
	(0.17)	(0.17)	(0.14)	(0.20)
v	2.52	1.96	1.96	4.07
	(0.20)	(0.19)	(0.16)	(0.15)
R	0.96	0.95	0.97	0.98
SE	0.11	0.09	0.08	0.15
F	109	84	121	308

Note: Statistically non-signficant results in bold, standard errors in parentheses.

6.2.2 Intercept (*c*) Descriptors

The first noticeable difference between the LSER descriptors in this regression series and typical LSER results was the very large *c* term. This indicated that either a significant amount of regression variance was unassigned, or that there was a significant contribution to retention that was a result of phase ratio effects. This is interesting given the previous study, which described the phase ratio effects on specific analytes, especially non-polar bulky compounds. It is also interesting that while not significantly different ($t = 0.53$, $df = 66$ for 160ºC and 180ºC), a decrease was observed in the 180ºC intercept in all regression studies. This approach may not resolve effects due to phase ratio at this sample size.

When this training set is regressed with the solute octanol-water coefficient instead of with the logarithm of retention factor, the scale of the intercept descriptor is much smaller and more in line with typical intercept values for LSERs. Torres-Lapasió et al. (2005) also performed this regression and their intercept value was on a similar scale as in this study (0.19±0.07 for Torres-Lapasió et al., and -0.04±0.19 in this study). The smallest relative intercept was observed for regressions of retention factors of the aromatic subset of solutes. Typically in LSERs of liquid chromatography samples all solutes are aromatic because a chromophore is used for retention monitoring. However, the intercept

of this regression still indicated a significant contribution to retention was not assigned.

6.2.3 Solvation Favorability (*e*) and Hydrophobicity *(v)* Descriptors

The two terms in the regression series that contribute to increased retention are the solvation favorability and hydrophobicity (*e* and *v*, respectively) descriptors. Solvation favorability correlates to the Van der Waal's forces between solutes and solvents due to excess polarizability relative to a reference alkane. However, the sign for all regressions for this term is positive, indicating that excess molar refraction will increase the retention factor; thus more polarizable compounds are more favorably solvated by the octadecane phase than by the aqueous phase. For all regression sets, the effect increases with temperature, indicating favorable solvation interactions with the octadecane phase are more favorable at high temperatures, which is also somewhat counterintuitive. What would be expected is that the solvation favorability should decrease with temperature, because the difference between phases decreases as temperature increases; this effect is seen in LSERs with mobile phase composition modification. In a study by Tan and Carr (1998), the *e* descriptor was found to be 0.49 (0.10) in a RPLC system with 20% THF as a mobile phase modifier, and 0.0 (0.06) at 50% THF. This indicates the likelihood of a function of

induced dipoles and dispersion interactions, which become more energetically favorable at high temperatures.

The volume of the analyte is expected to be the largest descriptor coefficient for any LSER and should increase retention because larger volume solutes should be more energetically excluded from the mobile phase than smaller volume compounds, due to the energetic cost of cavity formation. As is expected, the *v* term is larger than other coefficients and is positive. The statistically significant ($t = 2.68$, $df = 66$) difference between the *v* terms for 160ºC and 180ºC confirm a change in mobile phase. At this temperature range, the mobile phase changes behavior from pure water to one more like a hydroorganic phase, because the solvent cavity energetic value has reduced. This change correlates well with expected changes in mobile phase hydrogen bond reordering, which explains the reduction in the hydrophobic exclusion, as a rigid cavity is less formally established at elevated temperature. Temperature dependent changes in hydrophobicity and solvent favorability descriptors are presented in Figure 6.6, and demonstrate the relative shift in cavity formation as opposed to the unexpected shift in solvation favorability. This figure also depicts the relative size of effect of the two parameters; the change in hydrophobicity was approximately 10 times greater than the shift in solvation, and with the inherently larger contribution from the hydrophobicity term, it is not surprising that changes in this term dominate retention effects.

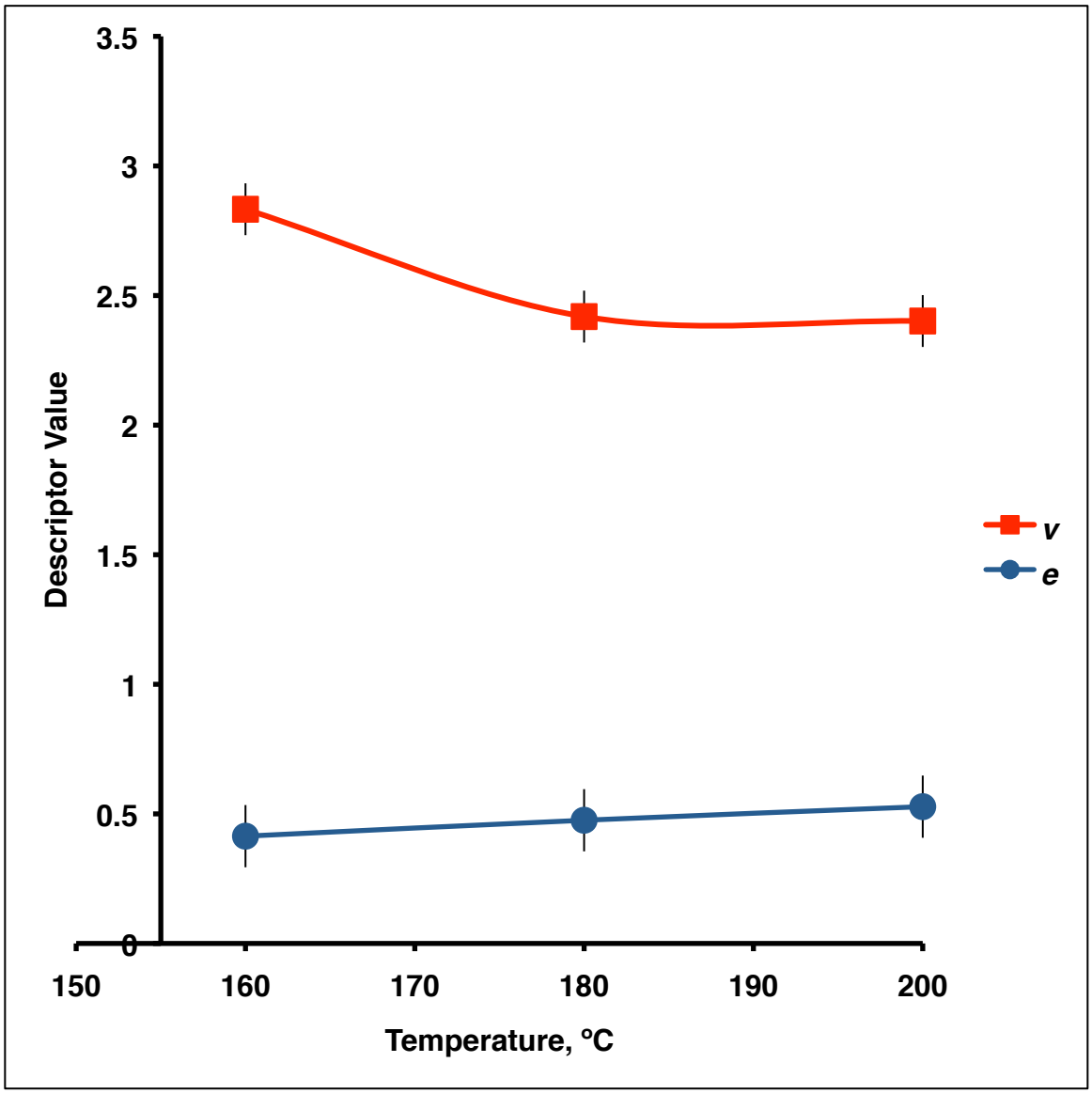

Figure 6.7 LSER solvent descriptors *e* and *v* as a function of temperature. Data derived from the full training set. Error bars are the standard error of the regression for each descriptor.

6.2.4 Temperature Dependent Hydrogen Bond Characteristics

The polarizability/dipolarity and hydrogen bonding terms *s*, *a*, and *b* are expected to contribute to partitioning into the mobile phase, giving these descriptors negative charges. It is difficult to deconvolute the *s* descriptor from the *e* term, as the two terms tend to overlap in solute parameters. The general description given to the *s* term is a correlation to the solvatochromic π* term, which is more like the traditional understanding of analyte and solvent polarity. The hydrogen bonding terms *a* and *b* are complimentary to the analyte terms, thus acidic analytes like phenol will compliment the hydrogen bond acceptor term in the solvent. The hydrogen bond donation and acceptance descriptors are expected to change as a function of temperature in correlation to the observed solvatochromic changes in the hydrogen bonding of the mobile phase. From the solvatochromic changes, the acidity of the solvent, *b*, should decrease with temperature, while the basicity, *a*, should remain relatively unchanged.

The solvent acidity term *b* was the largest contributor to reducing analyte retention. The trend from all tested analytes was a shift from a slightly greater value at 160ºC to a lower value above 180ºC. While a local minimum is observed at 180ºC, the value is not significantly lower than at 200ºC. Thus, hydrogen bond donation from the solvent was functionally reduced between 160ºC and 180ºC, which indicated the temperature at which the reorganization stops having a significant impact on the retention of analytes.

Solvent basicity was approximately a factor of 3 smaller in contribution to analyte retention than the acidity, and showed greater variation as a function of temperature. This was likely due to limited variation in hydrogen bond acidity parameters of the solute series. Frequently, acidic probe analytes have donation parameters that are very large (i.e., phenol, 1,4-dihydroxybenzene) indicating hydrogen bond donation to the point of acidic dissociation, or values of zero. Thus, solvent basicity descriptors are often difficult to probe, and this may account for the local minimum magnitude seen for this descriptor at 180ºC. Comparison of the three descriptor values for the full solute set did not demonstrate statistically significant difference, indicating variance is relatively limited for this descriptor as a function of temperature.

The solvent polarizability and dipolarity term *s* had a small contribution to retention relative to other descriptors, which was interesting as typically in liquid chromatography the facile description of solvent modification is the reduction of solvent dipolarity. This value iss effectively a measure of the difference in the polarity of the polar phase and non-polar phase, but the relatively small *s* term is observed for RPLC LSERs. At 180ºC, a relative maximum magnitude was observed to be -0.46 (0.12), which is comparable to the Tan and Carr (1998) citation for 20% THF, which had a statistically identical value of -0.41 (0.10) on an ambient temperature C_8 column. While the approximation given by Bolliet and Poole for temperature to organic modifier is 5ºC for every 1% modifier, the 20%

acetonitrile system of comparison had a *s* descriptor of -0.29 (0.05), which is slightly different from this system. Another interesting comparison to composition modification is that for increasing organic content in RPLC, the *s* descriptor decreases, indicating a smaller difference between stationary and mobile phase polarities. In this study, no such trend was recognized statistically, and it is possible an opposing trend was actually observed, with the polarity trend increasing between 160ºC and 180ºC. Again, the trend would be counterintuitive for what is expected to occur as mobile phase is modified. However, if the stationary phase changed orientation between these temperature points, then a large portion of previously unexposed non-polar surface became exposed and the solvent polarity would be observed to increase.

The values of *a* and *s* are very similar in scale, and show an opposite temperature trend in the full analyte set. This indicates that while solvent hydrogen bond donation (*b*) is a large contributor to retention, the hydrogen bond acceptance and polarity are comparably smaller. When these three descriptors are plotted together, as is seen in Figure 6.7, the relative scale of the descriptors demonstrates how much larger the effect of hydrogen bond donation is on retention as compared to the other descriptors. Thus, for polar analytes, retention can be largely predicted as a function of only the *b* and *v* parameters. The regression results using only the *b* and *v* terms are provided in Table 6.10.

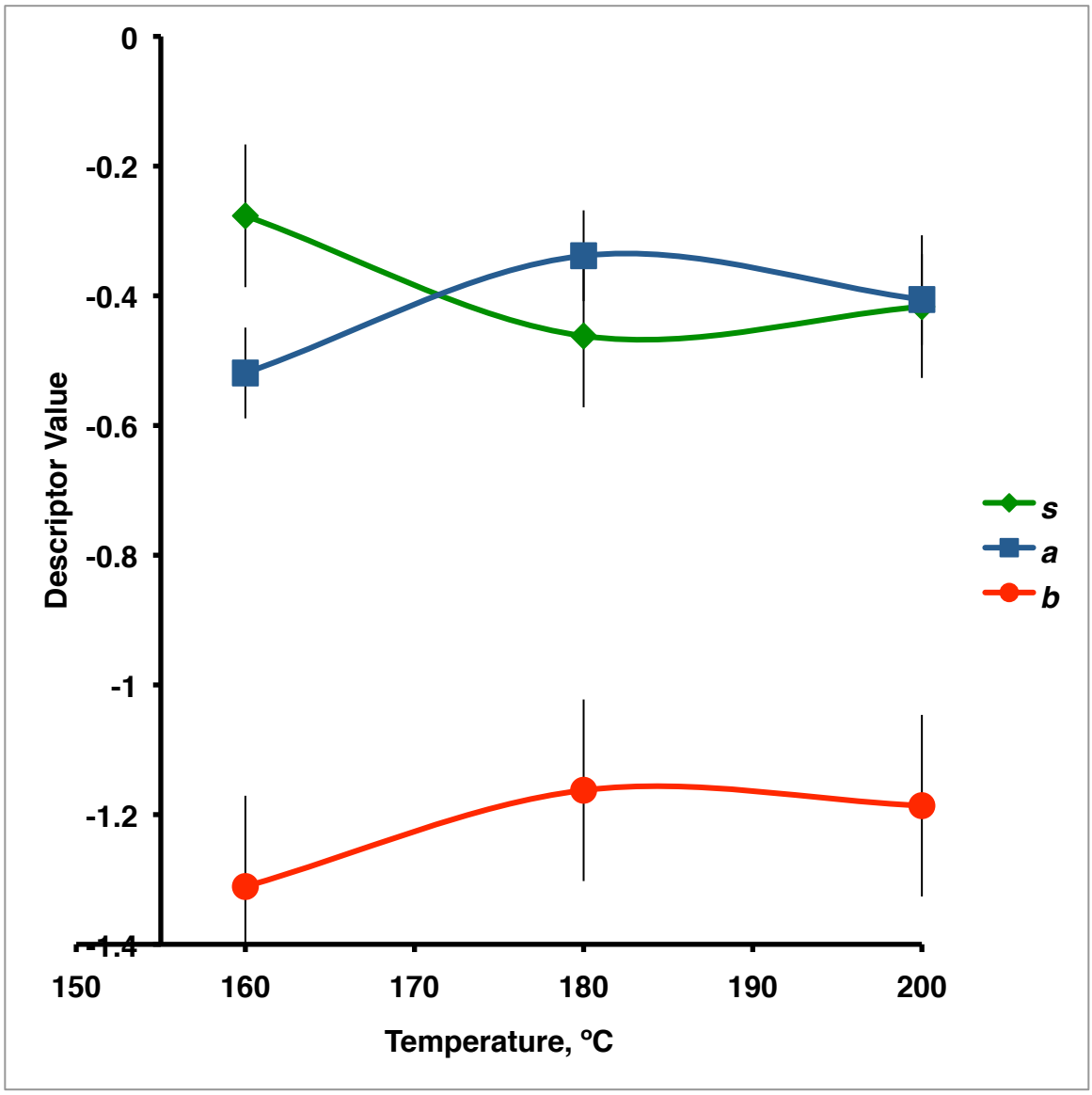

Figure 6.8 LSER solvent descriptors with a negative contribution to retention, from the regression of all test solutes. Error bars are the standard error of the regression for each descriptor.

Table 6.10 LSER regression values using B and V parameters only

Descriptor (SE)	B and V terms only		
	160	**180**	**200**
c	-1.43	-1.41	-1.47
	(0.18)	(0.16)	(0.16)
b	-1.79	-1.57	-1.68
	(0.18)	(0.16)	(0.16)
v	2.74	2.38	2.33
	(0.17)	(0.16)	(0.16)
R	0.92	0.91	0.92
SE	0.18	0.16	0.16
F	186	172	184

Note: Standard errors in parentheses

In Table 6.10, regression descriptors are provided for the full probe set with regression of the two most important parameters. When compared to the full set of parameters, the standard error of the regression increases and the overall fit decreases, but not by a wide margin. The correlation coefficient for the *b* and *v* was ~0.91 for the limited regression, and ~0.97 for the full correlation. The size of the intercept coefficient is similar, indicating little difference to the full LSER parameter set in the amount of unassigned variance.

6.2.5 Prediction of Analyte Retention based on LSER Parameters

The intent of producing a LSER is to be able to accurately predict the retention of an analyte in a chromatographic system based upon physical parameters, so that separations can be optimized for specific analytes and

analyte pairs. In addition, the prediction of analyte retention provides valuable data in the prediction of partitioning behavior in more complex systems. The LSER solute parameters of the training set were used to calculate predicted retention factors, which was then regressed against measured analyte retention factors in Figure 6.8. Next, a series of analytes were examined to test if the LSER parameter set could predict retention accurately. These analytes were not included in the training set, but have similar chemical structures and as such would be expected to have predictable retentions based upon their LSER parameters. The summarized measured retentions and predicted retentions are provided in Table 6.11. Some of the differences between predicted *k'* and the measured values are due to the low retention factor, such as acetone and propionaldehyde. However, compounds with similar structures to those in the training set, like ethanol and 2-propanol, show greater correlation. A long retaining analyte, 2-naphthol, demonstrated relatively accurate prediction of retention factor.

Table 6.11 Predicted and Measured *k'* of non-training set analytes at 200ºC

Compound	**Predicted *k'***	**Measured *k'***
Acetone	0.079	0.03
Ethanol	0.049	0.055
2-propanol	0.09	0.06
propionaldehyde	0.11	0.34
2-naphthol	9.68	9.16

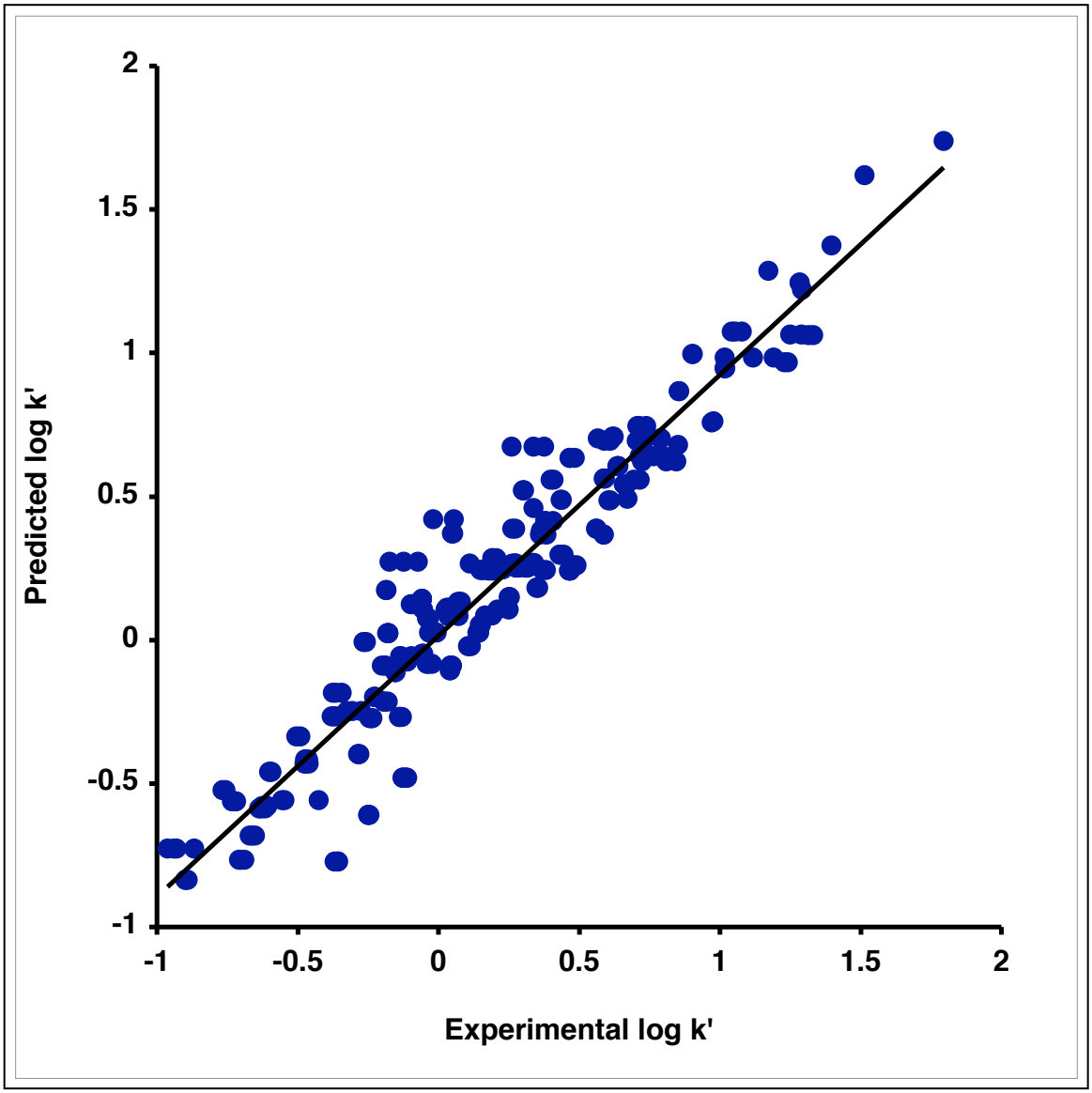

Figure 6.9 Correlation of measured retention factors to theoretical retention factors derived from LSER parameters. A measured correlation coefficient of R^2 = 0.97 is found for this comparison. Single retention factor values are presented.

6.4 Summary

Formal descriptions of the mechanisms of reversed-phase retention demonstrated the primary effect that controls solute partitioning was the energetic favorability of mass transfer between a stationary phase and a mobile phase. Stationary phase makeup controlled mass transfer through orientation (exposure volume of the non-polar phase) and favorability of cavity formation, with other contributions due to unmodified surface solvation and sorption effects. Mobile phase makeup controlled transfer through the changes in the favorability of cavity formation and the energetics of hydrophobic exclusion, which changed as a function of temperature and organic content.

Van't Hoff analysis of probe analytes demonstrated the temperature dependent phase transition observed in the stationary phase at around 175ºC, a temperature correlated to about 15% acetonitrile content in conventional RPLC. At temperatures above this transition, retention behaved like a solvated brush phase, whereas at lower temperatures, hydrophobic exclusion causes the partial collapse of the phase. Hydrophobic exclusion effects were also observed in computational simulations of water: octadecane phases, in which hydrophobicly driven aggregation was observed at 50ºC but solvation is observed at 200ºC.

In order to formalize contributions of solute size, polarity and hydrogen bonding characteristics, linear solvation energy relationships of solute parameters were used to produce solvent descriptors at three temperatures.

Temperature dependent changes in retention were correlated most strongly with changes in the energetic penalty of cavity formation, which decreased with increased temperature. The next largest contribution to retention was the hydrogen bond donation behavior of the solvent, which also reduced in contribution as temperature increased. Other solvent effects also had significant contributions, and the solvent polarizability/dipolarity term demonstrates changes that may also reflect a change in the orientation of the stationary phase. Using the derived solvent descriptors, correlation was demonstrated between measured and predicted retention both for the training set and for solutes not used for descriptor development, especially for compounds like 2-naphthol and ethanol with similar structures in the training set.

The partitioning of real dissolved organic/aqueous systems was modeled with the use of subcritical water as a mobile phase, which allowed for the measurements of partitioning of weakly polar molecules without the addition of another partial phase of organic modifier. The major predictor in solute partitioning to a dissolved organic layer is expected to be the solvent cavity formation descriptor; thus large non-polar molecules are expected to more readily partition to organic phases than small polar solutes. Methylation of a compound also increased organic partitioning, while polarizability decreased it.

Chapter 7: Removal of Organic Compounds with a Subcritical Water Oxidation Reactor

In this study, the usage of a wet oxidation process was examined for the removal of trace organic contaminants. A lab-scale, rotating tube reactor was used to perform subcritical wet oxidation, which caused accelerated oxidation, hydrolysis, and thermal degradation of organics. Subcritical water oxidation is more efficient than oxidation processes in ambient water due to the increased solubility of both organic contaminants and molecular oxygen. While molecular oxygen is more soluble in subcritical water, the mass transport from air is slow; a Taylor bubble was used to increase mixing the liquid and vapor phases in the reactor. The oxidation products of a series of simulated and actual wastewater streams were analyzed and results are reported in this section.

7.1 Metrics of Treatment in Wastewater Treatment

Two primary metrics of waste treatment are the reduction of solids and the removal of oxygen demand. For initial tests of reactor efficacy, wastewater

analogs were used to determine removal efficiency, with results summarized in Table 7.1.

Table 7.1 Oxidation of model compounds

Treatment of total solids[a]			
Treatment temperature, ºC	Initial total solids mg L^{-1}	Final total solids mg L^{-1}	% TS reduction
200	8750	5640	35.5
260	8750	168	98.1
260	17500	175	99.0
Oxidation products and chemical oxygen demand[b] reduction at 260ºC			
Initial COD mg L^{-1}	Final COD mg L^{-1}	% COD reduction	Residual organic acids, mg L^{-1}
2000	608	69.6	550 (60)
6000	1030	82.8	1700 (10)
10000	1960	80.4	3200 (20)
COD reduction at 260ºC with a 10 minute high temperature hold			
Initial COD mg L^{-1}	Final COD mg L^{-1}	% COD reduction	Residual organic acids, mg L^{-1}
6000	270	95.6	1140 (170)

[a] ASTM-208 A Method for total solids measurement
[b] ASTM-508 Method for measurement of chemical oxygen demand
Note: Standard errors in parentheses

Cellulose was derived from filter paper and was homogenized with water to make a solution with suspended solids. Initial solid concentrations were tested using the American Society for Testing and Materials (ASTM)-208 A method for total solids (TS) testing at 104-105ºC (the weighed initial sample was dried at 104ºC for at least an hour, then reweighed to measure percent solids).

With continuous mixing in the reactor tube, 500mL of sample was treated at 200 or 260ºC at a pressure of 4.32 MPa, held at maximum temperature for 10

minutes, then cooled to room temperature before testing the final total solid concentration. Total solids reduction was observed at both tested temperatures; however, a much greater reduction was observed for the higher temperature test. An increase in initial concentration did not decrease the % reduction, as both initial concentrations were less than the stoichiometric balance for oxygen provided during pressurization. Figure 7.1 depicts the results of removal of solids from the model cellulose solution.

Chemical oxygen demand (COD) was used as a measure of the reduction of dissolved organic carbon by reactor treatment. Solutions of glucose were used as a COD test compound, and treated at 260ºC and 4.32MPa pressure, with no hold at the maximum temperature. COD was tested via the ASTM-508a method before and after treatment, and residual organics were quantified via ion chromatography. Samples with initial COD levels of 2000, 6000 and 10000 mg/L all demonstrated significant reductions in COD, with higher concentration solutions demonstrating a higher final concentration of residual organic acids (primarily formic and acetic acid). A ten minute temperature hold resulted in further reduction in COD and residual organic acids, which suggested that at least some time dependency exists for oxidation, which may be related to the mixing mechanism between the vapor and liquid phase as a limit to reaction efficiency.

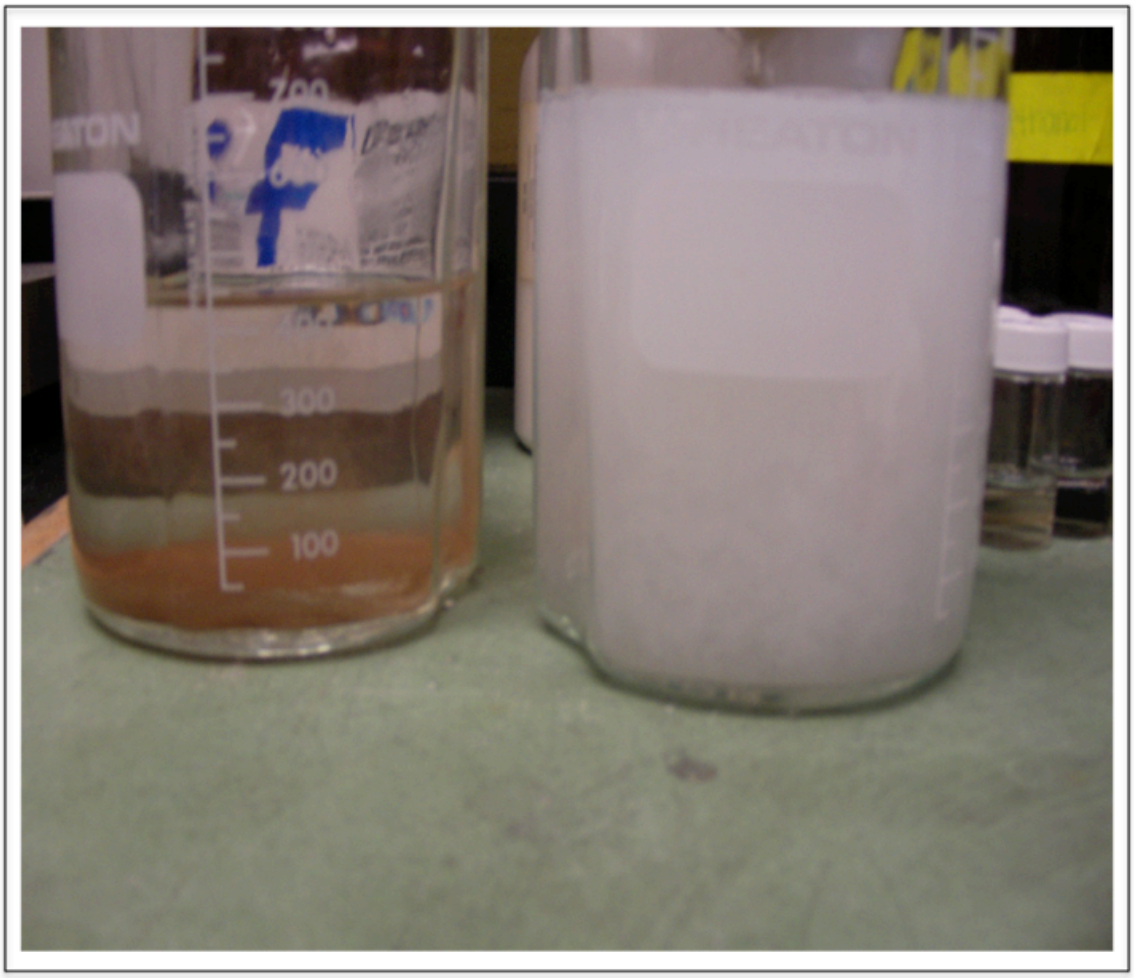

Figure 7.1 Cellulose solids before (right) and after (left) wet oxidation treatment.

7.2 Oxidation Products and Breakdown Mechanisms

Using simple solutions of glucose, predictions of all reaction products is possible, allowing for the estimation of conversion to CO_2. All solution concentrations were produced well beneath the equimolar ratio of carbon to oxygen as to assist in favorable conversion to oxidation products. Based upon the measured residual carbon in solution, and assuming a stoichiometric molar oxygen ratio for glucose combustion is 6 oxygen to 1 glucose, oxygen consumption can be measured by the change in pressure observed through the reaction to the amount of CO_2. In Table 7.2, measured residual organics in solution suggested that about 60% of the glucose present is converted to CO_2.

Table 7.2 Oxidation conversion efficiency and mass balance

Glucose oxidation products at 260ºC			
Initial moles glucose	Moles C as dissolved organics	Moles CO_2 produced	% Glucose converted to CO_2
0.00555	0.0125	0.0208	62.4
0.0166	0.0386	0.0612	61.3
0.0277	0.0727	0.0938	56.3
Reactor pressures at 260ºC			
Initial moles glucose	Predicted pressure (MPa)	Measured pressure (MPa)	Relative Percent Difference
0.00555	11.6	12.07	3.9
0.0166	11.2	11.83	5.7
0.0277	10.5	11.07	5.1

Figure 7.2 demonstrates the pressure and temperature changes as a function of time for a pure water solution. Figure 7.3 reflects the net pressure as

of a system as a function of initial glucose concentration, after the intrinsic pressure from the air and water are subtracted. Three runs of pure water and an initial pressure of 4.32MPa were heated to 260ºC and cooled to determine average values of water and air pressure as a function of temperature. Higher initial concentrations of glucose demonstrated a greater pressure drop relative to pure water, due both to the consumption of oxygen and high solubility of CO_2 at elevated temperatures. Predictions of CO_2 production were made by calculation of residual organic acids and subtraction from initial concentration, with the assumption that all other mass was converted to CO_2. The predicted pressure change due of the CO_2 produced and oxygen consumed in the reactor from Table 7.2 correlated strongly with measured pressure values at 260ºC, with a relative difference between predicted and measured pressure of less than 6%, which was reasonable, given the likelihood that other products were also produced besides organic acids and CO_2 (e.g., aldehydes).

Time resolution of pressure changes demonstrated pressure continues to increase after the maximum temperature was reached before gradually reducing back to the initial pressure value. When higher concentrations of glucose were used, net pressure reduction is observed relative to the low concentrations. This indicated oxygen was used up by oxidation processes early in the reaction (0-15 minutes) and was not replaced by CO_2 until later in the process (15-25 minutes). Thus, the pressure change from 25 minutes until the pressure maximum

predicted the degree of mineralization (complete conversion to CO_2). The 2000mg L^{-1} glucose sample showed a much higher degree of mineralization than the other two samples, which correlated with the lower concentration of residual dissolved organic acids found in this sample. The predicted conversion to CO_2 was not dramatically different from 2000mg L^{-1} to 10000mg L^{-1} from mass balance calculations of residual organic acids. This may indicate that at higher glucose concentrations mass was lost through volatile organic components, especially aldehydes.

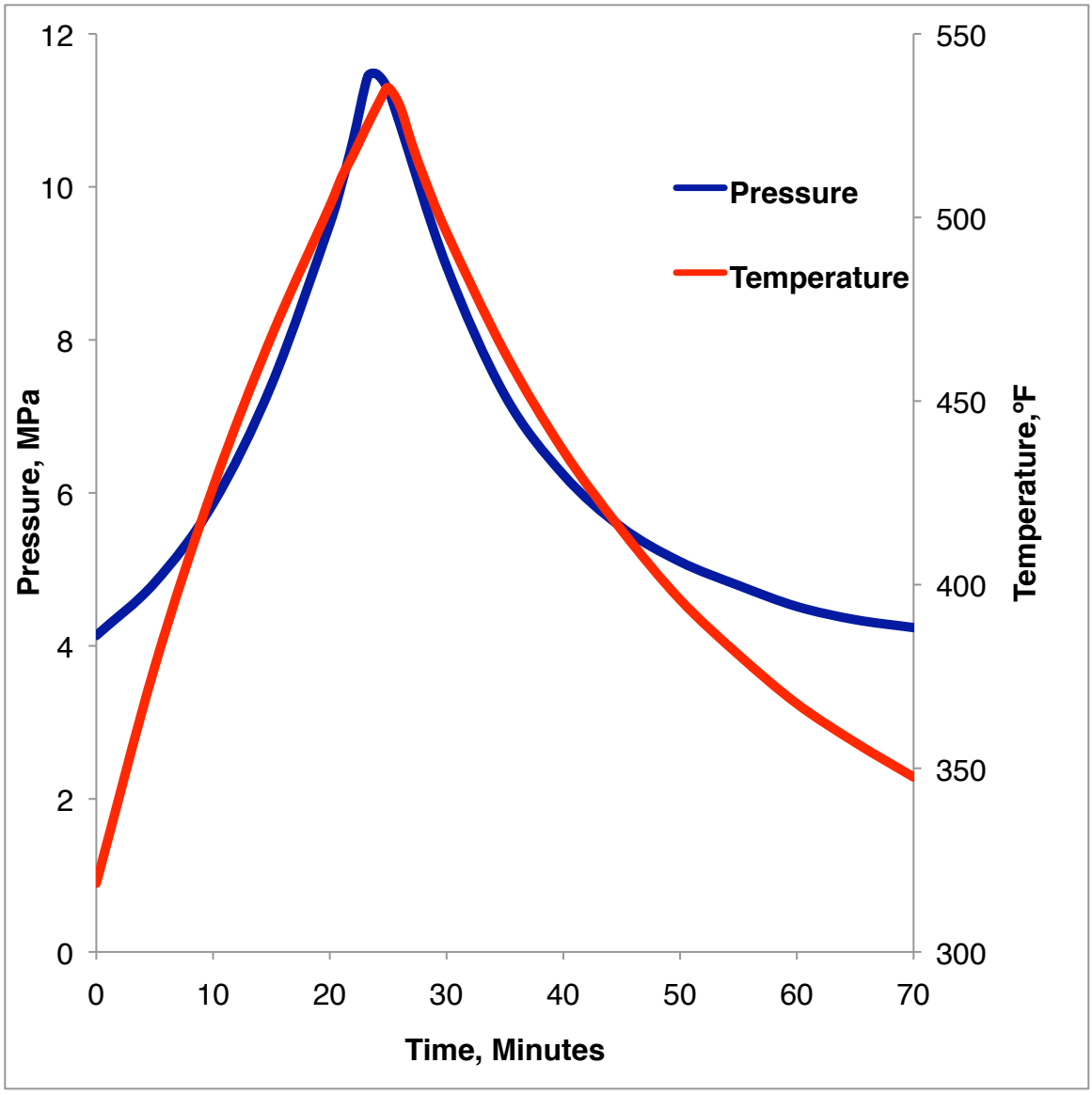

Figure 7.2 Temperature and pressure values of a pure water solution.

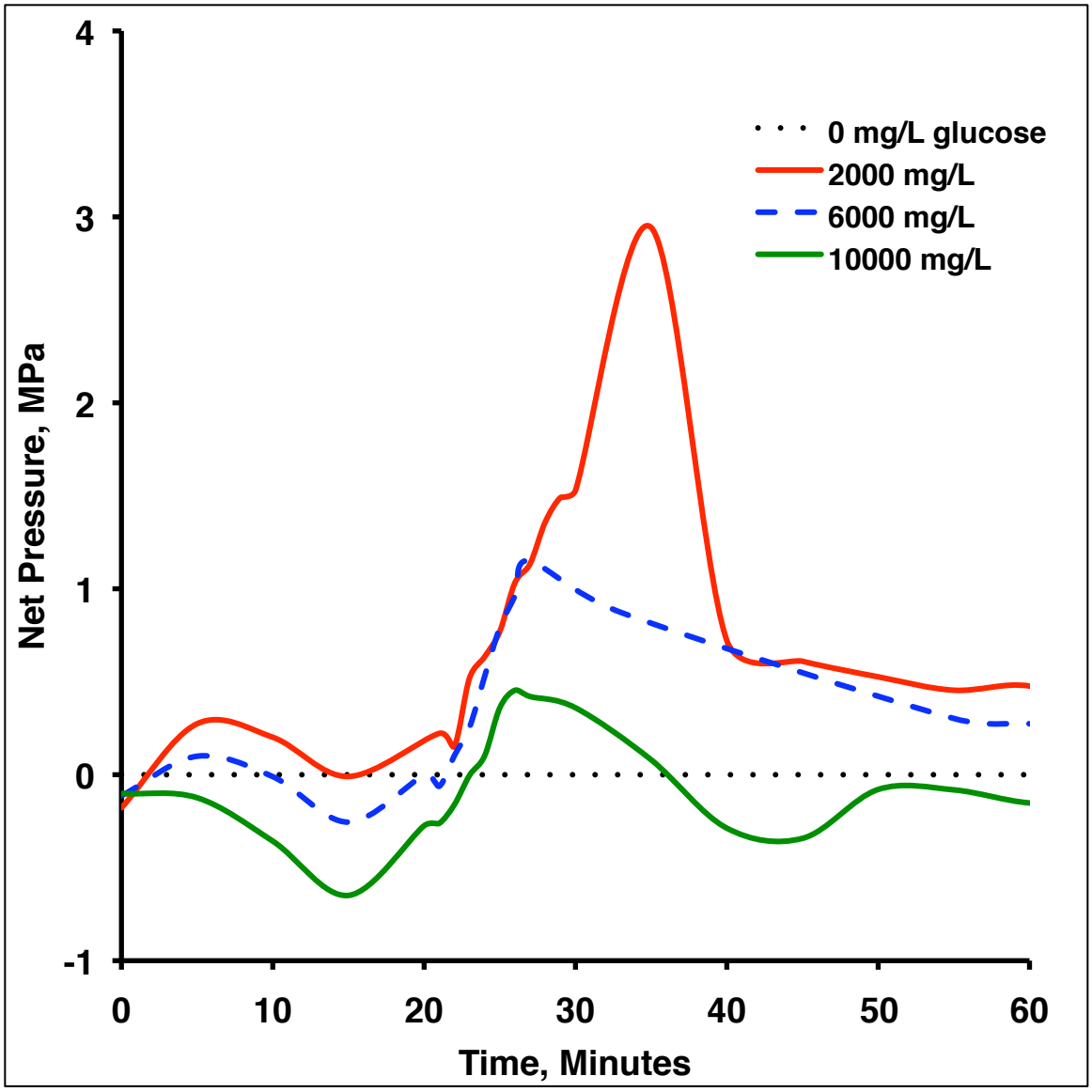

Figure 7.3 Changes in measured pressure as a function of reaction time. Changes in pressure were measured against the mean pressure production due to pure water. Maximum temperatures occurred at ~25 minutes. All samples had the same initial pressurization to 4.32MPa, and the same volume of liquid was added.

7.3 Treatment of Surrogate Waste Mixtures with the Lab-Scale Reactor

Two model wastewater systems were tested for treatment with the lab-scale reactor. The first system used bovine waste, which is high in cellulosic content. The second system was derived from hog waste and was of particular interest because of the environmental impact of large-scale hog operations, which typically collect the liquid waste in lined lagoons. The odor of hog waste is a concern, and the full-scale wet oxidation reactor has been suggested as a process for on-site treatment for commercial hog farms.

7.3.1 Treatment of Bovine Waste

A solution of bovine manure was made to an approximate concentration of 11400 mg/L of solids and then homogenized to produce a model wastewater solution. Treatment was tested at a constant initial pressure of 4.32MPa and temperature was raised to 200-260^{o}C, with a ten-minute maximum temperature hold. Solution total solids and COD were tested before and after treatment, and total organic acids were measured via ion chromatography (IC) after treatment. An example of the residual compounds detected by IC is provided in Figure 7.3.

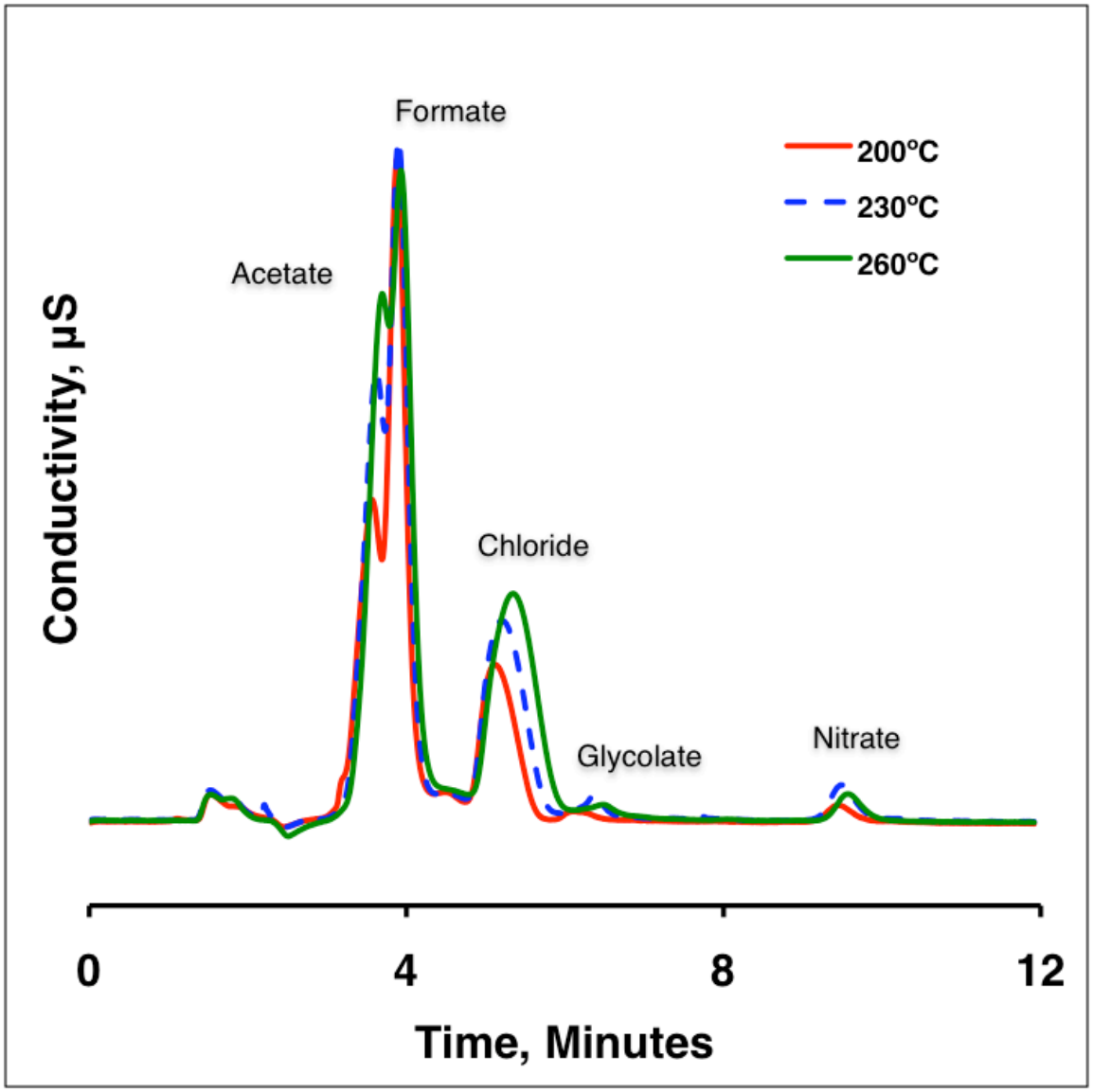

Figure 7.3 Ion chromatograph of treated bovine waste.

The major observable change in the IC plot was the increase in acetate at higher temperatures. Li et al. (1999) correlated acetate as a product likely to derive from oxidation instead of hydrothermolysis. This follows, as the solubility of oxygen increases with temperature, increasing the likelihood of oxidation.

Treatment results are summarized in Table 7.3. Of the three tested temperatures, similar reductions in TS and COD were observed, with the high temperature showing the most dramatic reduction in total solids. Residual organic acids were observed to increase in concentration as a function of temperature, although the measured concentrations were significantly lower relative to the pure glucose solutions. Due to the far more complex mixture present in the manure test, it is not surprising that a greater variance was observed in the COD and TS reduction. It is likely that with actual complex waste streams, less easily oxidizable compounds will be present, and therefore either longer residence time at maximum temperature, or greater stoichiometric balances of oxygen, or both will be required for effective treatment. Example surrogate solutions, before and after treatment are shown in Figure 7.4.

Table 7.3 Treatment of bovine waste solution

Initial concentration mg L^{-1}	Treatment temperature, °C	% COD reduction	% TS reduction	Residual organic acids mg L^{-1}
11600	200	71.2	66.0	86 (13)
11600	230	85.6	57.5	101 (15)
11400	260	75.4	> 99.9	105 (16)

Note: Single point values. Errors reported are derived from regression.

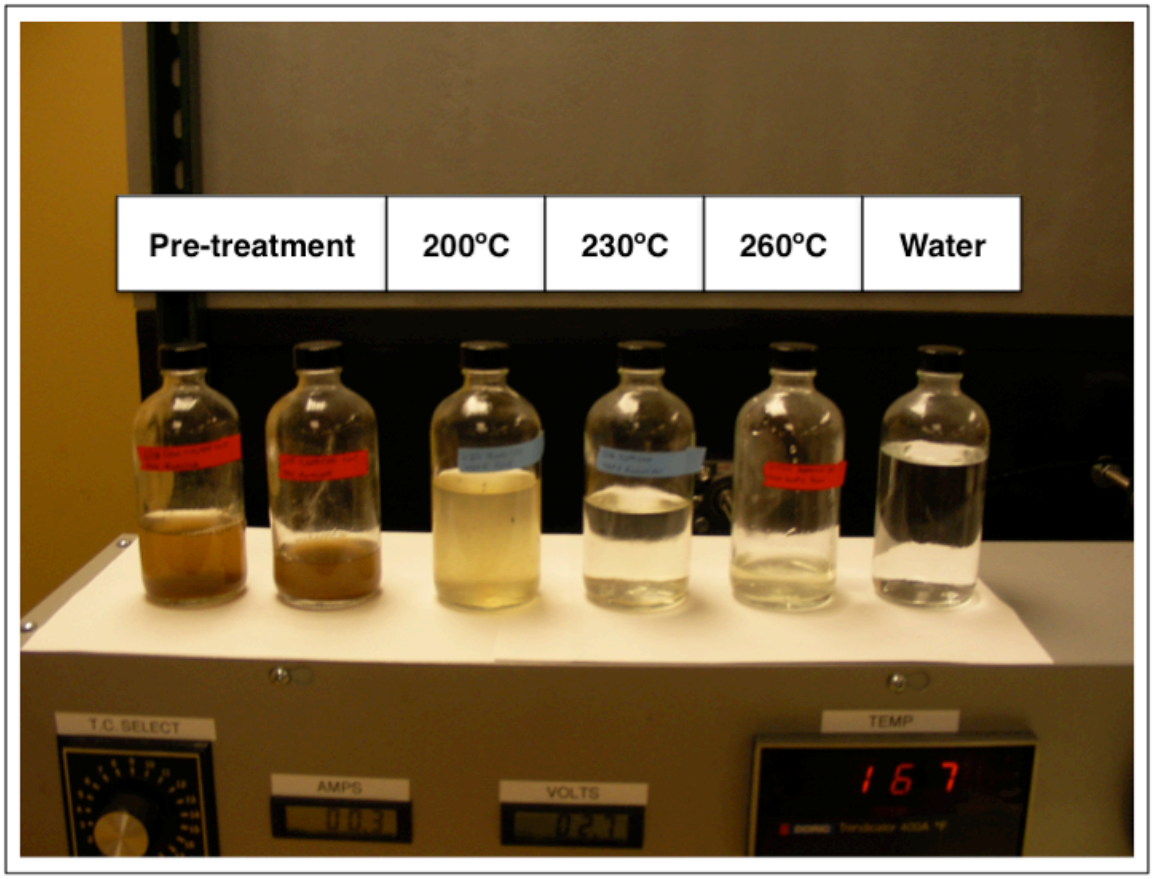

Figure 7.4 Bovine waste surrogate solutions, and resulting post-treatment products as compared to water. Residual solids and color are removed more efficiently at higher temperatures.

7.3.2 Treatment of Hog Waste with the Lab-Scale Reactor

Hog waste is usually considered to be a more difficult matrix for waste treatment, as it is more explicitly a mixture of feces and urine, which increases the nitrogen content of the material. However, the nitrogenous waste has great potential as a liquid fertilizer if offensive and potentially harmful organic contaminants such as antibiotics can be removed. Thus, the carbon and nitrogen concentrations of the effluent were monitored for treatment effects. Solids and COD were monitored using the same methods described previously, and nitrogen mineralization was monitored via ion chromatography for nitrate concentration. The results of the hog waste treatment studies are summarized in Table 7.4.

Table 7.4 Treatment of hog waste solution

Treatment Temperature, °C	Initial Concentration, mg L^{-1}	% COD reduction	% TS reduction	Residual organic acids (mg L^{-1})
200	12880	72.0	60.2	507
230	12880	70.3	91.0	312
260	12880	73.7	43.9	291
Treatment temperature, °C	**Conductivity, µS cm^{-1}**	**pH**	**Nitrate, mg L^{-1}**	
200	3200	7.4	3.7	
230	3500	7.2	10.6	
260	4900	7.5	30.6	

Note: COD, Residual acid concentrations and pH are average values of two trial sets.

The relative COD and TS reduction of hog waste was not as effective as the removal observed with the bovine waste. This may be due to the high ionic

strength of the hog waste, which may interfere with the acid-base catalysis observed in low ionic strength matrices. In addition, while the odor of the effluent had changed, it was not removed to a satisfactory level. This may indicate that highly volatile compounds are able to avoid oxidation or thermolysis by residing in the vapor phase. Nitrate levels were determined using a total water analysis performed by Colorado State University (CSU), using a LECO CN-2000 dry combustion method (Leco, St. Joseph, MI). A trend towards nitrogen mineralization is observed with the CSU method. IC was also used to attempt to quantify the nitrate levels; however no clear trend was observed, indicating a co-eluting compound in the effluent. Thus, the CSU results are reported in Table 7.4.

7.4 Removal of Sulfonamides with the Lab-Scale Reactor

Several studies were performed to measure the efficacy of decomposition of sulfonamide antibiotics using this reactor. Two relatively non-polar sulfonamides, sulfadiazine (SDZ) and sulfadimethoxine (SMZ) were selected as model compounds. SMZ is one of the least water-soluble sulfonamides and was chosen to test whether or not solubility within subcritical water would impact the breakdown. SDZ is moderately non-polar and was selected for the remainder of the studies due to its use in veterinary applications. Standards of 10ppm SMZ or 125ppm SDZ were added to approximately 5000 mg/L of analogs (i.e., glucose for SDZ, acetonitrile for SMZ) to simulate a background chemical oxygen

demand. The high concentration SDZ tested whether or not the breakdown would be limited by the time of treatment and if the reaction is temperature dependent. The lower concentration SMZ tested the likelihood of breakdown of a trace component and whether the concentration would result in reduced breakdown efficiency. Pre- and post-treatment samples were then quantified via RPLC. Results of these treatment measurements are reported in Table 7.5**.**

Table 7.5 Treatment of sulfonamide antibiotics

Compound	**Mean % reduction**
sulfadiazine	97.5 (0.14)
sulfadimethoxine	93.8 (0.31)

% Reduction of sulfadiazine by reactor temperature

Treatment Temperature, ºC	Mean % reduction
120	24.2 (1.72)
190	60.1 (0.70)
260	97.5 (0.14)

% Reduction of sulfadiazine with a 60 minute high temperature hold

Treatment temperature, ºC	Mean % reduction
190	94.0 (0.62)

Note: Standard errors in parentheses

Compound structure had a slight impact on the efficacy of treatment of the two antibiotics. SDZ treated at 260ºC, with no hold at the maximum temperature, showed an average concentration reduction of 97.5%, whereas SMZ showed on average a 93.8% concentration reduction. This difference may also correlate to

the background analogs, which were not the same due to differences between analyte water solubilities. The initial concentrations of the two compounds differed by a factor of ten; however, the measured reduction in concentration also scaled appropriately. Average residual concentrations of SDZ were measured at 3.8ppm from an initial concentration of 125ppm, whereas the SMZ showed a residual concentration of 0.63ppm from an initial concentration of 10ppm.

To test the minimum reactor temperature for effective reduction of SDZ, several temperatures were tested without holds. At a temperature of 120ºC, the concentration of SDZ was only reduced by 24.2%, whereas at higher temperature the degradation was much more pronounced. A sample hold of 60 minutes at a temperature of 190ºC results in degradation similar to a treatment of 260ºC without a hold. Degradation kinetics can be controlled by temperature and residence time, thus allowing for fine-tuning of the reactor to optimize target analyte degradation.

7.5 Sample Disinfection

A major step in normal wastewater treatment is the disinfection of biologically treated effluents to remove bacteria and other biota, typically using chlorine or other chemical disinfection methods. The wet oxidation process is functionally similar to an autoclaving process, in which high temperatures and pressures sterilized organic materials. By using a wet oxidation process for

disinfection, a value-added arrangement can be made for the removal of trace organics and bacteria. A Coliscan Easygel test (Micrology Laboratories, Goshen, NJ, USA) of treated bovine waste and of a biologically treated municipal wastewater was performed. Neither treated material resulted in colony-forming units, indicating the complete removal of *E. coli* and other fecal coliforms. Bacterial sterility was confirmed after a week of room temperature storage of the treated samples.

7.6 Summary

Several studies of wet oxidation processes in a lab-scale reactor were performed to determine breakdown processes of modeled waste streams. Initial studies of surrogate waste compounds indicated efficient reduction in COD and in solids concentrations. Surrogate waste solutions derived from animal wastes showed less efficient treatment but resulted in disinfected products with significantly lower COD and TS concentrations.

The breakdown process was controlled by two competing reactions: 1) the hydrothermolysis of compounds due to the inherent acid-base catalysis of subcritical water, and 2) the oxidation of compounds due to the free radical oxygen mechanism (Shanableh, 2005 and Li et al., 1991). Oxidation was enhanced in this reactor due to the efficient transport and solubility of oxygen in the subcritical medium, but hydrothermolysis was also observed. The reaction

process can be time-resolved as a function of system pressure, with initial net decreases in pressure corresponding to oxygen consumption and later increases corresponding to CO_2 production. Mineralization was observed to occur most completely in low COD systems, where full oxidation or breakdown occurs. At higher COD concentrations, more side products were observed and less CO_2 measured. Higher temperatures corresponded to greater dissolved oxygen concentrations, which correlated to a greater rate of oxidation.

Using sulfonamide antibiotics as a model trace organic contaminant, the removal efficiency was found to be greatest at high temperatures or in long residence times at high temperatures and pressures. Breakdown was more efficient for more water-soluble compounds, which was consistent, as all breakdown was expected to take place in the liquid phase. This suggests parent or breakdown products that are highly volatile are unlikely to be completely treated using the wet oxidation process; however, further testing is required to determine if this is the case.

The most likely place where PPCPs and associated compounds enter natural waters is through wastewater treatment plants, and, as such, WWTPs are the best position for the removal of trace organic contaminants. Conventional wastewater treatment focuses on the removal of bulk organic material, but trace organics could potentially be treated using mechanistically orthogonal techniques such as wet oxidation. Further studies of wet oxidation will expand the

examination of matrix effects on trace organic breakdown, as well as determine efficiencies of removal of expanded classes of compounds.

Chapter 8: Conclusions and Future Directions

The use of subcritical water technology has allowed for the investigation of partitioning behavior of polar solutes in pure water and also has been used as a reaction medium for the breakdown of polar solutes. Both of these research directions have a common goal -- quantification and removal of polar organic environmental contaminants of anthropogenic origin. In the case of quantification of polar analytes, new instrumentation was designed, and mechanistic studies were performed to determine the concentrations and partitioning behaviors of solutes. Previous work has often required complex mass spectral detection. In addition, little is known of the behavior of polar analytes once they enter a natural water system with organic, aqueous, and mineral phases. Polar analytes of anthropogenic origin usually belong to broad classes of compounds derived from pharmaceuticals, personal care products, high production volume chemicals and industrial surfactants, all of which are likely to pass through municipal wastewater treatment plants. Because wastewater plants are not designed for the removal of trace organic analytes, new technologies for the removal of PPCPs must be

developed. Using subcritical water and oxygen, efficient organic compound breakdown and disenfection was performed, by a wet oxidation mechanism. In order to prevent environmental effects from PPCPs, quantification, fate and WWTP treatment efficiency must be explored further. In addition to protecting biota from the unintended consequences of consumer and industrial products, a greater understanding of the chemical processes involved with the transport and fate of polar compounds will assist in the future designs of environmentally benign chemistry.

8.1 Detection of Polar Organic Compounds with SWC-FID

A basic design for a subcritical water chromatography system with flame ionization detection (SWC-FID) was constructed, using the work of Miller and Hawthorne (1997) as a guideline for system components. SWC-FID has advantages for the detection of environmental analytes due to the universal detector response to organic molecules. Mass spectrometry is most typically used for this purpose, but MS requires a complex, expensive system and cannot easily detect small polar molecules. Using SWC-FID as a primary screening tool for organic contaminants in aqueous systems would likely be more cost effective and simple, as a single separation could be used as a “go: no go” analysis for the presence or absence of contaminant classes. This would allow mass spectral

techniques to be used as a confirmatory technique, when structural information or more refined separations are required.

A new injection and sample preheating design, which kept the mobile phase and injection loop at the same temperature as the chromatography column, was built to remove thermal mismatch as a contribution to band broadening. The primary limitations of this system are the mobile phase flow requirements with the FID and the thermal limits on system components, especially the chromatography column. Using a weighted least squares regression, the detection limits of several compounds were found to be on the order of 1ng injected or less, with more volatile compounds demonstrating lower detection limits than non-volatile compounds. These detection limits were significantly lower than values reported in literature, but come with a cost of separation efficiency. A large column was used for greater analyte capacity, and no post-column split was used for maximum detector efficiency; however, low mobile phase flow rates are required so as to not extinguish the FID flame, resulting in poor separation efficiencies.

Because of the large linear response range of the FID, this system can deal with analyte concentrations from the part per billion up to mass percentages of analyte. This linear range means quantification of high production volume chemicals without chromophores can be performed, which is especially relevant to agricultural and food applications.

The FID can also readily hyphenate with other gas phase detection methods, and, as long as the other detection methods are also insensitive to steam, they can be used in conjunction with the SWC-FID system. Food chemistry applications are often interested in the detection of malodorous compounds containing sulfur, and so a sulfur chemiluminescent detector was hyphenated to the SWC-FID. Adding a selective sulfur channel allowed for increased peak capacity by the addition of a selective data channel, which allows for the recognition of co-eluting compounds separately. This is demonstrated by the identification of a surrogate contaminant, β-mercaptoethanol, in a high mass percentage alcohol matrix.

Separations are possible on the SWC-FID system as currently designed. Separation order is controlled by solute size and polarity and is similar to separations in RPLC. Thermal programming is demonstrated to be analogous to mobile phase composition programming in conventional RPLC, with isothermal and thermally programmed separations resulting in similar chromatograms to isocratic and composition program separations. Thermal programming demonstrated more efficient peak shapes than isothermal separations.

8.1.1 Future Directions and Applications of SWC-FID

Continued research on the SWC-FID system will need to focus on improving separation efficiency, without sacrificing linear range or detection

limits. For effective detection of polar analytes in the environment the detection limit range of any system must be in the low part per billion range. Separation efficiency will also be required so that complex environmental samples can be separated meaningfully. The simplest method for improving trace analyte detection may be to use narrower columns, which can be commonly purchased at 1mm internal diameter sizes. For even lower flow rates, micro-LC columns could be used, providing that a suitable stationary phase can be acquired.

A second method of improving peak capacity may be the adaptation of two-dimensional liquid chromatography (2DLC). The second separation dimension in 2DLC has often used elevated temperature chromatography as a method for accelerating separations, with the second dimension often designed for ultra-fast separations. Typically, 2DLC uses UV-Visible detection in both separation dimensions; however, a split to a FID may be possible, allowing for universal organic detection. The minimization of organic mobile phase modifiers would also simplify mass spectral detection for a 2DLC system, as current technology requires the use of two different modifiers in each of the separation dimensions.

In addition, different stationary phases are required for more efficient usage of the SWC-FID system. However, stationary phase collapse is a major concern for columns in pure water, so future column selection must take this into account. While zirconia-based columns can be used for many compounds,

exposed zirconium atoms behave as Lewis acids and can cause irreversible binding of many common functional groups, especially phosphates. Carbon-clad zirconia, used in many of the studies, can help prevent this type of inorganic interaction; however, zirconia columns still have much less passive stationary phases than typical RPLC silica columns, limiting operational flexibility.

The subcritical water chromatography system has numerous advantages in the field of green chemistry, and the pure mobile phase simplifies mechanistic studies of solute retention considerably. Flame ionization detection has been used for decades as a universal organic detector in gas chromatography, and the application of universal organic detection has significant use for the examination of polar compounds in the environment. Compounds in aqueous matrices can be directly injected into a SWC system with minimal sample preparation. Using efficient analytical techniques like SWC-FID can allow for more rapid responses to contamination events, eliminating the need for time-consuming techniques on samples without relevant contamination. SWC-FID cannot replace mass spectral detection, but may be considered a complementary technique for rapid screening of aqueous samples for organic classes of interest. Using SWC-FID as a screening tool may allow for more complete environmental analysis, and response in adequate time to promote environmental benefit.

8.2 Mechanistic Studies of Polar Analytes in Pure Water at Ambient and Elevated Temperatures

Partitioning of polar analytes in complex environmental matrices is a possible predictor of bioavailability, and models of polar solute partitioning between organic and aqueous phases are required to better correlate solute structure to behavior in the environment. Results of using reversed-phase retention as a model of partitioning between organic and aqueous phases provide insight into the mechanisms and statistical favorability of mass transport. In order to use RPLC as a model system organic modifiers are required to increase the solvent strength of the mobile phase, which changes the microstructure of the organic/aqueous interface. Using subcritical water as a mobile phase allows for increased solvent strength, while providing a partitioning interface more similar to natural organic/aqueous interfaces than observed with hydroorganic mobile phases.

Using a zirconia-based high temperature octadecane column and a pure water mobile phase at subcritical temperatures and pressures, the retention behavior of a number of analytes was tested. The enthalpy of transfer was measured for a series of carefully selected analytes. Some analytes displayed a linear response between retention and temperature, while others demonstrated significant deviations from linearity, indicating transfer favorability changed as a function of temperature. Using the selectivity between analytes was expected to

cancel out the most likely contributions to non-linearity -- specifically the contribution of volume phase ratio between the stationary and mobile phases. However, this assumes the effective phase volume is identical between analytes, which is incorrect when comparing polar and non-polar analytes.

Polar analytes, as well as linear, relatively non-polar analytes like 4-heptanone, are more likely to partition to the surface of a non-polar phase, as it is energetically unfavorable to remove hydrogen bonds from a polar functional group but not replace them in a fully hydrophobic cavity. Fully non-polar analytes, especially toluene and ethylbenzene are more likely to partition deeply into a non-polar phase, requiring a greater initial energy of cavity formation, which is energetically balanced by the entropic favorability of hydrophobic exclusion. In a collapsed stationary phase, the effective phase volume of the non-polar phase is smaller for a non-polar analyte than it is for a polar one, which is observed in the non-linearity in selectivity in van't Hoff plots of toluene and ethylbenzene, as compared to benzene and 4-heptanone. Once temperature is sufficient (i.e., ~ 175ºC, equivalent to ~15% acetonitrile in RPLC), the mobile phase appears to have been adequately modified to solvate the non-polar stationary phase, and the phase transitions from partial collapse to full extension.

While energetic descriptions of phase transfer provide a partial picture of what drives mass transfer in organic: aqueous phase interactions, this method poorly describes how molecular structure correlates to partitioning. Using a set of

34 solutes, retentions were measured at three temperatures: 160ºC, where the stationary phase is largely collapsed; 180ºC, where the phase has begun to extend; and at 200ºC, where the phase is most likely fully extended. Using these three temperatures can assist in the description of natural waters, where in the absence of miscible organic modifiers in the aqueous phase, much of the dissolved organic phase is likely to be compacted. Solvent descriptors were calculated from the retention factors and solute parameters of the training set. From this regression, it was determined that the largest contribution to mass transfer is the hydrophobicity of the solute, which is measured as a function of solute size. Larger analytes were found to retain longer, correlating to hydrophobic exclusion from an aqueous phase. The next largest contribution is from the hydrogen bond acceptor character of the solute. Hydrogen bond base sites on analytes decrease retention; this is the same as hydrogen bond donation in the aqueous phase. The hydrophobicity and hydrogen bond donation both decrease in magnitude as a function of temperature in subcritical water, resulting in decreased overall retention at higher system temperatures.

8.2.1 Future Directions in Mechanistic Studies of Polar Analyte Partitioning

Partitioning effects between organic and aqueous phases provide a valuable description of the bioavailability of polar contaminants; however, natural waters are considerably more complex than the chromatographic model used in

this study. In addition extrapolations to natural waters from a subcritical system are at least as difficult as extrapolations from mixed mobile phases, making descriptions of ambient organic-water phases very difficult to produce. In reality, polar analytes can partition to organics, as well as sorb to minerals or solid particles through ion pairing or exchange and other mechanisms. In addition, the dissolved organic phase in natural waters is considerably more complex than the uniform octadecane phase in a RPLC column. Using the approach in this study, a better model of polar partitioning may be designed.

Inorganic carbon stationary phases, which would be similar in structure to the black carbon found in natural waters and sediments, may provide a measure of how polar compounds interact with π donor surfaces. This would be a useful study to extend with the described subcritical water mobile phase, as carbon stationary phases have high thermal tolerances and would not undergo any phase change as a function of temperature. By performing a van't Hoff analysis of retention of the identical analytes used in this study, linear selectivities would be expected, as no stationary phase reorientation would be possible. Other columns with more humic-like stationary phases would also be of use in better describing natural aqueous systems and to determine the effects of stationary phase collapse. Phenyl and naphthalene stationary phases, which currently are not available with subcritical temperature tolerances, would be ideal in this

regard, as many models of dissolved humic matter suggest a large percentage of dissolved organics are aromatic.

Mineral and nano-particle surface sorption is likely to be a significant contributor to polar contaminant mass transfer. Because these surfaces may act as a breakdown catalyst for some compounds and concentrators for others, a better description of the interactions of polar compounds with these surfaces is required. Newly designed flow injection studies of nano-particle sorption performed by Sorauf et al. (2009, manuscript in preparation) may provide insight into this process. While sorbed compounds are not bioavailable, desorption without transformation may result in continuous concentrations of organic contaminants.

8.2.2 Computational Analysis of Pure Water-Organic Phase Microstructure

In order to correlate the findings of the thermodynamic studies performed in the partitioning studies to actual mechanistic behaviors of pure water and organics in more complicated systems, computational models of the partitioning of organic molecules and the effects of hydrogen bonding at elevated and ambient temperatures are needed. Preliminary data collected using the University of Denver Natural Sciences and Mathematics server are presented here. Unfortunately, the computational power required for the processing of complex Monte Carlo simulations is far greater than what is currently available for

this study; further computation will be required to confirm the findings presented. Typical Monte Carlo simulations must be run for at least 100000 cycles, and this was not possible at this time.

The first study simply sought to predict temperature dependent hydrogen-bonding changes from ambient to elevated temperatures at the higher than ambient pressures seen in the subcritical water system. This was required to prove that the simulation system accurately reflected previously observed temperature effects on water hydrogen bonding and to see if the elevated pressure affected hydrogen bonding in ambient water.

The second study simulated the effects of a model dissolved organic model system at several temperatures to determine if local augmentation of hydrogen bonding between phases was observed at elevated temperatures. This study sought to observe phase interactions between an octadecane phase (modeling a dense organic system) and a water phase to determine changes in ordering parameters at elevated temperatures.

A final simulation modeled the partitioning of a weakly hydrophobic compound – phenol -- between phases in order to predict how solute behavior changes as a function of temperature.

8.2.3 Hydrogen Bond Reordering at Elevated Temperatures

In this study, a 30Å× 30Å× 30Å CBMC simulation box was created with periodic boundary conditions and populated with 1000 water molecules designed using the TIP4P forcefield. An external pressure bath of 1.5MPa was used for all simulations, and the NPT ensemble was used. Box dimensions were allowed to change during the equilibration phase (1000 MC cycles) and then densities were measured. Simulation densities, which were calculated by the system, correlated well with published values for water in this temperature and pressure regime. After initial equilibration, the system was allowed to equilibrate for 10000 additional MC cycles to maximize local density interactions. The thermodynamic properties determined from the simulations are summarized in Table 8.1.

Table 8.1 Thermodynamic values of subcritical water from CBMC simulation

System temperature, K	Final volume, nm^3	Specific bulk density, g mL^{-1}	Literature value of density, g mL^{-1}
293.15	30.069	0.995	1.0023
373.15	32.47	0.921	0.9593
423.15	34.499	0.867	0.9225
473.15	38.05	0.787	0.8709

Note: literature value from Wagner and Pruss (2002).

The hydrogen bonding of an aqueous system can be determined by an empirical relationship to the pairing distance density functions determined by the CBMC simulation. Pairing densities are normalized functions that measure the relative likelihood of a given pair of atoms to be a given radial distance from each other, relative to the overall bulk density of the phase. Local density

augmentation relative to the background density results in the indication of a favorable interaction between molecules, which in this case would indicate a favorable distance for a hydrogen bond pair. Thus, as is observed in Figure 8.1, a local field augmentation of the 20ºC radial density function at approximately 1.8Å correlated to the equilibrium hydrogen bond length. While the 20ºC simulation plot gave the most resolved local density augmentation, all temperature simulations showed augmentation from about 1.6Å to 2Å, and local density depletion from 2Å to 2.6Å, which correlated to the distances of hydrogen bond favorability, and anti-favorability respectively. As expected from solvatochromic measurements, as temperature is increased from ambient to subcritical, the formalized hydrogen bonding seen in ambient water was broken down, and as a result less discrete hydrogen bonding density augmentation was found. Raw pairing densities of Oxygen: Hydrogen atoms are provided in Figure 8.2, which also showed the enrichment of radial distance density about the equilibrium hydrogen bond length. This indicated that formal hydrogen bonding decreases in subcritical temperatures but is not absent.

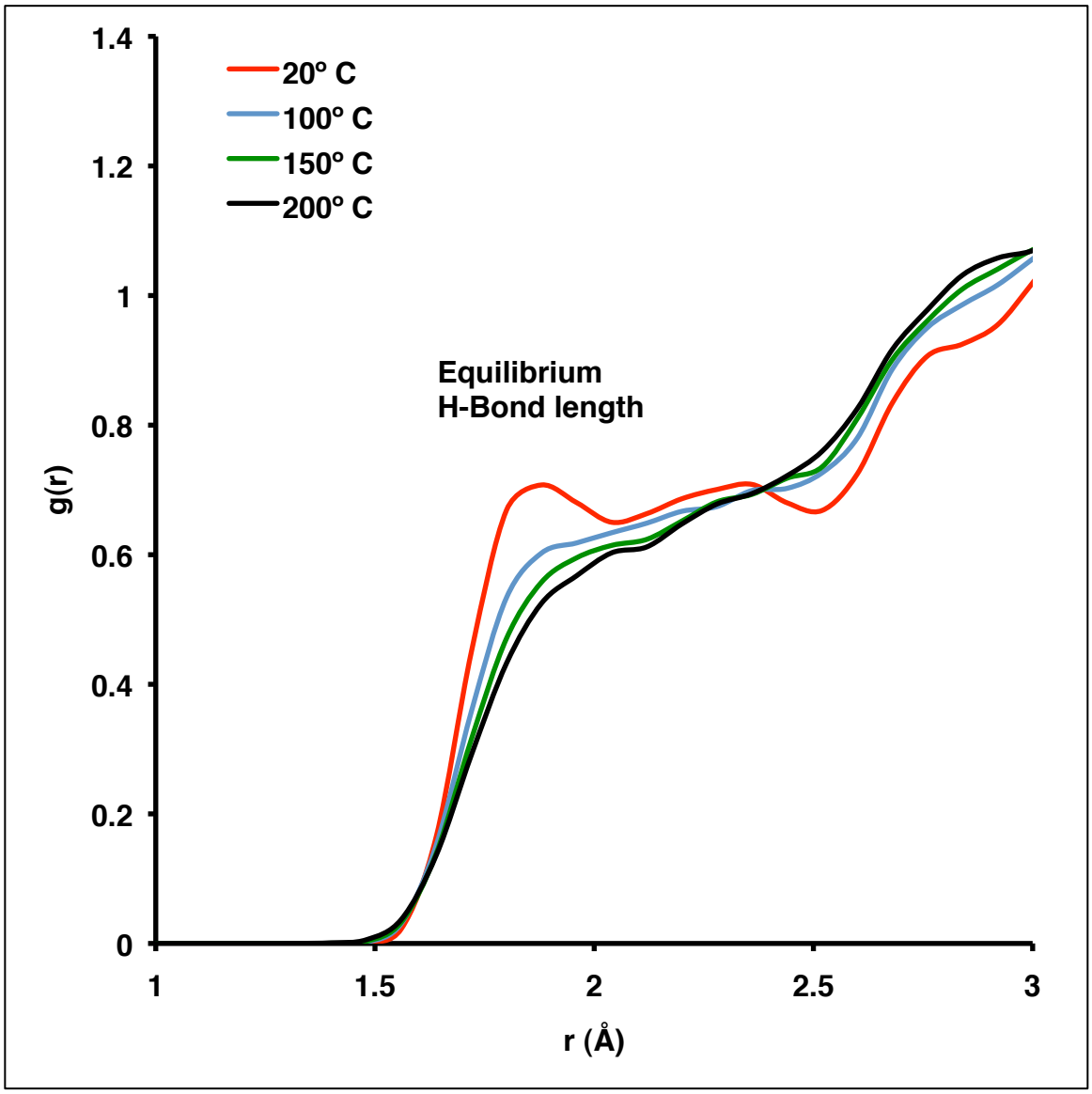

Figure 8.1 Composite density function of water at ambient and elevated temperatures, at 1.5MPa. A broad enhancement from 1.5 to 2.25Å is seen at all temperatures with corresponding deficits from 2.25 to 2.75Å, demonstrating hydrogen bonding.

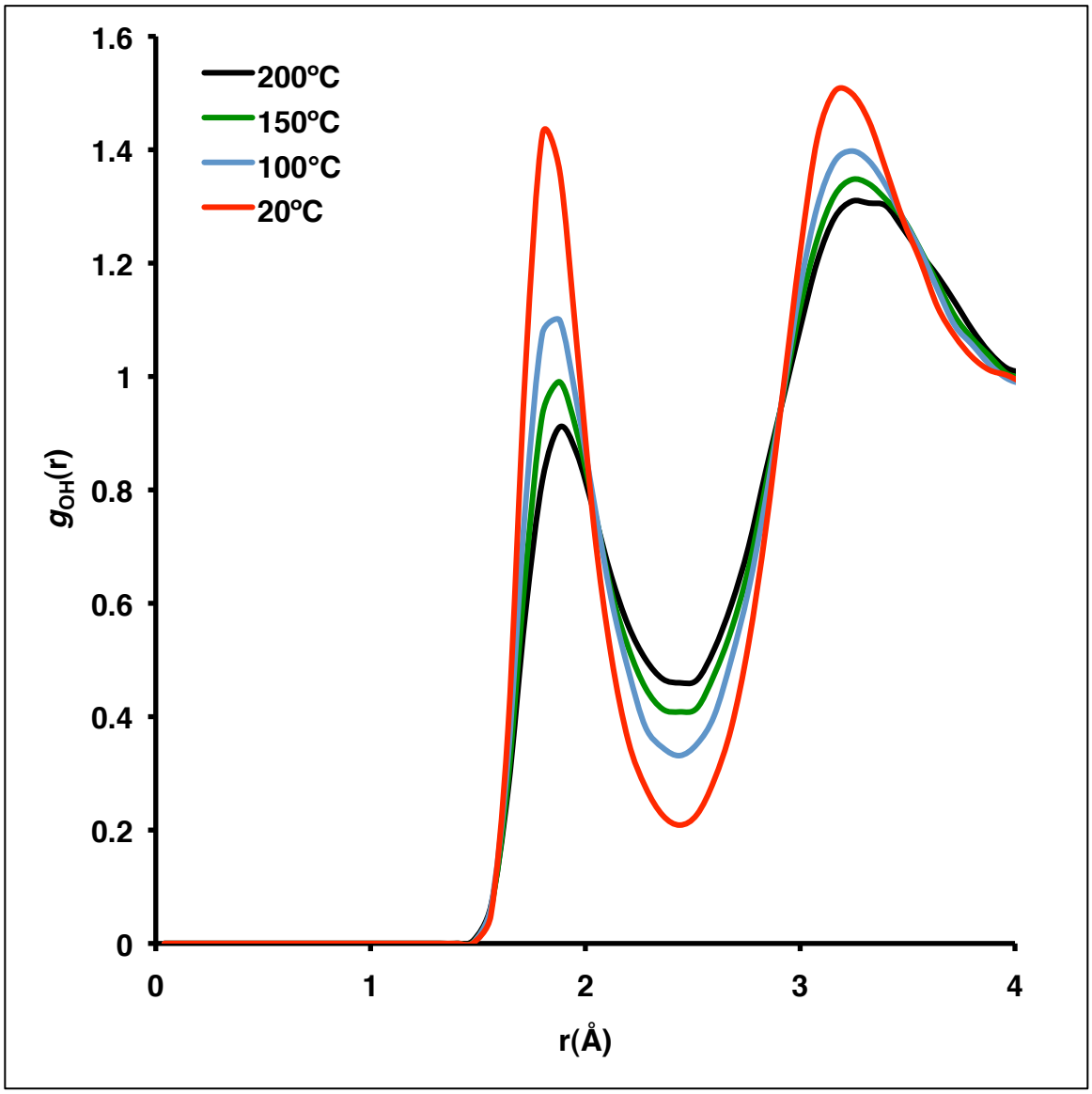

Figure 8.2 Pairing density of oxygen to hydrogens. The maximum observed at approximately 2A correlates with the relative measure of hydrogen bonding in the system, with high concentrations of hydrogen bonding at ambient and decreasing concentrations at elevated temperatures.

8.2.4 Solvation of a Model Organic Phase

In order to model the effects of solvation of an octadecane organic phase as a function of temperature, atomic density profiles were used to determine the sampling space of the center of the octadecane mass. A reasonable approximation of the center of mass for the octadecane is to average the atomic density values of the C9 and C10 atoms in the chain. Using the analyse_movie function, density profiles of sampled space were calculated and projected onto an XY plane. Actual centers of mass, although calculated in the system, are not outputted, and, as such, the main concern is observing the relative positions of the centers of the molecules. This density profile allows for the normalized quantification of sample space tested by the system, with greater sample coverage indicating that a thermodynamic minimum is not reached; thus MC cycles continue to move the center of mass in order to search out a thermodynamic minimum. If favorable solvation occurs, then the center of mass is expected to be less likely to move in the sample space, and local densities should be observed. In addition, it is more likely that, due to hydrophobic exclusion, aggregation would be observed in simulations where solvation is unfavorable.

For this simulation, two boxes were allowed to interact thermodynamically in the NPT ensemble; the first box contained five *n*-octadecanes while the second contained one thousand water molecules. While the density of the

octadecane phase was lower than is expected in RPLC phases, it was required to prevent aggregation that would not be statistically broken up by the simulation. After initial configuration, the simulation was allowed to process for 10000 MC cycles. The movie file created recorded the atomic density profiles of all atoms during and projected the density as a function of likelihood of finding a given atom in the averaged equilibrium. The density plots were produced by plotting the density function in the X direction against the density in the Y direction. It is important to note that XYZ coordinates were relatively arbitrary in this case, as no reference point is used, and simulation boxes have periodic boundaries, so a plot of XZ or YZ would give equivalent data. Figure 8.3 shows the approximate center of mass density function of the octadecane at 20ºC. Figure 8.4 depicts the density function at 50ºC, and Figure 8.5 shows the results of the 200ºC plot. Examples of the molecular arrangement of the aqueous phase and organic phase are provided in the molecular visualizations in Figures 8.6 and 8.7.

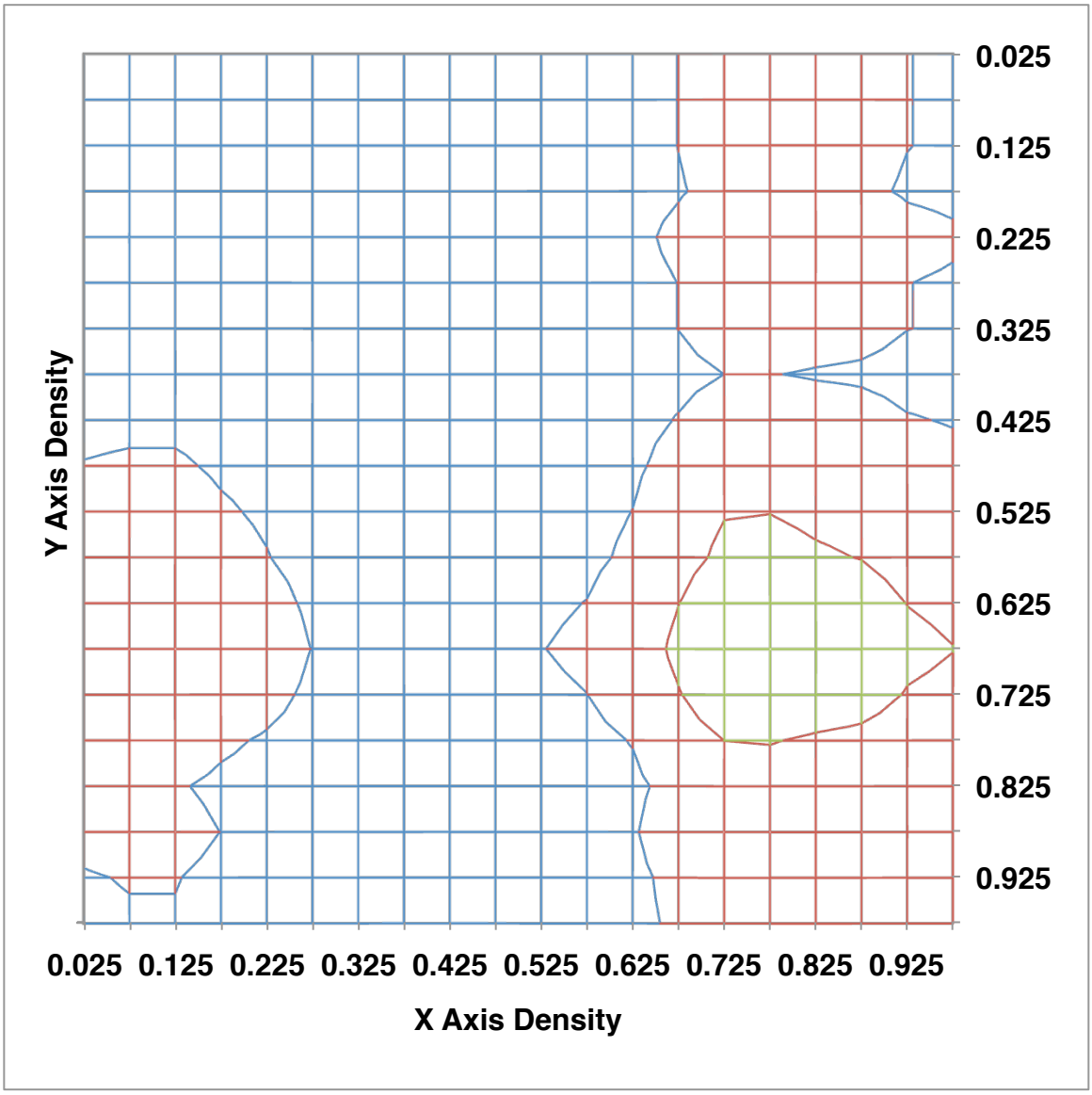

Figure 8.3 Density plot of octadecane center of mass at 20°C and 1.5MPa. Relatively low densities are observed over a large amount of simulation space, indicating a high degree of translational mobility for the center of mass. Translations correlate to energetic repulsion between the phases; however octadecanes cannot be removed from water, so the energy of the system is not reduced.

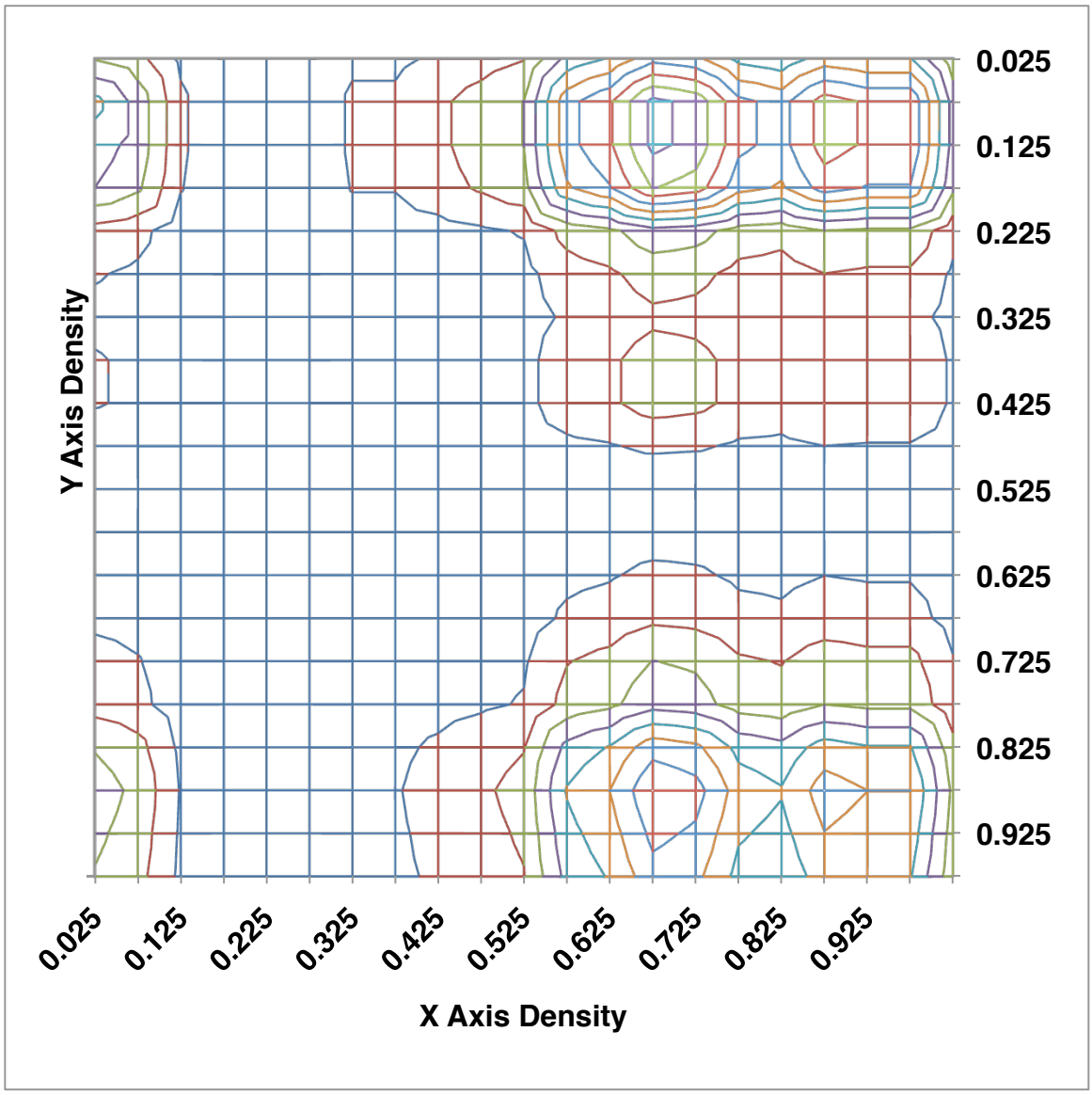

Figure 8.4 Density plot of octadecane center of mass at 50°C and 1.5MPa. At this temperature, hydrophobic exclusion of octadecanes is still expected, but less space is sampled via translational moves. A localized density is observed, correlating to the octadecane aggregation in Figure 8.7.

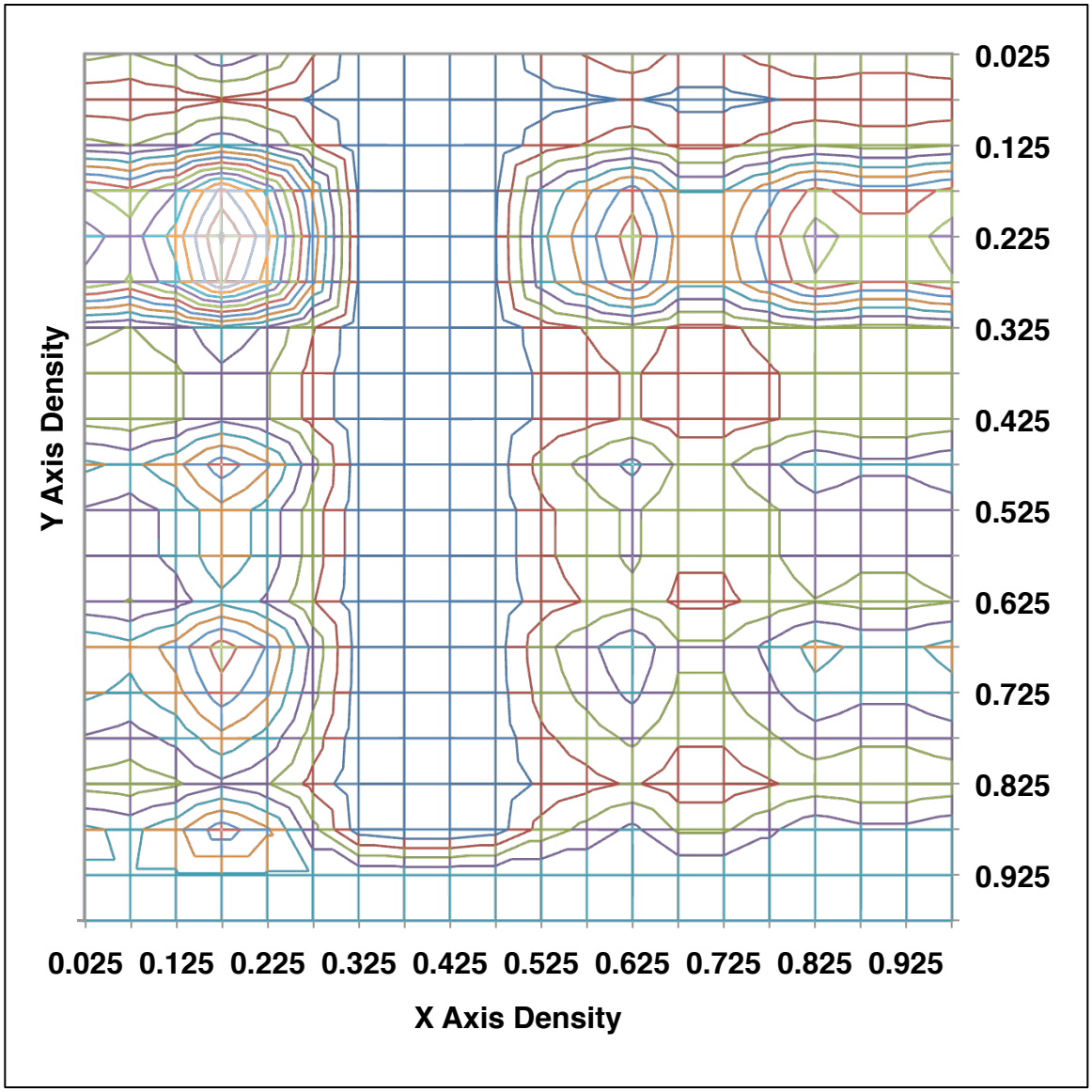

Figure 8.5 Density contour plot of octadecane mass at 200ºC and 1.5MPa. In this plot, much less space sampling is observed, resulting in greater density values in specific regions.

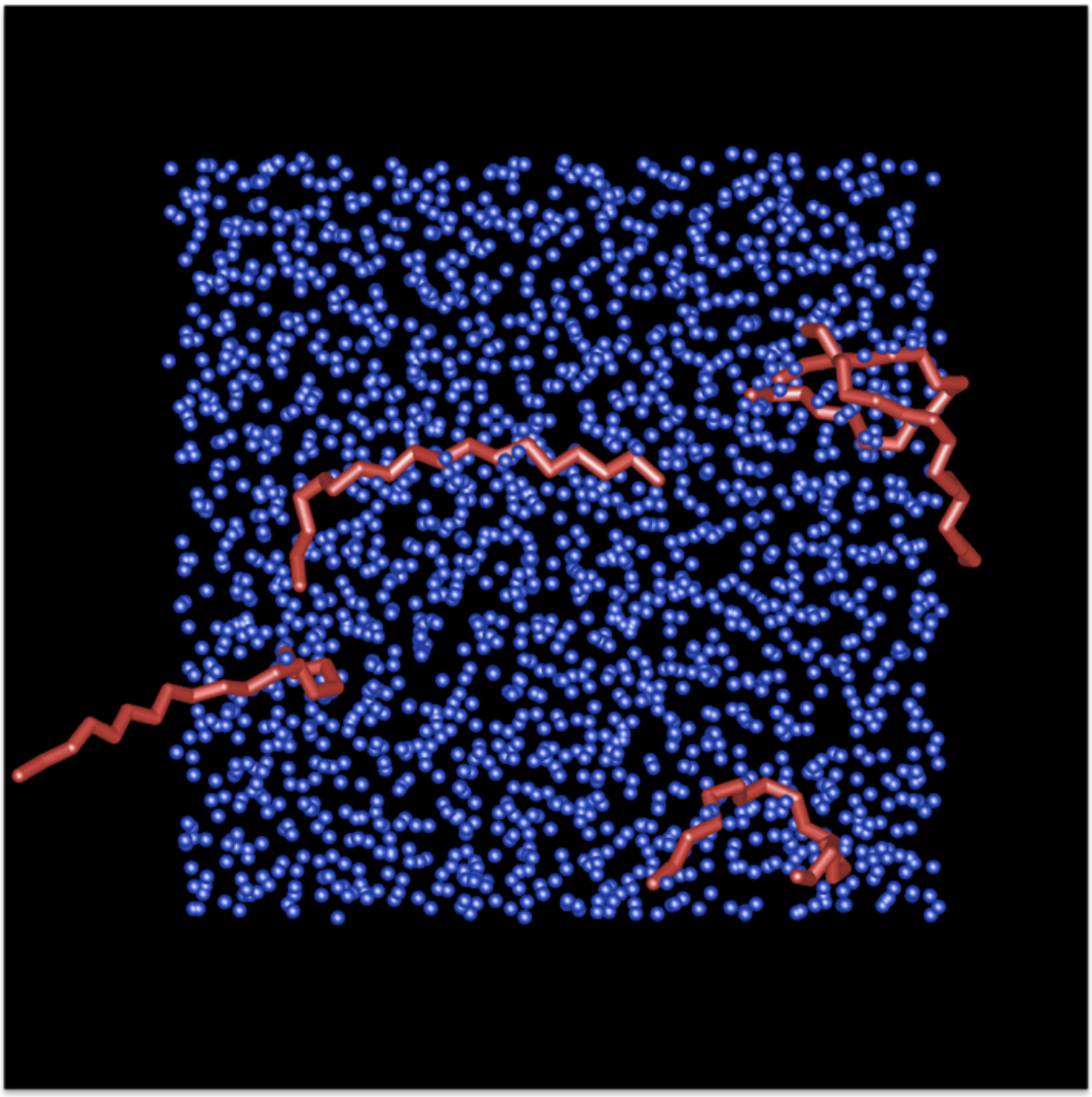

Figure 8.6 Molecular visualization of octadecane chains interacting with an aqueous phase at 200ºC, projected along the Z-axis. Octadecanes are in red; hydrogens have been removed for clarity. Note the relatively wide distribution of conformations for the octadecanes; apparently exposed octadecanes are actually interacting with additional periodic boxes.

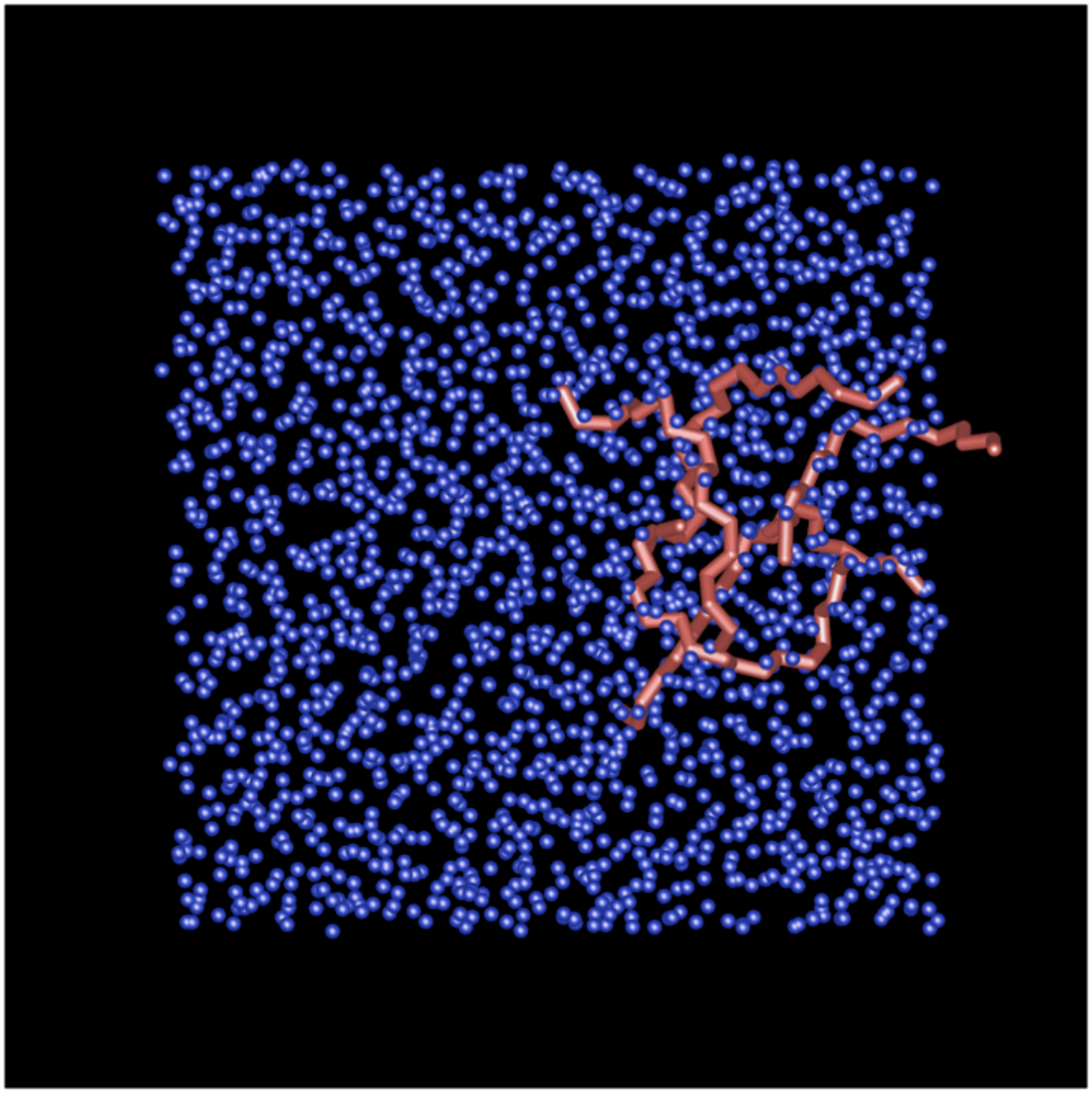

Figure 8.7 Molecular visualization of octadecane in water at 50ºC and 1.5MPa, projected along the Z-axis. At this temperature, the solvation favorability is much lower for octadecane, resulting in the hydrophobic aggregation of the sample.

The density plots and molecular visualizations in this study revealed the relative mobility of the octadecane at low temperatures, demonstrated by the relatively equal distribution of centers of mass in 20ºC as opposed to high local densities in the 200ºC simulation. At the same time aggregation was observed in lower temperatures but not at higher ones. Energetically, this indicated no minimum was found for the hydrophobic exclusion of the octadecane, and the simulation algorithm attempted to compensate by performing translational moves on the octadecane center of mass. Frequent center of mass translational moves were observed as broad, low intensity density distributions. A local minimum is found at lower temperatures when a large spherical solvent cage is formed, and the octadecanes aggregate, as was seen in Figure 8.7.

Increased octadecane solvation correlated to the center of mass density plot in Figure 8.6 and 8.7, which demonstrated greater localized density. Greater local density regions correlated to centers of mass that were in relatively energetically favorable environments. Furthermore, more density peaks are seen in Figure 8.5 than in 8.4, which correlated to non-aggregated octadecanes that were also not translationally shifting. This can be taken as an indication of energetic favorability for octadecane interactions with the aqueous phase.

8.2.5 Simulations of Polar Molecule Partitioning

The partitioning function of analytes can be measured as a function of the density of a probe analyte, phenol, which can partition between the polar and non-polar phase. This experiment explicitly excluded interactions between any stationary phase support and the probe, so the only interaction that could occur was the partitioning of an analyte between phases. As has been demonstrated in literature (Zhang et al. 2005), partitioning directly between phases is inefficient in Monte Carlo simulations, so a three box system was designed containing the non-polar phase (10 octadecanes), polar phase (1000 waters) and a gas phase (20 helium atoms); statistical controls only allowed transfer of the probe molecules to and from the gas phase. Experiments were carried out at 200ºC and 1.5MPa of pressure in the NPT ensemble.

Phenol, which has a normal K_{OW} of 1.16 at room temperature, but is also strongly polar, was expected to be found to partition on the surface of the phase, as deep partitioning would remove hydrogen bonding to the hydroxyl group. In the visualization of phenol in octadecane in Figure 8.8, one phenol behaved as was expected, appearing on the surface layer of the octadecane. However, two other phenols also appear to be aligned in such a manner as to suggest hydrogen bonding to one another, which may have allowed for more favorable partitioning deeper into the non-polar phase.

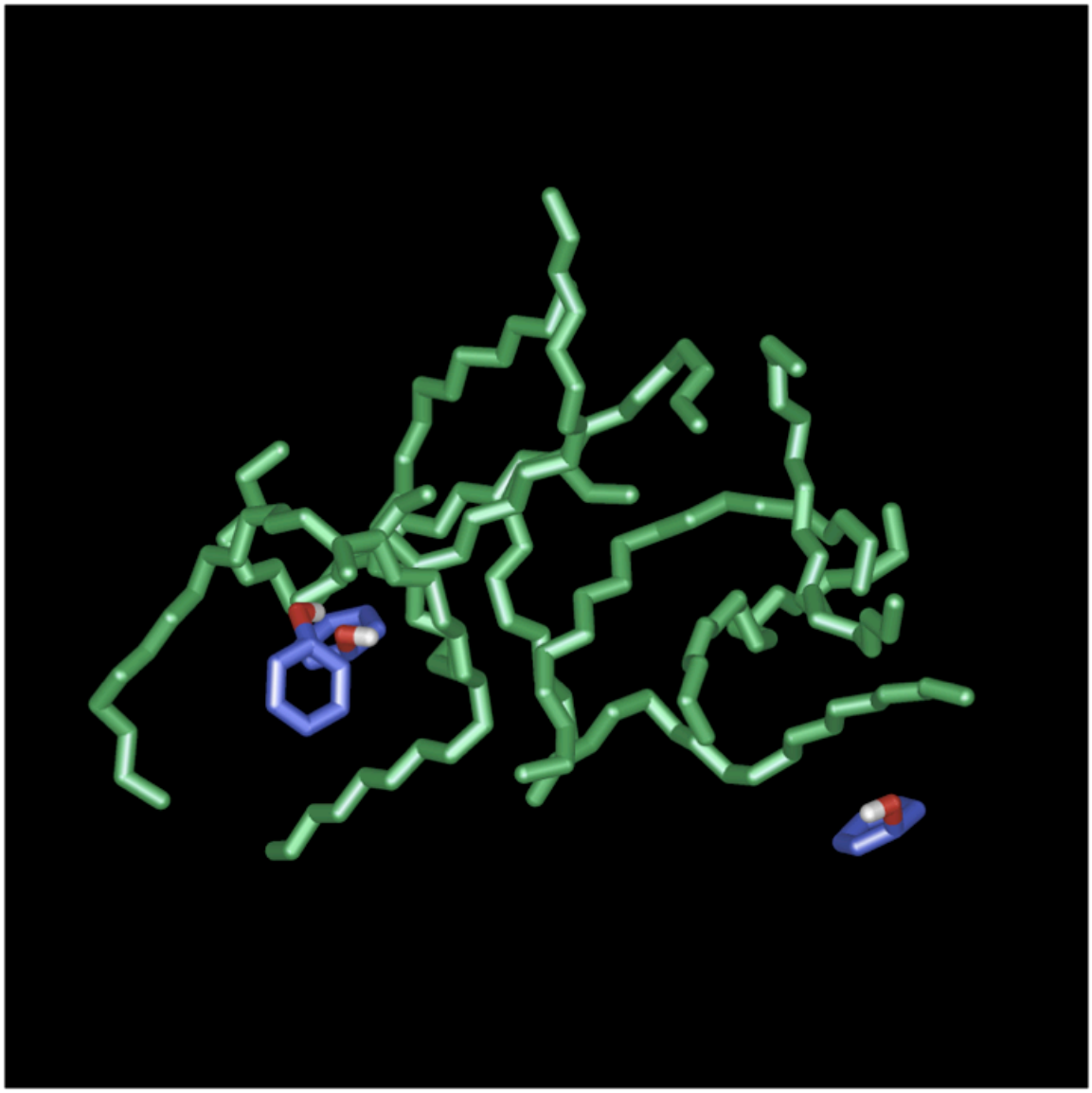

Figure 8.8 Distribution of phenol in octadecane phase. Note the hydrogen bond pairing of the two phenols in the left side of the visualization. Phenols are presented in blue, with the hydroxyl groups highlighted in red and white. Water phase overlay has been excluded for clarity.

8.3 Removal of Polar Contaminants with Subcritical Water Wet Oxidation

The most likely setting to prevent environmental contamination from PPCPs is wastewater treatment plants. However, current WWTPs are not designed for the removal of trace contaminants, and as such many contaminants of concern pass through wastewater treatment unmodified. In order to improve the treatment of PPCPs, orthogonal treatment methods have been designed. Wet oxidation with subcritical water uses a chemical process for treatment rather than the biological treatment process used for the removal of bulk organics, and can be used to compliment current WWTP designs.

While wet oxidation reactors would likely use a vertical tube dug into the ground to produce subcritical temperatures and pressures, a lab-scale apparatus was designed to pressurize the system externally and heat the system to appropriate temperatures. Because oxidation is limited by the concentration of oxidant in the system, a Taylor bubble mixing mechanism was used to maximize the air-liquid interface; oxidation was also improved at higher temperatures due to the increased solubility of oxygen.

Tests of the removal of chemical oxygen demand and total solids in surrogate solutions indicate that the wet oxidation reactor is effective as a treatment method, with typical reductions in both metrics at greater than 90% in optimized operation. While oxidation is the expected breakdown mechanism, the

acid-base catalysis of organic molecules also takes place due to the subcritical reaction medium, resulting in concentration dependent effectiveness of organic molecule mineralization. High concentrations of organic compounds decrease the effectiveness of the reaction, and greater concentrations of non-mineralized side products are observed. Higher temperatures, on the other hand, increase oxygen solubility, and residual products that correlate to the oxidation mechanism increase.

Using two surrogate solutions, one derived from bovine waste and the other from hog waste, treatment of more realistic waste stream surrogates was performed. Treatment efficiency was decreased as compared to pure surrogate solutions. It is likely some compounds volatilize and, therefore, avoid oxidation or hydrothermolysis. In some cases salt concentrations may interfere with organic oxidation. Ion chromatography of waste components does demonstrate, however, that a significant portion of the residual organic matter has been converted to simple organic acids or mineralized salts.

The removal of example organic microcontaminants was also tested, using the veterinary antibiotics sulfadiazine and sulfamethoxine. Both analytes were tested for removal, which was quantified via LC. In optimized oxidations, both contaminants were found to break down at efficiencies greater than 90%. Sulfadiazine was found to be slightly more susceptible to breakdown, likely due to its greater water solubility.

8.3.1 Future Directions for Lab-Scale Wet Oxidation Reactor Studies

Two primary studies are implicated for future investigation with wet oxidation reactor -- expanded testing of polar contaminants, and testing of endocrine-disrupting behavior of real and surrogate waste streams.

Polar contaminants of varying classes may be examined for breakdown using wet oxidation. Of particular interest may be compounds demonstrated to survive wastewater treatment. A specific compound of interest is the antimicrobial compound triclocarban, which is poorly treated by conventional wastewater processes, although many other compounds can also be studied. Caffeine is ubiquitous in wastewater streams, and while not generally indicated as an emerging contaminant by itself, could be indicative of poor polar contaminant treatment by WWTPs. The main focus in current research on emerging contaminants is on alkylphenols and their derivatives, due to their endocrine-disrupting characteristics. Using improved detection techniques (i.e., LC-MS, fluorescence), actual wastewater streams may be tested for trace organic contaminants after biological treatment. After treatment with wet oxidation, removal efficiency could be quantified for analytes at real world concentrations, and the breakdown products could be examined with MS detection. Because of significantly different treatment regimes from one WWTP to another, a greater number of waste effluents will need to be tested for PPCP contamination. In addition, the effluents should also be tested for matrix effects

on wet oxidation reactors. A further discussion of matrix effects from wastewater treatment effluents is provided in Appendix B.

Endocrine disruption is a significant concern for wastewater effluents, even with advanced treatment methods. A primary metric for future studies with the wet oxidation reactor may include measures of change of endocrine-disrupting compounds as to the extent of compatibility with biological endocrine receptors. Typical endocrine disruption occurs because organic molecules match the estrogen receptor in vertebrates. Unfortunately most compounds with a phenol-like structure will match. Using bioassays, especially estrogen receptor ELISAs, will allow for the quantification of endocrine disruption from effluents.

The wet oxidation process is likely useful in the removal of small polar analytes from waste streams where the significant bulk of organic contaminants has already been removed. The economic realities of replacing conventional biologically based wastewater treatment make the complete conversion to a wet oxidation process unlikely, but using wet oxidation in conjunction with biological processes may have potential. Combining disinfection processes with additional compound treatment is a value added approach to wastewater treatment, and if endocrine-disruptive chemicals can be removed, a significant improvement in treatment efficacy will result. It is likely polar organic contaminants will continue to be a significant environmental concern. Improved identification of structural risk contributions and more effective treatment of contamination before exposure to

the environment will both increase understanding of the types of chemicals which need to be of concern now, and what chemicals may have environmental impacts in the future.

Works Cited

Abraham, M.H.; McGowan, J.C., The characteristic volume to measure cavity terms in reversed-phase chromatography. *Chromatographia,* **1987**, 23(4), 243-246

Abraham, M. H.; Ibrahim, A.; Zissimos, A. M., Determination of sets of solute descriptors from chromatographic measurements. *J.Chromatogr. A* **2004,** 1037, 29-47.

Andreu, V.; Ferrer, E.; Rubio, J. L.; Font, G.; Picó, Y., Quantitative determination of octylphenol, nonylphenol, alkylphenol ethoxylates and alcohol ethoxylates by pressurized liquid extraction and liquid chromatography-mass spectrometry in soils treated with sewage sludges. *Sci. Total. Environ.* **2007,** 378, 124-129.

Asghari, F. S.; Yoshida, H., Kinetics of the decomposition of fructose catalyzed by hydrochloric acid in subcritical water: Formation of 5-hydroxymethylfurfural, levulinic, and formic acids. *Ind. Eng. Chem. Res.* **2007,** 46, 7703-7710.

Bajad, S.; Shulaev, V., Highly-parallel metabolomics approaches using LC-MS-MS for pharmaceutical and environmental analysis. *Trends* **2007,** 26, (6), 625-635.

Bandura, A. V.; Lvov, S. N., The ionization constant of water over a wide range of temperatures and densities. *J. Phys. Chem. Ref. Data* **2006,** 35, 15-30.

Barry, E. F., *Modern practice of gas chromatography*. 4th ed.; John Wiley & Sons: Hoboken, NJ, USA, 2004.

Baugros, J.-B.; Giroud, B.; Dessalces, G.; Grenier-Loustalot, M.-F.; Cren-Olivé, C., Multiresidue analytical methods for the ultra-trace quantification of 33

priority substances in the list of REACH in real water samples. *Anal. Chim. Acta* **2008,** 607, 191-203.

Beens, J.; Adahchour, M.; Vreuls, R. J. J.; Brinkman, U. A. T., Moving cryogenic modulator for the comprehensive two-dimensional gas chromatography (GC X GC) of surface water contaminants. *J. Microcolumn Separations* **2001,** 13, (3), 134-140.

Beltrán, F. J.; Aguinco, A.; García-Araya, J. F.; Oropesa, A., Ozone and photocatalytic processes to remove the antibiotic sulfamethoxazole from water. *Water Research* **2008,** 42, 3799-3808.

Benfenati, E.; Barcelò, D.; Johnson, I.; Galassi, S.; Levsen, K., Emerging organic contaminants in leachates from industrial waste landfills and industrial effluent. *Trends* **2003,** 22, (10), 757-765.

Benijts, T.; Dams, R.; Günther, W.; Lambert, W.; De Leenheer, A., Analysis of estrogenic contaminants in river water using liquid chromatography coupled to ion trap based mass spectrometry. *Rapid Commun. Mass Spectrom.* **2002,** 16, 1358-1364.

Benner, R.L.; Stedman, D.H., Universal sulfur detection by chemiluminescence. *Anal. Chem.* **1989,** 61, 1268-1271.

Berek, D.; Tarbajovská, J., Evaluation of high-performance liquid chromatography column retentivity using macromolecular probes 2. Silanophilic interactivity traced by highly polar polymers. *J.Chromatogr. A* **2002,** 976, 27-37.

Bertrand, G. L. *Linear Least Squares Calculator*, University of Missouri: Rolla, 2000.

Blackwell, J. A.; Stringham, R. W., Characterization of Temperature Dependent Modifier Effects in SFC Using Linear Solvation Energy Relationships. *Chromatographia* **1997,** 46, (5/6), 301-308.

Bobeldijk, I.; Vissers, J. P. C.; Kearney, G.; Major, H.; van Leerdam, J. A., Screening and identification of unknown contaminants in water with liquid chromatography and quadrupole-orthoganal acceleration-time-of-flight tandem mass spectrometry. *J.Chromatogr. A* **2001,** 929, 63-74.

Boethling, R. S.; Sommer, E.; DiFiore, D., Designing small molecules for biodegradability. *Chem. Rev.* **2007,** 107, 2207-2227.

Bolliet, D.; Poole, C. F., Influence of temperature on retention and selectivity in reversed phase liquid chromatography. *Analyst* **1998,** 123, 295-299.

Brown, T. N.; Wania, F., Screening chemicals for the potential to be persistent organic pollutants: A case study of Arctic contaminants. *Environ. Sci. Technol.* **2008,** 42, 5202-5209.

Bruckner, C. A.; Ecker, S. T.; Synovec, R. E., Simultaneous Flame Ionization and Absorbance Detection of Volatile and Nonvolatile Compounds by Reversed-Phase Liquid Chromatography with a Water Mobile Phase. *Anal. Chem.* **1997,** 69, (17), 3465-3470.

Buerge, I.J.; Poiger, T.; Müller, M.D.; Buser, H.R., Caffeine, an anthropogenic marker for wastewater contamination of surface waters. *Environ. Sci. Technol.* **2003,** 37, 691-700.

Butler, M. N.; Weber, W. J., Accelerated transformation and deactivation of erythromycin in superheated water. 1. Temperature effects, transformation rates, and the impacts of dissolved organic matter. *Environ. Sci. Technol.* **2005,** 39, (7), 2294-2300.

Butler, M. N.; Weber, W. J., Accelerated transformation and deactivation of erythromycin in superheated water. 2. Transformation reactions and bioassays. *Environ. Sci. Technol.* **2005,** 39, (7), 2301-2306.

Cabooter, D.; Heinisch, S.; Rocca, J. L.; Clicq, D.; Desmet, G., Use of the kinetic plot method to analyze commercial high-temperature liquid chromatography systems I: Instrinsic performance comparison. *J.Chromatogr. A* **2007,** 1143, 121-133.

Carr, P. W.; Li, J.; Dallas, A. J.; Eikens, D. I.; Tan, L. C., Revisionist look at solvophobic driving forces in reversed-phase liquid chromatography. *J.Chromatogr. A* **1993,** 656, 113-133.

Carson, R. *Silent Spring*, 40th Anniversary Edition; Houghton Mifflin: New York, NY, 2002.

Castillo, M.; Alonso, M. C.; Riu, J.; Barceló, D., Identification of polar, ionic and highly water soluble organic pollutants in untreated industrial wastewaters. *Environ. Sci. Technol.* **1999,** 33, 1300-1306.

Castillo, M.; Riu, J.; Ventura, F.; Boleda, R.; Scheding, R.; Schröder, H. F.; Nistor, C.; Émneus, J.; Eichhorn, P.; Knepper, T. P.; Jonkers, C. C. A.; de Voogt, P.; González-Mazo, E.; León, V. M.; Barceló, D., Inter-laboratory comparison of liquid chromatographic techniques and enzyme-linked immunosorbent assay for the determination of surfactants in wastewaters. *J.Chromatogr. A* **2000,** 889, 195-209.

Caulfield, J. A. Analytical studies of sorption phenomena for nitrogen heterocycles. University of Denver, Denver, 2008.

Chen, M. H.; Horváth, C., Temperature programming and gradient elution in reversed-phase chromatography with packed capillary columns. *J.Chromatogr. A* **1997,** 788, 51-61.

Chen, S. H.; Teixeira, J., Structure and dynamics of low-temperature water as studied by scattering techniques. *Adv. Chem. Phys.* **1986,** 64, 1-46.

Chester, T. L.; Coym, J. W., Effect of phase ratio on van't Hoff analysis in reversed-phase liquid chromatography, and phase-ratio-independent estimation of transfer enthalpy. *J.Chromatogr. A* **2003,** 1003, 101-111.

Chung, J.; Lee, M.; Ahn, J.; Bae, W.; Lee, Y.-W.; Shim, H., Effects of operational conditions on sludge degradation and organic acids formation in low-critical wet air oxidation. *J. Hazard. Mater.* **2009,** 162, 10-16.

Cole, L. A.; Dorsey, J. G., Temperature dependence of retention in reversed-phase liquid chromatography. 1. Stationary -phase considerations. *Anal. Chem.* **1992,** 64, (13), 1317-1323.

Cole, L. A.; Dorsey, J. G.; Dill, K. A., Temperature dependence of retention in reversed-phase liquid chromatography. 2. Mobile phase considerations. *Anal. Chem.* **1992,** 64, (13), 1324-1327.

Conn, K. E.; Barber, L. B.; Brown, G. K.; Siegrist, R. L., Occurance and fate of organic contaminants during onsite wastewater treatment. *Environ. Sci. Technol.* **2006,** 40, 7358-7366.

Cox, G. B., The influence of silica structure on reversed-phase retention. *J.Chromatogr. A* **1993,** 656, 353-367.

Coym, J. W.; Dorsey, J. G., Reverse-phase retention thermodynamics of pure-water mobile phases at ambient and elevated temperature. *J.Chromatogr. A* **2004,** 1035, 23-29.

Croley, T. R.; Hughes, R. J.; Koenig, B. G.; Metcalfe, C. D.; March, R. E., Mass spectrometry applied to the analysis of estrogens in the environment. *Rapid Commun. Mass Spectrom.* **2000,** 14, 1087-1093.

Cunningham, A. R.; Ronsenkranz, H. S., Estimating the extent of the health hazard posed by high-production volume chemicals. *Environ. Health Perspect.* **2001,** 109, (9), 953-956.

Dantas, R. F.; Contreras, S.; Sans, C.; Esplugas, S., Sulfamethoxazole abatement by means of ozonation. *J. Hazard. Mater.* **2008,** 150, 790-794.

Dugo, P.; Buonasera, K.; Crupi, M. L.; Cacciola, F.; Dugo, G.; Mondello, L., Superheated water as chromatographic eluent for parabens separation on octadecyl coated zirconia stationary phase. *J. Sep. Sci.* **2007,** 30, 1125-1130.

Engelhardt, H.; Löw, H.; Götzinger, W., Chromatographic characterization of silica-based reversed phases. *Chrom.* **1991,** 544, 371-379.

Environmental Protection Agency. Testing of Certain High Production Volume Chemicals; Final Rule. In Agency, E. P., Ed. Washington, D.C., 2006; Vol. 71, pp 13708-13735.

Esperanza, M.; Suidan, M. T.; Nishimura, F.; Wang, Z.-M.; Sorial, G. A.; Zaffiro, A.; McCauley, P.; Brenner, R.; Sayles, G., Determination of sex hormones and nonylphenol ethoxylates in the aqueous matrixes of two pilot-scale municipal wastewater treatment plants. *Environ. Sci. Technol.* **2004,** 38, 3028-3035.

Farré, M.; Ramón, J.; Galve, R.; Marco, M.-P.; Barceló, D., Evaluation of newly developed enzyme-linked immunosorbent assay for determination of linear alkyl benzenesulfonates in wastewater treatment plants. *Environ. Sci. Technol.* **2006,** 40, 5064-5070.

Feng, L.; Ling, L.; Peng, S.; Yutian, W., Sub-critical Column and Capillary Chromatograpy with Water as Mobile Phase and Flame Ionization Detection. *Journal of Chinese Pharmaceutical Sciences* **2001,** 10, (1), 39-41.

Fields, S. M.; Ye, C. Q.; Zhang, D. D.; Branch, B. R.; Zhang, X. J.; Okafo, N., Superheated water as eluent in high-temperature high-performance liquid chromatographic separations of steroids on a polymer-coated zirconia column. *J.Chromatogr. A* **2001,** 913, 197-204.

Frenkel, D.; Smit, B., *Understanding Molecular Simulation: From Algorithms to Applications*. Academic Press: San Diego, 1996.

Gabryelski, W.; Wu, F.; Froese, K. L., Comparison of high-field asymmetric waveform ion mobility spectrometry with GC methods in analysis of haloacetic acids in drinking water. *Anal. Chem.* **2003,** 75, 2478-2486.

García-Reyes, J. F.; Ferrer, I.; Thurman, E. M.; Molina-Diaz, A.; Fernández-Alba, A. R., Searching for non-target chlorinated pesticides in food by liquid chromatography/ time-of-flight mass spectrometry *Rapid Commun. Mass Spectrom.* **2005,** 19, 2780-2788.

Geissler, P. L.; Dellago, C.; Chandler, D.; Jürg, H.; Parrinello, M., Autonionization in liquid water. *Science* **2001,** 291, 2121-2124.

Gibson, R.; Tyler, C. R.; Hill, E. M., Analytical methodology for the identification of estrogenic contaminants in fish bile. *J.Chromatogr. A* **2005,** 1066, 33-40.

González, S.; Petrovic, M.; Barceló, D., Removal of a broad range of surfactants from municipal wastewater - Comparison between membrane bioreactor and conventional activated sludge treatment. *Chemosphere* **2007,** 67, 335-343.

Grange, A. H.; Sovocool, G. W., Identification of compounds in water above a pollutant plume by high-resolution mass spectrometry. *Environ. Forensics* **2007,** 8, (4), 391-404.

Griffith, J. W.; Raymond, D. H., The first commercial supercritical water oxidation sludge processing plant. *Waste Manage.* **2002,** 22, 453-459.

Guillarme, D.; Heinisch, S.; Rocca, J. L., Effect of temperature in reversed phase liquid chromatography. *J.Chromatogr. A* **2004,** 1052, 39-51.

Guo, R.; Liang, X., Chen, J.; Zhang, Q.; Kettrup, A., Prediction of soil adsorption from retention paramters on three reversed-phase liquid chromatographic columns. *Anal. Chem.* **2002,** 74, 655-660.

Halden, R. U.; Paull, D. H., Analysis of tricocarban in aquatic samples by liquid chromatography electrospray ionization mass spectrometry. *Environ. Sci. Technol.* **2004,** 38, 4849-4855.

Harbers, J. V.; Huijbregts, M. A.; Posthuma, L.; van de Meent, D., Estimating the impact of high-production-volume chemicals on remote ecosystems by toxic pressure calculation. *Environ. Sci. Technol.* **2006,** 40, 1573-1580.

Harris, D. C., *Quantitative Chemical Analysis*. W.H. Freeman and Company: New York, 2007.

Hao, C.; Shepson, P.B.; Drummond J.W.; Muthuramu, K., Gas chromatographic detector for selective and sensitive detection of atmospheric organic nitrates. *Anal. Chem.* **1994**, 66, 3737-3743.

He, P.; Yang, Y., Studies on the long-term thermal stability of stationary phases in subcritical water chromatography. *J.Chromatogr. A* **2003,** 989, 55-63.

Heberer, T., Tracking persistent pharmaceutical residues from municipal sewage to drinking water. *J. Hydrol.* **2002,** 266, 175-189.

Hernández, F.; Portolés, T.; Pitarch, E.; López, F. J., Target and nontarget screening of organic micropollutants in water by solid-phase microextraction combined with gas chromatography/high-resolution time-of-flight mass spectrometry. *Anal. Chem.* **2007,** 79, 9494-9504.

Hewlett-Packard HP 6890 Series Gas Chromatograph Service Manual; Hewlett-Packard: Wilmington, 1997.

Hildebrand, J. H.; Prausnitz, J. M.; Scott, R. L., *Regular and Related Solutions*. Prentice Hall: New York, 1962.

Holliday, R. L.; Jong, B. Y. M.; Kolis, J. W., Organic synthesis in subcritical water: Oxidation of alkyl aromatics. *Journal of Supercritical Fluids* **1998,** 12, 255-260.

Hooijschuur, E. W. J.; Kientz, C. E.; Brinkman, U. A. T., Potential of Flame Ionization Detection Coupled On-Line with Microcolumn Liquid Chromatography Using Aqueous Eluents and an Eluent-Jet Interface. *J. High Resol. Chromatogr.* **2000,** 23, (4), 309-316.

Houdiere, F.; Fowler, P. W. J.; Djordjevic, N. M., Combination of Column Temperature Gradient and Mobile Phase Flow Gradient in Microcolumn and Capillary Column High-Performance Liquid Chromatography. *Anal. Chem.* **1997,** 69, (13), 2589-2593.

Ibáñez, M.; Sancho, J. V.; Pozo, Ó. J.; Niessen, W.; Hernández, F., Use of quadrupole time-of-flight mass spectrometry in the elucidation of unknown compounds present in environmental water. *Rapid Commun. Mass Spectrom.* **2005,** 19, 169-178.

Ingelse, B. A.; Janssen, H.-G.; Cramers, C. A., HPLC-FID with Superheated Water as the Eluent: Improved Methods and Instrumentation. *J. High Resol. Chromatogr.* **1998,** 21, (11), 613-616.

Isaacson, C.; Mohr, T. K. G.; Field, J. A., Quantitative determination of 1,4-dioxane and tetrahydrofuran in groundwater by solid phase extraction GC/MS/MS. *Environ. Sci. Technol.* **2006,** 40, 7305-7311.

Jin, F.; Yun, J.; Li, G.; Kishita, A.; Tohji, K.; Enomoto, H., Hydrothermal conversion of carbohydrate biomass into formic acid at mild temperatures. *Green Chemistry* **2008,** 10, 612-615.

Jin, F.; Zhou, Z.; Enomoto, H.; Moriya, T.; Higashijima, H., Conversion mechanism of cellulosic biomass to lactic acid in subcritical water and acid-base catalytic effect of subcritical water. *Chemistry Letters* **2004,** 33, (2), 126-127.

Jin, F.; Zhou, Z.; Kishita, A.; Enomoto, H., Hydrothermal conversion of biomass into acetic acid. *J. Mater. Sci.* **2006,** 41, 1495-1500.

Jobling, S.; Sheahan, D.; Osborne, J. A.; Matthiessen, P.; Sumpter, J. P., Inhibition of testicular growth in rainbow trout (Oncorhynchus mykiss) exposed to estrogenic alkylphenolic chemicals. *Environ. Toxicol. Chem.* **1996,** 15, (2), 194-202.

Jorgensen, W. L.; Chandrasekhar, J.; Madura, J. D.; Impey, R. W.; Klein, M. L., Comparison of simple potential functions for simulating liquid water. *Journal of Chemical Physics* **1983,** 79, (2), 926-935.

Khetan, S. K.; Collins, T. J., Human Pharmacueticals in the Aquatic Environment: A Challeng to Green Chemistry. *Chem. Rev.* **2007,** 107, 2319-2364.

Klopman, G.; Chakravarti, S. K., Screening of high production volume chemicals for estrogen receptor binding activity (II) by the MultiCASE expert system. *Chemosphere* **2003,** 51, 461-468.

Koester, C. J.; Moulik, A., Trends in environmental analysis. *Anal. Chem.* **2005,** 77, 3737-3754.

Köhler, J.; Chase, D. B.; Farlee, R. D.; Vega, A. J.; Kirkland, J. J., Comprehensive characterization of some silica-based stationary phases for high-performance liquid chromatography. *Chrom.* **1986,** 352, 275-305.

Kolpin, D. W.; Furlong, E. T.; Meyer, M. T.; Thurman, E. M.; Zaugg, S. D.; Barber, L. B.; Buxton, H. T., Pharmaceuticals, hormones and other organic wastewater contaminants in U.S. streams, 1999-2000: A national reconnaissance. *Environ. Sci. Technol.* **2002,** 36, 1202-12211.

Kördel, W.; Stutte, J.; Kotthoff, G., HPLC-screening method to determine the adsorption coefficient in soil-comparison of immobilized humic acid and clay mineral phases for cyanopropyl columns. *Sci. Total. Environ.* **1995,** 162, 119-125.

Kubátová, A. K.; Lagadec, A.; Hawthorne, S. B., Dechlorination of lindane, dieldrin, tetrachloroethane, trichloroethene, and PVC in subcritical water. *Environ. Sci. Technol.* **2002,** 36, 1337-1343.

Lee, H.-B.; Peart, T. E.; Bennie, D. T.; Maguire, R. J., Determination of nonylphenol polyethoxylates and their carboxylic acid metabolites in sewage treatment plant sludge by supercritical carbon dioxide extraction. *J.Chromatogr. A* **1997,** 785, 385-394.

Li, J.; Carr, P. W., Characterization of polybutadiene-coated zirconia and comparison to conventional bonded phases by use of linear solvation energy relationships. *Anal. Chim. Acta* **1996,** 334, 239-250.

Li, J.; Hu, Y.; Carr, P. W., Fast separations at elevated temperatures on polybutadiene-coated zirconia reversed-phase material. *Anal. Chem.* **1997,** 69, 3884-3888.

Li, L.; Chen, P.; Gloyna, E.F. Generalized kinetic model for wet oxidation of organic compounds. *AIChE Journal,* **1991,** *37*, 1687. s

Li, L.; Portela, J. R.; Vallejo, D.; Gloyna, E. F., Oxidation and hydrolysis of lactic acid in near-critical water. *Ind. Eng. Chem. Res.* **1999,** 38, (7), 2599-2606.

Lide, D.R. Ed. *CRC Handbook of Chemistry and Physics, 85th Ed.* (2004). CRC Press. Boca Raton. 8–141.

Liew, C. C.; Inomata, H.; Arai, K.; Saito, S., Three-dimensional structure and hydrogen bonding of water in sub- and supercritical regions: A molecular simulation study. *Journal of Supercritical Fluids* **1998,** 13, 83-91.

Liu, C.-Q.; Li, S.-L.; Lang, Y.-C.; Xiao, H.-Y., Using δ15N- and δ18O-values to identify nitrate sources in Karst ground water, Guiyang, Southwest China. *Environ. Sci. Technol.* **2006,** 40, 6928-6933.

Liu, Y.; Grinberg, N.; Thompson, K. C.; Wenslow, R. M.; Neue, U. D.; Morrison, D.; Walter, T. H.; O'Gara, J. E.; Wyndham, K. D., Evaluation of C18 hybrid stationary phase using high-temperature chromatography. *Anal. Chim. Acta* **2005,** 554, 144-151.

Long, G. L.; Winefordner, J. D., Limit of Detection: A Closer Look at the IUPAC Definition. *Anal. Chem.* **1983,** 55, (7), 712A.

Loos, R.; Hanke, G.; Eisenreich, S. J., Multi-component analysis of polar water pollutants using sequential solid-phase extraction followed by LC-ESI-MS. *J. Environ. Monit.* **2003,** 5, (3), 384-394.

Loos, R.; Wollgast, J.; Huber, T.; Hanke, G., Polar herbicides, pharmaceutical products, perfluorooctanesulfonate (PFOS), perfluoroocotonoate (PFOA), and nonyphenol and its carboxylates and ethoxylates in surface and tap waters around Lake Maggiore in Northern Italy. *Anal. Bioanal. Chem.* **2007,** 387, 1469-1478.

Loraine, G. A.; Pettigrove, M. E., Seasonal variations in the concentrations of pharmaceuticals and personal care products in drinking water and reclaimed wastewater in Southern California. *Environ. Sci. Technol.* **2006,**

40, 687-695.

Loyo-Rosales, J. E.; Rice, C. P.; Torrents, A., Fate of octyl- and nonylphenol ethoxylates and some carboxylated derivatives in three American wastewater treatment plants. *Environ. Sci. Technol.* **2007,** 41, 6815-6821.

Lu, J.; Brown, J. S.; Liotta, C. L.; Eckert, C. A., Polarity and hydrogen-bonding of ambient to near critical water: Kamlet-Taft solvent parameters. *Chem. Commun.* **2001**, 665-666.

Lucas, L.; Jauzein, M., Use of principal component analysis to profile temporal and spatial variations of chlorinated solvent concentration in groundwater. *Environ. Pollut.* **2008,** 151, 205-212.

Martí, J., Dynamic properties of hydrogen-bonded networks in supercritical water. *Physical Review E* **2000,** 61, (1), 449-456.

Mart'ianov, A. A.; Dzantiev, B. B.; Zherdev, A. V.; Eremin, S. A.; Cespedes, R.; Petrovic, M.; Barcelò, D., Immunoenzyme assay of nonylphenol: study of selectivity and detection of alkylphenolic non-ionic surfactants in water samples. *Talanta* **2005,** 65, 367-374.

Martin, M. G.; Siepmann, J. I., Novel Configurational-Bias Monte Carlo Method for Branched Molecules. Transferable Potentials of Phase Equilbria. 2. United-Atom Description of Branched Alkanes. *Journal of Physical Chemistry B* **1999,** 103, 4508-4517.

McFarlane, J.; Ridenour, W. B.; Luo, H.; Hunt, R. D.; DePaoli, D. W.; Ren, R. X., Room temperature ionic liquids for separating organics from produced water. *Separation Science and Technology* **2005,** 40, (6), 1245-1265.

McNeff, C. V.; Yan, B.; Stoll, D. R.; Henry, R. A., Practice and theory of high temperature liquid chromatography. *J. Sep. Sci.* **2007,** 30, 1672-1685.

Miller, D. J.; Hawthorne, S. B., Subcritical Water Chromatography with Flame Ionization Detection. *Anal. Chem.* **1997,** 69, 623-627.

Miller, D. J.; Hawthorne, S. B., Method for determining the solubilities of hydrophobi organics in subcritical water. *Anal. Chem.* **1998,** 70, 1618-1621.

Milman, B. L., Identification of chemical compounds. *Trends* **2005,** 24, (6), 493-507.

Mukai, S.-a.; Deguchi, S.; Tsujii, K., A high-temperature and -pressure microscope cell to observe colloidal behaviors in subcritical and supercritical water: Brownian motion of colloids near a wall. *Colloids and Surfaces A: Physiochemical and Engineering Aspects* **2006,** 282-283, 483-488.

Neff, W. E.; List, G. R.; Byrdwell, W. C., Analysis of triacylglycerol positional isomers in food products as brominated derivatives by high-performance liquid chromatography coupled with a flame ionization detection. *J.Chromatogr. A* **2001,** 912, 187-190.

Neue, U.D. Theory of peak capacity in gradient elution. *J. Chromatogr. A* **2005,** 1079, 153-161.

Nguyen, T. H.; Goss, K.-U.; Ball, W. P., Polyparameter linear free energy relationships for estimating the equilibrium partition of organic compounds between water and the natural organic matter in soils and sediments. *Environ. Sci. Technol.* **2005,** 39, (4), 913-924.

Nigmatulin, T. R., Surface of a Taylor bubble in vertical cylindrical flows. *Dokl. Phys.* **2001,** 381, (1), 53-55.

Osada, M.; Katsunori, T.; Mizutani, T.; Minami, K.; Watanabe, M.; Adschiri, T.; Arai, K., Estimation of the degree of hydrogen bonding between quinoline and water by ultraviolet-visible absorbance spectroscopy in sub- and supercritcal water. *Journal of Chemical Physics* **2003,** 118, (10), 4573-4577.

Ozen, R.; Kus, N. S., Oxidation of alcohols to carbonyl compounds, benzylic carbonds to their ketones, and arenes to their quinones with molecular oxygen in subcritical water. *Monatsh. Chem.* **2006,** 137, 1597-1600.

Pan, B.; Ning, P.; Xing, B., Part IV—sorption of hydrophobic organic contaminants. *Environ. Sci. Pollut. Res.* **2008,** 15, 554-564.

Pan, B.; Ning, P.; Xing, B., Part V—sorption of pharmaceuticals and personal care products. . *Environ. Sci. Pollut. Res.* **2009,** 16, 106-116.

Pan, Y.-P.; Tsai, S.-W., Solid phase microextraction procedurefor the determination of alkylphenols in water by on-fiber derivitization with N-*tert*-butyl-dimethylsilyl-N-methyltrifluoroacetamide. *Anal. Chim. Acta* **2008,** 624, 247-252.

Petrović, M.; Barceló, D., Determination of anionic and nonionic surfactants, their degradation products, and endocrine-disrupting compounds in sewage sludge by liquid chromatography/ mass spectrometry. *Anal. Chem.* **2000,** 72, 4560-4567.

Pawlowski, T. M.; Poole, C. F., Solvation characteristics of pressurized hot water and its use in chromatography. *Anal. Commun.* **1999,** 36, 71-75.

Pesek, J. J.; Leigh, I. E., *Chemically modified surfaces*. Royal Society of Chemistry: Cambridge, 1994; Vol. 139,

Petrovic, M.; Barceló, D., Application of liquid chromatography/ quadrupole time-of-flight mass spectrometry (LC-QqTOF-MS) in the environmental analysis. *J. Mass Spectrom.* **2006,** 41, 1259-1267.

Polettini, A.; Gottardo, R.; Pascali, J. P.; Tagliaro, F., Implementation and performance evaluation of a database of chemical formulas for the screening of pharmaco/toxicologically relevant compounds in biological samples using electrospray-ionization-time-of-flight mass spectrometry. *Anal. Chem.* **2008,** 80, 3050-3057.

Pomati, F.; Castiglioni, S.; Zuccato, E.; Fanelli, R.; Vigetti, D.; Rosetti, C.; Calamari, D., Effects of a complex mixture of therapeutic drugs at environmental levels on human embryonic cells. *Environ. Sci. Technol.* **2006,** 40, 2442-2447.

Poole, C.F. *The essence of chromatography*. Elsevier: Amsterdam, NL, 2003.

Poole, C. F.; Kiridena, W.; DeKay, C.; Koziol, W. W.; Rosencrans, R. D., Insights into the retention mechanism on an octadecylsiloxane-bonded silica stationary phase (HyPURITY C18) in reverse-phase liquid chromatography. *J.Chromatogr. A* **2006,** 1115, 133-141.

Pussemier, L.; Szabo, G.; Bulman, R.A., Prediction of the soil adsorption K_{OC} for aromatic pollutants. *Chemosphere* **1990,** 21, 1199-1212.

Quina, F. H.; Carroll, F. A.; Cheuy, D. M., A Linear Solvation Energy Relationship to Predict Vapor Pressure from Molecular Structure. *J. Braz. Chem. Soc.* **2005,** 16, (5), 1010-1016.

Rafferty, J. L.; Zhang, L.; Siepmann, J. I.; Schure, M. R., Retention Mechanism in Reversed-Phase Liquid Chromatography: A Molecular Perspective. *Anal. Chem.* **2007,** 79, 6551-6558.

Rafferty, J. L.; Siepmann, J. I.; Schure, M. R., Influence of bonded-phase coverage in reversed phase liquid chromatography via molecular simulation 1. Effects on chain conformation and interfacial properties. *J.Chromatogr. A* **2008,** 1204, 11-19.

Rafferty, J. L.; Siepmann, J. I.; Schure, M. R., Influence of bonded-phase coverage in reversed-phase liquid chromatograpy via molecular simulation 2. Effects on solute retention. *J.Chromatogr. A* **2008,** 1204, 20-27.

Rai, N.; Siepmann, J. I.; Schultze, N. E.; Ross, R. B., Pressure dependence on the Hildebrand Solubility parameter and the internal pressure: Monte Carlo simulations for external pressures up to 300MPa. *J. Phys. Chem. C* **2007,** 111, 15634-15641.

Reddersen, K.; Heberer, T., Multi-compound methods for the detection of pharmaceutical residues in various waters applying solid phase extraction (SPE) and gas chromatography with mass spectrometric (GC-MS) detection. *J. Sep. Sci.* **2003,** 26, 1443-1450.

Richardson, S.D., Environmental Mass Spectrometry. *Anal. Chem.* **2000**, 72, 4477-4496.

Richardson, S.D., Environmental Mass Spectrometry: Emerging Contaminants and Current Issues. *Anal. Chem.* **2004,** 74, 3337-3364.

Richardson, S. D., Environmental Mass Spectrometry: Emerging Contaminants and Current Issues. *Anal. Chem.* **2006,** 78, 4021-4045.

Richardson, S. D., Environmental Mass Spectrometry: Emerging Contaminants and Current Issues. *Anal. Chem.* **2008,** 80, 4373-4402.

Richardson, S. D.; Ternes, T. A., Water Analysis: Emerging Contaminants and Current Issues. *Anal. Chem.* **2005,** 77, 3807-3838.

Routledge, E.J.; Sheahan, D.; Desbrow, C.; Brighty, G.C.; Waldock, M.; Sumpter, J.P., Identification of estrogenic chemicals in STW effluent. 2. In Vivo responses in trout and roach. *Environ. Sci. Technol.* **1998,** 32, 1559-1565.

Ryerson, T. B.; Dunham, A. J.; Barkley, R. M.; Sievers, R. E., Sulfur-selective detector for liquid chromatography based on sulfur monoxid-ozone chemiluminescence. *Anal. Chem.* **1994,** 66, (18), 2841-2851.

Sanderson, H.; Dyer, S. D.; Price, B. B.; Nielsen, A. M.; van Compernolle, R.; Selby, M.; Stanton, K.; Evans, A.; Ciarlo, M.; Sedlak, R., Occurance and weight-of-evidence risk assessment of alkyl sulfates, alkyl ethoxylates, and linear alkylbenzene sulfonates (LAS) in river water and sediments. *Sci. Total. Environ.* **2006,** 368, 695-712.

Savage, P. E.; Hunter, S. E.; Hoffee, K. L.; Schuelke, T. J.; Smith, M. J., Bisphenol E decomposition in high-temperature water. *Ind. Eng. Chem. Res.* **2006,** 45, (23), 7775-7780.

Schreiber, I. M.; Mitch, W. A., Occurence and fate of nitrosamines and nitrosamine precursors in wastewater-impacted surface water using boron as a conservative tracer. *Environ. Sci. Technol.* **2006,** 40, 3203-3210.

Serrano, J. M.; Silva, M., Rapid and sensitive determination of aminoglycoside antibiotics in water samples using a strong cation-exchange chromatography non-derivatization method with chemiluminescence detection. *J.Chromatogr. A* **2006,** 1117, 176-183.

Shanableh, A., Generalized First-order kinetic model for biosolids decomposition and oxidation during hydrothermal treatment. *Environ. Sci. Technol.* **2005,** 39, 355-362.

Shanableh, A.; Imteaz, M., First-order hydrothermal oxidation kinetics of digested sludge compared with raw sludge. *Environ. Tech.* **2008,** 29, 1009-1020.`

Shao, B.; Hu, J.; Yang, M.; An, W.; Tao, S., Nonylphenol and nonylphenol ethoxylates in river water, drinking water, and fish tissues in the area of Chongqing, China. *Arch. Environ. Contam. Toxicol.* **2005,** 48, 467-473.

Shearer, R. L. a. S., R.J., Supercritical Fluid Chromatography of Petroleum Products Using Flameless Sulfur Chemiluminescence Detection. *J. High Resol. Chromatogr.* **1994,** 17, 251-254

Siepmann, J. I.; Martin, M. G. *MCCCS Towhee*, 6.1.1; GNU public License: 1999.

Sievers Model 355 SCD and Model 255 NCD with Dual Plasma™ Controller and Burner Manual; Ionics Instruments: Boulder, 2004.

Sirivedhin, T.; Gray, K. A., Part 1. Identifying anthropogenic markers in surface waters influenced by treated effluents: a tool in potable water reuse. *Water Research* **2005,** 39, 1154-1164.

Skoog, D. A.; Holler, F. J.; Nieman, T. A., *Principles of Instrumental Analysis*. Fifth ed.; Saunders College Publishing: Philadelphia, 1998.

Skoog, D. A.; West, D. M.; Holler, F. J.; Crouch, S. R., *Fundamentals of analytical chemistry*. 8th ed.; Thomson Brooks/Cole: Belmont, CA, 2004

Smith, R. M., Superheated water: the ultimate green solvent for separation science. *Anal. Bioanal. Chem.* **2006,** 385, 419-421.

Smith, R. M., Superheated water chromatography -- A green technology for the future. *J.Chromatogr. A* **2008,** 1184, 441-455

Squillace, P. J.; Scott, J. C.; Moran, M. J.; Nolan, B. T.; Kolpin, D. W., VOCs, pesticides, nitrate and their mixtures in groundwater used for drinking water in the United States. *Environ. Sci. Technol.* **2002,** 36, 1923-1930.

Stackelberg, P. E.; Furlong, E. T.; Meyer, M. T.; Zaugg, S. D.; Henderson, A. K.; Reissman, D. B., Persistence of pharmaceutical compounds and other organic wastewater contaminants in a conventional drinking-water-treatment plant. *Sci. Total. Environ.* **2004,** 329, 99-113.

Stoll, D. R.; Cohen, J. D.; Carr, P. W., Fast, comprehensive online two-dimensional high performance liquid chromatography through the use of high temperature ultra-fast gradient elution reversed-phase liquid chromatography. *J.Chromatogr. A* **2006,** 1122, 123-137.

Stoll, D.R.; Wang, X.; Carr, P.W., Comparison of the practical resolving power of one- and two-dimensional high-performance liquid chromatography analysis of metabolomic samples. *Anal. Chem.* **2008,** 80, 268-278.

Sultan, J.; Gabryelski, W., Structural identification of highly polar nontarget contaminants in drinking water by ESI-FAIMS-Q-TOF-MS. *Anal. Chem.* **2006,** 78, 2905-2917.

Szabo, G.; Prosser, S.L.; Bulman, R.A., Adsorption coefficient (K_{OC}) and HPLC retention factors of aromatic hydrocarbons. *Chemosphere* **1990,** 21, 495-505.

Szabo, G.; Prosser, S.L.; Bulman, R.A., Prediction of the adsorption coefficient (K_{OC}) for soil by a chemically immobilized humic acid column using RP-HPLC. *Chemosphere* **1990,** 21, 729-739.

Tan, L.C.; Carr. P.W., Study of retention in reversed-phase liquid chromatography using linear solvation energy relationships. II. The mobile phase. *J. Chromatogr. A* **1998**. 799, 1-19.

Tchapla, A.; Colin, H.; Guiochon, G., Linearity of homologous series retention plots in reversed-phase liquid chromatography. *Anal. Chem.* **1984,** 56, 621-625.

Teske, S. S.; Arnold, R. G., Removal of natural and xeno-estrogens during conventional wastewater treatment. *Rev. Environ. Sci. Biotechnol.* **2008,** 7, 107-124.

Touba, H.; Mansoori, G. A., Structure and property prediction of sub- and supercritical water. *Fluid Phase Equilibria* **1998,** 150-151, 459-468.

Torres-Lapasió, J. R.; García-Alvarez-Coque, M. C.; Rosés, M.; Bosch, E.; Zissimos, A. M.; Abraham, M. H., Analysis of a solute polarity parameter in reversed-phase liquid chromatography on a linear solvation relationship basis. *Anal. Chim. Acta* **2004,** 515, 209-227.

Tyler, C. R.; Jobling, S., Roach, sex, and gender-bending chemicals: The feminization of wild fish in English rivers. *BioScience* **2008,** 58, (11), 1051-1059.

Uematsu, M.; Franck, E. U., Static Dielectric Constant of Water and Steam. *J. Phys. Chem. Ref. Data* **1980,** 9, (4), 1291-1306.

Vailaya, A.; Horváth, C., Solvophobic theory and normalized free energies of nonpolar substances in reversed phase chromatography. *Journal of Physical Chemistry B* **1997,** 101, 5875-5888.

Vailaya, A.; Horváth, C., Retention in reversed-phase chromatography: partition or adsorption? *J.Chromatogr. A* **1998,** 829, 1-27.

Vanderford, B. J.; Pearson, R. A.; Rexing, D. J.; Snyder, S. A., Analysis of endocrine disruptors, pharmaceuticals, and personal care products in water using liquid chromatography/tandem mass spectrometry. *Anal. Chem.* **2003,** 75, 6265-6274.

Vanhoenacker, G.; Sandra, P., High temperature liquid chromatography and liquid-chromatography-mass spectrometry analysis of octylphenol ethoxylates on different stationary phases. *J.Chromatogr. A* **2005,** 1082, 193-202.

Vetter, W.; Alder, L.; Palavinskas, R., Mass Spectrometric Characterization of Q1, a C9H3Cl7N2 Contaminant in Environmental Samples. *Rapid Commun. Mass Spectrom.* **1999,** 13, 2118-2124.

Vetter, W.; Jun, W. Elucidation of a polychlorinated bipyrrole structure using enantioselective GC. *Anal. Chem.* **2002**, 74 (16), 4287-4289.

Vial, J.; Jardy, A., Experimental comparison of the different approaches to estimate LOD and LOQ of an HPLC method. *Anal. Chem.* **1999,** 71, 2672-2677.

Vitha, M.; Carr, P. W., The Chemical Interpretation and practice of linear solvation energy relationships in chromatography. *J.Chromatogr. A* **2006,** 1126, 143-194.

Voutsa, D.; Hartmann, P.; Schaffner, C.; Giger, W., Benzotriazoles, alkylphenols and bisphenol A in municipal wastewaters and in the Glatt River, Switzerland. *Environ. Sci. Pollut. R.* **2006,** 13, (5), 333-341.

Wagner, W.; Pruss, A., The IAPWS formulation 1995 for the thermodynamic properties of ordinary water substance for general and scientific use. *J. Phys. Chem. Ref. Data* **2002,** 31, (2), 387-535.

Wick, C. D.; Siepmann, J. I.; Schure, M. R., Simulation studies on the effects of mobile-phase modification on partioning in liquid chromatography. *Anal. Chem.* **2004,** 76, 2886-2892.

Wu, N.; Tang, Q.; Lippert, J. A.; Lee, M. L., Packed Capillary Column Solvating Gas Chromatography Using Neat Water Mobile Phase and Flame Ionization Detection. *J. Microcolumn Separations* **2001,** 13, (2), 41-47.

Yang, Y. A model for temperature effect on column efficiency in high temperature liquid chromatography. *Anal. Chim. Acta* **2006,** 558, 7-10.

Yang, Y., Subcritical Water Chromatography: A Green Approach to High Temperature Liquid Chromatography. *J. Sep. Sci.* **2007,** 30, 1131-1140.

Yang, Y.; Jones, A. D.; Mathis, J. A.; Francis, M. A., Flame ionization detection after splitting the water effluent in subcritical water chromatography. *J.Chromatogr. A* **2002,** 942, 231-236.

Yoshii, N.; Yoshie, H.; Miura, S.; Okazaki, S., A molecular dynamics study of sub- and supercritical water using a polarizable potential model. *Journal of Chemical Physics* **1998,** 109, (12), 4873-4884.

Zangwill, A., *Physics at surfaces*. Cambridge University Cambridge, 1988.

Zhang, B.; Li, X.; Yan, B., Advances in HPLC detection -- Toward universal detection. *Anal. Bioanal. Chem.* **2008,** 390, 299-301.

Zhang, C.; Wang, F.; Wang, Y. Solubilities of Sulfadiazine, Sulfamethazine, Sulfadimethoxine, Sulfamethoxydiazine, Sulfamonomethoxine, Sulfamethoxazole, and Sulfachloropyrazine in Water from (298.15 to 333.15) K. *J. Chem. Eng. Data.* **2007**, *52*, 1563.

Zhang, L.; Sun, L.; Siepmann, J. I.; Schure, M. R., Molecular simulation study of the bonded-phase structure in reversed-phase liquid chromatography with neat aqueous solvent. *J.Chromatogr. A* **2005,** 1079, 127-135.

Zhang, L.; Rafferty, J. L.; Siepmann, J. I.; Chen, B.; Schure, M. R., Chain conformation and solvent partitioning in reversed-phase liquid chromatography: Monte Carlo simulations for various water/methanol concentrations. *J.Chromatogr. A* **2006,** 1126, 219-231.

Zhao, J.; Carr, P. W., A comparative study of the chromatographic selectivity of polystyrene-coated zirconia and related reversed-phase materials. *Anal. Chem.* **2000,** 72, (2), 302-309.

Zhuravlev, N. D.; Siepmann, J. I.; Schure, M. R., Surface coverages of bonded-phase ligands on silica: A computational study. *Anal. Chem.* **2001,** 73, 4006-4011.

Appendix A. Monte Carlo Simulation Input Files

Several simulations were performed using the MCCCS Towhee program (Siepmann et al., 1999), a coupled-decoupled, configurational-bias Monte Carlo algorithm. Towhee has its own input system, in which the Monte Carlo favorabilities, system constraints, and molecular structures are designed. An extensive description of the Towhee system and inputs is provided through the authors at http://towhee.sourceforge.net/. These example inputs demonstrate the three major study classes:

1. The simulation of subcritical water in the NPT ensemble at elevated pressure
2. The simulation of phase interaction between subcritical water and a non-polar analog, octadecane
3. Partitioning of phenol between a non-polar and polar phase.

For all studies, water was designed using the TIP4P forcefield, which describes atomic motion of water in terms of hard spheres with discrete point charges on hydrogens, and a simulated p orbital set containing the point charge of the

oxygen. For organic molecules and helium, the TraPPE-United Atom forcefield was used. This forcefield has been designed for use with long chain and branched molecules, and was extended experimentally by D.C. to be able to describe substituted aromatics, specifically phenol. TraPPE-UA uses united atoms, which include hydrogens with the carbon structure. Simulations were designed in boxes of arbitrary size, and then allowed to equilibrate using favorable box volume moves in the CBMC statistics. For most studies, water was placed in initial coordinates from a pre-equilibrated system that was allowed to come to equilibrium for 10000 cycles before use, using input A.1 as a starting input system. A note on the formatting in this section: input files must be exactly formatted in the provided spacing and tabbing, and have been provided in the correct arrangement for Towhee operation.

A.1. Simulation of Subcritical Water in the NPT Ensemble

```
inputformat
'Towhee'
randomseed
 1302002
random_luxlevel
 3
random_allow_restart
T
ensemble
'npt'
temperature
473.0d0
pressure
1500.0d0
nmolty
1
```

nmolectyp
1000
numboxes
1
stepstyle
'cycles '
nstep
10000
controlstyle
'manual'
printfreq
100
blocksize
1000
moviefreq
200
backupfreq
200
runoutput
full
pdb_output_freq
2000
loutdft
.false.
loutlammps
.false.
loutdlpoly
.false.
pressurefreq
10
trmaxdispfreq
10
volmaxdispfreq
10
potentialstyle
'internal'
ffnumber
 1
ff_filename
/home/200610-CHEM3320/dconnors/Documents/towhee-
6.1.0/ForceFields/towhee_ff_
classical_potential

'Lennard-Jones '
classical_mixrule
'Lorentz-Berthelot '
lshift
F
ltailc
T
rmin
0.5
rcut
15.
rcutin
10.
electrostatic_form
'coulomb '
coulombstyle
'ewald_fixed_kmax '
kalp
5.6
kmax
5
dielect
1.
max_bond_length
3.
nfield
0
solvation_style
'none'
linit
.false.
initboxtype
'dimensions'
initstyle
'full cbmc'
initlattice
'simple cubic'
initmol
1000
inix iniy iniz
10 10 10
hmatrix

30.0d0 0.0d0 0.0d0
0.0d0 30.0d0 0.0d0
0.0d0 0.0d0 30.0d0
pmvol
0.01d0
    pmvlpr
    1.00d0
    rmvol
    1.00d0
    tavol
    0.50d0
pmcell
0.00d0
    pmcellpr
    1.00d0
    pmcellpt
    1.00d0
    rmcell
    2.00d0
    tacell
    0.50d0
pm1boxcbswap
0.10d0
    pm1cbswmt
    1.0000
pmcb
0.6600
    pmcbmt
    1.0000
    pmall
    1.000
pmpivot
0.00d0
    pmpivmt
    1.00d0
pmconrot
0.0000
    pmcrmt
    1.00d0
pmtracm
1.0000
    pmtcmt

```
        1.00d0
        rmtrac
        5.00d0
pmrotate
0.6600
        pmromt
        1.00d0
        rmrot
        0.1d0
        tarot
        0.50d0
cbmc_style
'coupled-decoupled'
coupled_decoupled_form
'Martin and Siepmann JPCB 1999'
cbmc_setting_style
'default ideal'
#TIP4P water
input_style
'basic connectivity map'
nunit
4
nmaxcbmc
4
lpdbnames
F
forcefield
'TIP4P'
charge_assignment
'manual'
unit ntype qqatom
1    'O'   0.0d0
vibration
3
2 3 4
improper torsion
0
unit ntype qqatom
2    'H'   0.52d0
vibration
1
1
```

```
improper torsion
0
unit ntype qqatom
3    'H'   0.52d0
vibration
1
1
improper torsion
0
unit ntype qqatom
4    'M'   -1.04d0
vibration
1
1
improper torsion
0
```

A.2 Simulation of Phase Interactions Between Octadecane and Water

```
inputformat
'Towhee'
randomseed
1302002
random_luxlevel
3
random_allow_restart
.false.
ensemble
'npt'
temperature
473.15d0
pressure
1500.0d0
nmolty
3
nmolectyp
5 1000 30
numboxes
3
stepstyle
'cycles'
nstep
5000
```

controlstyle
'manual'
printfreq
1000
blocksize
1000
moviefreq
200
backupfreq
1000
restartfreq
2000
runoutput
'full'
pdb_output_freq
1000
loutdft
.false.
loutlammps
.false.
loutdlpoly
.false.
pressurefreq
200
trmaxdispfreq
100
volmaxdispfreq
100
potentialstyle
'internal'
ffnumber
2
ff_filename
/home/200610-CHEM3320/dconnors/Documents/towhee-
6.1.0/ForceFields/towhee_ff_
/home/200610-CHEM3320/dconnors/Documents/towhee-
6.1.0/ForceFields/towhee_ff_
classical_potential
'Lennard-Jones'
classical_mixrule
'Lorentz-Berthelot'
lshift

.false.
ltailc
.true.
rmin
0.5d0
rcut
15.0d0
rcutin
10.0d0
electrostatic_form
'coulomb'
coulombstyle
'ewald_fixed_kmax'
kalp
5.6d0
kmax
5
dielect
1.0d0
solvation_style
'none'
linit
.false.
initboxtype
'dimensions'
initstyle
'full cbmc' 'coords' 'full cbmc'
'full cbmc' 'coords' 'full cbmc'
'full cbmc' 'coords' 'full cbmc'
initlattice
'simple cubic' 'none' 'none'
'none' 'none' 'none'
'none' 'none' 'simple cubic'
initmol
5 0 0
0 1000 0
0 0 30
inix iniy iniz
2   2   2
12   12   12
6   6   6
hmatrix

40.0d0 0.0d0 0.0d0
0.0d0 40.0d0 0.0d0
0.0d0 0.0d0 40.0d0
40.0d0 0.0d0 0.0d0
0.0d0 40.0d0 0.0d0
0.0d0 0.0d0 40.0d0
40.0d0 0.0d0 0.0d0
0.0d0 40.0d0 0.0d0
0.0d0 0.0d0 40.0d0
pmvol
0.75d0
    pmvlpr
    1.0d0 1.0d0 1.0d0
    rmvol
    5.0d0
    tavol
    0.5d0
pmcell
0.25d0
    pmcellpr
    1.0d0 1.0d0 1.0d0
    pmcellpt
    0.5d0
    rmcell
    5.0d0
    tacell
    0.5d0
pm2boxrbswap
0.0d0
    pm2rbswmt
    1.0d0 1.0d0 0.0d0
    pm2rbswpr
    0.0d0 1.0d0 1.0d0
pm2boxcbswap
0.1d0
    pm2cbswmt
    1.0d0 1.0d0 0.0d0
    pm2cbswpr
0.0d0 1.0d0 1.0d0
pm1boxcbswap
0.1d0
    pm1cbswmt

1.0d0 1.0d0 0.0d0
pmavb1
0.1d0
pmavb1in
0.5d0
pmavb1mt
1.0d0 0.0d0 0.0d0
pmavb1ct
1.0d0 0.0d0 0.0d0
0.0d0 1.0d0 0.0d0
0.0d0 0.0d0 1.0d0
avb1rad
4.0d0
pmcb
1.0d0
pmcbmt
1.0d0 1.0d0 1.0d0
pmall
1.0d0 1.0d0 1.0d0
pmpivot
1.0d0
pmpivmt
1.0d0 0.0d0 1.0d0
pmconrot
0.5d0
pmcrmt
1.0d0 0.0d0 0.0d0
pmtraat
1.0d0
pmtamt
1.0d0 1.0d0 1.0d0
rmtraa
2.0d0 2.0d0 3.0d0
tatraa
0.5d0
pmtracm
1.0d0
pmtcmt
0.1d0 1.0d0 1.0d0
rmtrac
1.0d0 2.0d0 3.0d0
tatrac

```
        0.5d0
pmrotate
1.0d0
        pmromt
        0.1d0 1.0d0 0.0d0
        rmrot
        0.1d0 0.1d0 0.1d0
        tarot
        0.5d0
cbmc_style
'coupled-decoupled'
coupled_decoupled_form
'Martin and Siepmann JPCB 1999'
cbmc_setting_style
'default ideal'
#octadecane
input_style
'basic connectivity map'
nunit
18
nmaxcbmc
18
lpdbnames
F
forcefield
'TraPPE-UA'
charge_assignment
'bond increment'
unit ntype
1    'CH3*(sp3)'
vibration
1
2
improper torsion
0
unit ntype
2    'CH2**(sp3)'
vibration
2
1 3
improper torsion
0
```

unit ntype
3 'CH2**(sp3)'
vibration
2
2 4
improper torsion
0
unit ntype
4 'CH2**(sp3)'
vibration
2
3 5
improper torsion
0
unit ntype
5 'CH2**(sp3)'
vibration
2
4 6
improper torsion
0
unit ntype
6 'CH2**(sp3)'
vibration
2
5 7
improper torsion
0
unit ntype
7 'CH2**(sp3)'
vibration
2
6 8
improper torsion
0
unit ntype
8 'CH2**(sp3)'
vibration
2
7 9
improper torsion
0

unit ntype
9 'CH2**(sp3)'
vibration
2
8 10
improper torsion
0
unit ntype
10 'CH2**(sp3)'
vibration
2
9 11
improper torsion
0
unit ntype
11 'CH2**(sp3)'
vibration
2
10 12
improper torsion
0
unit ntype
12 'CH2**(sp3)'
vibration
2
11 13
improper torsion
0
unit ntype
13 'CH2**(sp3)'
vibration
2
12 14
improper torsion
0
unit ntype
14 'CH2**(sp3)'
vibration
2
13 15
improper torsion
0

```
unit ntype
15    'CH2**(sp3)'
vibration
2
14 16
improper torsion
0
unit ntype
16    'CH2**(sp3)'
vibration
2
15 17
improper torsion
0
unit ntype
17    'CH2**(sp3)'
vibration
2
16 18
improper torsion
0
unit ntype
18    'CH3*(sp3)'
vibration
1
17
improper torsion
0
#TIP4P water 20c
input_style
'basic connectivity map'
nunit
4
nmaxcbmc
4
lpdbnames
F
forcefield
'TIP4P'
charge_assignment
'manual'
unit ntype qqatom
```

```
1    'O'   0.0d0
vibration
3
2 3 4
improper torsion
0
unit ntype qqatom
2    'H'   0.52d0
vibration
1
1
improper torsion
0
unit ntype qqatom
3    'H'   0.52d0
vibration
1
1
improper torsion
0
unit ntype qqatom
4    'M'   -1.04d0
vibration
1
1
improper torsion
0
#helium
input_style
'basic connectivity map'
nunit
1
nmaxcbmc
1
lpdbnames
F
forcefield
'TraPPE-UA'
charge_assignment
'manual'
unit ntype qqatom
1    'He'  0.0d0
```

vibration
0
improper torsion
0

A.3 Simulation of Phase Partitioning with Phenol

inputformat
'Towhee'
randomseed
1302002
random_luxlevel
3
random_allow_restart
.false.
ensemble
'npt'
temperature
473.15d0
pressure
1500.0d0
nmolty
4
nmolectyp
10 1000 20 10
numboxes
3
stepstyle
'cycles'
nstep
1000
controlstyle
'manual'
printfreq
100
blocksize
200
moviefreq
100
backupfreq
1000
restartfreq
100

runoutput
'full'
pdb_output_freq
100
loutdft
.false.
loutlammps
.false.
loutdlpoly
.false.
pressurefreq
200
trmaxdispfreq
100
volmaxdispfreq
100
potentialstyle
'internal'
ffnumber
2
ff_filename
/home/200610-CHEM3320/dconnors/Documents/towhee-
6.1.0/ForceFields/towhee_ff_
/home/200610-CHEM3320/dconnors/Documents/towhee-
6.1.0/ForceFields/towhee_ff_
classical_potential
'Lennard-Jones'
classical_mixrule
'Lorentz-Berthelot'
lshift
.false.
ltailc
.true.
rmin
0.5d0
rcut
15.0d0
rcutin
10.0d0
electrostatic_form
'coulomb'
coulombstyle

'ewald_fixed_kmax'
kalp
5.6d0
kmax
5
dielect
1.0d0
solvation_style
'none'
linit
.true.
initboxtype
'dimensions'
initstyle
'coords' 'full cbmc' 'full cbmc' 'full cbmc'
'coords' 'full cbmc' 'full cbmc' 'full cbmc'
'coords' 'full cbmc' 'full cbmc' 'full cbmc'
initlattice
'none' 'none' 'none' 'simple cubic'
'none' 'simple cubic' 'none' 'simple cubic'
'none' 'none' 'simple cubic' 'none'
initmol
10 0 0 5
0 1000 0 5
0 0 20 0
inix iniy iniz
6   6   6
12   12   12
6   6   6
hmatrix
40.0510614d0 0.0d0 0.0d0
0.0d0 40.0510614d0 0.0d0
0.0d0 0.0d0 40.0510614d0
40.0d0 0.0d0 0.0d0
0.0d0 40.0d0 0.0d0
0.0d0 0.0d0 40.0d0
40.0d0 0.0d0 0.0d0
0.0d0 40.0d0 0.0d0
0.0d0 0.0d0 40.0d0
pmvol
0.0d0
        pmvlpr

1.0d0 1.0d0 1.0d0
rmvol
5.0d0
tavol
0.5d0
pmcell
0.0d0
pmcellpr
1.0d0 1.0d0 1.0d0
pmcellpt
0.5d0
rmcell
5.0d0
tacell
0.5d0
pm2boxcbswap
1.0d0
pm2cbswmt
0.0d0 0.0d0 0.0d0 1.0d0
pm2cbswpr
0.0d0 1.0d0 1.0d0
pm1boxcbswap
0.5d0
pm1cbswmt
1.0d0 1.0d0 0.0d0 1.0d0
pmavb1
0.1d0
pmavb1in
0.5d0
pmavb1mt
1.0d0 0.0d0 0.0d0 0.1d0
pmavb1ct
1.0d0 0.0d0 0.0d0 0.0d0
0.0d0 1.0d0 0.0d0 0.0d0
0.0d0 0.0d0 1.0d0 0.0d0
0.0d0 0.0d0 0.0d0 1.0d0
avb1rad
4.0d0
pmcb
0.5d0
pmcbmt
1.0d0 1.0d0 1.0d0 1.0d0

```
        pmall
        1.0d0 1.0d0 1.0d0 1.0d0
pmpivot
0.5d0
        pmpivmt
        1.0d0 0.0d0 1.0d0 0.0d0
pmconrot
0.5d0
        pmcrmt
        1.0d0 0.0d0 0.0d0 0.0d0
pmtraat
1.0d0
          pmtamt
        1.0d0 1.0d0 1.0d0 1.0d0
        rmtraa
        2.0d0 2.0d0 3.0d0 2.0d0
        tatraa
        0.5d0
pmtracm
1.0d0
        pmtcmt
        0.1d0 1.0d0 1.0d0 1.0d0
        rmtrac
        1.0d0 2.0d0 3.0d0 2.0d0
        tatrac
        0.5d0
pmrotate
1.0d0
        pmromt
        0.1d0 1.0d0 0.0d0 0.0d0
        rmrot
        0.1d0 0.1d0 0.1d0 0.1d0
tarot
        0.5d0
cbmc_style
'coupled-decoupled'
coupled_decoupled_form
'Martin and Siepmann JPCB 1999'
cbmc_setting_style
'default ideal'
#octadecane
input_style
```

'basic connectivity map'
nunit
18
nmaxcbmc
18
lpdbnames
F
forcefield
'TraPPE-UA'
charge_assignment
'bond increment'
unit ntype
1   'CH3*(sp3)'
vibration
1
2
improper torsion
0
unit ntype
2   'CH2**(sp3)'
vibration
2
1 3
improper torsion
0
unit ntype
3   'CH2**(sp3)'
vibration
2
2 4
improper torsion
0
unit ntype
4   'CH2**(sp3)'
vibration
2
3 5
improper torsion
0
unit ntype
5   'CH2**(sp3)'
vibration

2
4 6
improper torsion
0
unit ntype
6 'CH2**(sp3)'
vibration
2
5 7
improper torsion
0
unit ntype
7 'CH2**(sp3)'
vibration
2
6 8
improper torsion
0
unit ntype
8 'CH2**(sp3)'
vibration
2
7 9
improper torsion
0
unit ntype
9 'CH2**(sp3)'
vibration
2
8 10
improper torsion
0
unit ntype
10 'CH2**(sp3)'
vibration
2
9 11
improper torsion
0
unit ntype
11 'CH2**(sp3)'
vibration

2
10 12
improper torsion
0
unit ntype
12   'CH2**(sp3)'
vibration
2
11 13
improper torsion
0
unit ntype
13   'CH2**(sp3)'
vibration
2
12 14
improper torsion
0
unit ntype
14   'CH2**(sp3)'
vibration
2
13 15
improper torsion
0
unit ntype
15   'CH2**(sp3)'
vibration
2
14 16
improper torsion
0
unit ntype
16   'CH2**(sp3)'
vibration
2
15 17
improper torsion
0
unit ntype
17   'CH2**(sp3)'
vibration

```
2
16 18
improper torsion
0
unit ntype
18    'CH3*(sp3)'
vibration
1
17
improper torsion
0
#TIP4P water 20c
input_style
'basic connectivity map'
nunit
4
nmaxcbmc
4
lpdbnames
F
forcefield
'TIP4P'
charge_assignment
'manual'
unit ntype qqatom
1    'O'   0.0d0
vibration
3
2 3 4
improper torsion
0
unit ntype qqatom
2    'H'   0.52d0
vibration
1
1
improper torsion
0
unit ntype qqatom
3    'H'   0.52d0
vibration
1
```

```
1
improper torsion
0
unit ntype qqatom
4    'M'   -1.04d0
vibration
1
1
improper torsion
0
#helium
input_style
'basic connectivity map'
nunit
1
nmaxcbmc
1
lpdbnames
F
forcefield
'TraPPE-UA'
charge_assignment
'manual'
unit ntype qqatom
1    'He'  0.0d0
vibration
0
improper torsion
0
#TraPPE-UA phenol
input_style
'basic connectivity map'
nunit
8
nmaxcbmc
8
lpdbnames
F
forcefield
'TraPPE-UA'
charge_assignment
'manual'
```

```
unit ntype qqatom
1    'Ho'  0.435d0
vibration
1
2
improper torsion
0
unit ntype qqatom
2    'Och(sp3)' -0.700d0
vibration
2
1 3
improper torsion
0
unit ntype qqatom
3    'Caac(aro)' 0.205d0
vibration
3
2 4 8
improper torsion
0
unit ntype qqatom
4    'CHaa(aro)' 0.03d0
vibration
2
3 5
improper torsion
0
unit ntype qqatom
5    'CHaa(aro)' 0.0d0
vibration
2
4 6
improper torsion
0
unit ntype qqatom
6    'CHaa(aro)' 0.0d0
vibration
2
5 7
improper torsion
0
```

```
unit ntype qqatom
7    'CHaa(aro)' 0.0d0
vibration
2
6 8
improper torsion
0
unit ntype qqatom
8    'CHaa(aro)' 0.03d0
vibration
2
3 7
improper torsion
0
```

Appendix B: Chloride Stress Corrosion in the Wet Oxidation Reactor

B.1 Stress Corrosion of Steel Alloys

During the study of operation of the lab-scale wet oxidation reactor, it was discovered that a significant contribution to effluent color and residual solids resulted from the corrosion of the high strength steel in the reactor chamber. In previous work with pilot scale wet oxidation reactors, passivation of the reactor became a significant concern, requiring frequent additions of nitric acid to the reactor to maintain a passive surface. Reactor stress is a result of the combination of high concentrations of oxygen and chlorine in a reactive liquid medium, although the reaction mixture is less corrosive than supercritical water solutions, which can react very rapidly with typical steel alloys.

In the usage of high temperature solutions with oxygen and chloride, stress cracking can occur rapidly. Stress corrosion cracking is when small corrosive pits expose unpassivated metal surfaces, which rapidly dissolve into the solvent. Small intragranular fissures develop in the underlying alloy, often with reactive Lewis acid sites that favor further reaction, until the fissures move

all the way through the alloy and result in stress fracture. Chlorine and oxygen both accelerate stress corrosion in the inherently corrosive subcritical water medium by weakening the passivated surface in the case of chlorine, or causing oxide production and corrosion with oxygen.

Even with very high grade stainless steel (alloy type 625) has been shown to crack under acidic, oxygenated conditions in subcritical water, sometimes leading to reactor failure after only hours (Kritzer, 2004). The reason for the specific danger with subcritical water is that mechanical and chemical stresses are both being placed on the reactor surface. As a result, corrosion types often become more severe, and entire surfaces are attacked, as opposed to just pitting effects.

A study of coupons of high-grade stainless steel (alloy 625, 21.6% chromium, 62.7% nickel, 2.3% iron, 9% molybdenum) demonstrated chloride related pitting at subcritical temperatures beneath 215ºC (Kritzer et al., 1998). Above 215ºC, the pitting changed to general corrosion, attacking the entire surface of the steel alloy. Transgranular cracks occurred as well at high temperatures, eventually leading to stress corrosion cracking.

Schroer et al. (2007) demonstrated the main problem resulting in wet oxidation corrosion is the ability of chloride and oxygen to pass through the passive layer of oxides on a metal surface, and react with alloy atoms, especially chromium, to produce chromate and lewis acid sites. These acid sites in turn

allow for the dissolution of all components, some of which produce oxide scale (Nickel) and others (iron and chromium) dissolving into the aqueous medium. Both acidic and basic solutions of chlorine and oxygen demonstrate corrosion capacity, and the most severe corrosion occurred at temperatures from 100-400ºC.

Son et al.(2008) demonstrated that alloy specific metals turned up in subcritical reaction effluents. Interestingly, the total metal mass reduction is greater in subcritcal wet oxidation reactors than in supercritical oxidation. Hastelloy C-276 coupons (the most similar alloy in this work to type 304 stainless steel) demonstrated a 0.06% mass reduction after 60 minutes of exposure to subcritical water, oxygen and chlorophenol as a chlorine source. The primary effluent metals detected were chromium, nickel and molybdenum.

B.2 Stress Corrosion in the Wet Oxidation Rotating Tube Reactor

It was observed that with natural products (waste stream surrogates) that full color removal did not occur. Furthermore, solutions with low soluble solids would often have slight residues of solids in effluents, with definite colors, indicating a possible corrosion product (see Figure 7.4 for an example of residual color in treated effluents). A more dramatic color was observed when a solution of biologically treated wastewater effluent was tested with the wet oxidation

reactor. Despite the relatively clear initial liquid, the final liquid was found to be a brilliant yellow. An example of this residual color is provided in Figure B.1.

To determine what metal ions, if any, were contributing to this residual color, atomic emission spectroscopy was used. A filtered sample of the effluent was aspirated into an Atomic Absorbance spectrometer, with monitoring performed at all wavelengths using an Ocean Optics Spectrometer. The signal was then interpreted using LoggerPro software. Once graphed, the emission lines of the spectrum were correlated to elements via the NIST atomic spectral database, with high intensity transitions of likely elements used to assign spectral lines. The resulting assignments are graphed in Figure B.2. The predominantly observed elements found in the effluent are iron, molybdenum, copper and chromium, with likely concentrations of chlorine, magnesium and lithium also found. This would correlate well with the expected chemical makeup of the reactor, which is a type 304 alloy made predominantly from iron, chromium and nickel. Nickel oxides have been found in literature to retain as scale on the inside of reactor surfaces, so it is possible this is why no nickel lines were observed in the effluent.

A test of glucose spiked with sodium chloride resulted in even more dramatic color changes and residual oxides. The effect of treatment of this solution is presented in Figure B.3, with both beakers containing effluent. The

agitated sample on the left is a deep reddish brown, corresponding to iron oxide. The settled sample is relatively clear, but with a definite yellow tint.

Future work on this problem will study how type 304 stainless can be repassivated after exposure to the wet oxidation medium. Typical treatment includes routine exposure to nitric acid, however this may not fully repassivate deep fissures. Future directions for wet oxidation design may follow the work of Son et al. (2008), who used ceramic liners for flow through supercritical water reactors.

B.3 Works Cited in Appendix B

Kritzer, P.; Boukis, N.; Dinjus, E., Corrosion of Alloy 625 in Aqueous Solutions Containing Chloride and Oxygen. *Corrosion* **1998,** 54, 824-834.

Kritzer, P., Corrosion in high-temperature and supercritical water and aqueous solutions: a review. *J. Supercrit. Fluids* **2004,** 29, 1-29.

Schroer, C.; Konys, J.; Novotny, J.; Hausselt, J., Material Performance in Chlorinated Supercritical Water Systems. *Corrosion* **2007,** 63, 46-62.

Son, S.H.; Lee, J.H.; Lee, C.H., Corrosion phenomena of alloys by subcritical and supercritical water oxidation of 2-chlorophenol. *J. Supercrit. Fluids* **2008**, 44, 370-378.

Figure B.1 Wet oxidation reactor effluent (left) and untreated (right) originating from a biologically treated wastewater stream.

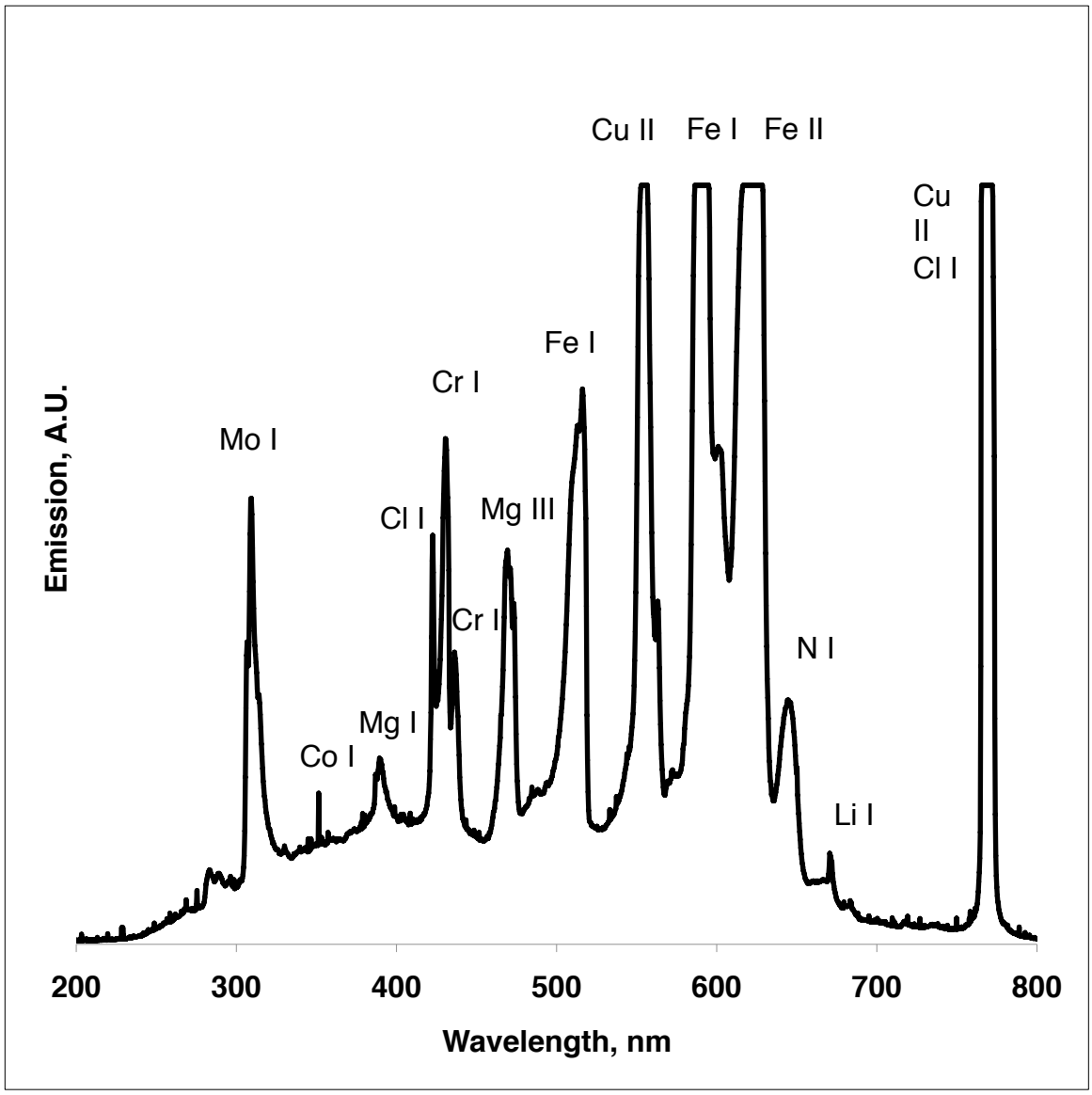

Figure B.2 Atomic Emission spectra of treated wastewater effluent with proposed identification from NIST Atomic Spectrum Database.

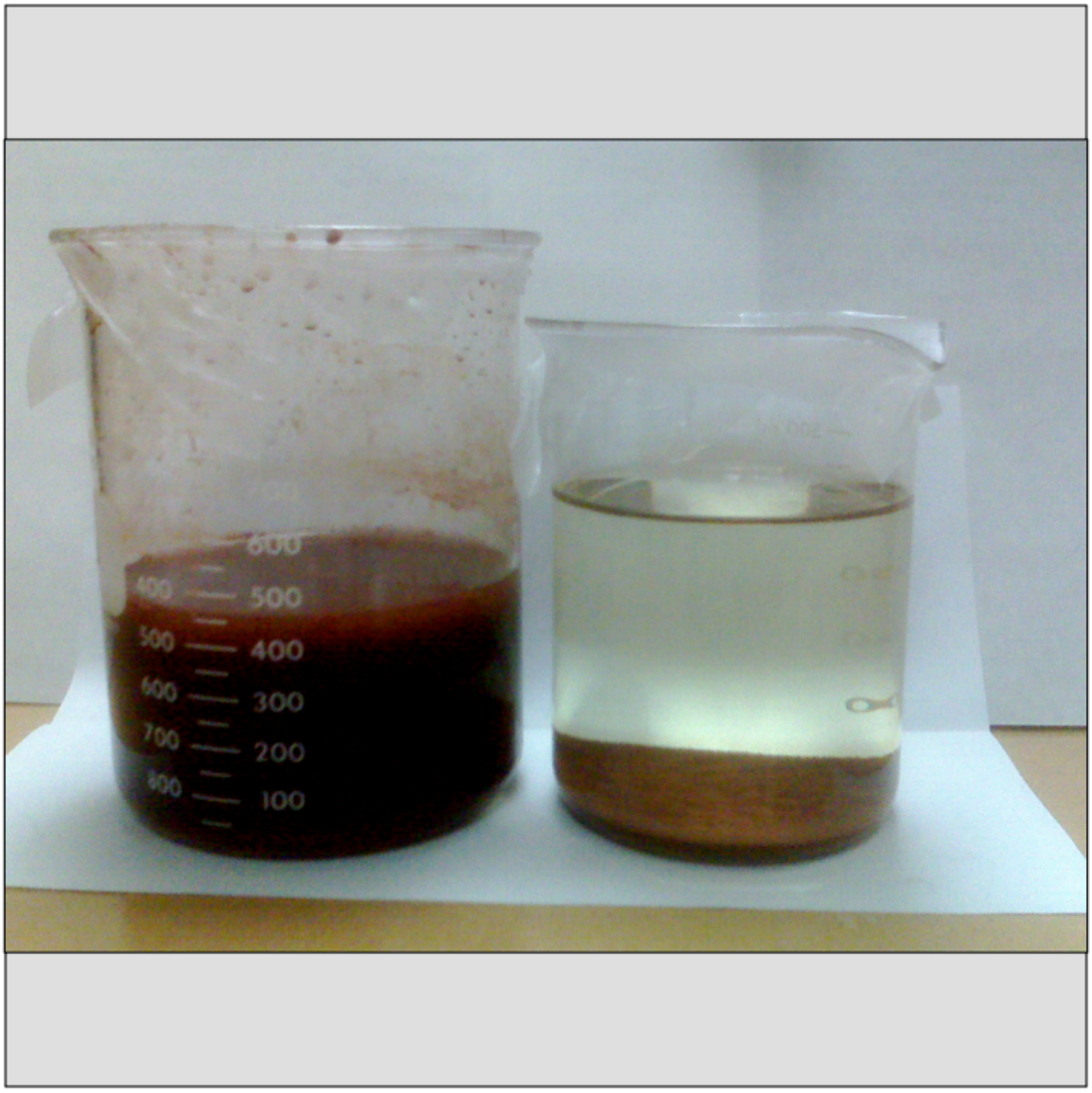

Figure B.3 Agitated (left) and settled (right) reaction products from treatment of glucose spiked with sodium chloride. The resulting solid is likely iron oxide, which settles out, leaving other residual products in solution.

Appendix C: Table of Abbreviations Used in This Dissertation

2DLC	Two dimensional Liquid Chromatography
ASTM	American Society for Testing and Materials
C18	Octadecane
CBMC	Configurational-Bias Monte Carlo
COD	Chemical Oxygen Demand
DDT	dichlorodiphenyltricholoroethane
ELISA	Enzyme-Linked Immunosorbent Assay
ELSD	Evaporative Light Scattering Detector
ESI	Electrospray Ionization
FAIMS	High-Field Assymetric Waveform Ion Mobility Spectrometry
FID	Flame Ionization Detector
GC	Gas Chromatography
GPM	Gallon per Minute
HPLC	High Performance Liquid Chromatography
HPVC	High Production Volume Chemical
HTLC	High Temperature Liquid Chromatography
ICP	Inductively Coupled Plasma
I.D.	Internal Diameter
IR	Infrared
K_{OC}	Organic Carbon/Water Partition Coefficient
K_{OW}	Octanol/Water Partition Coefficient
L	Liter
LC	Liquid Chromatography
LN	Natural Logarithm
LOD	Limit of Detection
LOG	Logarithm
LOQ	Limit of Quantification
LSER	Linear Solvation Energy Relationship
MC	Monte Carlo
MD	Molecular Dynamics
MPa	MegaPascal

MS	Mass Spectrometry
mg	milligram
µg	microgram
µL	microliter
NCD	Nitrogen Chemiluminescence Detector
ng	nanogram
nm	nanometer
NMR	Nuclear Magnetic Resonance
O.D.	Outer Diameter
ODS	Octadecylsilane
OECD	Organization for Economic Cooperation and Development
OLS	Ordinary Least Squares
OWC	Organic Wastewater Contaminant
Pa	Pascal
PAH	Polyaromatic Hydrocarbons
PBD	Polybutadiene
PEEK	Polyetheretherketone
pg	picogram
PPCPs	Pharmaceuticals and Personal Care Products
PPB	Part Per Billion
PPM	Part Per Million
PPT	Part Per Trillion
Q-TOF	Quadrupole-Time of Flight
RI	Refractive Index
RPLC	Reversed-Phase Liquid Chromatography
RSD	Relative Standard Deviation
SCD	Sulfur Chemiluminescence Detector
SCCM	Standard Cubic Centimeter per Minute
SD	Standard Deviation
SDZ	Sulfadiazine
SE	Standard Error
SMZ	Sulfadimethoxine
S/N	Signal to Noise Ratio
SPME	Solid Phase Microextraction
SPE	Solid Phase Extraction
SWC	Subcritical Water Chromatography
TOF-MS	Time of Flight Mass Spectrometry
TS	Total Solids
USGS	United States Geological Survey
UV-VIS	Ultraviolet-Visible
VOC	Volatile Organic Compound

VTR	VERTICAL TUBE REACTOR
WLS	WEIGHTED LEAST SQUARES
WWTP	WASTE WATER TREATMENT PLANT
YES	YEAST ESTROGEN RECEPTOR TRANSCRIPTION BIOASSAY